Novel Mechanisms in Control of Mitotic Exit

by

İdil KIRDÖK

A Dissertation Submitted to the
Graduate School of Sciences and Engineering
in Partial Fulfilment of the Requirements for
the Degree of
Master of Science
in
Molecular Biology and Genetics

May 2022

Novel Mechanisms in Control of Mitotic Exit

Koç University

Graduate School of Sciences and Engineering

This is to certify that I have examined this copy of a master's thesis by

İdil Kırdök

and have found that it is complete and satisfactory in all respects,
and that any and all revisions required by the final
examining committee have been made.

Committee Members:

Assistant Prof. Dr. Ayşe Koca Çaydaşı (Advisor-Koç University)

Prof. Dr. Halil Kavaklı (Koç University)

Prof. Dr. Mesut Muyan (Middle East Technical University)

Date: 26/05/2022

To my family, and my friends who always supported me

ABSTRACT

Novel Mechanisms in Control of Mitotic Exit

İdil Kırdök

Master of Science in Molecular Biology and Genetics

May 26, 2022

Mitotic exit network is a G-protein signaling process that regulates the exit from mitosis. This process must be tightly regulated for proper cell division. The aim of this thesis is to characterize novel mechanisms controlling mitotic exit. For this purpose, two independent but related mechanisms are studied in *Saccharomyces cerevisiae*, budding yeast.

The first mechanism focuses on an unanticipated effect of the daughter cortex localized bud site selection protein Bud14 on Cdc14 which is the main protein phosphatase that triggers the mitotic exit in budding yeast. Our data shows that in the absence of *BUD14* or if Bud14 cannot bind to the protein phosphatase 1 (*bud14-F379A*), Cdc14 stays longer at the spindle pole body (SPB). SPB localization of Cdc14 was dependent on the Cdc14 release mechanisms FEAR and MEN as well as the mitotic exit inhibitor protein Bfa1. Thus, Bud14-Glc7 is part of the mechanism that controls Cdc14 localization to SPBs.

The second part of the thesis investigates the mechanisms by which Cdc36 influences mitotic exit. Cdc36 is a component involved in CCR4-NOT complex which have roles in a variety of mechanisms in mRNA regulation and translation. Our data show, *cdc36-16* mutant rescues a mitotic exit defective yeast strain. We performed RNAseq analysis of WT and *cdc36-16* cells during their synchronous progression in the cell cycle from anaphase onset until mitotic exit. Many cell cycle related genes were found to be differentially regulated in *cdc36-16*. Our data thus suggest Cdc36 dependent expression is important for a timely mitotic exit.

Taken together, in this thesis, we discovered novel conserved proteins (Bud14-Glc7 and Cdc36) that take part in mitotic exit control. We anticipate that these conserved proteins may have similar functions in higher eukaryotes.

ÖZETÇE

Mitozdan Çıkış Mekanizmasında Yeni Mekanizmalar

İdil Kırdök

Moleküler Biyoloji ve Genetik, Yüksek Lisans

Mayıs 26, 2022

Mitozdan çıkış mekanizması, mitozdan çıkışı düzenleyen bir G-protein sinyalleşme sürecidir. Bu süreç, doğru hücre bölünmesi için sıkı bir şekilde düzenlenmelidir. Bu tezin amacı, mitozdan çıkışı kontrol eden yeni mekanizmaları karakterize etmektir. Bu amaçla, maya hücresi olan *Saccharomyces cerevisiae*'de birbirinden bağımsız fakat ilişkili iki mekanizma incelenmiştir.

İlk mekanizma, yavru kortekste tomurcuk bölgesi seçim proteini Bud14'ün fosfataz Cdc14 üzerindeki beklenmeyen bir etkisi üzerinedir. Cdc14, mitozdan çıkışı tetikleyen ana protein fosfatazdır ve anafaz başlangıcından sonra mil pol gövdelerine (SPB) yerleşir ve mitozdan çıkışla birlikte SPB'lerden kaybolur. Verilerimiz, BUD14'ün yokluğunda veya Bud14'ün protein fosfataz 1'e (bud14-F379A) bağlanamaması durumunda, Cdc14'ün Mil Pol Gövdesinde (SPB) daha uzun süre kaldığını göstermektedir. Cdc14'ün SPB lokalizasyonu, Cdc14 salım mekanizmaları FEAR ve MEN'nin yanı sıra mitotik çıkış inhibitörü protein Bfa1'e bağlıdır. Bu nedenle, Bud14-Glc7, Cdc14'ün SPB lokalizasyonunu kontrol eden mekanizmanın bir parçasıdır.

Tezin ikinci kısmı, Cdc36'nın mitotik çıkışı etkilediği mekanizmaları araştırır. Cdc36, mRNA regülasyonu ve translasyonunda çeşitli mekanizmalarda rolleri olan CCR4-NOT kompleksinde bir bileşendir. Verilerimiz, *cdc36-16* mutantının mitozdan çıkış sorununu kurtardığını göstermektedir. Anafaz başlangıcından mitotik çıkışa kadar senkronize hücre döngüsü sırasında WT ve *cdc36-16* hücrelerinin RNAseq analizini gerçekleştirdik. Birçok hücre döngüsü ile ilgili genin, *cdc36-16*'da farklı şekilde düzenlendiği bulundu. Bu nedenle verilerimiz, Cdc36'ya bağlı ifadenin mitozdan çıkış için önemli olduğunu göstermektedir.

Bu tezde, mitotik çıkış kontrolünde yer alan yeni proteinleri (Bud14-Glc7 ve Cdc36) keşfettik. Bu proteinlerin daha yüksek ökaryotlarda benzer işlevlere sahip olabileceğini tahmin ediyoruz.

ACKNOWLEDGEMENTS

Firstly, I would like to thank The Scientific and Technological Research Council of Turkey (TUBITAK). This project was funded by the TUBITAK 118Z979 awarded to Ayşe Koca Çaydaşı.

I would like to thank my supervisor Assist. Prof Ayşe Koca Çaydaşı. I started to work with her as a fresh graduate. She helped me through this journey and taught me to be a better scientist. I learn so many things from her, and I am thankful for all the support she has provided me. She helped me to become better and learn from my mistakes. She was always here for me when I needed. I remember the first time we talked about the projects; her enthusiasm made me more excited about research and MSc. Thank you for always being so enthusiastic about doing research.

I would like to thank our collaborators; Dr. Şeref Gül, Prof. Dr. Halil Kavaklı, Assoc. Dr. Nurcan Tunçbağ. It was a pleasure to work with you.

I would like to thank to all the current and previous lab members; Şeyma, Mariam, Barış, Gülden, Dilara, Mukadder, Betül, Sevilay, Atakan, Cansu and Hüseyin, whom I was very lucky to work with side by side. I enjoyed this journey together with you. You were always there when I needed help. I still don't know how Şeyma used to show up unexpectedly when I was about to make a mistake. We made the work turn into fun. We spent so much time in the lab with you, and I couldn't do so much without you.

I would like to thank my family. Thank you so much for always supporting me. You were always there for me when I needed you. You helped me achieve my goals. My mother was the role model when I was growing up. She was the strongest woman in my life, and I want to thank her for all the support and love. I want to dedicate this thesis to her. Moreover, I want to thank my brother. He made me follow my dreams when I was about to give up. Thank you for believing me. I would like to thank my grandparents; your memories were always a support to me.

I would like to thank the people who survived with me through this challenging journey; Tuğce, Cansu, Beste, and Hüseyin. We have been through so much with you, and we had so much fun at the same time. You were always with me when I needed support or fun. I loved living here with you, and you will always be with me wherever we go. Even though we will be in separate cities or countries, I know you are always there, and I am always here for you. Cansu and Hüseyin, we spent so many late nights and weekends at the lab with you, and when I look back, I only remember how much we used to laugh together. Thank you for so many great memories.

I would like to thank Berk; thank you so much for the calm and happiness you brought to me. I am so happy to have you in my life. I will always be looking forward to watching sitcoms with you after a long day and preparing food that has too much cheese in it.

I would like to thank Kutlu and Kıymet. You have been a family to me since we met at the university. You gave me the best birthdays even though we were in separate countries. I am looking forward to the day we are near each other again. I am so happy that we shared so many great memories, and we will continue to do so.

I would like to thank Eda, Yasemin, Esma, Ezgi, Elif Ayşe, Mine, Elif Nur, İlayda, and Batuhan, Berkay. Eda, you were always there for me, even though you are hours away physically. You are one of the first people I always need to consult about anything. Yasemin, thank you so much for making me laugh all the time. I know I can always speak to you whenever I need. Esma, thank you so much for the fun we had. I always loved hanging out with you and finding us in unexpected situations. Ezgi, thank you so much for our talks; you always had the best logical ideas. Elif Ayşe, I would only be sorry we didn't use to know each other earlier. Thank you for being such a good friend to me. Mine, I remember the first field trip we met, and I am so happy to have your friendship. Elif Nur, you were the greatest lab partner; I am so glad we chose each other on the first day of the MBGE lab. İlayda, thank you for your positivity, I am looking forward to doing so much next year. Batuhan, thank you so much for your friendship; music will always be with you.

I would like to thank my flat mates; Elif, Buse, Saliha, and Ceku. Elif, you were a significant part of my life in Ankara and İstanbul. I will always be looking forward to doing music and having a long walk to talk about everything. Buse, I will always miss having tea and talking to you at night; thank you so much. Saliha, thank you for bringing Ceku to us, and I would like to thank Ceku for being big emotional support with her cuteness.

I would like to thank Selin, Buse, and Gaye. You are my oldest friends, and I feel your support every day. We spent so many great memories through these years, and we will have so much more in the future.

I would like to thank Melis; we had a great time during the internship, and I am so happy we are going to continue to do so in Ph.D. I am looking forward to traveling and having a lot of fun with you next year.

I would like to thank Buğra and Gizem (Bülbül). Bülbül, you always knew what to say to make me laugh even in my saddest times. Buğra, I always loved talking to you, and we will continue to have times in the future. Thank you both for being such good friends to me.

Lastly, I want to thank my professors at the Middle East Technical University; you were an inspiration to me and made me more and more excited about research. Thank you so much.

TABLE OF CONTENTS

LIST OF TABLES

LIST OF FIGURES

ABBREVIATIONS

FEAR: Fourteen Early Release Pathway

MEN: Mitotic Exit Network

SPB: Spindle Pole Body

APC/C: Anaphase Promoting Complex/Cyclosome

APS: Ammonium Persulfate

DMSO: Dimethyl Sulfoxide

PFA: Paraformaldehyde

TCA: Trichlorocacetic acid

CDK: Cyclin Dependent Kinase

CKI: Cyclin Dependent Kinase Inhibitor

SPOC: Spindle Positioning Checkpoint

SAC: Spindle Assembly Checkpoint

Gap: GTPase Activating Protein

GEF: Guanine Exchange Factor

MTOC: Microtubule Organizing Center

PP1: Protein Phosphatase 1

CCR: Cell Cycle Regulated

Chapter 1: INTRODUCTION

1.1 *Saccharomyces cerevisiae* as a Model Organism

S. cerevisiae, also known as budding yeast, is a widely used model organism. The first eukaryote, whose genome is sequenced, budding yeast, has a long history and multiple applications developed for industrial and scientific manipulations (Goffeau et al., 1996). *S. cerevisiae* is a member of fungi Familia. *S. cerevisiae* is a eukaryote and it provides an efficient research tool for complex organisms, including humans (Hanson, 2018). Sequence analyses of *S. cerevisiae* showed that 31% of its coding genome has clear homologs in the human genome (Botstein et al., 1997).

Many experimental strains of budding yeast have been constructed; for example, S288C is one of the most common experimental strains used. It was constructed by Robert Mortimer in the early 1950s (Mortimer & Johnston, 1986). A haploid *S. cerevisiae* cell contains 12,000 kb of genomic DNA in 16 chromosomes that are thought to occur from a whole-genome duplication event of 8 ancestral chromosomes (Kellis et al., 2004).

Budding yeast is a single cellular microorganism and resembles bacteria in terms of growth, maintenance, and suitability for applications of molecular genetic methods. At the same time, as a eukaryote, yeast shares the fundamental cellular properties of eukaryotes which makes yeast applicable for eukaryotic studies (Botstein & Fink, 1988). Budding yeast provides an effective research tool in cost-effectiveness and usability because it is easy to handle and proliferates rapidly. As sufficient nutrients are provided, the doubling time of budding yeast is around 100 min (Herskowitz, 1988).

More importantly, budding yeast provides an easy model to analyze genetic studies because it is easily manipulated. Budding yeast has a high recombination rate, enabling easiness in genetic manipulations. With a high frequency, budding yeast can be transformed with PCR-made DNA fragments such as cassettes that can be exchanged with endogenous genes in the chromosomal DNA (Gardner & Jaspersen, 2014; Knop, Siegers, et al., 1999). The easiness of gene editing, such as gene deletions and N- terminal and C- terminal epitope tagging of proteins, makes *S. cerevisiae* a critical model organism as it has been commonly used in the history of biological sciences (Duina et al., 2014). It can be transformed with plasmids

containing genes from yeast and other organisms (Hanson, 2018; Osborn & Miller, 2007). For example, the human version of a gene can be transformed to a yeast strain with a loss of function mutation. This provides a reversal of the phenotype, which indicates the similar function of the gene in both organisms.

Budding yeast provides a great tool to study mutant phenotypes to understand gene functions in detail. Most commonly, temperature-sensitive (*ts*) mutants are used to study the role of essential genes. This type of mutant contains a specific type of mutation in the gene of interest that does not affect the product in permissive temperatures. However, at restrictive temperatures, this type of mutation leads to a non-functional or drastically reduced phenotype (Hartwell, 1967).

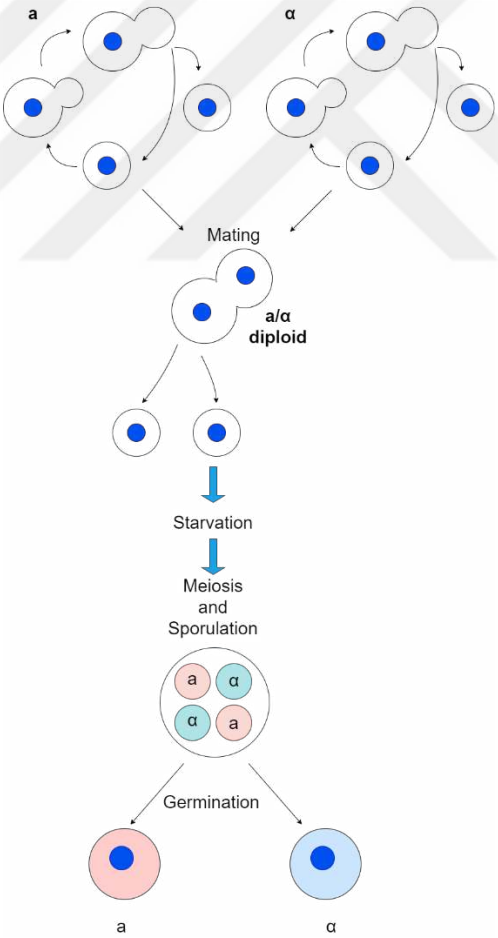

Figure 1. 1: Life cycle of budding yeast. In the haploid form budding yeast contains either Mat-a or Mat-α. It can undergo mitosis in both haploid and diploid form (Duntze et al., 1970). This figure is adapted from Morgan et al. (Morgan, 2007)

Many aspects of the cell cycle of *S. cerevisiae* make it a valuable tool to study the cell cycle. One of them is that *S. cerevisiae* can undergo mitosis in both haploid and diploid forms. In the haploid form, *S. cerevisiae* contains either Mat-a or Mat-α mating types (Duntze et al., 1970). Under nutritionally and environmentally efficient conditions, cells maintain their haploid state. Maintaining both diploid and haploid forms gives an advantage in which the haploid forms enable isolation of recessive mutations, and the diploid form allows the analysis of the complementation (Hartwell, 1974).

Moreover, using a light microscope, one can easily estimate the cell cycle stage of *S. cerevisiae.* A cell that has no bud is in the G1 phase. The daughter cell can be recognized at the early stages of mitosis as the bud formation on the mother cell's surface. As bud starts to emerge, the cells go through the G1/S transition. Cells with a small bud are either in G1/S transition or S or G2 phases. As the cells progress further from G1/S, the bud grows bigger and bigger. The ratio between bud size and parent cell increases positively during the cell cycle. Thus, the daughter and mother cell ratio provides a guide to assess the cell cycle stage (Hartwell et al., 1974).

Apart from that, *S. cerevisiae* can be synchronized during the cell cycle and arrested at specific stages easily by using chemicals, drugs, and activation or depletion of certain genes. For example, mating hormone, alpha factor, is used to arrest Mat-a type cells at the G1 phase (Udden & Finkelstein, 1978). Also, the expression of a specific type of Clb2, which lacks its destruction site, makes the cells arrest at anaphase with elongated, intact spindles and separated chromosomes (Irniger et al., 1995).

1.2 The cell cycle of *S. cerevisiae*

Duplication and partition of genetic information from mother cells generate a new generation called daughter cells. The cell cycle is highly regulated to perform this event with high accuracy. The cell cycle is divided into four intervals which are G1, S, G2, and M.

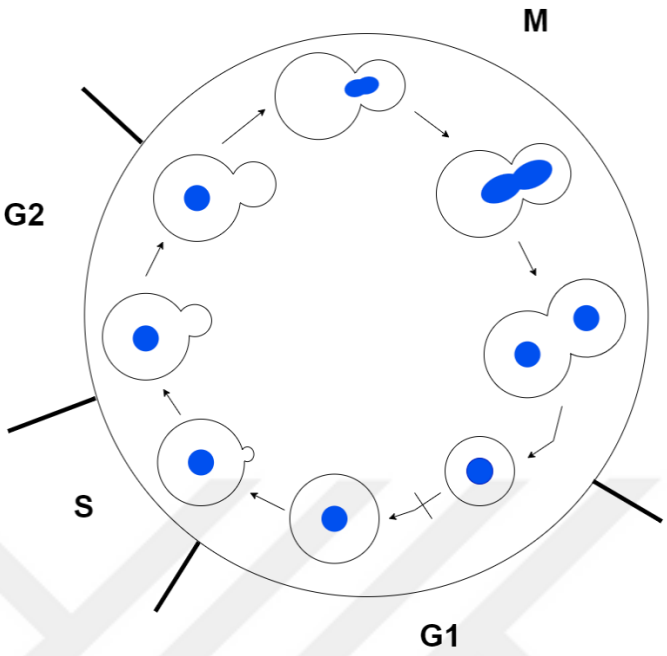

Figure 1. 2: The cell cycle of the budding yeast. The budding yeast cell cycle is composed of 4 main stages. G1, S G2 and M.

Budding yeast cell division takes place asymmetrically (Hartwell & Unger, 1977; Lew & Reed, 1995). G1 is the stage where growth signals are received, and the decision to divide is given. For the replication to start, the cell must reach a critical size (Johnston et al., 1979; Johnston et al., 1977). Later, G1 phase cells enter the S phase, where duplication events occur. During the S phase, duplication of genetic information occurs, and then cells get ready for mitosis in the G2 phase. S phase constitutes 25% of the cell cycle. Moreover, in this stage, spindle plaques separate to form the spindle (Hartwell, 1974). Bud emergence occurs in similar timing as these duplication events (Lew & Reed, 1995). During bud emergence, actin cortical patches polarize to the bud site, indicating that they may have a role in bud growth (Amberg, 1998). As budding starts, the daughter cell starts to grow with the bud. Later, the M phase, where the division of the cells' nucleus into two equal cells, takes place in mitosis. During the M phase, the cell goes through four distinct phases: namely prophase, metaphase, anaphase, and telophase. During prophase, duplicated chromosomes pair and condense and form sister chromatids (Guacci et al., 1994). Sister chromatids are held together by a complex called Cohesin. The Cohesin complex regulates the establishment and separation of sister

chromatids (Michaelis et al., 1997). Moreover, during this stage, spindles emerge from centromeres, spindle pole bodies in yeast. Later, spindles attach to sister chromatids from their kinetochores and align them during metaphase. Cohesion between sister chromatids holds sister chromatids together, resisting against the spindle forces. However, in early anaphase Cohesin complex is cleaved from its kleisin subunit (Scc1 in budding yeast) by Separase (Esp1), enabling its removal from sister chromatids (Uhlmann et al., 2000). Separase protease is held inactive by Securin (Pds1) at the earlier stages of mitosis. Later Securin is degraded by APC/Cdc20 complex to activate the Separase (Ciosk et al., 1998). These events lead to the separation of sister chromatids into opposite poles by the forces applied by spindles. Regulation of these events is highly crucial for the cells to obtain only one copy of the duplicated DNA. As chromatids are pulled to opposite poles, the cell enters telophase, where condensed chromosomes decondense. Starting at the late anaphase and during telophase, cytokinesis occurs. Cytokinesis is the separation of the duplicated cell into two by the separation of the plasma membrane in various ways (Schroeder, 1968).

Cells go through either closed or open mitosis depending on the nuclear envelope disassembly. In open mitosis nuclear envelope disperses; however, in closed mitosis nuclear envelope stays intact (Newport & Forbes, 1987). Thus, if the cell goes through closed mitosis nuclear envelope does not disassemble at prophase and reassemble in the telophase. Budding yeast goes through closed mitosis (Hartwell, 1974).

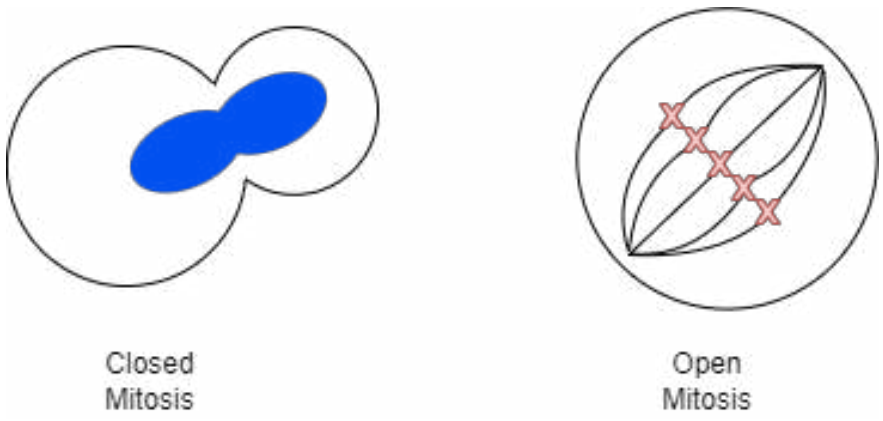

Figure 1. 3: Open and Closed mitosis. In the open mitosis, the nuclear envelope disperses but in the closed mitosis, the nuclear envelope remains intact (Newport & Forbes, 1987).

A family of proteins called cyclin-dependent kinases (CDKs) is key elements of tight cell cycle regulation. CDKs are proline-directed kinases that phosphorylate serine or threonine

residues (Langan et al., 1989). The regulation of CDKs is highly crucial for proper cell division. They interact with other proteins called cyclin, and this active complex regulates the cycle in an oscillatory manner. Cyclins have a conserved domain called the “cyclin box” (Kobayashi et al., 1992). During the cell cycle, CDK levels remain unchanged, but cyclins periodically degrade and are produced, enabling the CDK activity regulation. cyclins provide substrate specificity to the CDKs (Bhaduri & Pryciak, 2011). Another regulation of the CDK/cyclin activity is made by CDK inhibitors (CKIs) (Mendenhall, 1993).

In *S. cerevisiae*, the main CDK is the Cdc28. Previously the search for identification of cell cycle genes showed that cdc28 mutants show a deficiency in START signal of cell division (Reid & Hartwell, 1977; Wittenberg & Reed, 1988). Cdc28 can interact with two families of cyclins, CLNs and CLBs. While the CLB family takes place for S, G2, and M phases, interaction with the CLN family works in the G1 phase (Jimenez et al., 2015). A family of CLNs: namely Cln1, Cln2, and Cln3, take parts in triggering the START signal of mitosis as they are G1 specific cyclins. For proper START of the cell cycle, at least one of them is necessary as a triple mutant of these genes shows lethality (Richardson et al., 1989). SBF (SCB binding factor) and MBF (MluI binding factor) regulate the family of genes transcribed at the late G1 phase. Upon activation of SBF and MBF-mediated transcription by Cln3-Cdc28 kinase, Cln1 and Cln2 accumulate through a positive feedback loop and start the yeast cell cycle (Dirick et al., 1995).

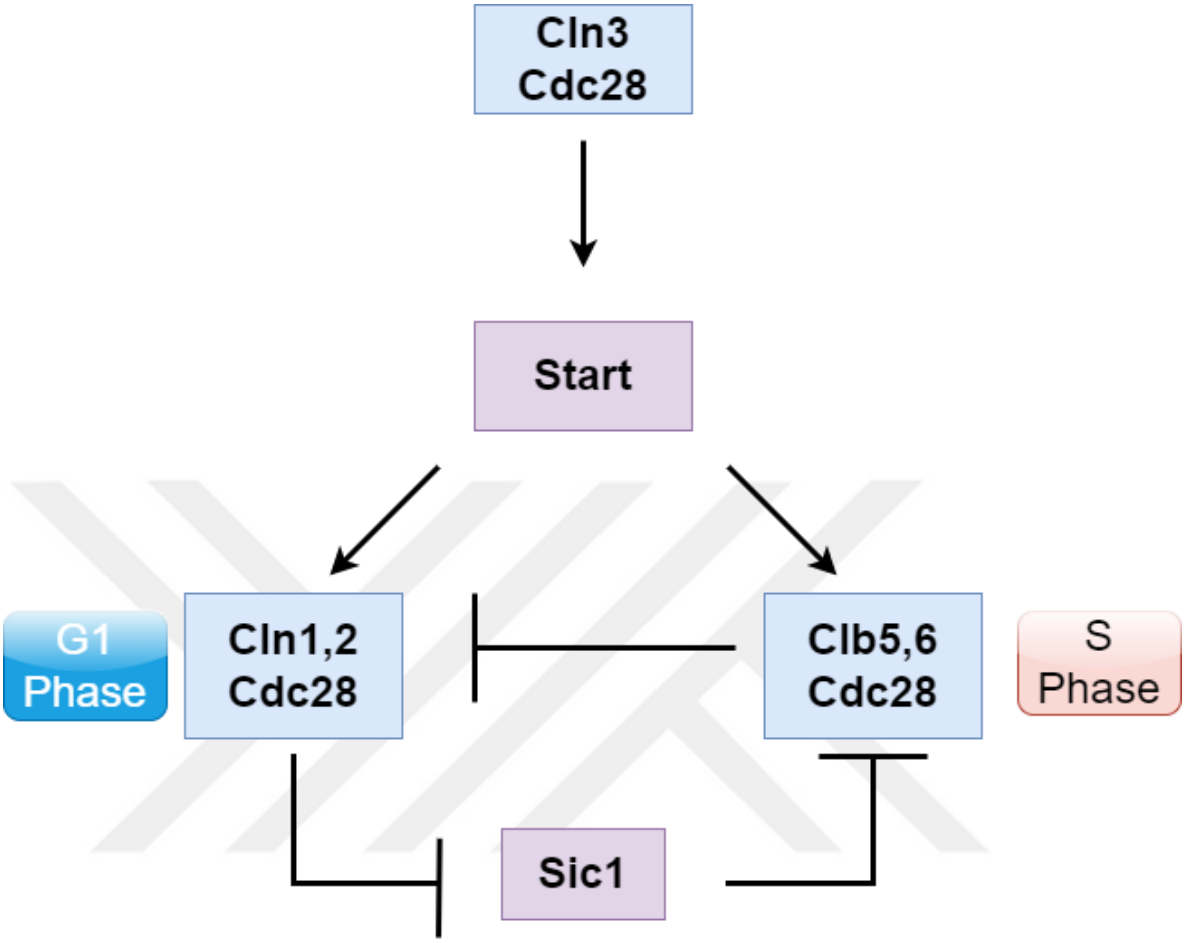

Figure 1. 4: Budding yeast Cyclin CDK regulation. The Cyclin CDK regulation provides cell cycle machinery control. The S phase cyclins prevent re-initiation of the replication. Even though they are expressed simultaneously, S phase cyclins are kept inactive by Sic1 until the activities of G1 Cyclins. This figure is adapted from Mendenhall et al. (Mendenhall & Hodge, 1998)

Clb5 and Clb6 are S-phase cyclins as they prevent re-initiation of replication origins. Even though Clb5 and Clb6 are expressed simultaneously with Cln1 and Cln2, they are kept inactive by Sic1 until the Cln1-Cdc28 and Cln2-Cdc28 activities (Schwob et al., 1994).

Clb1, Clb2, Clb3 and Clb4 are M phase cyclins. They have roles in spindle formation and elongation (Fitch et al., 1992). They inhibit mitotic exit until the cell division is over (Bloom & Cross, 2007). Their levels fall after the mid-mitosis as they are destructed by the APC (Anaphase promoting complex) activity (King et al., 1996; Rudner & Murray, 2000).

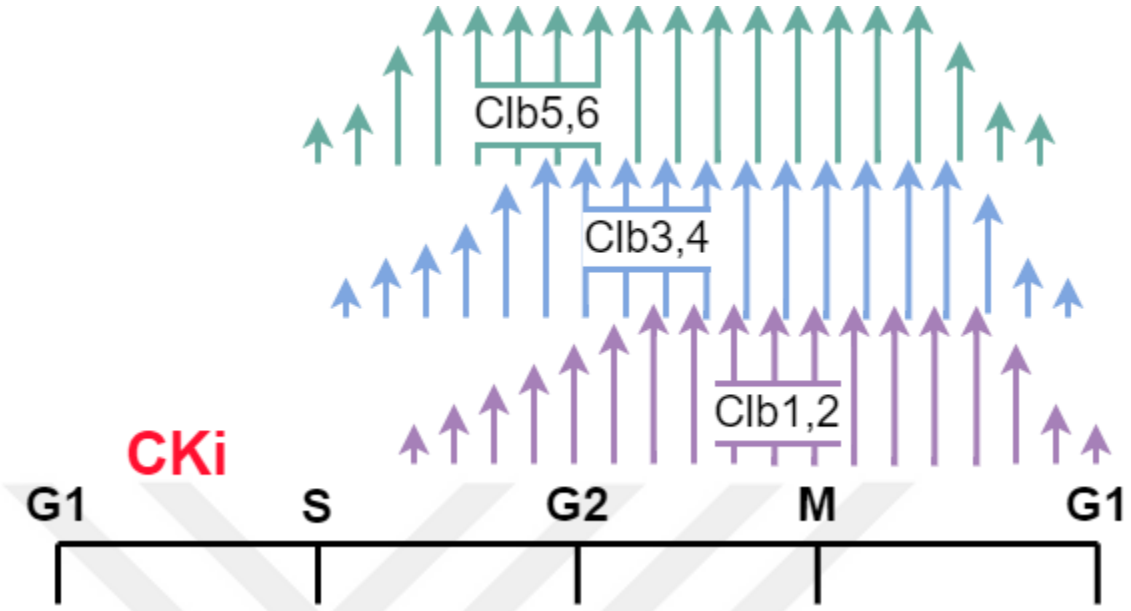

Figure 1. 5: Budding yeast cyclin waves. Cyclin CDK activities are tightly regulated for a proper cell cycle. This figure is adapted from Barberis et al. (Barberis, 2021)

For a proper cell division, the cyclin-CDK activity must be tightly regulated. Various mechanisms regulate Cyclin-CDK activity; transcription of the cyclins, degradation of the cyclins, cyclin-CDK inhibition (CKIs), and cyclin localization (Bloom & Cross, 2007). CKIs are cyclin-CDK inhibitory proteins as their binding results in inhibiting the complex. Sic1 inhibition of Clb5 and Clb6 at the S phase is an example of CKIs inhibition (Schwob et al., 1994). Moreover, differences in the cyclin localization provide cycling-specific targeting of the substrates. For example, G1 cyclin Cln3 localization is nuclear, yet G1 cyclin Cln2 is cytoplasmic. This enables substrate specificity to regulate different substrates (Miller & Cross, 2000). Ubiquitin-mediated proteolysis of cyclins is another regulatory event for cyclin-CDK activity (Seufert et al., 1995). G1 cyclins Cln1 and Cln2 and S cyclin Clb6 are degraded in an SCF-dependent mechanism (Berset et al., 2002; Jackson et al., 2006). S cyclin Clb5 and M phase cyclins Clb1, Clb2, Clb3, and Clb4 are degraded by the activity of the APC complex (Rudner & Murray, 2000; Shirayama et al., 1999). Destruction of S phase and M phase cyclins are essential for proper cell division.

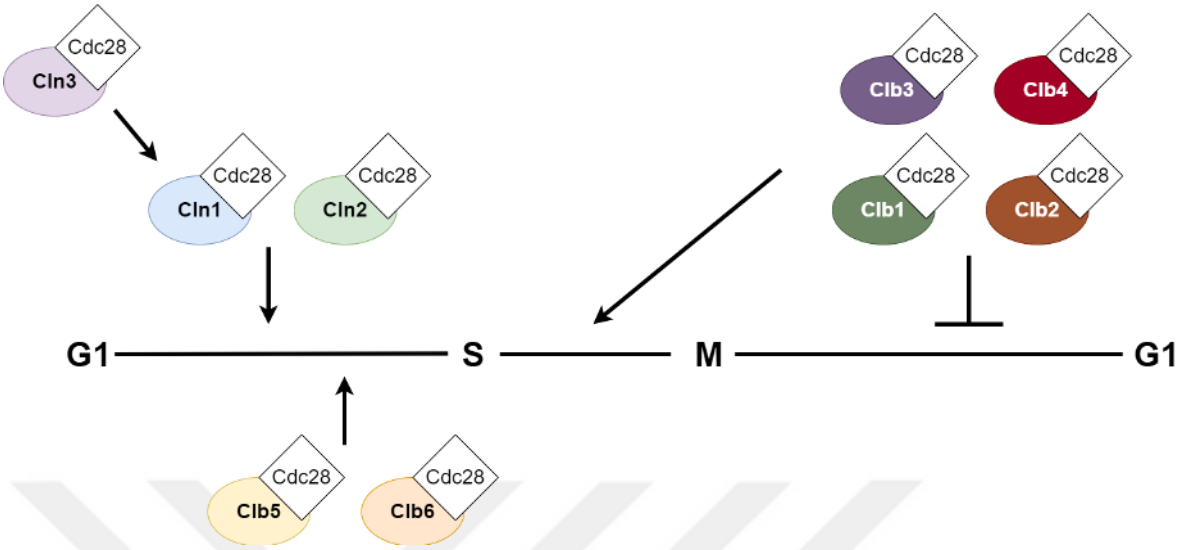

Figure 1. 6: Cyclin dependent regulation of the cell cycle. Cdc28 is the main CDK in budding yeast. Different cyclins regulate cell cycle in complex with the CDK. Even though CDK remains through the cell cycle, the cyclins change. This figure is adapted from Bloom et al. (Bloom & Cross, 2007)

1.3 Cell Cycle Regulation Mechanisms

To obtain healthy progeny, cells must duplicate without any errors in the process. Various mechanisms control the proper cell division to avoid problems. These mechanisms detect the mistakes and activate other mechanisms to fix them while they halt the cell cycle for the cell to correct the problem. Control mechanisms that control the proper division are called Checkpoints (Hartwell & Weinert, 1989). If a problem is detected, the cell must fix the problem to complete the mitosis. If the problem cannot be repaired, the cell is destined for cell death. Mechanisms in the cell cycle checkpoints safeguard the cell division's integrity and are crucial for healthy progeny.

As mentioned before, the cell cycle comprises four phases: G1, S, G2, and M phases. The checkpoint mechanisms control the events conducted in the previous phases, either pausing the cell division in case of a mistake or letting the cell enter the next phase.

G1/S is the first cell cycle checkpoint. Here, the cell must have reached a significant size in optimum environmental conditions to give the START signal for DNA and other components replication (Hartwell & Unger, 1977; Nurse, 1975). In this phase, the cell commits to mitosis. In the mammalian cells, START is referred to as Restriction Point (Zetterberg et al., 1995). In budding yeast, START signal depends on a CLN family protein; Cln3, and its interaction

with yeast CDK; Cdc28 (Nasmyth, 1993). As cells reach a critical size, Cln3 activates two transcription mechanisms called SBF and MPF to transcribe other G1 cyclins named Cln1 and Cln2, S phase cyclins Clb5 and Clb6, and many different cycle-related genes (Futcher, 1996). This process pushes the cell to START mitosis (Schneider et al., 2004).

Multicellular eukaryotes that are not dividing are in the G0 phase and can be activated to enter G1 via extracellular components (Pardee, 1989). In the presence of mitogens, the cells can either enter to cell cycle via passing the restriction point or go back to the G0 quiescent state (Planas-Silva & Weinberg, 1997). In the presence of mitogens, G1 cyclin-CDKs get activated and pushes the cells to enter the S phase. G1 cyclin-CDKs are the limiting factors for passing the restriction point (Connell-Crowley et al., 1998).

DNA damage is the second cell cycle checkpoint. It is a surveillance mechanism against the errors that may happen during DNA replication. These errors may occur from various external and internal reasons. For example, carcinogens, overexpression of oncogenes, ionizing radiation, attrition of telomeres, UV radiation, etc. In this checkpoint, if there is an error cell cycle is halted so that the cell has time to fix the problem before going to the subsequent phases. There are specific DNA damage responses depending on the type of lesion on the DNA. The main role of the checkpoint is to maintain CDKs inactivated until the lesion is repaired (Noguchi et al.).

One of the pathways in this process is the highly conserved Chk1 pathway. Chk1 is profoundly activated in the S and G2 phases as it is needed in the initiation of the checkpoint and the maintenance of the checkpoint (Latif et al., 2004). In mammalian cells, activation of this pathway involves activation of ATR (Mec1 homolog in budding yeast) and ATM (Tel1 homolog in budding yeast) protein kinases. These kinases are termed as PIKKs because they share homolog sequences with PI-3Ks (O'Connell et al., 2000). Other than PIKKs, activation of Chk1 requires some other proteins; a PCNA related complex Rad9-Hus1-Rad1(9-1-1) (MacDougall et al., 2007). PIKKs phosphorylates several other checkpoint members, including ATRIP, PCNA-related complexes, and RFC (Replication factor complex) members (O'Connell et al., 2000). In case of a lesion on the DNA, an ssDNA-binding protein replication protein A (RPA) comes to the lesion, and it triggers the Ckh1 to be activated by ATR (O'Connell & Cimprich, 2005). Checkpoint-related proteins and ATR assemble onto the RPA covered damage point. The activated Chk1 is released to maintain the CDK Cdc2

inactive in its Y15 site phosphorylated. To maintain this inhibitory phosphorylation, Chk1 phosphorylates Wee1 kinase and Cdc25 phosphatase (Raleigh & O'Connell, 2000). After the error is fixed, Chk1 gets dephosphorylated by Type I phosphatases, and mitosis resumes (den Elzen et al., 2004).

RAD9, the first checkpoint gene to be defined, works as an adaptor to couple activation of Mec1 (upstream kinases) and Rad53 and Ckh1 (downstream effector kinases) (Melo & Toczyski, 2002; Weinert & Hartwell, 1988). Rad53 gets activated via phosphorylation, and it is released to the nucleus to transmit the signal. Cdc5 Polo-like kinase is one of the downstream targets of Rad53. Rad53 inhibits anaphase entry and mitotic exit via the Cdc5 pathway (Sanchez et al., 1999). Another downstream target of Rad53 is a Dun1 protein kinase. Dun1 protein kinase regulates the transcription of RNR (Ribonuclease Reductase) genes, transcriptional induction of DDR genes, and has roles in NHEJ (de la Torre Ruiz & Lowndes, 2000).

Pds1 is an anaphase inhibitor, and in the presence of DNA damage, it gets phosphorylated in a Mec1 and Rad9 dependent manner. Pds1 and Rad53 work in parallel branches in DNA damage response because the phosphorylation is Rad53 independent. In the presence of DNA, damage Pds1 is involved in implementing the mitosis arrest (Cohen-Fix & Koshland, 1997).

Moreover, in yeast, there is another mechanism regulating the firing of replication origin. Mec1 phosphorylated Mrc1 has a role in the activation of Cds1 (Chk2 homolog), which functions as a checkpoint effector that delays DNA replication (Tanaka & Russell, 2001).

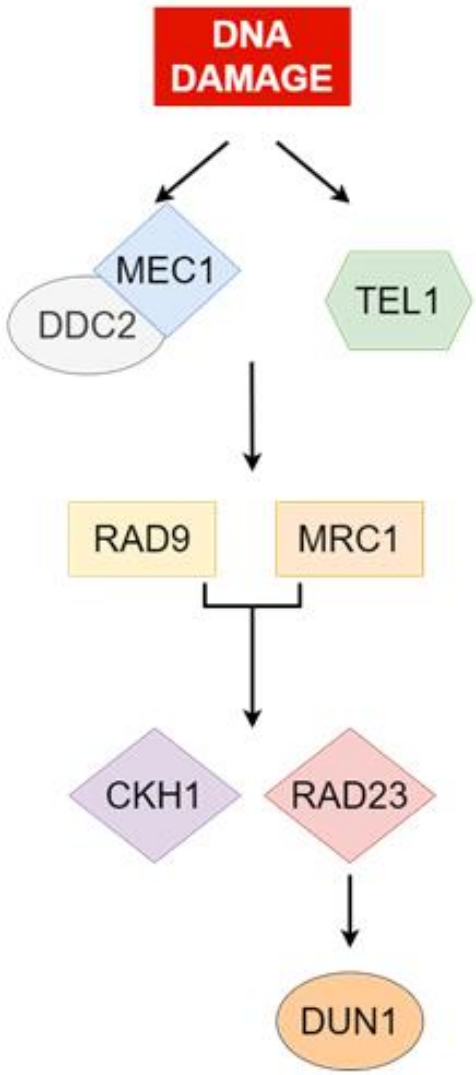

Figure 1. 7: DNA damage response in budding yeast. DNA damage checkpoint is a surveillance mechanism against the errors that may happen during DNA replication. This figure is adapted from Zhou et al. (Zhou et al., 2010)

Spindle Assembly Checkpoint, M-phase checkpoint, is the third checkpoint whose primary role is to monitor proper binding of spindles to the kinetochores. If spindles are not correctly attached to the kinetochores, kinetochores activate the SAC network to halt the progression. SAC is activated in case a kinetochore is not attached to a spindle. Kinetochores are complex structures that are assembled at the centromeres of each sister chromatid. Some of the proteins in this complex such as RZZ have role in recruiting SAC components such as Mad1 and Mad2. SAC components (Karess, 2005).

SAC arrests the cells at metaphase-anaphase transition by acting against the APC/C complex (Anaphase Promoting Complex/Cyclosome) that it cannot target cyclin B1 and Securin for ubiquitination. At the anaphase onset Securin (Pds1) is targeted to proteosome to remove the inhibition on Separase (Esp1). As Separase is active, it cleaves the Scc1 subunit of the Cohesin complex. Cleavage of Scc1 subunit triggers unloading of the Cohesin from sister chromatids which leads to separation of the sister chromatids and pulling to the opposite poles by spindles (Ciosk et al., 1998). SAC inhibition of the activity of the APC/C complex arrest the cells in a way that sister chromatids cannot be separated (Yu, 2002). SAC targets APC/C by inactivating its activator Cdc20.

There are two forms of Mad2: O-Mad2 (open) and C-Mad2 (closed) (Mapelli et al., 2007). Mad1-C-Mad2 is recruited to the unattached kinetochores as a first step of signaling of SAC. C-Mad2 is converted to O-Mad2 which can bind the Cdc20. However, it is not enough to maintain the SAC arrest. Later O-Mad2 is recruited to Mad1-C-Mad2. Cdc20 is captured by Mad2 (Luo et al., 2000). It is the first step for formation of mitotic checkpoint complex. BubR1 and Bub3 are other components of this complex (Sudakin et al., 2001). Cdc20 is not only kept inactive, but it is also targeted for degradation by APC/C (Nilsson et al., 2008). Thus, an empty kinetochore leads to inhibition of the APC/C complex.

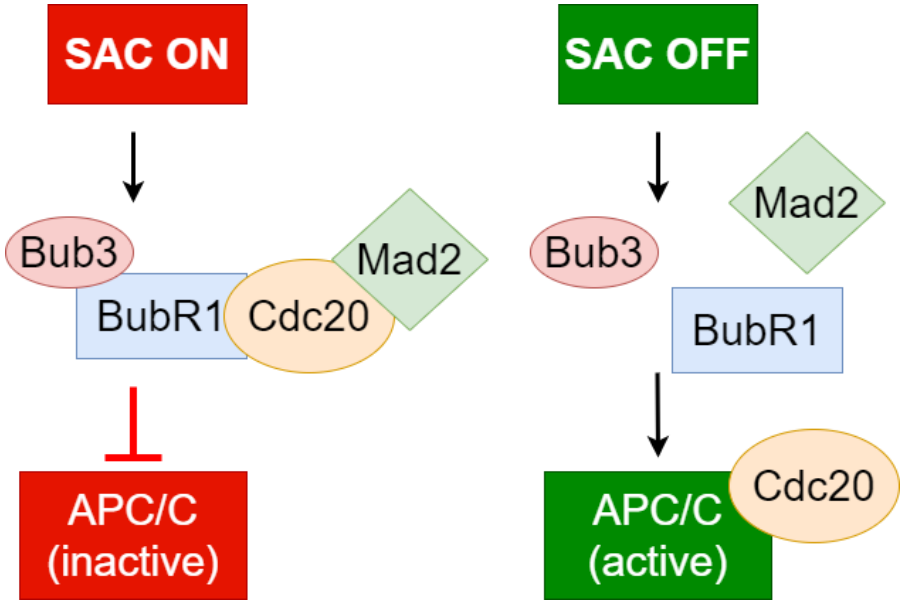

Figure 1. 8: Spindle Assembly Checkpoint. Spindle assembly checkpoint is the M phase checkpoint. It monitors proper binding of spindles to the kinetochores.

Budding yeast cells divide asymmetrically and correct positioning of the mitotic spindle along mother-daughter axis is critical for the fidelity chromosome segregation. SPOC (Spindle Position Checkpoint) is another checkpoint mechanism that safeguards the spindle positioning along the mother-daughter axis. To maintain the correct alignment, budding yeast developed two microtubule associated pathways; namely Kar9 and Dynein related pathways (Eshel et al., 1993; Miller & Rose, 1998). In response to mutations affecting the microtubule associated pathways, cells misalign their spindles and SPOC pathway is the checkpoint mechanism safeguarding this error. In budding yeast, cleavage plane is determined at the G1/S stage by bud neck. Thus, where the cytokinesis will occur is pre-determined. For correct ploidy, the cell must maintain spindle positioning correctly (Lew & Burke, 2003).

If the spindle is misaligned SPOC gets activated to inhibit MEN (Mitotic Exit Network) which regulates the mitotic exit progression. Bfa1-Bub2 GAP complex is the guardian of this mispositioning. As the GAP complex gets activated, it acts against the Tem1 GTPase, which is the upstream of MEN, and keeps it inactive (Geymonat et al., 2002). Thus, mitotic exit progression is halted until the problem is fixed.

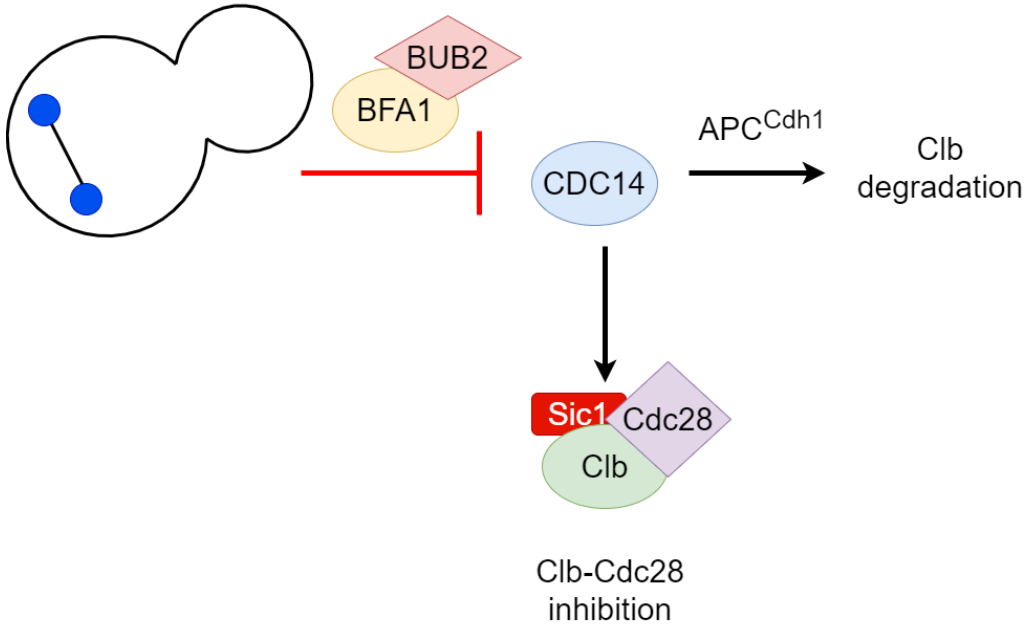

Figure 1. 9: Spindle Positioning Checkpoint. Correct positioning of the mitotic spindle along mother-daughter axis is critical for budding yeast. SPOC pathway is the checkpoint mechanism safeguarding this process.

1.4 Cdc14 Phosphatase

Cdc14 phosphatase acts as a key regulator of mitosis and controls events in the cell such as chromosome compaction, segregation, transcription, cytokinesis, autophagy, centrosome duplication, and many others. Cdc14 family of phosphatases shows extraordinary evolutionary conservation. The N-terminal of Cdc14 is highly conserved and contains two domains essential for the enzyme's enzymatic activity; A domain shows peptide substrate specificity, and B domain is the catalytic domain (Gray et al., 2003). The C-terminal of Cdc14 is where the nuclear export sequence is located (Mohl et al., 2009). NLS and NES regions of Cdc14 are significant for regulating Cdc14 because Cdc14's localization in the cell affects its activity (Mohl et al., 2009). Before its release, Cdc14 is kept sequestered in the RENT (regulator of nuclear silencing and telophase) complex in the nucleolus by Net1/Cfi1 (Shou et al., 1999). During the cell cycle, the amount of Cdc14 remains; however, its localization and activity are changed by its interaction with Cfi1 (Visintin et al., 1999). Cdc5 is suggested to have a role in both release and re-sequestration by Net1. CDK, Cdc5, and Cdc14 execute an autonomous oscillator cycle that regulates Cdc14 activity by controlling its localization (Manzoni et al., 2010).

Cdc14 has essential regulatory roles in regulating the cell cycle and exit from mitosis in budding yeast. Cdc14 is essential to reverse CDK phosphorylation events to inhibit mitotic cyclins. Cdc14 has many substrates which it dephosphorylates to promote the mitotic exit. Cdc14 dephosphorylates Sic1 and the transcription factor Swi5, responsible for Sic1 production, leading to its stabilization and accumulation of Sic1 protein (Visintin et al., 1998). Moreover, Cdh1/Hct1 is another target of Cdc14. Cdh1/Hct1 phosphorylated at its CDK consensus sites by Cdc28 to inhibit its association with APC/C complex. Cdc14 dephosphorylates Cdh1/Hct1 promotes its association with the APC/C complex. The dephosphorylation is an event that leads to cyclin destruction (Jaspersen et al., 1999). All these dephosphorylation events lead to resetting the cell cycle back to its G1 state.

Cdc14 release occurs in two steps. Cdc14 is transiently released by the FEAR network in early anaphase; then, it is fully released and sustained in late anaphase by MEN. Its full release is necessary for the initiation and progression of the Mitotic exit (Stegmeier & Amon, 2004). However, auxin-inducible models of Cdc14 depletion show that Cdc14 depletion has

no effects on the kinetics of mitotic exit and CDK substrate dephosphorylation. Yet, it causes detrimental separation defects, which leads to lethality. Thus, additional phosphatases might contribute to dephosphorylation events and regulation of mitotic exit in budding yeast (Powers & Hall, 2017). In terms of mitotic exit, the primary function of Cdc14 activity is acting as a switch for positive-feedback mechanism yet, a small fraction of Cdc14 is sufficient to trigger this mechanism. Additionally, for the proper order of CDK substrate dephosphorylation, Cdc14 may have intrinsic roles in regulating this process.

Apart from its functions in the mitotic exit network, Cdc14 has many roles in the cell division progression. Cdc14 has roles in spindle midzone assembly, chromosome arm recoiling, rDNA segregation, and nuclear positioning. When Cdc14 is released, its activity downregulates CDK phosphorylation, which promotes telomere and rDNA condensation by inhibiting RNA polymerase to facilitate proper segregation of chromosomal regions, which primes the MEN pathway (Clemente-Blanco et al., 2011; Tomson et al., 2006). Since rDNA condensation and MEN are regulated by the same phosphatase, cells can initiate nuclear compaction only when the Cdc14's activity is dynamically obtained. Cdc14 regulates rDNA segregation via Condensin related pathways (Sullivan et al., 2004). Moreover, Cdc14 phosphatase has roles in DNA damage response. In budding yeast, Cdc14 release from nucleolus is stimulated in response to DNA damage. It anchors DNA lesions to the spindle pole bodies (SPBs), facilitating their repair (Villoria et al., 2017). Furthermore, Cdc14 works in signaling pathways such as High-Osmolarity Glycerol Pathway (HOG) and Target of Rapamycin Pathway (TORC1) (Kondo et al., 2018; Reiser et al., 2006). Thus, it is highly important in terms of stress response and response to environmental signals, and it can induce autophagy under starvation by inactivating TORC1. However, having multiple crucial roles in regulating the cell cycle and its regulation, Cdc14's most conserved role is the control of cytokinesis to ensure proper segregation of dividing cells. Spindle midzone assembly is another mechanism that Cdc14 has a role in. It regulates spindle midzone assembly via Sli15-Ipl1 (Pereira & Schiebel, 2003). Localization of Cdc14 to bud neck during cytokinesis and its identified substrates involved in cytokinesis and septation is crucial in budding yeast. Thus, normal levels of Cdc14 are necessary for proper cytokinesis. (Powers & Hall, 2017)

Moreover, Cdc14 has role in regulation of the SPB duplication. High CDK activity inhibits the duplication of SPBs via multiple phosphorylation of one of the critical components of the

duplication. This inhibitory phosphorylation limits the SPB duplication events to once in every cell cycle. Cdc14 removes the inhibitory phosphorylation made by CDK1 as it is released at the anaphase. It leads the promotion of the SPB replication (Avena et al., 2014). The oscillation between CDK1 and Cdc14 activity restrict the duplication of the SPB per cycle (Ruthnick & Schiebel, 2016).

1.5 Spindle Pole Body

In *S. cerevisiae*, Spindle pole bodies (SPB) are organelles that are embedded in the nuclear envelope and organizes the cytoplasmic, mitotic and meiotic microtubules (Rout & Kilmartin, 1990). The yeast SPB is the equivalent of the mammalian centrosomes as they are names as Microtubule Organizing Centers (MTOCs). They can nucleate the microtubules from tubulin subunits (Rose et al., 1993). Mitotic spindle mediates the proper segregation of the sister chromatids (Inoue, 1981). Microtubules are polar structures that have minus and plus ends which enable their directional growth (Bergen & Borisy, 1980). Microtubules attach to the kinetochores through their plus end which is nucleated by SPBs. Microtubule depolymerization provides the energy for the movement of chromosome pulling to the opposite poles by microtubules (Koshland et al., 1988). Like centrosomes, SPBs duplicate once in a cell cycle and it uses mother SPB as a platform produce the daughter SPB (Ruthnick & Schiebel, 2016).

The SPB provides organization of two different microtubule arrays: the cytoplasmic microtubules and nuclear microtubules. The cytoplasmic microtubules are directed to the cell cortex, and they are important for positioning of the nucleus (Shaw et al., 1997). Cytoplasmic microtubules have role in regulating the proper orientation of the mitotic spindle (Carminati & Stearns, 1997). The alignment of the nucleus and mitotic spindle is important to maintain the mother to bud axis for proper cell division. Moreover, they also have role in nuclear migration during mating, reorientation of SPB after cytokinesis (Knop, Pereira, et al., 1999). On the other hand, the nuclear microtubules are directed to the nucleoplasm as they originate at the nuclear side of the SPB. Nuclear microtubules have role in SPB separation, chromosome segregation, mitotic and meiotic spindle formation, and DNA damage repair (Jacobs et al., 1988; Oshidari et al., 2018)

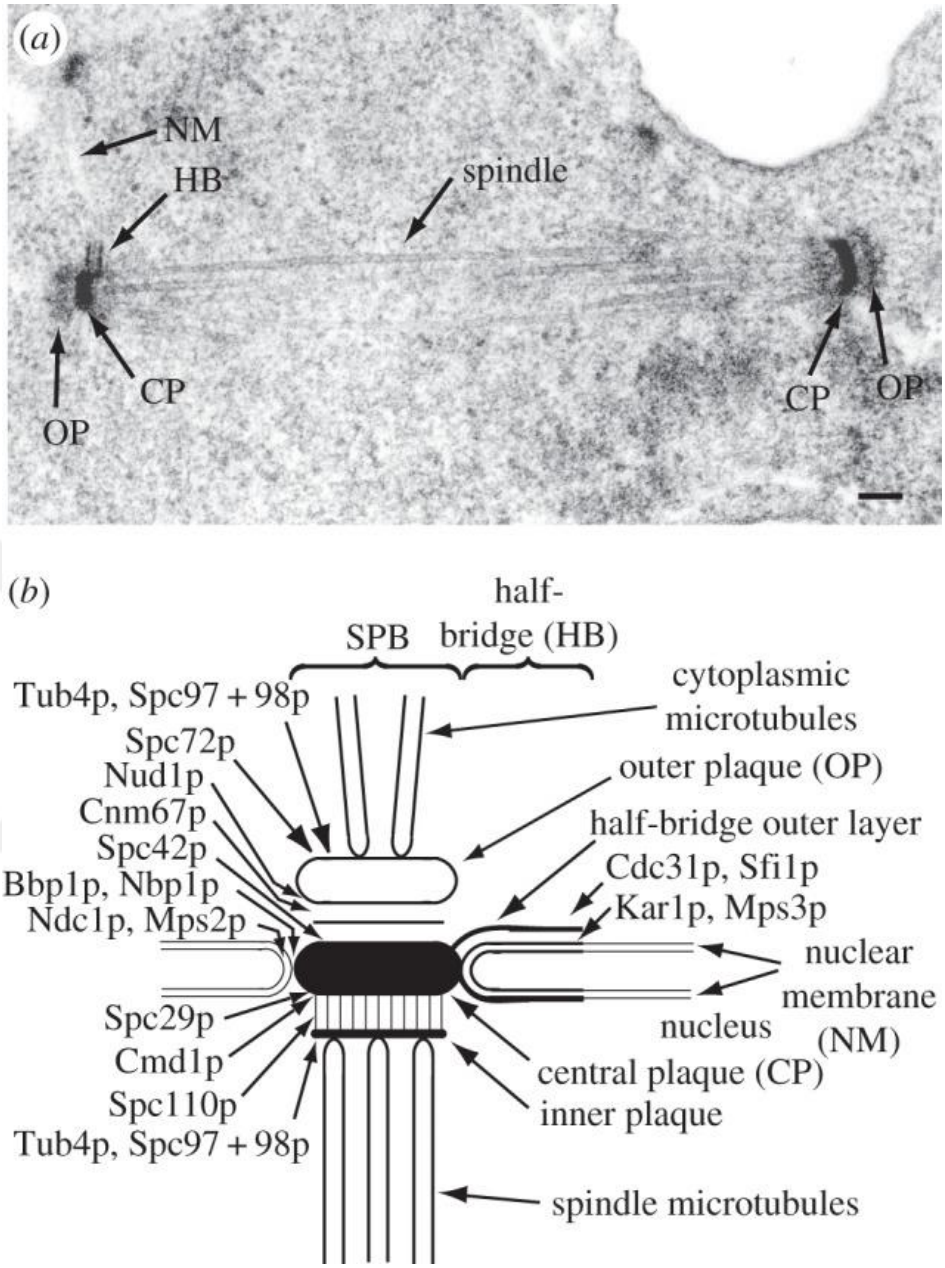

Figure 1. 10: Spindle pole body structure. Spindle pole body electron microcopy image (a) and the components of the SPB (b) This figure is taken from Kilmartin et al. (Kilmartin, 2014).

1.6 Spindle Pole Body Structure

Electron microscopy studies has been utilized to study the SPB structure. SPBs are cylindrical organelles that are consist of an outer plaque which faces cytoplasm and interacts with cytoplasmic microtubules, an inner plaque which faces the nuclear membrane and interacts with nuclear microtubules and a central plaque which spans the nuclear membrane

(Jaspersen & Winey, 2004; Moens & Rapport, 1971). Later studies using cryo-EM and electron tomography added two more layers to our knowledge as first and second intermediate layers (O'Toole et al., 1999).

SPBs are dynamic structures in that they change during cell cycle and mating (Bullitt et al., 1997; Yoder et al., 2003). SPB structure is composed of many components. The central core of SPB is mainly composed of a coiled-coil protein namely Spc42 (Donaldson & Kilmartin, 1996; Snyder, 1994). The N-terminus of the Spc42 interacts with other two coiled coil proteins: Spc29 and Spc110 which are localized to the nuclear face of the SPB. Spc29 links central plaque protein Spc42 and inner plaque protein Spc110 (Elliott et al., 1999). Spc100 acts as a spacer protein connecting inner and central plaque. Cmd1 (Calmodulin) is another interaction partner of Spc110 (Spang et al., 1996). Spc110 binds to Spc29 and Cmd1 through its C-terminus (Stirling et al., 1994). Moreover, Calmodulin binding site affects Spc110 interaction with Spc29 (Elliott et al., 1999). The N-terminus of Spc110 interacts with Spc98, which is a γ tubulin binding protein. This interaction links γ tubulin (Tub4) to the SPB complex and regulates the Spc110 and Spc97 interaction which is another γ tubulin binding protein (Nguyen et al., 1998). γ tubulin is involved in microtubule nucleation (Marschall et al., 1996). The C-terminus of Spc42 which faces the cytoplasm, interacts with the Cnm67 through its C-terminus (Adams & Kilmartin, 1999). Cnm67 functions as a spacer between first and second intermediate layers by dimerization (Schaerer et al., 2001). Cnm67 interacts with an outer plaque protein called Nud1. From their C- terminuses, Nud1 interacts with another outer plaque protein called Spc72 whose N-terminus interacts with the γ tubulin complex (Gruneberg et al., 2000).

1.7 Spindle Pole Body Duplication

Daughter SPB is produced from mother SPB once in every cell cycle. The daughter SPB is produced next to the mother SPB using the mother as a template in the process. Duplication process starts from the half-bridge which is a one-sided extension from the central plaque at the early G1 (Byers & Goetsch, 1975). The half-bridge contains: Cdc31 (yeast centrin), Sfi1and Kar1 proteins at its cytoplasmic site and Mps3 proteins at its nuclear site (Biggins & Rose, 1994; Jaspersen et al., 2002; Kilmartin, 2003; Spang et al., 1993; Spang et al., 1995). Multiple Sfi1 proteins are localized to the cytoplasmic site of the half bridge. Kar1 attaches

the Sfi1 to the Nuclear Envelope with its C-terminal membrane anchor (Seybold et al., 2015). Sfi1 contains conserved centrin binding sites and each Sfi1 binds up to 21 Cdc31 (Li et al., 2006). Cdc31 and Sfi1 dimerization is the first step of the SPB duplication. Mutants of Cdc31 cannot perform satellite formation, which is the first step of this process (Schiebel & Bornens, 1995). In yeast Sfi1 phospho-regulation by CDK1 and Cdc14 is important for SPB duplication events. High CDK1 activity prevents SPB duplication by phosphorylating CDK1 consensus sites. This phosphorylation inhibits C- to C- tail dimerization of Sfi1 molecules. Cdc14 dephosphorylation allows the Sfi1 dimerization and it leads to increase in the length of half-bridge (Avena et al., 2014). Dimerization of Sfi1 molecules also exposes free N-terminus end of Sfi1 at the bridge distal end. It promotes the "Satellite" formation, which is the SPB precursor (Elserafy et al., 2014). Satellite is mainly composed of Spc29 and Spc42 central plaque components. Spc29 binding to Cdc31 and N-Sfi1 interaction is necessary for satellite formation and satellite formation is the trigger for daughter SPB assembly (Ruthnick et al., 2021). Later, with high CDK1 activity SPB enlarges and forms the duplication plaque. It gets embedded in Nuclear Envelope (NE) and nuclear envelope assists the duplication plaque insertion (Ruthnick et al., 2017). At the late S phase, as SPB is duplicated, two side by side SPBs are separated by medial fission of the half-bridge. Phosphorylation of C-Sfi1 and activities of kinesin-5, Kip1 and Cin8 forces the SPBs to be separated (Elserafy et al., 2014).

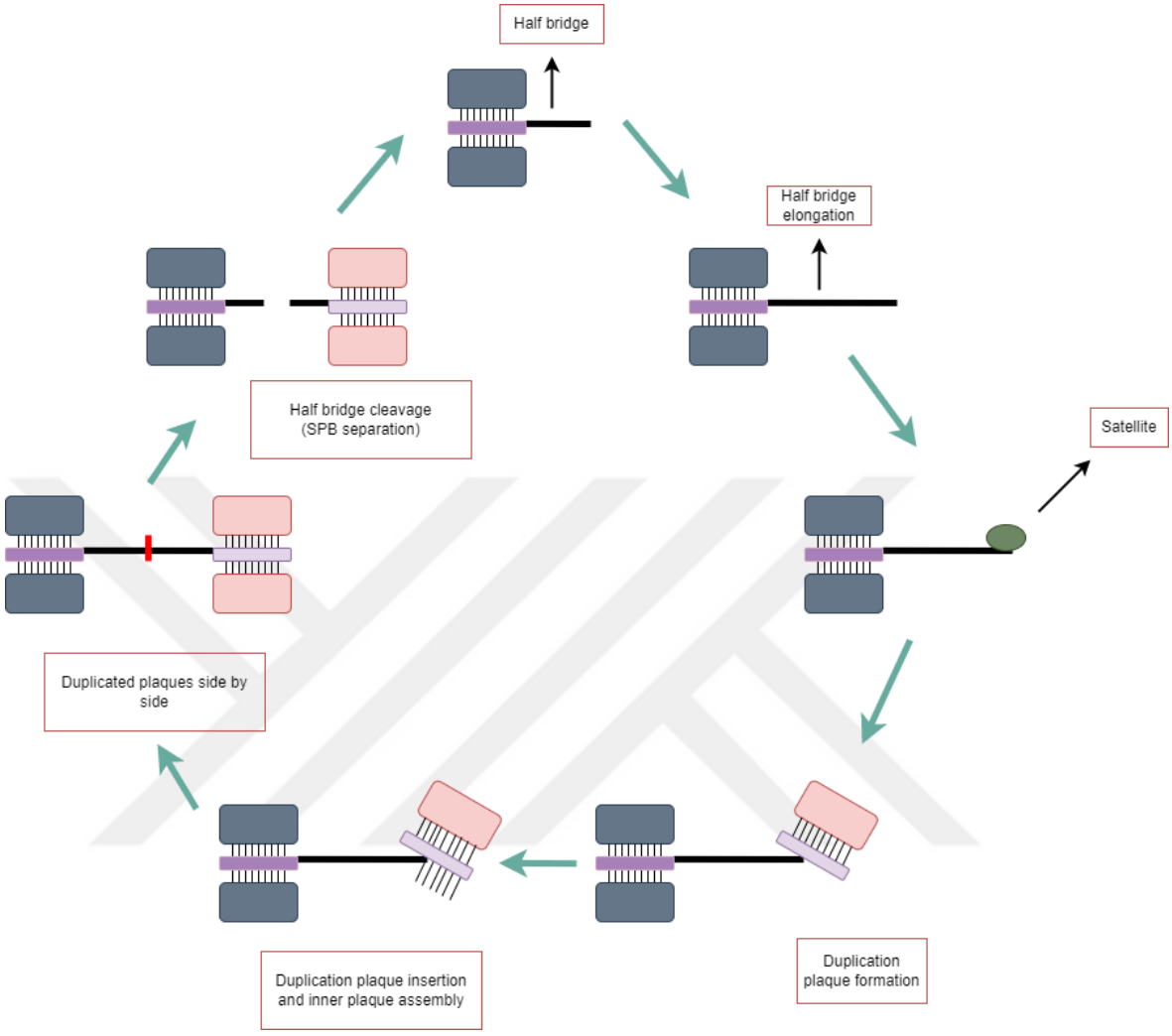

Figure 1. 11: Spindle Pole Body Duplication. New SPB is produced using the existing SPB as a template. New SPB is produced next to the old SPB. Later, half bridge is broken and the SPBs are separated to opposing poles. This figure is adapted from Seybold et al. (Seybold & Schiebel, 2013)

1.8 FEAR (Fourteen Early Anaphase Release) NETWORK

During mitotic exit progression Cdc14 phosphatase is released through two networks: FEAR network and mitotic exit network. At early anaphase Cdc14 is released from the nucleus transiently. The transient release of Cdc14 plays key roles in various mechanisms such as regulation of the spindle assembly, partitioning of the DNA, activation of microtubule forces and promotion of the mitotic exit (D'Amours & Amon, 2004). Partial released Cdc14 by the FEAR network is not enough to trigger mitotic exit instead mitotic exit is triggered by the Mitotic Exit Network (MEN). As explained in previous section, Cdc14 is sequestered in the

nucleus by RENT complex Net1/Cfi1 before the anaphase (Shou et al., 1999). Its localization and activity are changed by its interaction with Cfi1 but the amount of Cdc14 remains through cell cycle (Visintin et al., 1999). Previously, it is shown that Cdc14 is released from the nucleus in several MEN mutants which indicates the Cdc14 release apart from the MEN (Yoshida et al., 2002). The FEAR release Cdc14 have key roles in anaphase. The FEAR network components that have been identified are: Separase, Slk19 (Separase binding protein), Cdc5, Fob1 (replication fork protein), $PP2A^{Cdc55}$, Zds1, Zds2, some histone modifications, and cyclins Clb1 and Clb2 (Rock & Amon, 2009). Securin (Pds1) is ubiquitinated by activation of APC^{Cdc20} at the metaphase and targeted for degradation (Cohen-Fix et al., 1996). Separase is activated by degradation of its inhibitor Securin. Separase activation is another crucial event for Cdc14 activation. Separase and Zds1 down regulates the $PP2A^{Cdc55}$. Upon this down regulation Cdc55 phosphorylation is increased and it is dependent on the Cdk1-Clb2. This controls the $PP2A^{Cdc55}$ activity, and it promotes the Net1 phosphorylation (Jativa et al., 2019). Net1 phosphorylation leads to Cdc14 release from the nucleus. Moreover, Cdc5 is essential for Cdc14 release (Shou et al., 2002; Yoshida et al., 2002). Spo12 is an inhibitor of another FEAR network protein, Fob1 interacts with Net1/Cfi1 and prevents Cdc14 release. Spo12 antagonizes the inhibitory function of Fob1 and promotes the Cdc14 release (Stegmeier et al., 2004). To conduct anaphase related functions FEAR released Cdc14 dephosphorylates components related to such as rDNA segregation, spindle assembly and spindle midzone formation (Pereira & Schiebel, 2003; Ross & Cohen-Fix, 2004; Sullivan et al., 2004).

1.9 MEN (Mitotic Exit Network)

Mitosis is a highly regulated cell cycle stage where the genomic and cellular content is duplicated and further divided into two new cells by cytokinesis. This process is regulated by multiple mitotic kinases of CDK1, Aurora, and Polo families. As the name implies, mitotic exit refers to a cascade of events that happen after the biorientation of chromosomes to cytokinesis, in which cells divide into two new cells. As an outcome of mitosis, two cells in the G1 phase of the cell cycle are obtained (Holder et al., 2019). Exit from mitosis requires the inactivation of cyclin-dependent kinases (CDKs), which establish cell cycle regulatory complexes with their cyclin subunits that promote the initiation and the transition through

the cell cycle (Matellan & Monje-Casas, 2020). Inactivation of these Cyclin/CDK complexes is carried out by anaphase-promoting complex/Cyclosome (APC/C) (King et al., 1995). APC complex is kept inactive until the end of mitosis. APC complex has two cofactors, Cdc20 and Cdh1, which provide the substrate specificity to the APC complex. Cdc20 is crucial for the metaphase-anaphase transition by directing the degradation of Pds1 (Shirayama et al., 1999). Cdc20 triggers the first wave of CDK inactivation in mitosis whereas, Cdh1 acts later in mitosis. This dual regulation on the APC complex is suggested to be important for the timely destruction of different APC substrates (Peters, 2002; Visintin et al., 1997).

In budding yeast, mitotic exit is highly regulated by the localization of a phosphatase Cdc14 which is kept inactive in the nucleolus and activated when released. Cdc14 release happens stepwise, first from the nucleolus to the nucleus and then to the cytoplasm. Once released, it leads to dephosphorylation of CDK substrates and leads to accumulation of CDK-inhibitor Sic1 (Visintin et al., 1998). Through these dephosphorylation events, it triggers mitotic exit and cytokinesis.

Mitotic exit network (MEN) is a G-protein signaling process associated with the localization of the spindle pole body (SPBs) (Jativa et al., 2019). Even though the activation of MEN is not well understood, the most upstream component is Tem1GTPase (Lee et al., 2001). Tem1 activates a signaling cascade, leading to the activation of Cdc15 and Dbf2-Mob1 kinases (Mah et al., 2001). Later, Dbf2-Mob1 promotes the release of Cdc14 to the cytoplasm (Mohl et al., 2009). Through these events, MEN lead to the complete release of Cdc14. Two main processes regulate Tem1 activity; it is negatively regulated by Bfa1-Bub2 (GTPase-activating complex) and positively regulated by Lte1 (Geymonat et al., 2009; Hu et al., 2001). Lte1 and Tem1 are localized at the bud after the nucleus entry to the bud in the nuclear division. The localization of Lte1 and Tem1 is required in mitotic exit (Bardin et al., 2000). Lte1 promotes MEN with a separate mechanism other than directly activating Tem1, in which it contributes to the mitotic exit through its role in cell polarity (Geymonat et al., 2009) and regulation of Kin4 activity and localization (Bertazzi et al., 2011). In case of spindle mispositioning SPOC gets activated and it inhibits the MEN. In normal aligned cells, Kin4 associates with the mother SPB and Bfa1-Bub2 complex is localized to the daughter SPB. However, in spindle misalignment Bfa1-Bub2 and Kin4 localize to both SPBs. Kin4 phosphorylates Bfa1 to inhibit Mitotic Exit during SPOC (Pereira & Schiebel, 2005). On the

other hand, Lte1 promotes mitotic exit by restricting Kin4 to the mother (Bertazzi et al., 2011). Moreover, Cdc5 is another regulator of MEN, it inhibits Bfa1's inhibitory function to promote mitotic exit (Hu et al., 2001). It also promotes MEN by assisting Cdc15 recruitment to SPBs in parallel to Tem1 (Rock & Amon, 2011). In parallel to Kin4 pathway, yeast protein phosphatase 1 (Glc7) with its regulatory subunit Bud14 promotes dephosphorylation of Bfa1 to activate the Bfa1-Bub2 Gap complex. These pathways independently activated SPOC effector Bfa1 in response to spindle misalignment (Kocakaplan et al., 2021).

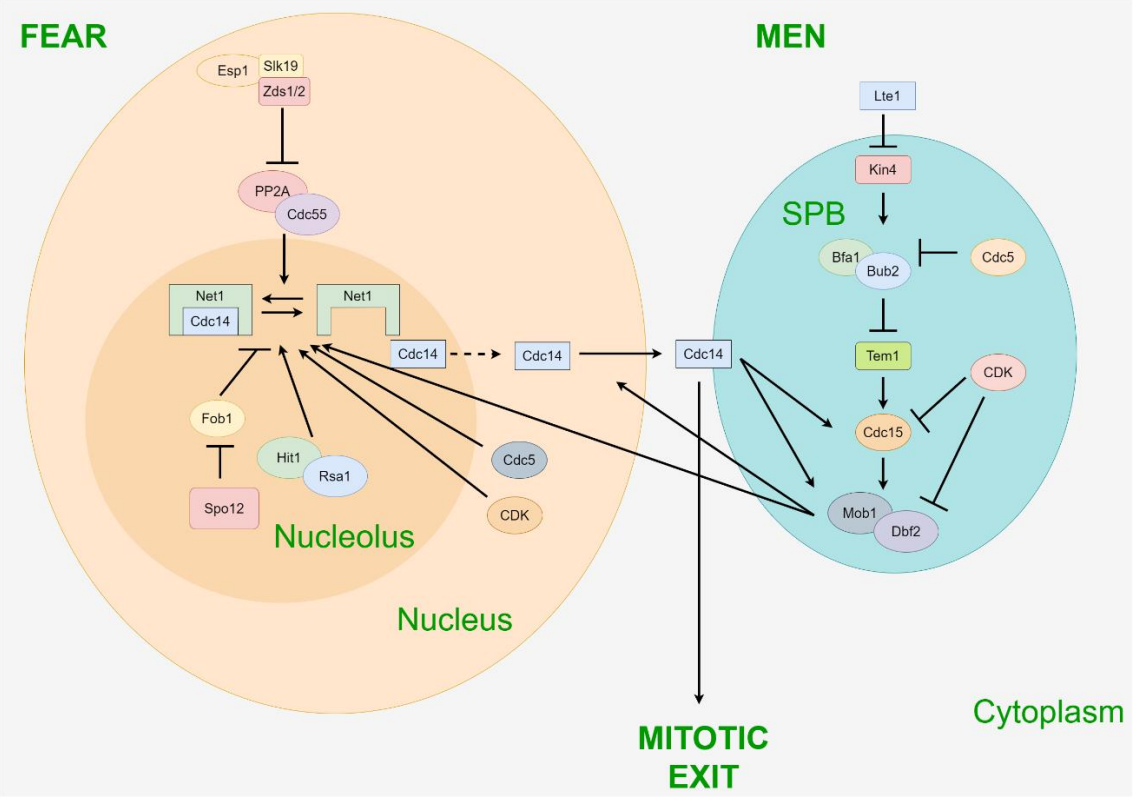

Figure 1. 12: Mitotic exit in budding yeast. Mitotic Exit progression is enabled with two sets of Cdc14 release mechanisms namely: FEAR and MEN. This figure is adapted from Howell et al. (Howell et al., 2020)

1.20 CCR4-NOT Complex

In all eukaryotes, Ccr4-Not complex has roles in regulation of gene expression at all steps of production of messenger RNAs to their destruction in the cytoplasm. Yeast Ccr4-Not complex contains 9 core subunits namely; Ccr4, Caf1, Caf40, Caf130 and Not1-5 (Bai et al., 1999). Cdc36 is the Not2 subunit of the complex. The Ccr4 and CAF1 function as exonucleases (Temme et al., 2010). The complex contains a scaffold protein called Not1

which a variety of evolutionary conserved proteins dock onto. Not1 is the only essential component of the complex in yeast but deletion of other subunits (Not2, Not4, or Not5) has effects on the strain growth as well (Maillet et al., 2000). Ccr4-Not complex is found in both nucleus and cytoplasm. In cytoplasm it is found in polysomes where mRNAs are translated, in P-bodies where mRNAs are inhibited by certain mechanisms (Panasenko & Collart, 2012; Teixeira & Parker, 2007). In nucleus, it is involved in a variety of mechanisms such as transcription initiation, elongation, RNA export, nuclear RNA surveillance and DNA damage repair (Chalabi Hagkarim & Grand, 2020).

Ccr4-Not complex has roles in a variety of regulatory mechanisms. One of them is translation. It is previously shown that all Ccr4-Not components are detected at polysomes. Moreover, in the absence of Not2. Not4 or Not5 the level of polysomes are reduced (Panasenko & Collart, 2012). Ccr4-Not complex has also roles in mRNA degradation processes. Ccr4-Not complex has roles in initiation of mRNA deadenylation (Alhusaini & Coller, 2016). Several studies show the role of deadenylation in certain cellular processes such as DNA-damage response, cell proliferation and cell cycle viability(Ito et al., 2011; Morel et al., 2003; Traven et al., 2005) . Moreover, Ccr4-Not complex has roles in P-bodies such as mRNA decapping (Muhlrad & Parker, 2005).

Depending on the cell needs, different subunits of Ccr4-Not are recruited by gene specific regulators for post-translational mechanisms. Ccr4-Not complex can also interact with nascent mRNA. It is proposed, Ccr4-Not may associate with mRNAs during their synthesis and remain bound to as they are transported to the cytoplasm (Collart, 2016).

1.21 Cell Cycle Regulation on Transcription

A proliferative cell carries out 4 main cell division events of two gap phases, one duplication and one division. Transcription of a variety of genes peaks depending on the specific cell cycle phases. Transcription of certain elements tends to start right before their necessity begins. Transcriptional control is a universal control over the cell division process. Different mechanisms mediate the transcriptional control at specific phases of initiation of DNA replication, entry into mitosis and exit from mitosis. Many studies identified cell cycle regulated gene expression (Cho et al., 1998; Spellman et al., 1998).

In the initiation of DNA replication there is a commitment step for cell to initiate division. This initiation depends on the expression of certain transcription factor complexes. In budding yeast, MBF (MCB binding factor) and SBF (SCB binding factor) transcription factor mechanisms are the main regulators of the process. G1 cyclins and other proteins that have role in DNA synthesis gets activated in late G1 by these transcription factors (Koch et al., 1993). These factors act in the same direction of the mechanism but activate distinct elements that work in different sides of cell cycle machinery (Iyer et al., 2001).

Entry into mitosis, G2/M transition, requires specific activation of certain pathways. For the activation of these pathways MCM1 is essential. Mcm1 with an Mcm1 recruited factor activates the Swi5 and Clb2 other G2/M specific activators (Althoefer et al., 1995). Moreover, forkhead factors are shown to regulate mitotic cluster of genes. Clb2 cluster of genes cannot oscillate which in the end affects activation of other mitotic gene clusters in forehead factor mutants (Zhu et al., 2000). Ndd1 is another forkhead interactor that regulates the G2/M specific transcription (Koranda et al., 2000).

Mcm1 also plays role in gene regulation of mitotic exit. Mcm1 has binding sites on early cell cycle box promoter element that is responsible for M/G1 specific transcription (McInerny et al., 1997). Swi5 and Ace2 are transcriptionally activated at the entry to Mitosis but act on activation of M/G1 specific genes. Swi5 and Ace2 factors both accumulate in the nucleus but bind DNA at different times (Sbia et al., 2008). They resemble MBF and SBF transcription factors in that Swi5 and Ace2 activate M/G1 transcription with their specific substrates (McBride et al., 1999).

Chapter 2 : MATERIAL AND METHODS

2.1 *Saccharomyces Cerevisiae* Methods

The descriptions and components of the media, buffers and reagents are listed in Table 9.4.

2.1.1 Growth Media and Yeast Strains

S288C isogenic yeast strains are used in this study, listed in Table 9.1. The strains were grown in selective medium regarding the cell type. D-(+)-Glucose (BioFroxx, #1191GR500) is used as the sole carbon source unless it stated otherwise. For general cell growth YPAD media is used. Agar plates are prepared with 20g per Liter Agar (Carl Roth #5210.2). All media and agar plates were sterilized via autoclave unless otherwise is stated.

2.1.2 Yeast Growth

The yeast strains are grown at the optimum temperature, 30 °C rich media if not stated otherwise. Synthetic complete (SC) media, lacks the respective auxotrophic nutrients are used for plasmid containing media. Filter sterilized SC media is used for cell growth prior microscopy experiments. Depending on the temperature sensitive status, respective degrees are used for cell culturing as permissive and non-permissive degrees.

Prior the experiments, cells are grown at respective agar plates. Next, the cells grown on agar plate is used for inoculation to respective liquid medium. The culture is grown overnight (12-18 h) at respective temperature to reach the stationary phase. Later, the stationary culture is diluted to 600nm OD value 0.15-0.2 in a fresh medium. Spectrophotometer (PG Instrument, T60 Visible Spectrophotometer) is used for spectrophotometric measurements. The cells are grown until they reach the OD value 0.8-1.0 which corresponds to 2.5~ doubling to obtain logarithmically growing culture.

2.1.3 Yeast Competent Cell Preparation and Transformation

Chemical method is used to prepare yeast competent cells. Firstly, 10 ml stationary culture is prepared by overnight growth at 30°C or 23°C for temperature sensitive strains. Then, the stationary culture is diluted to OD600 0.15-0.2 in 50 mL fresh media. The cells are grown until they reach to OD600 0.8-1.0 to obtain log phase. Later the log phase cells are

centrifugated at 3200 rpm 2 minutes at room temperature. All centrifugations are made at room temperature. Then, supernatant is removed, and the pellet is resuspended with 20-25 mL sterile double-distilled water. Next, the cells are centrifugated again at 3200 rpm for 2 minutes and supernatant is removed. Pellet is resuspended in 20-25 mL LiSORB, centrifugated as before and the supernatant is removed. Later the pellet is centrifugated once more to remove all the LiSORB. Finally, pellet is resuspended in for OD600 1.0 50 mL culture, 300 µl LiSORB AND 50 µl salmon sperm DNA. The amount of LiSORB and salmon sperm is scaled depending on the cell amount. Salmon sperm DNA is boiled at 95 °C for 5 minutes followed by 5 minutes ice incubation beforehand. Later, yeast competent cells can be used for transformation directly or they can be stored at -80 °C for some time.

Competent cells are used to get PCR products or plasmids into the cells. To obtain this, generally, 5 µl of PCR product; 5 µl of integration plasmid; 1-2 µl of circular plasmid is used. Firstly, cells are thawed at room temperature. After adding the PCR product or the plasmid, cells are incubated at room temperature for 15-20 minutes. Later 300 µl LiPEG is added to the cells and vortexed. The mixture is incubated at room temperature for 20 minutes. Then, 35 µl DMSO (Fisher Scientific #BP231-1) was added to the mixture and incubated at 42°C for 15 minutes (12 minutes for temperature sensitive mutants). After incubation, cells are centrifugated at 3200 rpm for 2 minutes and supernatant is removed by aspiration. Finally, cell pellet is resuspended in 150-200 µl 1X sterile PBS and plated out onto respective selective agar plate if the marker is an auxotrophic marker. If the selective marker is an antibiotic, the cells are grown overnight at respective temperature in YPAD then plated out to antibiotic containing agar plate. Then, the plates are incubated at 30 °C or 23 °C if the strain is temperature sensitive.

2.2 PCR-based methods

Casette PCR genome editing method is used for gene deletions and C- or N- terminal tagging. Later, yeast cells are confirmed depending on the tag or gene manipulation. Gene deletion is confirmed by PCR. Yeast colony PCR or PCR on yeast chromosomal DNA is conducted.

2.2.1 Casette PCR

All PCRs are conducted using Biometra TAdvenced Twin Analytik Jena PCR machine. S1/S2 primers are used for gene deletions; S2/S3 primers are used for C- terminal tagging; S1/S4 are used for N- terminal tagging. To obtain 50 µl cassette PCR reaction; 5 µL (20 ng/µL) plasmid as template, 3.2 µL forward S1 or S3 primers (10 µM), 3.2 µL reverse S2 or S4 primers (10 µM), 5 µL 10X PCR Buffer 8.75 µL dNTPs (NEB #N0446S), 0.6 µL enzyme mix (2X Taq polymerase (NEB #M0273L) + 1X Vent polymerase (2U/ µL, NEB #M0254S) and 24.25 double distilled water is mixed.

The PCR cycles are as followed; 2 min at 95 ºC (Step 1), 30 sec. at 95 ºC (Step 2), 30 sec at 52 ºC (Step 3), X min at 68 ºC, (X is calculated as 1 minute per 1000 bp of the expected product size) (Step 4). Steps 2 to 4 are repeated for 9 times before going through step 5. 30 sec at 95 ºC (Step 5), 30 sec at 52 ºC (Step 6), X min with an increment of 20 sec per step at 68 ºC (Step 7). Steps 5 to 7 are repeated 19 times. Finally, the reaction is held at 4 ºC. To check the PCR product, 0.8% agarose gel electrophoresis is conducted.

2.2.2 Yeast Colony PCR

To skip the chromosomal DNA isolation process and perform PCR using yeast cells directly from the solid culture PCR with Sarkosyl is used. A very small amount of cells are taken from solid culture to 50 µL Sarkosyl solution (0.01% Sarkosyl in 0.02 NaOH) and vortexed harshly. The mixture is then boiled at 95 ºC for 20 minutes followed by an incubation at -20 ºC degree for a couple of minutes to increase lysis efficiency. Usage of freshly grown plates and proper amount of cell usage increases the colony PCR efficiency.

The PCR cycle conditions: 5 min at 95 ºC (Step 1), 30 sec at 95 ºC (Step 2), 30 sec at 54 ºC (Step 3), X min at 68 ºC (Step 4), (X is calculated as 1 minute per 1000 bp of the expected product size). Steps 2 to 4 are repeated for 30-35 times. 3 minutes at 68 ºC (Step 5). Finally held at 4 ºC. PCR results were analysed on 0.8 % agarose gel electrophoreses prepared in 1X TAE buffer. To test gene deletions, WT PCR products are used as control.

2.2.3 Yeast Chromosomal DNA Isolation by Zymolase

To obtain yeast chromosomal DNA, the cells are grown to stationary phase in proper media. Then, 1 ml culture is pelleted at 3200 rpm for two minutes. Supernatant is removed by aspiration. 1 mL distilled water is used to resuspend the pellet and centrifugated as before. Supernatant is removed by aspiration. The pellet is resuspended in 750 µl P1 buffer, 1 µl mercaptoethanol, 0.15 mg Zymolase 20 T (MP Biomedicals, LLC #320921) and incubated at 37 °C with occasionally mixing for 1-2 h. Later, 150 µl P2 buffer is added to the mixture with mixing carefully and incubated at 65 °C for 20 minutes followed by incubating on ice until it cools down. 150 µl P3 buffer is added with carefully mixing and incubated on ice for 15 minutes. Then, the sample is centrifugated at 14000 rpm for 5 minutes. The supernatant is transferred to a new Eppendorf and 450 µl Isopropanol (ACS #0312.2500) is added. The mixture is mixed carefully and incubated 5 minutes at room temperature followed by centrifugation at 14000 rpm for 15 minutes. The supernatant is discarded, and 1 mL 70% molecular Ethanol is added. The sample is centrifugated once more and supernatant is removed. The sample is left to dry until all the liquid is evaporated. Later 20-30 µl pre-heated (65 °C) ddH_2O is added to elute the chromosomal DNA. The chromosomal DNA is stored at -20 °C.

2.2.4 MiniPrep (Plasmid Isolation with Manual Method)

A colony or little amount of grown E. coli on a plate is inoculated to respective antibiotic containing TY medium. The cells are grown overnight at 37 °C with shaking (12-18h). 1.5-2 mL culture is centrifugated at 6000 rpm for 5 minutes at room temperature. The supernatant is removed with aspiration. Then, 300 µl P1 buffer is added to resuspend the pellet. Next 300 µl of P2 buffer added with careful mixing (invert/rotate), followed by 300 µl P3 buffer with careful mixing (invert/rotate). Later, the mixture is centrifugated at 14000 rpm for 10 minutes at room temperature. The supernatant is transferred to a new Eppendorf that contains 500 µl Isopropanol (ACS #0312.2500). The mixture is centrifugated at 14000 rpm for 15-20 minutes. The supernatant is discarded and 500 µl 70% molecular Ethanol is added. The sample is centrifugated at 14000 rpm for 5 minutes. The supernatant is discarded and centrifugated once more. The supernatant is discarded again, and the Eppendorf is left to dry

to evaporate all the liquids. Finally, 30-50 µl pre-heated (65 °C) ddH_2O is added to elute the plasmid DNA. The plasmid DNA is stored at -20 °C.

2.2.4 Site-Directed Mutagenesis

Site directed mutagenesis is performed to obtain a desired mutation in a plasmid DNA. To construct 50 µL mutagenesis PCR; 5 µL (5 ng/µL) plasmid, 4 µL (2 mM) dNTPs (NEB #N0446S), 1.5 µL forward primer (10 µM), 1.5 µL reverse primer (10 µM), 1.5 µL Turbo PFU DNA Polymerase (Agilent #600250), 5 µL 10X PFU Turbo Buffer and 31.5 µL ddH_2O mixture is prepared. As PCR reaction control 5 µL (5 ng/µL) plasmid, 40 µL ddH_2O, 5 µL 10X Turbo PFU Buffer mixture is prepared.

The PCR conditions are set as; 30 sec at 95 ºC (Step 1), 30 sec. at 95 ºC (Step 2), 1 min at 54 ºC (Step 3), X min at 68 ºC (Step 4), (X is calculated as 2 minutes per 1 kb of the expected vector size). Steps 2 to 4 are repeated for 16 times. Finally, the reaction is held at 4 ºC. Then 2 µL DpnI (Thermo Fisher Scientific #ER1705) is added to the PCR mixture and incubated at 37 ºC overnight (at least 10 h). Then, 3 µL PCR product is transformed to *E. coli DH5α* competent cells for plasmid amplification. Finally, transformants are used for plasmid isolation and sent for sequencing for confirmation.

2.3 Biochemical Methods

2.3.1 TCA Total Cell Protein Extraction

2 mL of log phase cell culture with known optical density is pelleted with centrifugation 14000 rpm for two minutes. The supernatant is removed with aspiration. Next, the pellet is resuspended in 800 µl cold ddH_2O followed by addition of 150 µL of 1.85M NaOH (Merck, #106498) and 150 µL of 55 % (w/w) TCA (Trichloroacetic acid, Merck #100807). The mixture is vortexed well. Then, the mixture is incubated on ice for 10 minutes. Later the samples are centrifugated at 14000 rpm for 15-20 minutes at 4 °C. The supernatant is removed by aspiration. The samples are centrifugated at 14000 rpm for 1 minute and the supernatant is removed by aspiration to remove all the supernatant. The pellet is resuspended in HU-DTT. HU-DTT amount was decided depending on the cell density and the protein of desire. If an abundant protein, 150 µL of HU-DTT was used for 1 mL OD600 1.0, if not abundant 75 µL of HU-DTT was used for 1 mL OD600 1.0 is used. After HU-DTT addition,

if yellowish green colour is formed 2 µL of 2M Tris-HCI was added to neutralize the pH. Finally, the protein samples are boiled at 65 °C for 15 minutes and stored at -20 °C.

2.3.2 SDS- PAGE

SDS-PAGE method is used for separation of proteins. SDS-PAGE gels were prepared by using Mini-Protean II gel system. The separating gel was prepared by using the stock solutions of 1.5M Tris-HCl pH: 8.8, 6-15% polyacrylamide mixture (30%: 0.8% (w/v) Acrylamide:Bisacrylamide, Carl Roth, #3029.1), 10% (w/v) SDS, propriate amount of ddH_2O and polymerized using 10% (w/v) Ammonium persulfate (APS, Sigma #A3678) and TEMED (Sigma, #T7024). The stacking gel was prepared by using the stock solutions of 0.5M Tris HCl pH: 6.8, 10% (w/v) SDS, 4% polyacrylamide mixture, propriate amount of ddH_2O. Polymerization of the gels was obtained with 10% APS and TEMED.

Prior sample loading, the samples are centrifugated at 14000 rpm for 2 minutes and 15 µl samples are loaded.

2.3.3 Western Blotting

Following the SDS-PAGE, the samples are transferred to nitrocellulose membrane (Merck, GE10600002) in 1X Blotting Buffer for 1.5-2 hours at 0.1 A constant with Bio-Rad Mini-Trans-Blot transfer apparatus. The transfer is checked with Ponceau S staining. Then, Ponceau S staining is washed with 1X PBS-T (0.02% Tween-20) solution. Next, the membrane is blocked with 5% non-fat dried milk (AppliChem, # A0830) prepared with 1X PBS-T for 1 h at room temperature or overnight at 4 °C with proper shaking. The membrane is then introduced to the primary antibody which is prepared in 3mL of 3 % non-fat dried milk with appropriate concentration of the antibody. The membrane is incubated with primary antibody solution for 1 hour at room temperature or overnight at 4 °C with proper shaking. After incubation, the membrane is washed with PBS-T solution 5 minutes for 3 times with shaking. Next, membrane is introduced to the secondary antibody which is prepared in 3mL of 3 % non-fat dried milk with 1:1000 concentration of the antibody. Secondary antibodies used are; Goat-anti-rabbit (Advansta #R-05062-500) or Goat-anti-mouse (Advansta #R-05071-500) conjugated with HRP (Horse Radish Peroxidase). Then the

membrane is visualized at Chemidoc (BioRad) using home-made enhanced chemiluminescence (ECL).

2.3.4 Total RNA isolation

For total RNA isolation Direct-zol RNA Miniprep kit is used (Zymo Research R2051). Prior RNA isolation, OD600 3.0 OD cell pellet is obtained by centrifugation at 3200 rpm for 2 minutes. The pellet is resuspended with 15 mL ddH_2O and centrifugated once more. The supernatant is removed by aspiration. The pellet is centrifugated once more and the supernatant is aspirated. The samples are stored at -80 ºC until RNA isolation.

The pellet is resuspended with 800 µL TRI Reagent and lysed with glass beads (Sigma, #G8772), using a cell homogenizer (SpeedMill Plus AnalytikJena) for 8 times. After lysis the cell lysate is separated from the glass beads and cell debris by centrifugation at 3200 rm for 2 minutes. Later, protocol stated in Direct-zol RNA Miniprep kit is conducted.

2.4 Microscopy-based Methods

For fluorescent microscopy we carried out our microscopy experiments with Carl ZEISS Axio Observer 7 motorized inverted epifluorescence microscope equipped with Colibri 7 LED light source, Axiocam 702 Monochrome camera, 100X and 63X Plan Apochromat immersion oil objective lenses, Filter sets 95 (GFP/Cherry), 20 (Rhodamin), FITC and DAPI, and an XL incubation and climate chamber. For analysis of DAPU 63X objective was used. For mCherry-Tubulin and Cdc14-GFP we used 100 X objective.

2.4.1 Fixed-cell Imaging

For GFP and mCherry microscopy analysis, the cells are fixed using 8% PFA (Merck, 30525-89-4). 700 µL PFA is added to 700 µL culture. The mixture is incubated at room temperature for 10 minutes. Then, centrifugated at 6000 rpm for 2 minutes. The supernatant is removed, and the cell pellet is resuspended in 1 mL 1X PBS and stored at 4 °C up to 1 day. Before imaging, the cells are centrifugated at 3200 rpm for 2 minutes to obtain more concentrated culture. Then microscope slides are prepared for further imaging by 2 µl of culture sandwiched between the slide and the coverslip.

For DAPI analysis, the cells are fixed by Ethanol fixation. 700 µL molecular Ethanol is added to 300 µL culture. Then the samples are stored at 4 °C until visualization. Before staining, the cells are centrifugated and the supernatant is removed by aspiration. To get rid of all the Ethanol, the centrifugation s repeated. Finally, the cell pellet is resuspended in 10 µl of 1 mg/mL DAPI in 1X PBS (1:10000)

2.4.2 Image Analysis

Image analyses were performed using Image J. Graphs and statistical results were obtained using GraphPad Prism 8.0.1 (GraphPad, Le Jolla, Ca). Key followed for asterisk placeholders for p-values in the figures are: *P < 0.05, **P < 0.01, ***P < 0.001, **** P < 0.0001 or p value in numeric is stated.

2.4.3 The Localization Based Fluorescence Signals Quantifications

For signal intensity of Cdc14 localization to the SPBs. We took images of cells containing mCherry-*TUB1* cell cycle marker and CDC14-GFP. Each still image consisted of 10 z-stacks of 0.36 µm thickness of the images and Max-projected. Spindle pole body is selected (ROI) and the mean intensities of 0.343 μm^2 (25 pixels) square area is measured using Image J (NIH) software. A cellular area without signal is selected as well for background control. Background is used for correction of the signal by subtracting it from the SPB localization signal intensity.

2.4.3 Live Cell Imaging Preparation for FRAP

Prior the experiment, stationary culture is obtained with overnight growth in respective media and temperature. Then, the culture is diluted to OD600 0.15 - 0.2 and grown in the respective temperature with proper shaking until OD600 0.8 - 1.0. Cells are prepared on glass bottom petri dishes (WVR 10810-054 Matsunami). 150-200 µl of Concanavalin A (Canavalia ensiformis Jack Bean, type IV Sigma C2010-G) is put directly onto the center of the cover dish and incubated it at room temperature for 10 minutes. Next, the Concanavalin A is taken back by pipette and the dish is washed 3 times with 3 mL ddH_2O. All the water is removed by aspiration. Then, OD600 0.5-0.6 200 µl culture is directly added to the center. The dish is

incubated at respective temperature for 30 minutes. Then, the dish is washed 3 times with 3 mL fresh media. Finally, the dish is filled with 3 mL fresh media.

2.4.4 FRAP (Fluorescence Recovery After Photobleaching)

We carried out FRAP experiments using Live Cell Microscope DMI8 SP8 Leica. To obtain fastest acquisition, 256x256 imaging resolution is used. For FRAP analysis Argon laser power is used at 80%. 3 pre-bleaching images, 3 bleaching at 80% shift, and 75 post-bleaching images are taken with 0.653 ms intervals. Zoom in method is used. Images of a single plane with pinhole size 5.78 AU were taken. Pinhole size 5.78.

Image analysis is conducted using ImageJ software. All analysis is conducted as explained previously by Caydasi et al. (Caydasi & Pereira, 2009) 36 pixels square (ROI) at SPB is selected for Cdc14 localization mean intensity at pre and post bleaching images. An outside area selected for the correction for the mean intensity. SPB ROI is corrected by subtracting the outside control, as we will call corrected ROI. For bleaching control, another cell's Cdc14 nucleolus signal is used. Bleaching control is also corrected with an outside control near the cell, which we will call REF corrected. We obtained a corrected signal by dividing corrected SPB ROI mean intensity over corrected bleaching control mean intensity, which we will call ROI corrected 2. Then, the first image after bleaching is corrected to 0 by this formula:

ROI normalized = (ROI corrected 2 – ROI corrected 2 of Post-bleach (1^{st} time point after bleaching))/ (Mean ROI corrected 2 of Pre-Bleach - ROI corrected 2 of Post-bleach (1^{st} time point after bleaching))

And this formula is applied to the rest of the data. The graph is plotted at GraphPad and curve fitting is performed with One Phase Association exponential curve fitting. Plateau, rate constant and halftime are calculated with this curve fitting.

2.5 Yeast Two Hybrid Assay

Genes of interest are cloned under pMM5 (LexA-myc fusion, *HIS* +) and pMM6 (Gal4-HA fusion, *LEU2* +) backbones. The pmm5 and pmm6 plasmids are transformed to SGY37-VIII,3 strain. SGY37-VIII,3 strain contains a chromosomally integrated LexA(op)-LacZ reporter for activation of the ß-galactosidase gene. Transformants are selected on SC-His-

Leu Agar and SC-His-Leu liquid culture. Transformants are transferred to the liquid culture to obtain stationary phase. Cultures are diluted to OD600 1.0 and 10 µl from each are dropped to the agar plate. The drops are grown for 48 hours at 30 °C. Later, the plates are overlaid with soft agar solution (0.4%) containing 0.4 mg/ml X-Gal, 0.1% SDS, 10 mM KCl, and 1 mM $MgCl_2$

2.6 WT and *cdc36-16* RNAseq

The cells are grown in Filter sterilized YPAD medium (for nocodazole treatment) to the stationary phase at 23 °C. The stationary phase culture is diluted to OD600 0.2 OD and grown to OD600 0.8-1.0 log phase at 23 °C. Then, the culture is diluted to OD600 0.3-0.4 for alpha factor arrest. Alpha factor (1:100 1 mg/1ml in DMSO) is added to the diluted culture and grown for 1.5 doubling until the cells are arrested at G1 phase at 23 °C. After the arrest, the cells are released at the alpha factor free medium at 23 °C. Then, the culture is diluted to OD600 0.3-0.4 for nocodazole arrest and nocodazole is added (1:100 1.5 mg/1ml nocodazole in DMSO Sigma #M1404). The cells are grown at 30 °C for the temperature sensitive phenotype for 1.5 h and metaphase arrest. After the metaphase arrest, cells are released in metaphase free medium and alpha factor (1:100) is added to obtain cell synchrony at 30 °C. After 30 minutes incubation at 30 °C samples are collected with every 10 minutes. 30, 40,50, 60 minutes are collected for WT and 40,50,60,70 are collected for *cdc36-16.* OD600 3.0 cell pellet for RNA isolation, 1 mL cell pellet for TCA protein extraction and 300 µl culture for Ethanol fixation is taken. CLB2 levels and DAPI counts are compared, and respective time points are used. For example, WT 30-minute sample corresponds to the *cdc36-16* 40-minute sample.

Total mRNA is extracted from cell pellets using isolation Direct-zol RNA Miniprep kit is used (Zymo Research R2051). Then, cDNA libraries are prepared using NebNext Ultra II RNA Library Prep Kit for Illumina (E7490, E7335, E7770). Finally, the samples are sent for sequencing with Hiseq X platform. 3 sets of replicas is conducted.

Chapter 3 : BUD14 IS PART OF A MECHANISM THAT AFFECT CDC14 LOCALIZATION TO THE dSPB

3.1 Bud14 does not affect Cdc14 full and partial release in an unperturbed cell cycle

In our previous paper, we identified Bud14 as a Spindle Positioning Checkpoint regulator (Kocakaplan et al., 2021). This intrigued us to investigate more about Bud14's effect on mitotic exit in cells with correctly positioned spindles. To investigate the effect of *BUD14* on timing of mitotic exit, we compared Cdc14 release dynamics in wild type (WT) and in *bud14*Δ yeast strains that contain mCherry tagged Tubulin (mCherry-Tubulin) and GFP tagged Cdc14 (Cdc14-GFP). mCherry-Tubulin marks the mitotic spindle and enables us to observe the anaphase onset (start of spindle elongation) and mitotic exit (spindle breakage) (Bardin et al., 2000), whereas full release of Cdc14-GFP from the nucleolus into the cytoplasm directly shows MEN activity and mitotic exit (Shou et al., 1999).

To assess the timing of mitotic exit in WT and *bud14*Δ cells, we analyzed the full release of Cdc14. To do this, we arrested WT and *bud14*Δ cells in the G1 phase using alpha factor (mating pheromone) synchronization of cells. Subsequently, we removed the mating pheromone from the medium to allow synchronous cell cycle progression of cells. Samples were collected for microscopy every 10 minutes for one complete cell cycle after release from G1 arrest (Figure 3.1A-B). WT cells fully released their Cdc14 mainly at late anaphase (spindle length > 6 μm. Timing of full release of Cdc14 from nucleolus was similar in *bud14*Δ cells (Figure 3.1B-C)).

Later, we analyzed the FEAR release of Cdc14. Cdc14 release occurs in two steps. First, at the anaphase onset Cdc14 is partially released from the nucleolus by the action of the FEAR network (Stegmeier et al., 2002), subsequently Cdc14 is fully and persistently released into cytoplasm as a result of MEN activation (Shou et al., 1999). FEAR release is transient and is followed by the full release imposed by the MEN. Thus, FEAR release is not easily observed in cells progressing in the cell cycle. However, when the MEN is blocked, FEAR released Cdc14 can readily be detected. Therefore, to analyze Cdc14 FEAR release, we took advantage of *cdc15-1* cells, in which MEN is inhibited at restrictive temperature (37 ^{o}C) (Jaspersen et al., 1998). *cdc15-1* and *cdc15-1bud14*Δ cells were synchronized in G1 phase

using alpha-factor at 23 ºC. Then, cells were released from the G1 arrest at 37 ºC which is the restrictive temperature for MEN inactivation. In *cdc15-1* cells, Cdc14 FEAR release started at early anaphase, peaked during mid anaphase, and decreased at telophase (Figure 3.1D) which we didn't observe in *spo12*Δ, FEAR mutant. FEAR release of Cdc14 occurred similarly in *cdc15-1bud14*Δ cells (Figure 3.1D). Both *cdc15-1* and *cdc15-1bud14*Δ were significantly different than *cdc15-1spo12*Δ, which indicates we observed FEAR release. To conclude, the partial and full release of Cdc14 is not affected by the *BUD14* deletion.

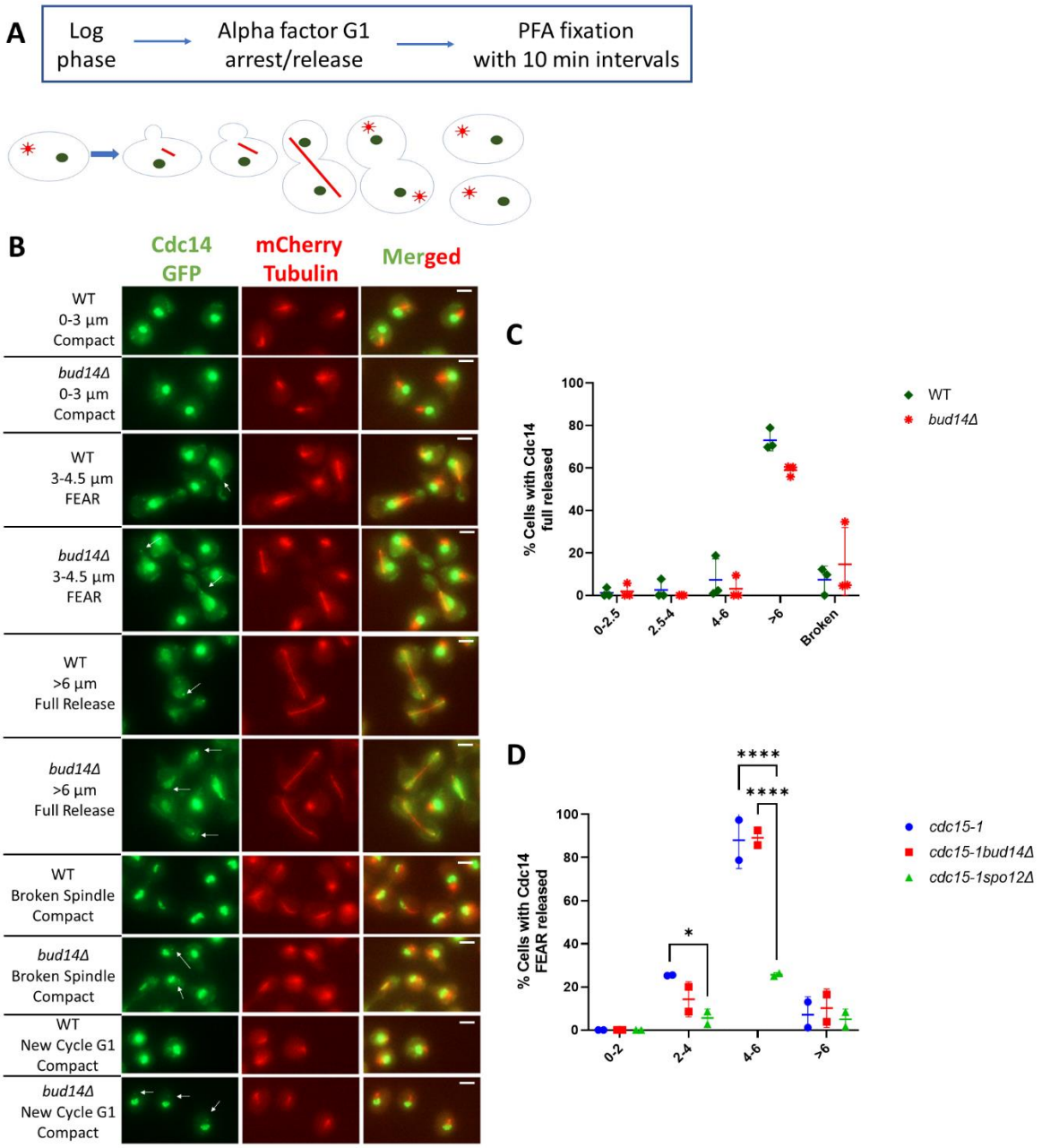

Figure 3. 1: Bud14 does not affect Cdc14 full and partial release in an unperturbed cell cycle. A. Experiment plan: Cells are grown to the log phase and arrested at the G1 phase with alpha-factor and then released from the G1 phase by removing the mating hormone. Microscopy samples are collected every 10 minutes interval. B. Representative images for Cdc14 release status and Cdc14 localization at SPBs. Images come from WT and *bud14*Δ cells that carry Cdc14-GFP and mCherry-Tubulin. C. Percentage of cells with Cdc14 full release grouped according to the tubulin length. Unpaired multiple t-test is conducted for significance analysis. D. Percentage of cells with Cdc14 FEAR release grouped according to the tubulin length in MEN mutant strain background. For C and D experiments were repeated

3 times and at least total of 148 cells were counted per spindle interval per experiment. Mean values of each repeat are shown in the graph as well as the standard deviation of the 3 repeats. Two-way Anova is conducted for significance analysis of D. Only the significant results are shown in the graphs.

3.2 Cdc14 localization at the dSPB is prolonged in *bud14*Δ cells

Cdc14 localizes to the Spindle Pole Bodies (SPBs) upon its release. At SPBs, Cdc14 regulates specific MEN components to activate Mitotic Exit network (Pereira et al., 2002). We analyzed SPB localization of Cdc14 in WT and *bud14*Δ cells. Cells were synchronized in G1 phase using alpha factor treatment and released from this arrest to allow synchronous cell cycle progression of cells (Figure 3.1A-B). In WT cells, Cdc14 localized to the SPBs after anaphase onset (spindle length: 2.5-4 μm) and stayed at the SPBs until telophase (spindle length> 6 μm) (Figure 3.2B, 3.2C). In *bud14*Δ cells, Cdc14 was detected at the SPBs after anaphase onset like WT. Surprisingly, Cdc14 did not diminish from SPBs at telophase but stayed there after mitotic exit (broken spindle) until next G1. (Figure 3.2B). Thus, Cdc14 stayed at the SPB during anaphase, telophase and G1 phases in *bud14*Δ cells.

Although Cdc14 was at the SPBs of *bud14*Δ cell in next G1, we didn't observe Cdc14 localization to SPBs in alpha-factor arrested G1 cells (Figure 3.2B). This discrepancy may have resulted from various events: First, alpha factor treatment is known to effect the SPB structure (Yoder et al., 2003). Second, cell cycle arrest in G1 may have provided enough time for Cdc14 to leave SPBs. Both may account for the observed discrepancy in Cdc14 SPB localization.

To avoid influence of alpha factor arrest on our results, we analyzed SPB localization of Cdc14 in asynchronous cells (Figure 3.2A-C). Cells were grouped according to the spindle length like the experiment that used alpha factor synchronization. Like the data from alpha factor release experiment, Cdc14 localized to the SPBs in WT cells after the anaphase onset (spindle length: 2.5-4 μm) and remained there until telophase (spindle length > 6 μm) (Figure 3.2C). Different than the WT phenotype, Cdc14 localized to the SPB in 40% of no budded (G1) *bud14*Δ cells and disappeared from SPBs soon after *bud14*Δ cells started budding (small-budded cells with less than 2.5 μm tubulin) (Figure 3.2C). After anaphase onset Cdc14 relocalized to the SPBs of *bud14*Δ cells, in a way like WT cells. We didn't observe SPB localization in WT cells after the telophase (broken spindle). However, in *bud14Δ* cells,

Cdc14 localization to the SPB remained during telophase. In concordance with the experiment that used alpha-factor synchronization, this experiment supported that Cdc14 does not disappear from the SPBs of *bud14*Δ cells during telophase (broken) and remains until the next G1/S.

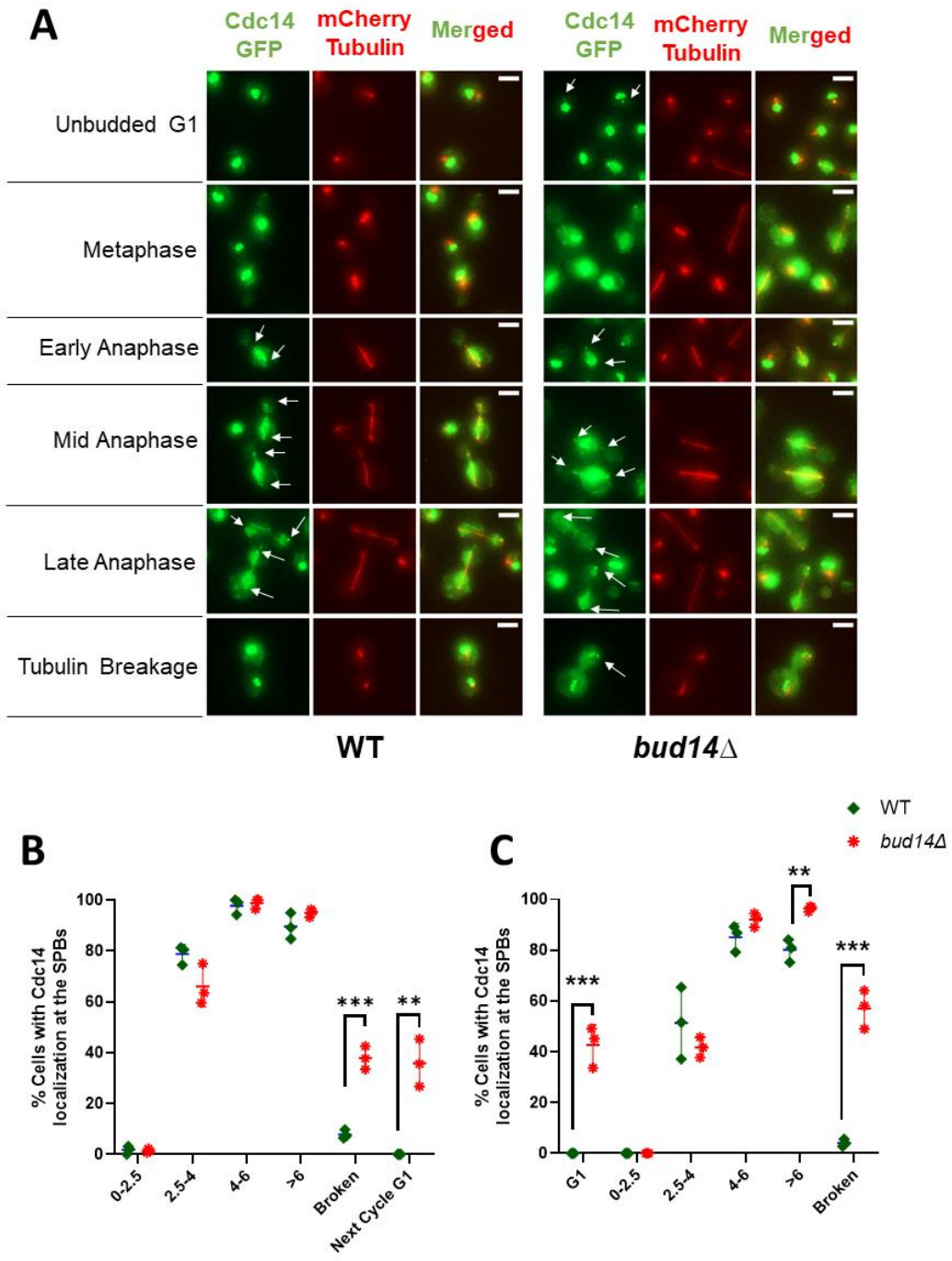

Figure 3. 2: Cdc14 localization to the SPBs is prolonged in *bud14*Δ until entry into the subsequent cell cycle. A. Representative images for Cdc14 localization to SPBs. Cells are

taken from logarithmically growing culture. B. % of cells with Cdc14 localization to the SPBs depending on the tubulin length, the cells are arrested at the alpha factor and released from arrest. Then PFA microscopy samples are taken in every 10-minute interval. C. % of cells with Cdc14 localization to the SPBs depending on the tubulin length, from logarithmically growing culture. Unpaired multiple t-test is conducted for significance analysis. Only the significant values are represented. Experiments were repeated 3 times and at least 48 cells were counted per spindle interval per experiment with at least total of 160 cells. Mean values of each repeat are shown in the graph as well as the standard deviation of the 3 repeats.

To understand Cdc14 SPB localization in more detail, we measured the relative intensities of Cdc14-GFP at the SPBs in WT and *bud14*Δ cells. In this analysis, we discriminated mother and daughter SPBs (mSPB and dSPB) (Figure 3.3). mSPB is the SPB localized to the mother cell and dSPB is localized to the daughter cell or that is directed to the daughter cell. To elucidate the localization timing in logarithmically growing cells, we measured the mean intensity of Cdc14 at SPBs as well as the tubulin length and budding, as markers for cell cycle progression. The levels of Cdc14 localization to the mSPB and dSPB exhibited different profiles during the cell cycle both in the wild type (Figures 3.3 C-E) and the mutant (Figures 3.3 C-E). Cdc14-GFP mSPB localization in *bud14*Δ and WT cells were similar in G1/S-S (tubulin length: 0-2.5 μm - budded), M-phases (tubulin length: 2.5-4, 4-6, >6 μm) and after mitotic exit (broken spindle) (Figure 3.3A). dSPB localization of Cdc14, however, remained high in *bud14*Δ cells after mitotic exit (broken spindle), whereas it started decreasing after mid-anaphase (tubulin length: 4-6 μm) in WT cells (Figure 3.3B). Importantly, when we quantified Cdc14-GFP at the SPB of no budded cells (G1), *bud14*Δ cells still had higher amount of Cdc14 at the SPB during this stage (Figure 3.3A-B). Although we cannot differentiate the origin of the SPB in no budded cells (whether it is coming the previous mother or the daughter), this increased localization may reflect the increase observed in dSPB after spindle breakdown. Taken together, these results are in line with the previous analysis shown in Figure 3.2 and it further shows that the Bud14 dependent change in Cdc14 SPB localization is mostly restricted to the dSPB. Bud14 is a protein that localizes to the daughter cell cortex, and it therefore may affect Cdc14 localization in the daughter cell. Moreover, Cdc14 localization to the SPBs is partly Bfa1-Bub2 dependent (Pereira et al., 2002) and the SPB carrying Bfa1-Bub2 complex is sent to the dSPB upon mitotic exit (Pereira et al., 2001). So, Bfa1 at dSPB may keep Cdc14 at its localization to the SPB.

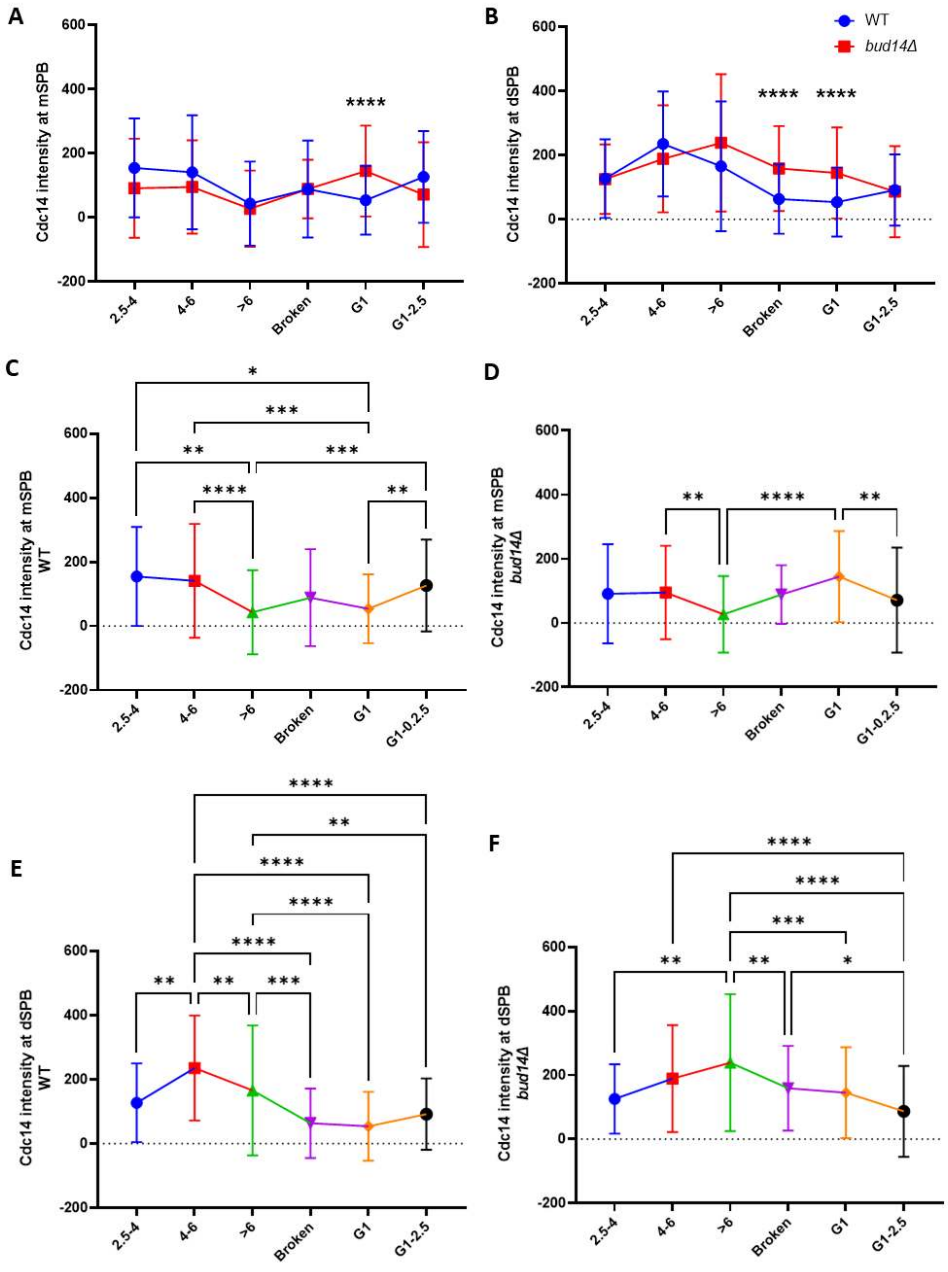

Figure 3. 3: Cdc14 is localization to the Spindle Pole Bodies are significantly prolonged in *bud14*Δ compared to WT. A. Cdc14 localization intensity to the mother SPB depending on the tubulin length. B. Cdc14 localization intensity to the daughter SPB depending on the tubulin length. Unpaired t-test is applied for A, B. C. Cdc14 localization intensity to the mother SPB in WT depending on the tubulin length with one-way Anova analysis for significance. D. Cdc14 localization intensity to the mother SPB in *bud14Δ* depending on the tubulin length with one-way Anova analysis for significance. E. Cdc14 localization intensity to the daughter SPB in WT depending on the tubulin length with one -way Anova analysis for significance. F. Cdc14 localization intensity to the daughter SPB in *bud14Δ* depending on the tubulin length with one-way Anova analysis for significance. Only the significant values are represented. 1 of 3 experimental set up in Figure 3.2 are counted and at least 30

SPBs were measured per spindle interval per experiment. Mean values of each repeat are shown in the graph as well as the standard deviation of these SPB intensities.

3.3 Cdc14 localization is FEAR and MEN dependent in WT and bud14Δ

Cdc14 is released from nucleolus with two subsequent mechanisms: FEAR and MEN (Stegmeier & Amon, 2004). These mechanisms are crucial for proper mitosis and mitotic exit. To understand the effects of MEN and FEAR pathways on Cdc14 localization to the SPB in *bud14*Δ cells, we performed microscopy analysis of *cdc15-1* cells released from alpha factor induced G1 arrest at 37 ºC (Figure 3.4A). *cdc15-1* is an MEN temperature sensitive mutant in which Cdc14 full release is prevented at 37 ºC, but FEAR release takes place in these cells at 37 ºC (Jaspersen et al., 1998; Mah et al., 2001). As a FEAR deficient control, *spo12*Δ cells were used. *cdc15-1 spo12*Δ double mutants cannot perform neither MEN nor FEAR. We analyzed Cdc14 localization to SPB depending on the tubulin length as a cell cycle progression marker.

*cdc15-1 spo12*Δ cells had markedly reduced Cdc14 SPB localization at the anaphase onset (spindle length: 2.5-4 μm) and during mid-anaphase (spindle length: 4-6 μm) based on population analysis (Figure 3.4B). Thus, FEAR release is necessary for Cdc14 localization to SPB. This is in line with previous reports (Stegmeier et al., 2002). However, unexpectedly, Cdc14 localization to the SPBs was reduced drastically at late anaphase arrested (spindle length: >6 μm) *cdc15-1* cells. This was not the case when we analyzed WT cells in which MEN activity was not blocked (Figure 3.2). This data suggests a probable effect of MEN in Cdc14 localization to the SPB. However, it is important to note that, in *cdc15-1* cells Cdc14 returns to the nucleolus during late anaphase, this is also reflected in our FEAR release analysis of Cdc14 in these cells (Figure 3.1D). Thus, a persistent Cdc14 release is necessary to keep Cdc14 at the SPBs in late anaphase. Taken together we conclude that FEAR (early and mid-anaphase) and MEN activity (late anaphase) is necessary for Cdc14 localization to the SPBs.

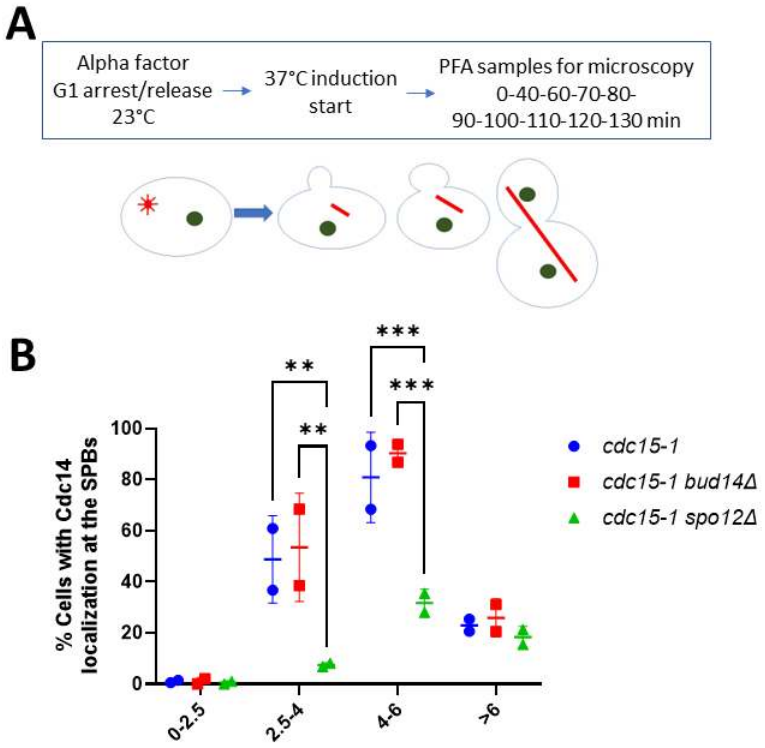

Figure 3. 4: Cdc14 localization is FEAR and MEN dependent. A. Experimental scheme. B. Percentage of cells that had Cdc14 localized to the SPBs. Data is grouped depending on the tubulin length. Two-way Anova is conducted for significance analysis. Only the significant values are represented. Experiments were repeated 2 times. Mean values of each repeat are shown in the graph as well as the standard deviation of the 2 repeats.

3.4 Cdc14 SPB localization is Bfa1 dependent in wild type and bud14Δ cells

Upon its release at the early anaphase from the nucleolus, Cdc14 is localized to the SPBs via its interaction with the Bfa1-Bub2 complex (Pereira et al., 2002). Accordingly in WT cells, Cdc14 SPB localization is Bfa1 dependent. We asked whether Cdc14 localization in *bud14*Δ cells are also Bfa1 dependent. To address this, we deleted *BFA1* from the WT and *bud14*Δ strains and quantified Cdc14-GFP localization at the SPBs (Figure 3.5A). First, we quantified the percentage of cells with Cdc14 SPB localization in these strains (Figure 3.5B-C). Next, we measured signal intensity of Cdc14-GFP at the dSPB of cells in log phase (Figure 3.5D-H). Cells were grouped according to the spindle length to provide grouping of cells in the same cell cycle progression. Upon *BFA1* deletion, percentage of cells that showed Cdc14 localization at their SPBs was greatly reduced in both WT and *bud14Δ* (Figure 3.5C). Even though the localization was visible in some cells, it was observed at a low intensity (Figure

3.5D-H). This indicates SPB localization of Cdc14 localization is dependent on Bfa1 irrespective of presence of *BUD14*. Prolonged localization of Cdc14 to the SPBs in *bud14Δ* is also reduced upon *BFA1* deletion. This indicates that Cdc14 at the SPBs of *bud14*Δ cells localize to the SPBs via Bfa1, as in wild type cells.

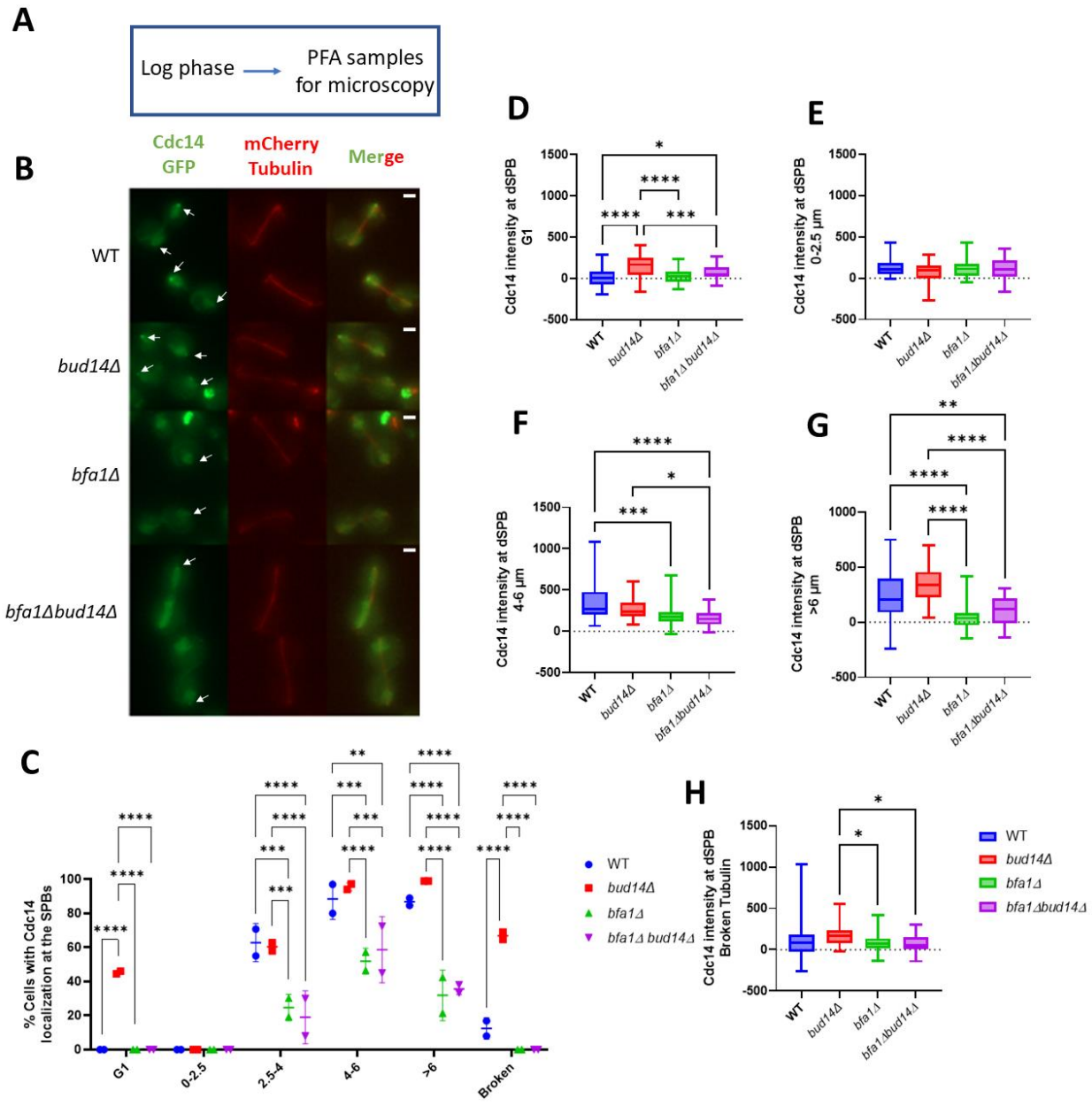

Figure 3. 5: *BFA1* deletion inhibits Cdc14 localization to the SPBs. A. Experimental scheme. B. Representative figure for SPB localization. C. Percentage of cells that had Cdc14 at the SPBs. D- Intensity of Cdc14-GFP at the SPB in G1. E-H. Intensity of Cdc14-GFP at the dSPB in G1/S-S-G2 cells (E), in mid anaphase cells (F) in late anaphase cells (G) and

after mitotic exit (H). At least 25 cell SPBs are counted and 20 cell SPB intensity is measured. Two-way Anova is conducted for C. One-way Anova is conducted for D to H.

3.5 Cdc14 is dynamically localized to the SPBs in both WT and *bud14*Δ.

We next asked whether the binding/dissociation dynamics of Bud14 to the SPBs change in the absence of *BUD14*. To investigate the localization dynamics of Cdc14 to the Spindle Pole body, we utilized the FRAP (Fluorescence recovery after photobleaching) technique. In this technique, a protein of interest tagged with GFP is photobleached using high intensity laser, and localization of new protein recruitment to the area is investigated. We successfully performed FRAP of Cdc14 localized to the daughter SPB during anaphase stage of the cell cycle (spindle >6). In WT cells, Cdc14-GFP quickly recovered after photobleaching with an average half-life of 2.366 sec and the Cdc14-GFP levels were restored up to 65% at the plateau. Thus, 65% of Cdc14 gets localized dynamically to the dSPB at late anaphase. In *bud14*Δ cells, as well, Cdc14 SPB interaction was dynamic with a half-life of 3.608 sec. The mobile fraction of Cdc14 in *bud14*Δ cells were around 58%. Of note, these values were not significantly different in WT and the *bud14*Δ. This means that Cdc14 localized to the daughter SPB with similar dynamics in both type of cells.

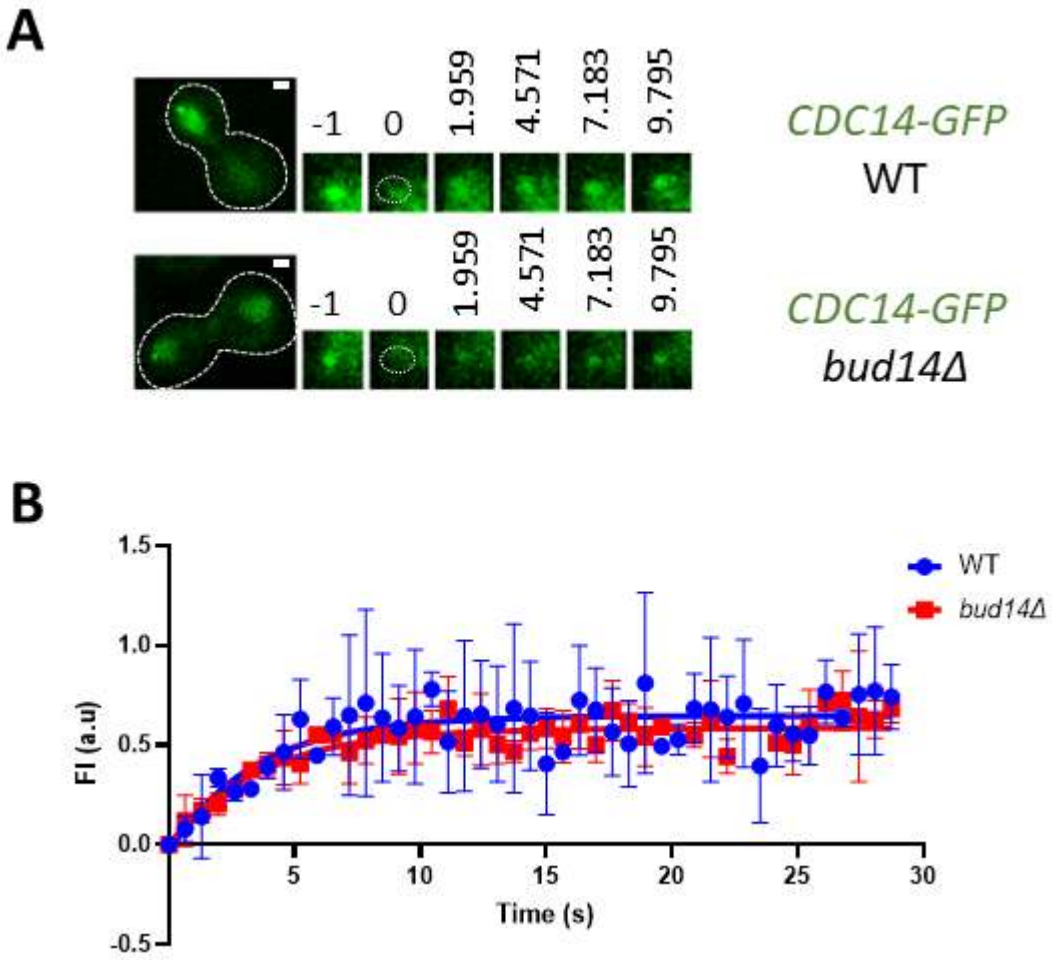

Figure 3. 6: Cdc14 is dynamically localized to the SPBs in both WT and *bud14*Δ. A. SPB ROI of FRAP recovery graph in WT. WT reaches the plateau 0.6462 (standard deviation = 0.2), halftime is 2.366 (standard deviation = 0.61), and the rate constant 0.2930 (standard deviation = 0.05) B. SPB ROI of FRAP recovery graph in *bud14Δ*. *bud14Δ* reaches the plateau 0.5843 standard deviation = 0.1), halftime is 3.608 (standard deviation = 1.2), and the rate constant 0.2772 (standard deviation = 0.12). Unpaired t-test is applied for significance analysis. 4 cells are analyzed for both strains. Average of cells were plotted. Error bars show standard deviation. Lines show the fitted graph.

3.6 Bfa1 is more abundantly localized to the SPBs upon BUD14 deletion.

Bfa1 association is necessary for Cdc14 localization to the SPBs. This association intrigued us to investigate Bfa1 localization in *bud14*Δ cells. Bfa1 levels at the dSPB of *bud14*Δ cells were significantly higher than that of WT cells at all cell cycle stages analyzed (Figure 3.7C), whereas increased Cdc14 dSPB localization was only observed during telophase and G1 in *bud14*Δ cells (Figure 3.3B). Cdc14 localization at the mSPB was not significantly altered by

deletion of *BUD14* (Figure 3.3A), whereas more Bfa1 localization to the mSPB were observed from G1 to early anaphase in *bud14*Δ cells than in WT cells (Figure 3.7B). These data altogether show that Bud14 dependent changes in Bfa1 localization does not correlate with Bud14 dependent changes in Cdc14 localization at the SPBs. This suggests that Bud14 may regulate Bfa1 and Cdc14 SPB localization independently of one another.

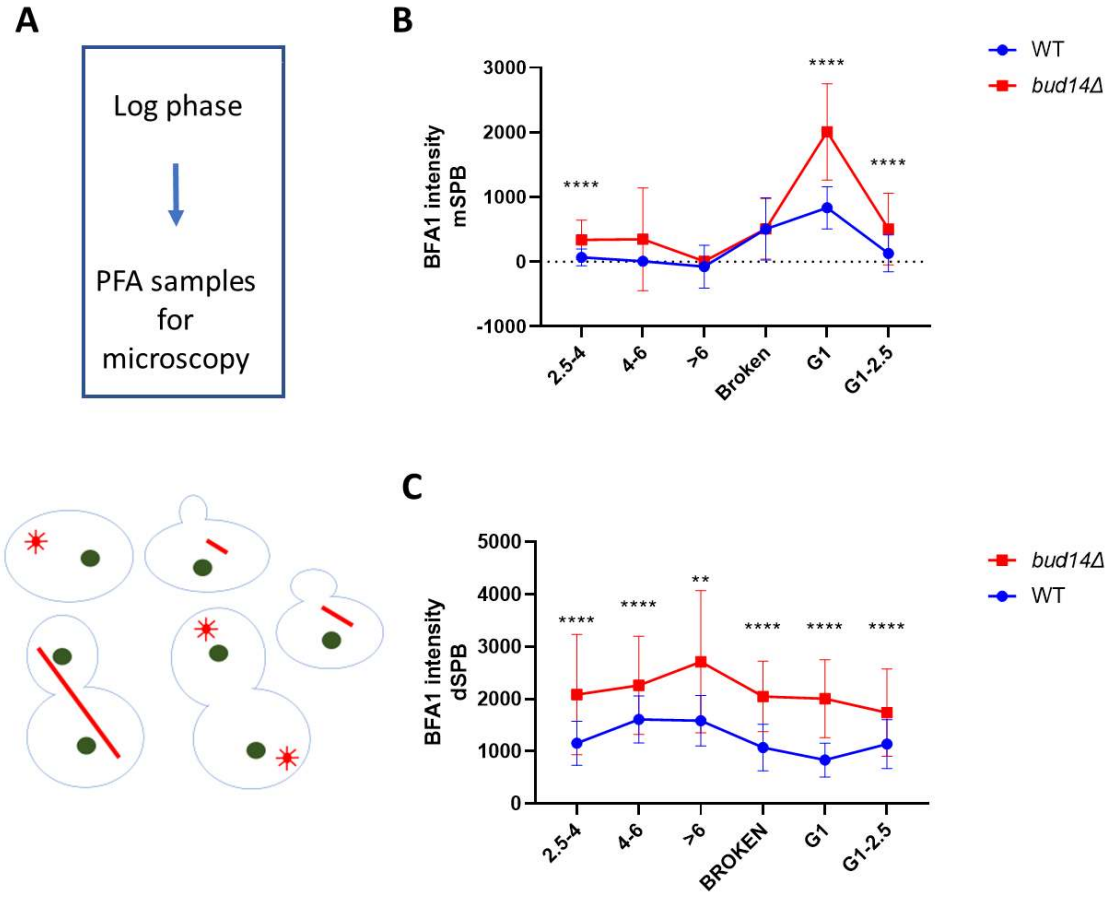

Figure 3. 7: Bfa1 is more abundantly localized to the SPBs upon Bud14 deletion. A. Experiment plan scheme. B. Bfa1 localization to the mother SPB depending on the tubulin length. C. Bfa1 localization to the daughter SPB depending on the tubulin length. At least 23 Bfa1 intensity is measured. Dots show the average of measurements. Error bars are standard deviation. Unpaired multiple t-test is applied for significance analysis.

3.7 Cdc14 interacts with Bud14 and Bfa1 in Yeast Two-Hybrid System, and the interaction is not dependent on each other.

We previously showed that Bud14 interacts with Bfa1 (Kocakaplan et al., 2021). Here, we wanted to understand whether Bud14 interacts with Cdc14 as well. To address this question, we took a yeast two hybrid approach. Cdc14, Bud14, and Bfa1 were expressed in fusion with LexA DNA binding protein or Gal4-activation domain. We investigated the interaction using both directions for all proteins. In this system, if two proteins interact or come too close to each other in a complex, we expect a blue color formation.

Bud14 and Cdc14 pair produced blue color indicating their proximity. We further tested the effect of some known Bud14 mutants in Cdc14 interaction, and in each case, we observed blue color formation as an indication of the interaction (Figure 3.8A). We asked whether this interaction is Bfa1 dependent. Thus, we analyzed the interactions in a *bfa1*Δ background. Interactions remained the same in the absence of *BFA1* in our yeast two-hybrid system. This means Bud14-Cdc14 interaction is not Bfa1 dependent (Figure 3.8A).

Moreover, we checked the known Cdc14 and Bfa14 interaction (Pereira et al., 2002) in our yeast two-hybrid system. As expected, it resulted in blue color formation (Figure 3.8B). Further, we sought to understand if Bud14 has a role in this interaction. We compared our yeast two-hybrid results with Bud14 deletion, and the interaction remained still. Thus, we conclude that the Cdc14-Bud14 interaction is not Bud14 dependent (Figure 3.8B).

These experiments altogether suggest that Bud14 and Cdc14 interact with Bfa1 independently of each other and likewise Bud14-Cdc14 interaction is not dependent on Bfa1.

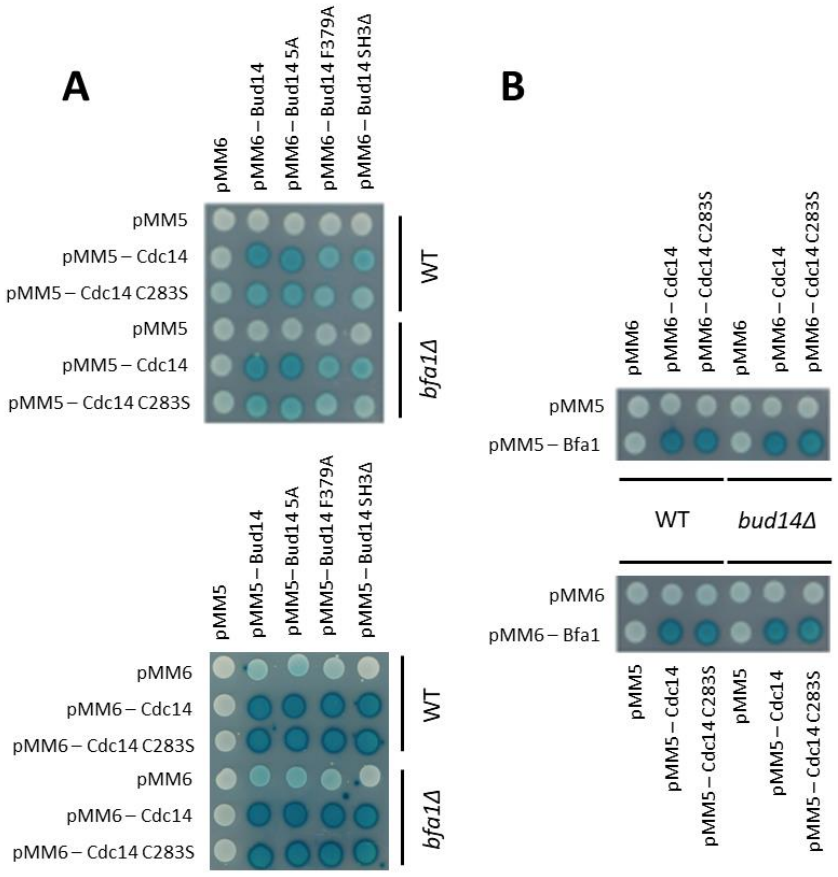

Figure 3. 8: Cdc14 interacts with Bud14 and Bfa1 in Yeast Two-Hybrid System, and the interaction is not dependent on each other. pMM5 with LexA DNA binding domain and pmm6 with GAL4 Activation domain. A. Cdc14 – Bud14 yeast two-hybrid interaction assay with Cdc14 (full length, substrate trap mutant) and Bud14 mutants (Bud14, F379A glc7 binding mutant, ΔSH3 which diminishes Bud14 bud cortex localization, 5A the formin regulatory motif mutant) in WT and *bfa1*Δ strain. B. Bud14 – Bfa1 yeast two-hybrid interaction assay.

3.8 Cdc14 localization is switched to the WT when the full-length Bud14 gene is introduced but not with the glc7 binding mutant.

Bud14 is one of many regulatory subunits of the protein phosphatase 1 (Cullen & Sprague, 2002; Knaus et al., 2005). We asked whether Bud14 influence on Cdc14 requires Bud14-Glc7 interaction. To test this, we cloned Bud14 gene and its endogenous promoter into the pRS405 backbone. Later we performed site-directed mutagenesis to obtain *bud14*-F379A mutation. *bud14*-F379A mutant fails to bind Glc7 (Knaus et al., 2005). Next, we integrated these plasmids into the Leu2 locus of *CDC14*-GFP mCherry-*TUB1 bud14*Δ cells to perform add-back experiments. Bud14 WT and mutant were expressed similarly (Figure 3.9B). As

expected, add-back of the full-length Bud14 (*BUD14*) showed the Cdc14 SPB localization phenotype as in WT cells (Figure 3.9A-C). However, add-back of the *bud14*-F379A resulted in a *bud14*Δ phenotype (figure 3.9C) while the expressions of Bud14 were comparable. These data indicate that Glc7-Bud14 interaction is essential for Bud14's role in Cdc14 SPB localization.

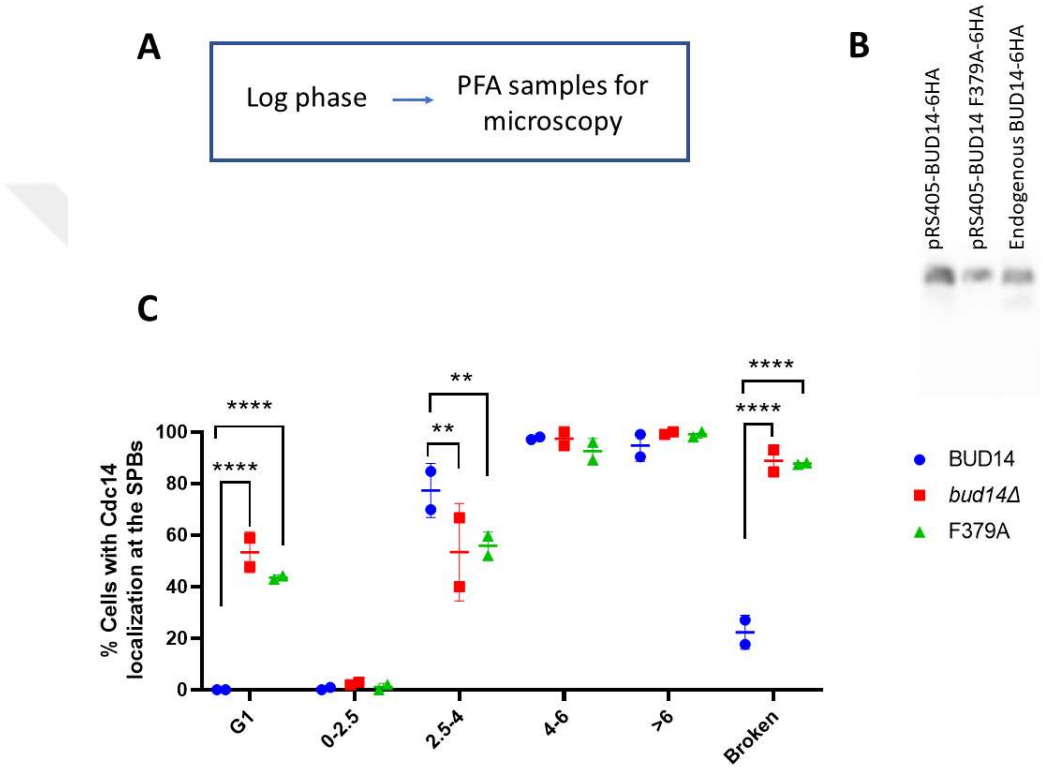

Figure 3. 9: Cdc14 localization is switched to the WT when the full-length Bud14 gene is introduced but not with the glc7 binding mutant. A. Experiment plan scheme. B. Representative Western Blot of integration BUD14, BUD14 F379A and endogenous Bud14 expressions C. CDC14 localization to the SPBs regarding the tubulin length. Two-way Anova is conducted for significance analysis. Only the significant values are represented.

Chapter 4 : CHARACTERIZATION OF THE ROLE OF *CDC36* ON MITOTIC EXIT

4.1 Partial inactivation of Cdc36 rescues Gal1-*KIN4* toxicity.

Kin4 is a known spindle position checkpoint (SPOC) activator. In case of spindle mispositioning, the Kin4 branch of SPOC gets activated, preventing the cell cycle through Mitotic Exit Network inhibition (D'Aquino et al., 2005). Thus, overexpression of Kin4 halts cells at telophase due to inhibition of the mitotic exit network (MEN). In a previous study conducted by Dr. Ayşe Koca Çaydaşı and Ms. Betül Sarı, they found that Kin4 overexpression was not any more toxic in the temperature-sensitive mutant which they named *rkt1-1* (Sarı, 2021) (Figure 5.1). Through whole-genome sequencing, we identify that *rkt1-1* is a temperature-sensitive mutant of *CDC36* (*cdc36-16*) (Reed, 1980). A nonsense mutation in the mutant gene produces a mutant protein truncated after the 136th amino acid. *CDC36* is a core subunit of the CCR4-Not complex which regulates mRNA levels (Alhusaini & Coller, 2016). Our aim is to investigate how the absence of Cdc36 activity supports mitotic exit.

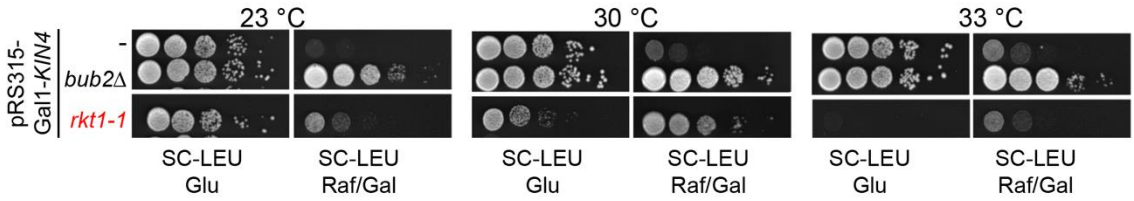

Figure 4. 1: *cdc36-16* rescues cell cycle arrest (Sarı, 2021)

4.2. Analysis of mRNA levels in WT and *cdc36-16* from anaphase onset until mitotic exit

Because Cdc36 is known to be involved in regulation of mRNA levels, we reasoned that differences in the mRNA levels likely accounts for the rescue phenotype observed. We hypothesized that especially differences during anaphase and telophase would be contributing to this phenotype the most. In order to collect samples in this window of the cell cycle we used the following experimental set up:

First, we synchronized WT and *cdc36-16* mutant at the G1 phase via alpha factor treatment at 23 ^{o}C. Then, we released the G1-arrested cells into nocodazole containing medium to allow metaphase arrest. At this stage, temperature was shifted to 30 ^{o}C, to allow partial inactivation of *cdc36-16*. Importantly, growth rescue phenotype was observed more pronouncedly at 30 ^{o}C (Figure 4.1). We then removed nocodazole from the medium to allow metaphase arrested cells (T0) progress into anaphase, and concomitantly added alpha factor to the medium to keep cells synchronized until the next G1 (Figure 4.2A). Samples were collected at indicated time points for western blot (Figure 4.2B), microscopy (Figure 4.2C), and for RNAseq experiments. Clb2 degradation served as a marker for mitotic exit and percentage of cells with separated 2 DAPI stained regions (nucleus) showed the cell percentage that transited into anaphase. Based on Clb2 blots, we observed a delay in Clb2 degradation in *cdc36-16* mutant compared to the WT. To better assess the Clb2 degradation profile, we quantified Clb2 protein band intensities and divided it to the Tubulin (Tub1) band intensities yielding relative Clb2 levels (Figure 4.2E). A delay of 10 min in complete degradation of Clb2 was noted in *cdc36-16* mutant compared to the wild type. Based on anaphase cell percentage graphs, mutant cells' progression in anaphase was 10 minutes slower (Figure 4.2C, E).

The decrease in percentage of cells with separated nucleus at the end of the experiment corresponds to a point after mitotic exit. Thus, we considered the point before this decrease (peak point of percentage of cells with separated nucleus) as the end point (t4) of samples to be analyzed with RNAseq. We reasoned that this peak point corresponds to a time around M/G1 transition. This time point is 60 min after release for WT and 70 min after release for the *cdc36-16.* We considered three consecutive time points before t4, to have a total of four time point for each type of cells (t1-t2-t3-t4). Accordingly, the initial point of samples (t1) was 30 min after release for WT and 40 min after release for the *cdc36-16.* This time point corresponded to a time where about 30% of the cells entered anaphase in both cell types.

Later, collected samples were processed for RNA sequencing in collaboration with Prof. Dr. Halil Kavaklı and Dr. Şeref Gül. Briefly, we isolated the total RNAs of the samples and prepared their cDNA library then we sent the samples for sequencing (see materials methods for details). We had two aims in this study: First, to identify the changes in the levels of single mRNAs from anaphase until M/G1 transition and pinpoint those mRNAs that are subjected to change at this window of the cell cycle. Second, to understand differentially expressed

genes in the mutant compared to the wildtype. We reasoned that these differentially expressed genes may help us understand how *cdc36-16* can exit mitosis upon Kin4 overexpression.

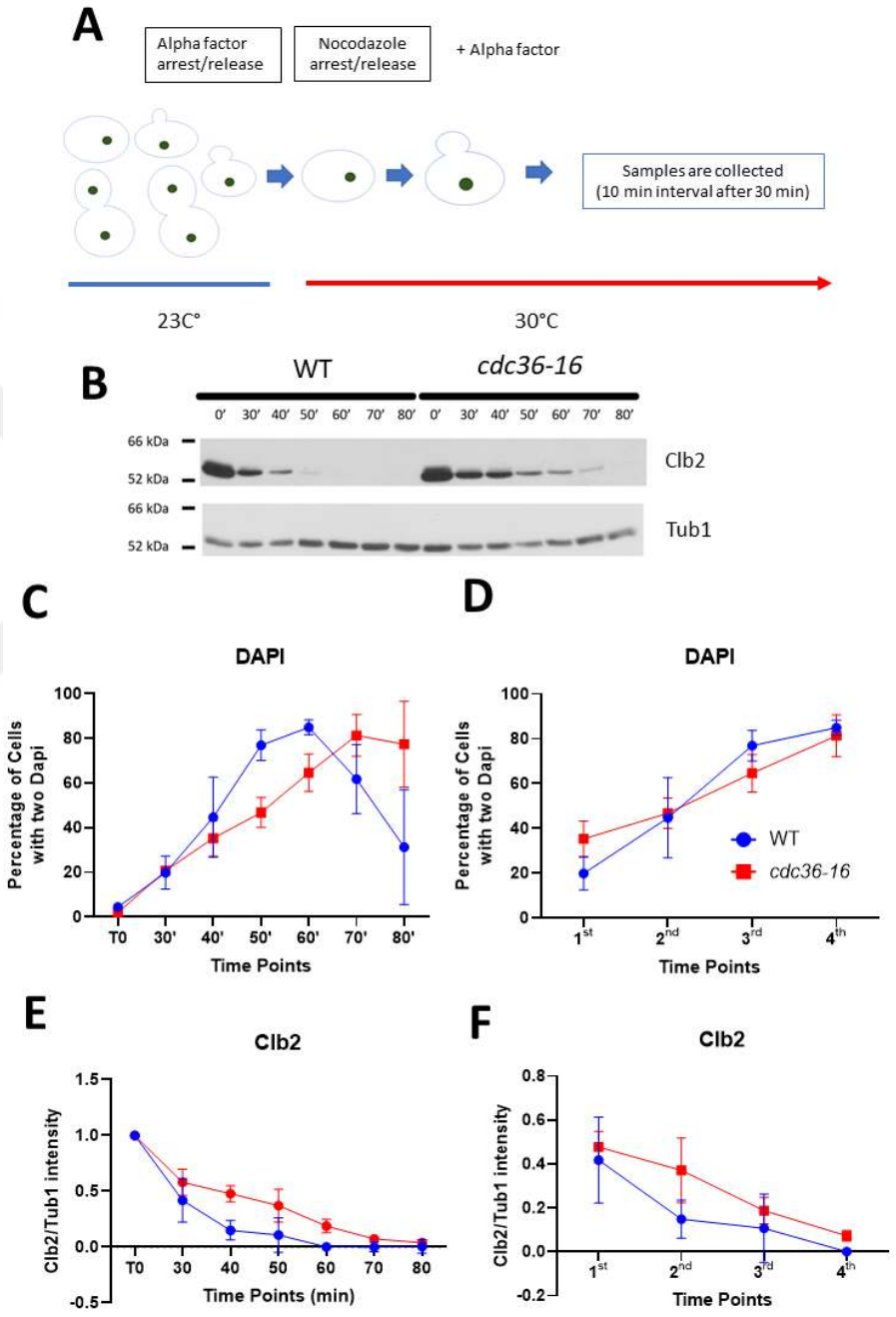

Figure 4. 2: WT and *cdc36-16* experimental set up. A. Experiment flow. See text for details. B. Representative Western Blots for Clb2 and Tub1 levels. Time points are minutes after release from metaphase C. Percentage of cells with separated nucleus (2 DAPI). D. As in C but focusing on the time points that are selected for RNA sequencing. E. Clb2 protein

levels normalized to the Tubulin and the first time point of WT. F. As in E but focusing on the time points that are selected for RNA sequencing. 1st, 2nd, 3rd, and 4th timepoints correspond to 30, 40, 50, 60 minutes and 40, 50, 60, 70 minutes after release from metaphase of WT and *cdc36-16* respectively. Graphs show average of 3 repeats. Error bars are standard deviation. For C and E, at least 100 cells were counted per timepoint.

4.3 1214 and 1324 genes were differentially expressed from anaphase onset to next G1 in wild type and the cdc16-16 respectively

To identify mRNAs, those levels change during anaphase onset until the next telophase, we performed the Time Series KMeans clustering algorithm, an unsupervised machine learning algorithm of tslearn (Romain Tavenard, 2020). This algorithm clusters time series with similar changing phenotypes. Thus, it enables visualization of genes that showed similar changes in their expression during the experiment. For example, if a gene is upregulated at the 2nd time point and downregulated at the 3rd time point, it will be found in a cluster that contains genes that show a similar phenotype. After clustering, mRNAs those levels did not deviate less than 1.5 -fold in any of the time points were considered as mRNAs not changing during course of the experiment. Rest of the genes were defined as differentially expressed genes from anaphase onset until next G1 (anaphase-telophase-G1) in our experimental set up. The number of genes which we found to be expressed in a cell cycle dependent manner was 1214 genes in the wild type (WT) and 1324 in *cdc36-16*. 694 of the genes were detected in both WT and the mutant. Depending on the change in their expression patterns during anaphase-to-G1, differentially expressed genes were successfully represented in 26 and 25 clusters in WT and the mutant respectively (Figure 4.3)

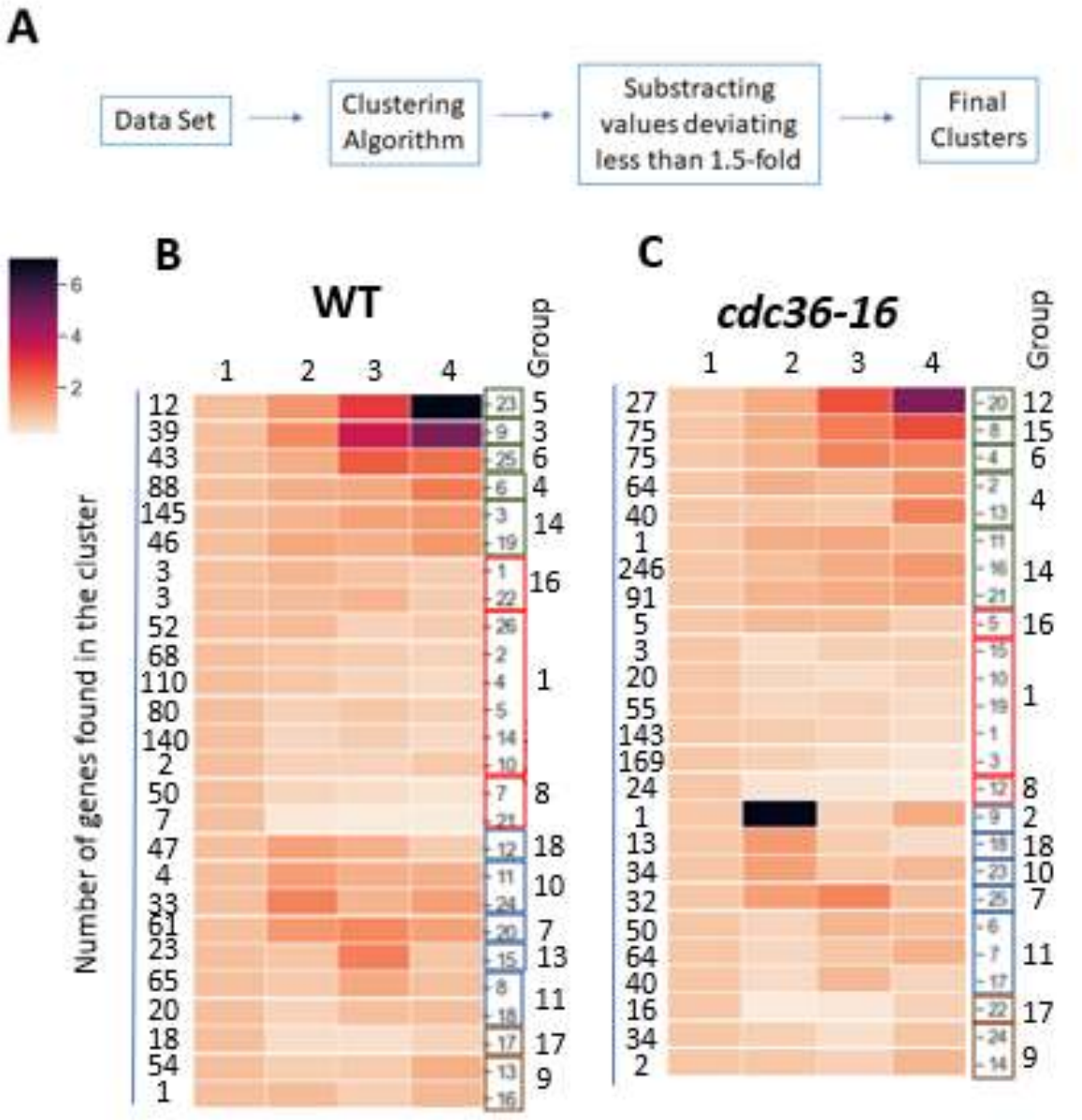

Figure 4. 3: 1214 genes were found to be cell cycle changed during anaphase onset to G1 transition in WT A. Data analysis scheme. See text for further detail. B-C. Clustermap of cluster means. "Cluster mean" is the average expression value of mRNAs in each cluster per timepoint. Note that expression value is normalized according to 1st time point. Cluster numbers are given on the right side of the map. Number of genes in each cluster is shown on the left. Clusters that show similar behavior are grouped together in new groups marked in squares (Section 5.6). Cluster number is indicated at each row withing the box. Group numbers are shown on the right side of the squares. See text for more detail. These groups represent: increasing expression profile (marked with green box), decreasing expression profile (marked with a red box), an expression profile where the expression peaks at the second or third time point (marked with a blue box) or where the expression undergoes a transient fall at the second or third time point (marked with a brown box). B shows the values in WT whereas, C shows the values in the mutant.

Previous studies identified various genes as transcriptionally changed during the cell cycle (Gauthier et al., 2010; Granovskaia et al., 2010; Rowicka et al., 2007; Spellman et al., 1998). 400 among 1214 genes identified in our analysis of wild type cells were previously identified in wild type cells (Figure 4.4A), whereas 814 transcripts (genes and dubious ORF) were not identified before as cell cycle regulated genes (Figure 4.4A). Among 814 genes, 148 of them were dubious open reading frames. Dubious open reading frames correspond to 13.7% of our data set. However, these previous studies identified fewer percentage of dubious open reading frames. (Granovskaia et al. 1.2%, Rowicka et al. 1.8%, Spellman et al 6.3%, Gauthier et al. 2.6%). It is important to note that data from previous studies mostly came from microarray analysis (Gauthier et al., 2010; Granovskaia et al., 2010; Rowicka et al., 2007; Spellman et al., 1998) while our data comes from RNA sequencing, which provides higher sensitivity. Furthermore, our samples came from cultures synchronously progressing from anaphase onset to the next G1 (M, M/G1, G1), whereas previous studies covered other phases as well. In other words, our analysis is in more depth and focused on a smaller time frame of the cell cycle. These may be the reasons why more genes and dubious open reading frames were detected in our study.

Indeed, our analysis of wild type data identified the vast majority (up to 95%) of the mRNAs that were previously shown to peak in M (Clb2 cluster), M/G1 (Sic1 Cluster), and M/G1 (MCM cluster) phases according to Zhu et al. (Gauthier et al., 2010; Zhu et al., 2000) (Figure 4.4C) and a significant amount of the mRNAs that were shown to peak in M/G1 and M according to Spellman et al. (Spellman et al., 1998) (Figure 4.4B). Intriguingly, data coming from *cdc36-16* mutant identified lesser amount of M, M/G1 phase specific genes identified by Zhu et al and Spellman et al (Figure 4.4C) and more of G1/S and G2 genes (Figure 4.4B), which may be a consequence of major gene expression changes in the mutant.

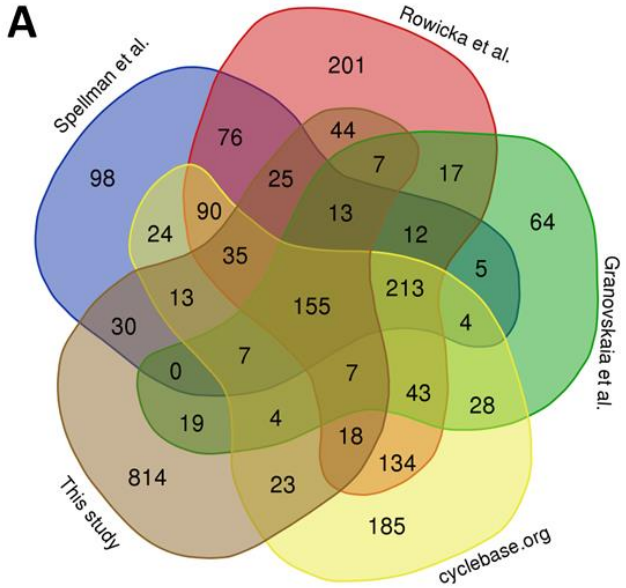

B

CELL PHASE	WT	*cdcc36-16*
G1	29.67	48.67
S	29.58	23.94
G2	19.83	22.31
M	42.05	34.87
M/G1	54.87	43.36

C

Cell Cycle Clusters	WT	*cdcc36-16*
CLB2 CLUSTER (M)	80.77	76.92
CLN2 CLUSTER (G1)	43.75	68.75
SIC1 CLUSTER (M/G1)	95	55
MCM CLUSTER (M/G1)	85.71	71.43
HISTONE CLUSTER (S phase)	87.5	25

Figure 4. 4: Comparison of cluster analysis with previously identified cell cycle changed genes. 155 of the genes we found in our clustering study is shared with 4 previous studies and 814 is unique to our study of which 148 are dubious open reading frames. B. % of genes in the Spellman et al. data set that were also identified in this study. C. % of genes in the Zhu et al. data set that were also identified in this study.

We compared our clusters in terms of the genes that they include. We used previously identified cell cycle clusters by Zhu et al to investigate this. Between the WT and the mutant, Clb2 (95%) and MCM (83%) shared the most similar genes. However, Sic1 (58%), CLN2 (29%) and Histone (29%) cluster show the least similarity in terms of the genes they include. When we compared genes from clusters defined by Zhu et al., that were also identified in our analysis, except the genes in CLN2 (G1) cluster and histone cluster (S phase) genes' expression profiles were similar in WT and mutant (Figure 4.5). Moreover, in CLN2 cluster genes, whereas we observed mostly downregulated genes in the mutant, in the WT most of the genes were upregulated (Figure 4.5). Moreover, we observed a smaller number of genes of histone cluster in the mutant that also shows a different phenotype than the mutant. It may also be important that expression levels of SIC1 cluster genes were also different. Notably, the different cluster of genes are mostly G1/S and S phase clusters. This shows the changes in account of the cell division machinery in WT and the mutant.

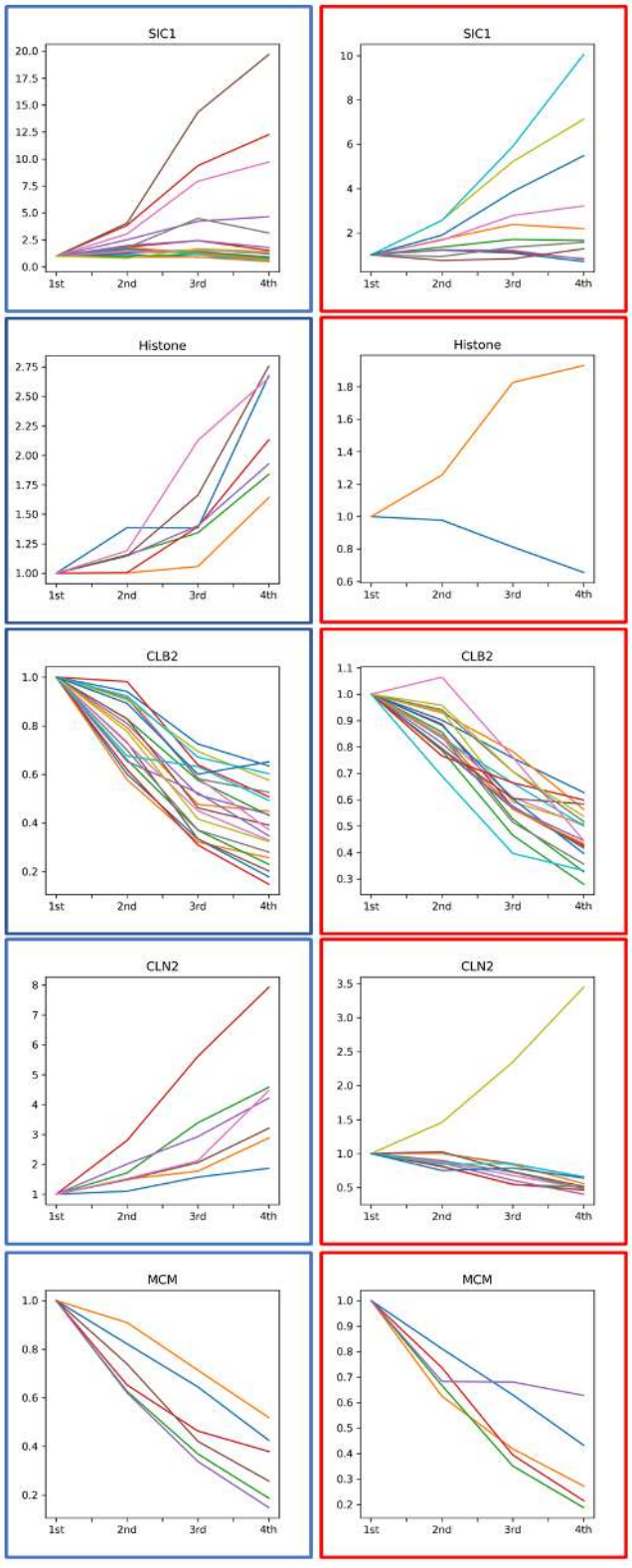

Figure 4. 5: Genes that are previously identified as cell cycle clusters. Blue boxes represent WT and red boxes represent the mutant. Y axis represents the transcript count normalized by the first time point. X axis represents corresponding time points. Here,

previously identified cell cycle cluster elements that are also found in our analysis are plotted. While some of the clusters show similar phenotype some don't. Note that the y axis limits are different for each graph.

4.4 Around half of the genes were found in both groups

So far, we identified 1214 genes for the WT and 1324 genes for the *cdc36-16* mutant to be deviating at least 1.5-fold in one of the time points. 694 of these genes were present in both WT and *cdc36-16*. These genes were later clustered into 26 and 25 clusters based on their change in time (Figure 4.3.B-C, each row represents a cluster).

To be able to compare clusters of WT and the mutant, we applied Time Series KMeans clustering algorithm to the means of 26 and 25 clusters and obtained 18 groups of clusters (Figure 4.6). 12 of them were shared by WT and the mutant, whereas 3 were unique to the WT, and 3 were unique to the mutant (Figure 4.6).

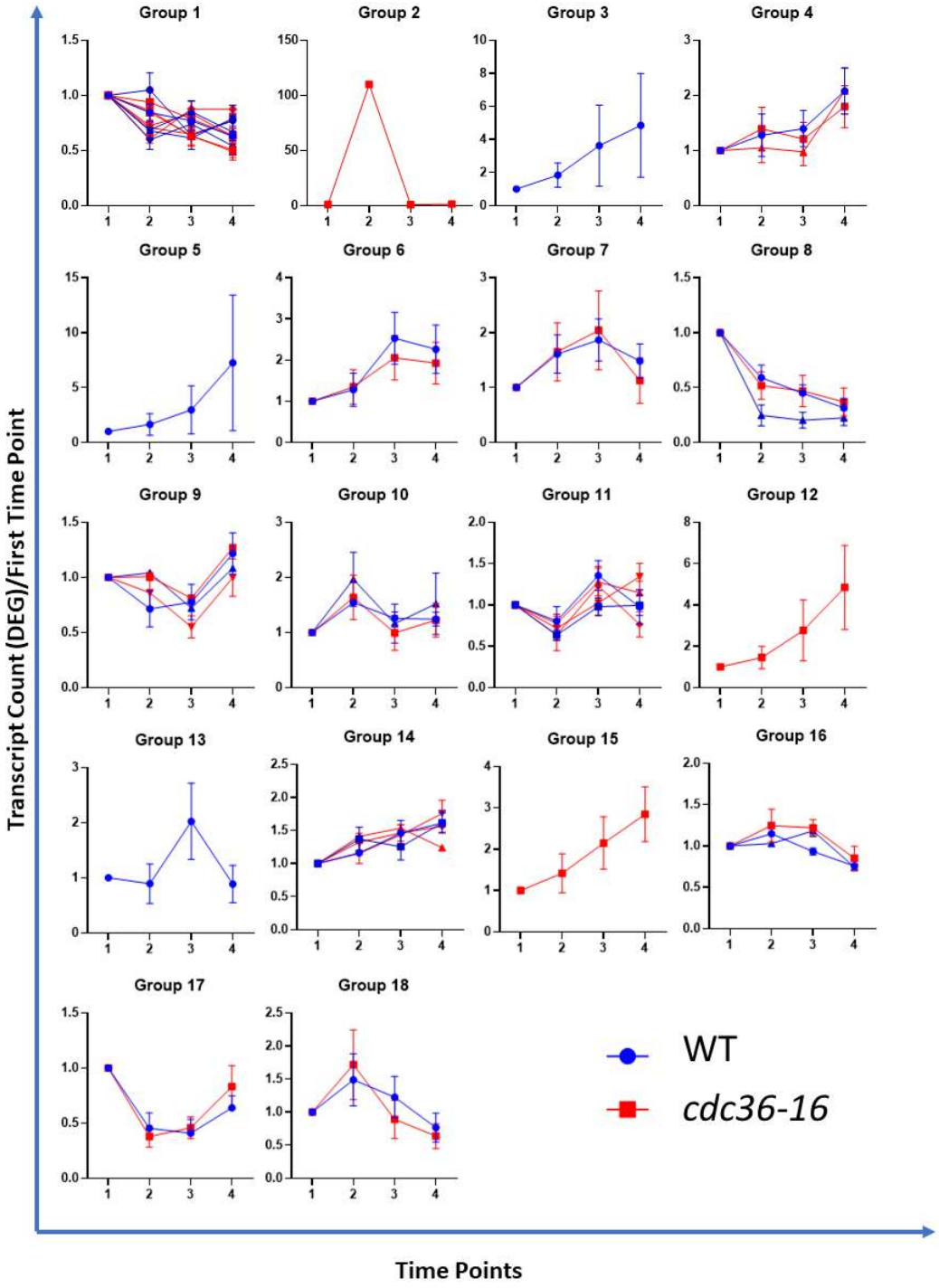

Figure 4. 6: Clusters of WT and *cdc36-16* mutant were clustered together in 18 groups. The error bars represent standard deviation. Blue and white lines represent individual clusters in wild type. The exact cluster numbers within each group can be visualized in Figure 4.3B-C.

To our surprise among the 694 genes common to both strains, only 227 fell into the same group in this analysis. This means that most of the cell cycle regulated genes identified in both wild type and the mutant are not behaving the same.

Later, we investigated whether the genes found in related groups were identical. Surprisingly, we observed WT and the mutant to be highly differentiated. While some groups contain identical genes for up to 19% of the cluster, some don't even have a single identical gene. As stated before, 694 of the deviating genes were common to both strains. However, only 227 of them were found in the same groups. This is interesting because even if expression of a gene was changing in a cell cycle dependent manner in both wild type and the mutant, the rate of expression changes or the direction of expression change differs between the wild type and the mutant.

Our grouping method is sensitive to rate changes thus differentiates between rates of mRNA change. We categorized the groups according to the outcome of mRNA changes in time, irrespective of changes in their rate and we obtained 4 categories of gene expression profiles during Anaphase-Telophase-G1. These categories were (1) increasing, (2) decreasing, (3) peaking at t2, (4) falling at t2-3. When we considered these four main categories in our analysis, 401 of the 694 common genes fell into the same category. This is a larger number compared to the 227 genes that fall into the same group. This suggests that 227 genes showed identical behavior while 174 genes showed similar behavior in WT and the mutant, but the remaining 293 genes' expression was completely different in the mutant than the wild type.

4.5 Deseq2 analysis of WT and *cdc36-16* show differences in a variety of mechanisms.

Corresponding time points of WT and *cdc36-16* were analyzed by Deseq2 to understand the WT and mutant differences in more detail. This was a collaborative work with Dr. Şeref Gül and Prof. Dr. Halil Kavaklı. Dr. Gül performed the analysis. As a result, we obtained genes that are down or upregulated in the mutant. A variety of pathways were shown to be upregulated or downregulated in the mutant compared to the WT. Complete results of this analysis are not shown in this thesis. However, it is worth mentioning that mRNA levels of many cell cycle related genes were changed significantly between the mutant and the WT. Among 143 mitotic cell cycle genes defined (Project; Wong et al., 2013), 90 of them show

differential regulation at least one point of the experiment time scale (Figure 4.7). It indicates that the mutant mitotic cell cycle machinery is highly differentiated than the WT.

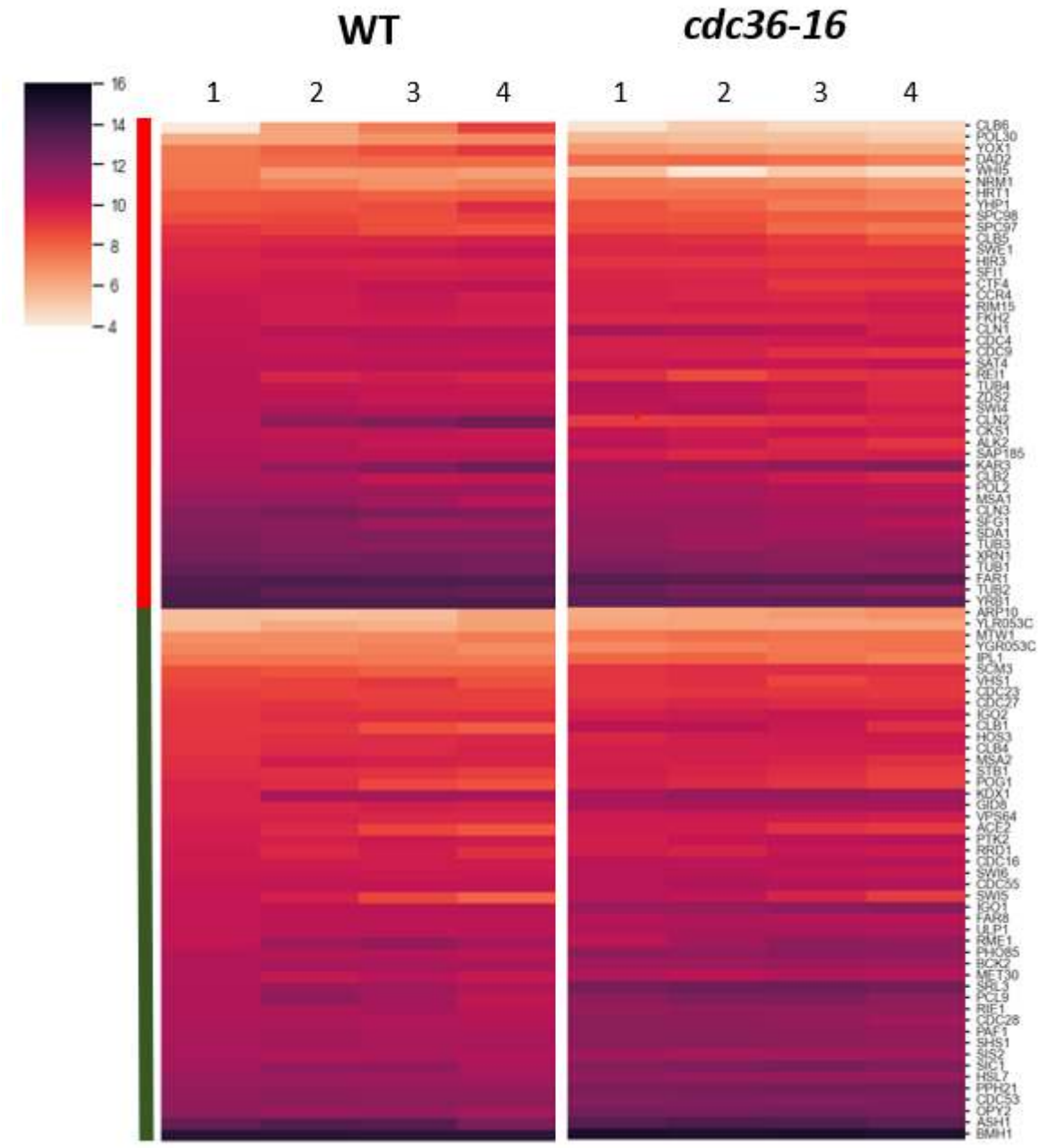

Figure 4. 7: Many mitotic cell cycle related genes were regulated according to Deseq2 analysis. Clustermap showing the mitotic cell cycle genes that upregulated or downregulated in at least one of the time points. Red part shows genes that were downregulated in *cdc36-16* and green part shows genes that were upregulated. All values are normalized using log2 conversion.

Mitotic Exit Network regulates the exit from mitosis. One of these genes that has role in this pathway is Mob1. It is known that Mob1 is a part of Ccr4 transcriptional complex and is required for activation of Dbf2 kinase for activation of Mitotic Exit Pathway (Komarnitsky et al., 1998). Our results indicate upregulation of Mob1 in *cdc36-16* mutant. Thus, we tested if Mob1 protein is also more expressed in *cdc36-16* in our experiment set up. We employed the same experimental set up that was used to obtain samples for RNAseq analysis. Total protein extracts of WT and *cdc36-16* cells that contain Mob1-3HA were run in SDS-PAGE and western blot was performed using anti-HA antibodies. Clb2 as a cell cycle marker and Tubulin as a loading control were used. Relative Clb2 levels from corresponding time points were calculated and were found to be similar to the previous experiment. Mob1 band intensities were quantified relative to the Tubulin intensity. We found that Mob1 protein levels were upregulated in *cdc36-16* (Figure 4.8). Increased levels of Mob1 may be leading to the cell cycle arrest rescue we observe.

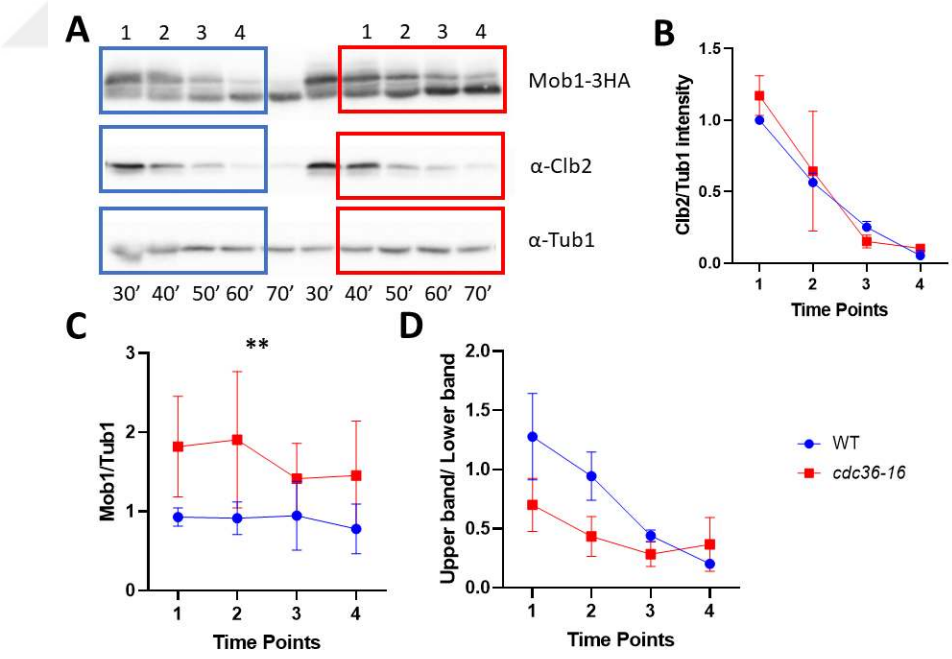

Figure 4. 8: Mob1 levels were upregulated in *cdc36-16.* A. Representative blot images. Corresponding timepoints are shown as 1,2,3,4 Blue is WT and red ones are the *cdc36-16* mutant. B. Corresponding anaphase onset to G1 samples are collected depending on their Clb2 degradation levels and Dapi counts (not shown). C. Mob1 levels were ** significantly different according to unpaired t-test D. Mob1 bands level comparison was not significantly different.

Moreover, we also observed many genes to be downregulated or upregulated in homeostasis and membrane transport related pathways. In literature, it is previously shown that MEN mutants exit from mitosis in response to HOG (High Osmolarity Glycerol Pathway) pathway induction (Reiser et al., 2006). The main role of HOG pathway is to regulate cell machinery to increased osmolarity conditions and our Deseq2 analysis showed many homeostatic and transport machineries to be differentially regulated in between WT and the *cdc36-16* mutant. We found 150 HOG pathway related gene among 270 defined HOG pathway genes (Project; Wong et al., 2013) to be differentially expressed at least one of the time points of which 69 of them were differentially expressed at all of the time points. We observed differential expression of HOG pathway genes when we visualized their transcript counts (Figure 4.9). Thus, HOG pathway can be another explanation for the rescue phenotype.

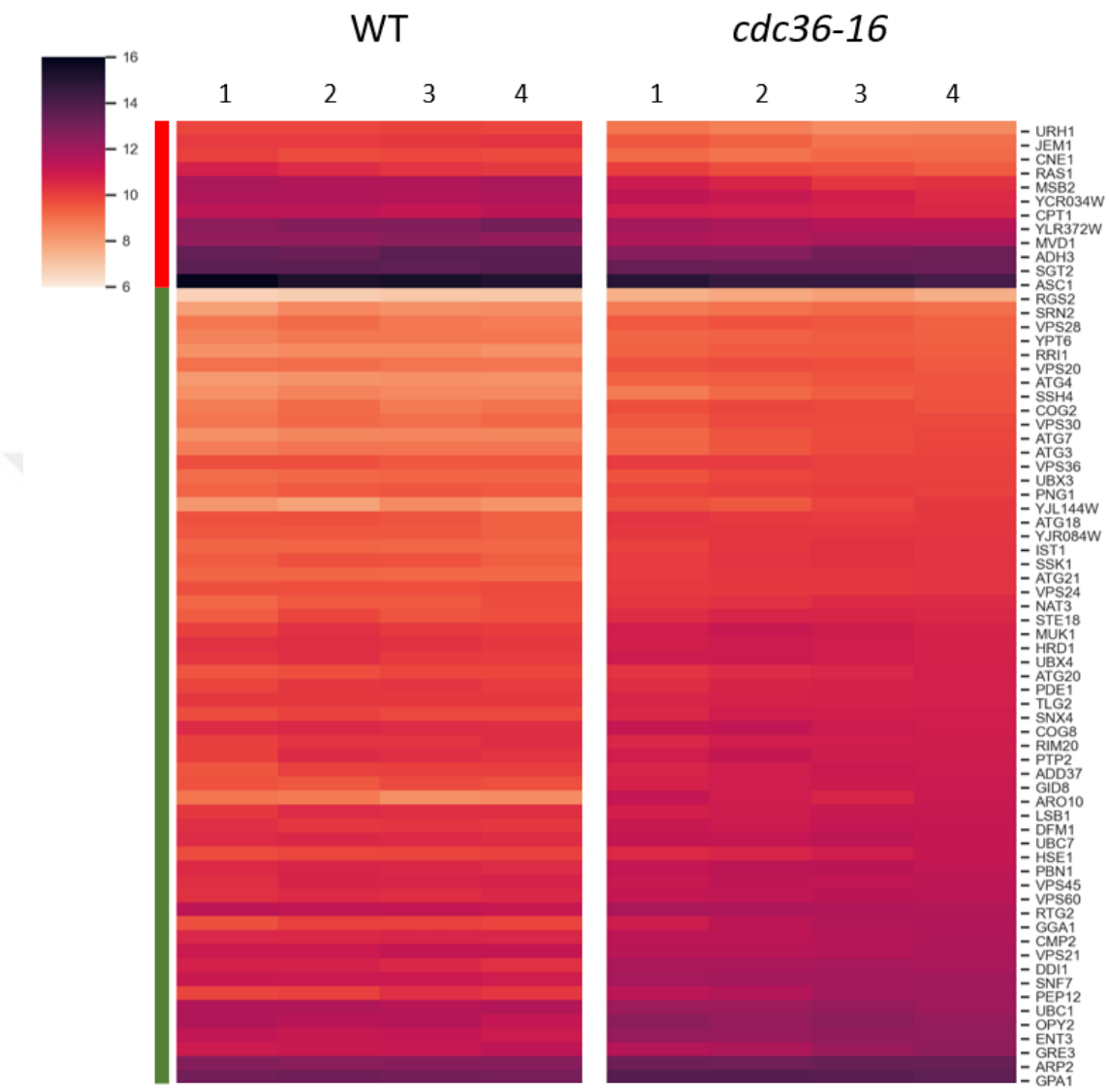

Figure 4. 9: Many HOG pathway related genes were regulated according to Deseq2 analysis. Clustermap showing the HOG pathway genes that upregulated or downregulated at each time point. Red part shows genes that were downregulated in *cdc36-16* and green part shows genes that were upregulated. All values are normalized using log2 conversion.

Chapter 5 : DISCUSSION

5.1 Characterization of the role of Bud14 in Cdc14 localization to the SPB

In this thesis, we showed that Cdc14 localization to the dSPB is altered in the absence of Bud14. Upon tubulin breakage Cdc14 is disappeared from the dSPB in WT cells while it remained on the dSPB until the next cycle (G1/S-S) in *bud14Δ* (Figure 3.2B, Figure 3.2C). This indicates prolonged Cdc14 localization at the dSPBs of *bud14*Δ cells. Thus, Bud14 may be part of a mechanism that removes Cdc14 from the dSPB in telophase. The prolonged Cdc14 localization phenotype was also observed in the Bud14-F379A mutant that cannot bind to Glc7 suggesting that Bud14-Glc7 plays a role in this process (Figure 3.9 B). Bud14 is a protein that localizes to the daughter (bud) cell cortex from the time cell starts budding until the end of mitosis. It also recruits Glc7 to this location. Bud14-Glc7 disappears, most likely is released from the daughter cortex into the cytoplasm upon mitotic exit. Thus, it is tempting to speculate that Bud14-Glc7 may be regulating Cdc14 and/or the SPB or associated factors specifically in the daughter cell, which may result in the observed Cdc14 localization phenotype in the dSPB.

Upon G1-S transition however the removal occurs in the absence of Bud14. Thus, a CDK dependent mechanism may be promoting removal at this stage in parallel to Bud14-Glc7.

Moreover, when we arrested cells at the G1 phase using alpha-factor mating hormone the SPB localization to the Cdc14 is diminished (Figure 3.2B). There may be possible reasons for this: First, G1 arrest by alpha factor may happen later than Cdc14 removal in *bud14Δ.* Second, the time required for the G1 arrest may be enough for Cdc14 removal in *bud14Δ.* Third, alpha-factor produces alterations on the SPB composition which in the end resets the Bud14 phenotype on Cdc14 localization. Fourth, there may be other factors affecting Cdc14 localization in alpha-factor arrested cells. To test these ideas, the progress of alpha-factor arrest can be visualized in sense of Cdc14 localization and other components of SPB.

In the literature it is shown that upon *bfa1Δ,* Cdc14 localization to the SPB is lost (Pereira et al., 2002). Our result is in accordance with the literature in that both *bfa1Δ* and *bud14 Δ bfa1Δ* double mutant loses the Cdc14 localization to the SPBs (Figure 3.5C). This indicates that the majority of Cdc14 localized to the SPBs via Bfa1 even in the absence of Bud14. Interestingly we observed significantly higher localization of the Bfa1 to the dSPB. The relationship

between Cdc14 localization to the SPBs and Bfa1 needs more investigation to understand. It is not clear whether more Cdc14 localization comes from the higher levels of Bfa1. However, since Bfa1 is still localized more in the cell stages where Cdc14 is removed from the SPB in *bud14Δ* there must be other elements regulating the process.

We observed that inhibitions of Cdc14 release pathways (FEAR and MEN) also limits Cdc14 localization to the SPBs. It is reasonable because if the Cdc14 cannot be released from the nucleolus it cannot localize to the SPBs as well. In the *cdc15-1* MEN mutant, FEAR pathway is still active and Cdc14 is localized to the SPBs in early and mid-anaphase cells. However, it is removed from the SPB at the late anaphase (Figure 3.4). It shows Cdc14 is removed from the SPB after the FEAR release if MEN is not activated and Cdc14 is localized to the SPBs at the late anaphase by MEN. Importantly, FEAR release is transient in *cdc15-1* cells, thus Cdc14 returns to the nucleolus at the late anaphase arrest point. Thus, a persistent Cdc14 release is necessary to keep Cdc14 at the SPBs in late anaphase.

Our FRAP experiments showed that Cdc14 localizes dynamically to the SPBs at the late anaphase (Figure 3.6). However, in our analysis the SPB binding dynamics of *bud14*Δ cells were similar to that of wild type cells. Also, majority of Cdc14 was bound to the SPBs via Bfa1 in both cell types in anaphase. So, Bud14 likely does not affect SPB binding site or dynamics of Cdc14. It could be possible that perhaps the number of Bfa1 and/or Cdc14 binding sites may be changing.

We showed the interaction between Cdc14-Bud14 using yeast two hybrid system and these interactions did not depend on Bfa1. This data also suggests a direct link between Cdc14 and Bud14. However, we do not now at this stage the functional importance of this interaction for Cdc14 localization. Also, we knew Cdc14 interacts with Bfa1.Our yeast hybrid data showed that this interaction is independent of Bud14. This is in line with our observation that Cdc14 SPB localization dependent on Bfa1 irrespective of Bud14.

Bud14 Glc7 binding mutant does not revert the Cdc14 localization phenotype, while showing an interaction with the Cdc14 in our yeast two hybrid system. This interaction may not be sufficient to revert the phenotype. Thus, it is not just interaction of Bud14 with Cdc14, but a possible activity of Bud14-Glc7 is necessary for altering Cdc14 SPB localization.

In this thesis it is shown that upon *BUD14* deletion the Cdc14 localization is prolonged at the SPB, but we cannot comment on its effects on the cell cycle machinery. Functional analysis

of the phenotype should be investigated. CDK and Cdc14 oscillations are key events regulating the SPB duplication. Cdc14 removes the inhibitory phosphorylation on SPB duplication elements made by CDK. Our data show presence of Cdc14 at the SPB in phases where CDK activity is high. The outcomes of this aspect can are intriguing and must be further investigated.

Moreover, we propose the origin of the SPB in no budded cells to be daughter SPB. Bud14 is a protein that localizes to the daughter cell cortex, and it therefore may affect Cdc14 localization in the daughter cell. Our data also indicates Bud14 dependent change in Cdc14 SPB localization is mostly restricted to the dSPB. In addition, Cdc14 localization to the SPBs is partly Bfa1-Bub2 dependent (Pereira et al., 2002). Upon mitotic exit the SPB which carries Bfa1-Bub2 complex is sent to the dSPB (Pereira et al., 2001). We also observed higher levels of Bfa1 localization at the SPB at no budded G1 cells (Figure 3.7). Higher Bfa1 levels may be the reason behind the prolonged Cdc14 localization.

To sum up, our results indicate that Cdc14 localization is altered upon Bud14 deletion, and this phenotype is dependent on other mechanisms that regulate the Cdc14 release and SPB regulation. Bud14 needs its interaction partner Glc7 to regulate the process. We cannot state whether the effect of Bud14 on Cdc14 localization is direct or indirect. In vitro reconstitution experiments should be performed to understand this.

5.2 The role of Cdc36 in M- G1 Transition

In this thesis, we investigated genes that were expressed in a cell cycle dependent manner in WT and in *cdc36-16* mutant during a time period from the anaphase onset until transition into next G1. We identified 1214 such genes in the WT and 1324 genes in the *cdc36-16* mutant (Figure 4.3). These genes were successfully clustered using Time Series KMeans clustering algorithm into 26 clusters for the WT and 25 clusters for *cdc36-16* (Figure 4.3). We identified 814 new cell cycle regulated genes or dubious open reading frames in our study, in addition to 400 genes identified in previous studies. We think that our experimental set up constitute a more sensitive analysis compared to previous studies for two reasons: First, previous studies of yeast cell cycle regulated genes were based on microarray analysis, whereas our work is based on RNAseq analysis. Second, our experiment setup focused on a

narrow period (Anaphase-Telophase-G1) of the cell cycle with 10-minute resolution of total 40 minutes.

When we analyzed the common genes identified in our study and previous studies, we found that our study of wild type transcriptome captured vast majority of the genes that were shown to peak in M and M/G1. However, the situation was different in the *cdc36-16.* Our transcriptome analysis of the mutant mostly captured genes that were reported to peak in M/G1 and G1 to show cell cycle dependent changes. Some of the expression patterns were also different between WT and the mutant. These changes in the cell cycle dependent genes may eventually lead to the rescue phenotype.

A previous study conducted by Zhu et al, identified specific cell cycle clusters. We took these clusters as a reference to understand cell cycle related genes in our analysis. As a result, we observed mitotic and early G1 cluster of genes to be show cell cycle changed phenotype in the WT. However, we detected more early G1 and G1/S gene clusters changes in the mutant. The phenotypes of these clusters were also different between the WT and the mutant. Surprisingly, while late G1 and G1/S gene expression was increasing in the WT, most of them were decreasing in the mutant such as CLN2 cluster genes. To sum up, in mutant, some cell cycle dependent genes show different phenotypes than the WT

Moreover, we identified plenty of more genes showing cell cycle dependent changes similar to those genes that were previously identified in cell cycle clusters. It is an interesting aspect to study the new genes and investigate if they have roles like or independent from them.

Around half of the genes we found to be changing in the inspected time window of the cell cycle were commonly detected both in the WT and the mutant. However, a significant portion of the common genes (293 genes out of 694) exhibited a different expression category in the mutant than the WT. This indicates, expression profile of many cell cycle regulated genes was drastically changed in the mutant.

Furthermore 520 genes, we found to be changing in a cell cycle dependent manner in the wild type were found not to be among the cell cycle regulated in the mutant. In other words, their cell cycle dependent regulation was lost in the mutant which means those regulatory pathways may no longer be effective.

Intriguingly, even though the clusters of gene expression profiles in wild type and the mutant did not contain the same genes, similar clusters contained a high level of similar GOs. This

means even though different genes were upregulated or downregulated, they had similar roles in the cell cycle. So, activation of redundant mechanisms in the mutant may be an adaptation. However, it is hard to pinpoint the roles of those genes specifically.

Another aspect came to our attention was the dubious open reading frames. We observed 166 dubious open reading frames for the WT and 164 dubious open reading frames for the mutant. 95 of these dubious open reading frames were shared between both strains. However, they showed less similarity in terms of their change phenotypes as well. 15.8% were in the same groups and 34.7% were in the same categories. Moreover, most of these dubious open reading frames were not previously defined as cell cycle changed before. These dubious open reading frames are not expected to produce meaningful products, but they still may have roles in the regulation of the cell cycle. Thus, we believe these dubious open reading frames should be further investigated as well. In our analysis 13.7% of the cell cycle regulated genes were dubious open reading frames. This proposes, even though they are not translated into products they can still have roles in mediating the cell cycle.

We also conducted a Deseq2 analysis to understand the differences between WT and the mutant in detail. We observed many pathways to be differentially regulated. Among those pathways cell cycle and cell homeostasis related pathways came mostly to our attention. As expected, many RNA machinery pathways were also differentially regulated. Among cell cycle genes we found Mob1 to be upregulated in the mutant, which may account for the rescue phenotype. It is notable that Mob1 interacting with Dbf2 was identified to be a Ccr4-Not complex component (Komarnitsky et al., 1998) which interacts physically (Miller et al., 2018). Moreover, homeostatic pathways are also notably critical; as previously shown, HOG pathway activation results in phenotypic rescue of MEN mutants (Reiser et al., 2006). We also investigated HOG pathway-related genes to observe the difference further, and we observed many of them be upregulated or downregulated. These two pathways may be working together or separately. However, it would be interesting to look for the link between Mob1 overexpression and HOG pathway activities.

In this thesis, we followed a broad way of understanding the events in the anaphase onset to G1 transition and the difference between WT and the mutant in this sense. We identified several genes that show similar phenotypes as previously identified cell cycle regulated genes. Their relation to cell cycle machineries should be investigated to understand other

elements working in the cell cycle. Moreover, we observed a level of dubious open reading frames which indicates their role in this cell cycle phase as well. It is also notable that, most of the changes between WT and the mutant were either different in the gene level or the behavior of the gene's activity. Many cell cycle regulated genes were not regulated anymore in the mutant, but we detected other genes that were not regulated in the WT. Moreover, some genes were cell cycle regulated in both WT and the mutant but in a different manner. These differences need further investigation.

Finally, our DEG analysis shows a variety of mechanisms differentiated between WT and the mutant which cell cycle machineries and cell homeostasis took most of our attention. Mob1 is a known component of the Ccr4-Not complex and we showed its upregulation in the mutant which may resulted in the cell cycle arrest rescue. Moreover, MEN mutants also show rescue phenotype in response to HOG pathway activation, however, the mechanism behind is not specified clearly. These two mechanisms may work in parallel or together. The relationship between these two responses is worth looking into. Moreover, we observed many other mechanisms to be differentiated in the mutant such as cell wall biogenesis, organelle organization processes as well as transcription and translation machineries. These functional aspects should also be investigated.

Chapter 6 : REFERENCES

Adams, I. R., & Kilmartin, J. V. (1999, May 17). Localization of core spindle pole body (SPB) components during SPB duplication in Saccharomyces cerevisiae. *J Cell Biol, 145*(4), 809-823. https://doi.org/10.1083/jcb.145.4.809

Alhusaini, N., & Coller, J. (2016, May). The deadenylase components Not2p, Not3p, and Not5p promote mRNA decapping. *RNA, 22*(5), 709-721. https://doi.org/10.1261/rna.054742.115

Althoefer, H., Schleiffer, A., Wassmann, K., Nordheim, A., & Ammerer, G. (1995, Nov). Mcm1 is required to coordinate G2-specific transcription in Saccharomyces cerevisiae. *Mol Cell Biol, 15*(11), 5917-5928. https://doi.org/10.1128/MCB.15.11.5917

Amberg, D. C. (1998, Dec). Three-dimensional imaging of the yeast actin cytoskeleton through the budding cell cycle. *Mol Biol Cell, 9*(12), 3259-3262. https://doi.org/10.1091/mbc.9.12.3259

Avena, J. S., Burns, S., Yu, Z., Ebmeier, C. C., Old, W. M., Jaspersen, S. L., & Winey, M. (2014, Oct). Licensing of yeast centrosome duplication requires phosphoregulation of sfi1. *PLoS Genet, 10*(10), e1004666. https://doi.org/10.1371/journal.pgen.1004666

Bai, Y., Salvadore, C., Chiang, Y. C., Collart, M. A., Liu, H. Y., & Denis, C. L. (1999, Oct). The CCR4 and CAF1 proteins of the CCR4-NOT complex are physically and functionally separated from NOT2, NOT4, and NOT5. *Mol Cell Biol, 19*(10), 6642-6651. https://doi.org/10.1128/MCB.19.10.6642

Barberis, M. (2021, Dec 13). Cyclin/Forkhead-mediated coordination of cyclin waves: an autonomous oscillator rationalizing the quantitative model of Cdk control for budding yeast. *NPJ Syst Biol Appl, 7*(1), 48. https://doi.org/10.1038/s41540-021-00201-w

Bardin, A. J., Visintin, R., & Amon, A. (2000, Jul 7). A mechanism for coupling exit from mitosis to partitioning of the nucleus. *Cell, 102*(1), 21-31. https://doi.org/10.1016/s0092-8674(00)00007-6

Bergen, L. G., & Borisy, G. G. (1980, Jan). Head-to-tail polymerization of microtubules in vitro. Electron microscope analysis of seeded assembly. *J Cell Biol, 84*(1), 141-150. https://doi.org/10.1083/jcb.84.1.141

Berset, C., Griac, P., Tempel, R., La Rue, J., Wittenberg, C., & Lanker, S. (2002, Jul). Transferable domain in the G(1) cyclin Cln2 sufficient to switch degradation of Sic1 from the E3 ubiquitin ligase SCF(Cdc4) to SCF(Grr1). *Mol Cell Biol, 22*(13), 4463-4476. https://doi.org/10.1128/MCB.22.13.4463-4476.2002

Bertazzi, D. T., Kurtulmus, B., & Pereira, G. (2011, Jun 13). The cortical protein Lte1 promotes mitotic exit by inhibiting the spindle position checkpoint kinase Kin4. *J Cell Biol, 193*(6), 1033-1048. https://doi.org/10.1083/jcb.201101056

Bhaduri, S., & Pryciak, P. M. (2011, Oct 11). Cyclin-specific docking motifs promote phosphorylation of yeast signaling proteins by G1/S Cdk complexes. *Curr Biol, 21*(19), 1615-1623. https://doi.org/10.1016/j.cub.2011.08.033

Biggins, S., & Rose, M. D. (1994, May). Direct interaction between yeast spindle pole body components: Kar1p is required for Cdc31p localization to the spindle pole body. *J Cell Biol, 125*(4), 843-852. https://doi.org/10.1083/jcb.125.4.843

Bloom, J., & Cross, F. R. (2007, Feb). Multiple levels of cyclin specificity in cell-cycle control. *Nat Rev Mol Cell Biol, 8*(2), 149-160. https://doi.org/10.1038/nrm2105

Botstein, D., Chervitz, S. A., & Cherry, J. M. (1997, Aug 29). Yeast as a model organism. *Science, 277*(5330), 1259-1260. https://doi.org/10.1126/science.277.5330.1259

Botstein, D., & Fink, G. R. (1988, Jun 10). Yeast: an experimental organism for modern biology. *Science, 240*(4858), 1439-1443. https://doi.org/10.1126/science.3287619

Bullitt, E., Rout, M. P., Kilmartin, J. V., & Akey, C. W. (1997, Jun 27). The yeast spindle pole body is assembled around a central crystal of Spc42p. *Cell, 89*(7), 1077-1086. https://doi.org/10.1016/s0092-8674(00)80295-0

Byers, B., & Goetsch, L. (1975, Oct). Behavior of spindles and spindle plaques in the cell cycle and conjugation of Saccharomyces cerevisiae. *J Bacteriol, 124*(1), 511-523. https://doi.org/10.1128/jb.124.1.511-523.1975

Carminati, J. L., & Stearns, T. (1997, Aug 11). Microtubules orient the mitotic spindle in yeast through dynein-dependent interactions with the cell cortex. *J Cell Biol, 138*(3), 629-641. https://doi.org/10.1083/jcb.138.3.629

Caydasi, A. K., Micoogullari, Y., Kurtulmus, B., Palani, S., & Pereira, G. (2014, Jul 15). The 14-3-3 protein Bmh1 functions in the spindle position checkpoint by breaking Bfa1 asymmetry at yeast centrosomes. *Mol Biol Cell, 25*(14), 2143-2151. https://doi.org/10.1091/mbc.E14-04-0890

Caydasi, A. K., & Pereira, G. (2009, Jan). Spindle alignment regulates the dynamic association of checkpoint proteins with yeast spindle pole bodies. *Dev Cell, 16*(1), 146-156. https://doi.org/10.1016/j.devcel.2008.10.013

Chalabi Hagkarim, N., & Grand, R. J. (2020, Oct 29). The Regulatory Properties of the Ccr4-Not Complex. *Cells, 9*(11). https://doi.org/10.3390/cells9112379

Cho, R. J., Campbell, M. J., Winzeler, E. A., Steinmetz, L., Conway, A., Wodicka, L., Wolfsberg, T. G., Gabrielian, A. E., Landsman, D., Lockhart, D. J., & Davis, R. W. (1998, Jul). A genome-wide transcriptional analysis of the mitotic cell cycle. *Mol Cell, 2*(1), 65-73. https://doi.org/10.1016/s1097-2765(00)80114-8

Ciosk, R., Zachariae, W., Michaelis, C., Shevchenko, A., Mann, M., & Nasmyth, K. (1998, Jun 12). An ESP1/PDS1 complex regulates loss of sister chromatid cohesion at the metaphase to anaphase transition in yeast. *Cell, 93*(6), 1067-1076. https://doi.org/10.1016/s0092-8674(00)81211-8

Clemente-Blanco, A., Sen, N., Mayan-Santos, M., Sacristan, M. P., Graham, B., Jarmuz, A., Giess, A., Webb, E., Game, L., Eick, D., Bueno, A., Merkenschlager, M., & Aragon, L. (2011, Oct 23). Cdc14 phosphatase promotes segregation of telomeres through repression of RNA polymerase II transcription. *Nat Cell Biol, 13*(12), 1450-1456. https://doi.org/10.1038/ncb2365

Cohen-Fix, O., & Koshland, D. (1997, Dec 23). The anaphase inhibitor of Saccharomyces cerevisiae Pds1p is a target of the DNA damage checkpoint pathway. *Proc Natl Acad Sci U S A, 94*(26), 14361-14366. https://doi.org/10.1073/pnas.94.26.14361

Cohen-Fix, O., Peters, J. M., Kirschner, M. W., & Koshland, D. (1996, Dec 15). Anaphase initiation in Saccharomyces cerevisiae is controlled by the APC-dependent degradation of the anaphase inhibitor Pds1p. *Genes Dev, 10*(24), 3081-3093. https://doi.org/10.1101/gad.10.24.3081

Collart, M. A. (2016, Jul). The Ccr4-Not complex is a key regulator of eukaryotic gene expression. *Wiley Interdiscip Rev RNA, 7*(4), 438-454. https://doi.org/10.1002/wrna.1332

Connell-Crowley, L., Elledge, S. J., & Harper, J. W. (1998, Jan 1). G1 cyclin-dependent kinases are sufficient to initiate DNA synthesis in quiescent human fibroblasts. *Curr Biol, 8*(1), 65-68. https://doi.org/10.1016/s0960-9822(98)70021-1

Cullen, P. J., & Sprague, G. F., Jr. (2002, Dec). The Glc7p-interacting protein Bud14p attenuates polarized growth, pheromone response, and filamentous growth in Saccharomyces cerevisiae. *Eukaryot Cell, 1*(6), 884-894. https://doi.org/10.1128/EC.1.6.884-894.2002

D'Amours, D., & Amon, A. (2004, Nov 1). At the interface between signaling and executing anaphase--Cdc14 and the FEAR network. *Genes Dev, 18*(21), 2581-2595. https://doi.org/10.1101/gad.1247304

D'Aquino, K. E., Monje-Casas, F., Paulson, J., Reiser, V., Charles, G. M., Lai, L., Shokat, K. M., & Amon, A. (2005, Jul 22). The protein kinase Kin4 inhibits exit from mitosis in response to spindle position defects. *Mol Cell, 19*(2), 223-234. https://doi.org/10.1016/j.molcel.2005.06.005

de la Torre Ruiz, M. A., & Lowndes, N. F. (2000, Nov 24). DUN1 defines one branch downstream of RAD53 for transcription and DNA damage repair in Saccharomyces cerevisiae. *FEBS Lett, 485*(2-3), 205-206. https://doi.org/10.1016/s0014-5793(00)02198-0

den Elzen, N., Kosoy, A., Christopoulos, H., & O'Connell, M. J. (2004, May). Resisting arrest: recovery from checkpoint arrest through dephosphorylation of Chk1 by PP1. *Cell Cycle, 3*(5), 529-533. https://www.ncbi.nlm.nih.gov/pubmed/15020842

Dirick, L., Bohm, T., & Nasmyth, K. (1995, Oct 2). Roles and regulation of Cln-Cdc28 kinases at the start of the cell cycle of Saccharomyces cerevisiae. *EMBO J, 14*(19), 4803-4813. https://www.ncbi.nlm.nih.gov/pubmed/7588610

Donaldson, A. D., & Kilmartin, J. V. (1996, Mar). Spc42p: a phosphorylated component of the S. cerevisiae spindle pole body (SPD) with an essential function during SPB duplication. *J Cell Biol, 132*(5), 887-901. https://doi.org/10.1083/jcb.132.5.887

Duina, A. A., Miller, M. E., & Keeney, J. B. (2014, May). Budding yeast for budding geneticists: a primer on the Saccharomyces cerevisiae model system. *Genetics, 197*(1), 33-48. https://doi.org/10.1534/genetics.114.163188

Duntze, W., MacKay, V., & Manney, T. R. (1970, Jun 19). Saccharomyces cerevisiae: a diffusible sex factor. *Science, 168*(3938), 1472-1473. https://doi.org/10.1126/science.168.3938.1472

Elliott, S., Knop, M., Schlenstedt, G., & Schiebel, E. (1999, May 25). Spc29p is a component of the Spc110p subcomplex and is essential for spindle pole body duplication. *Proc Natl Acad Sci U S A, 96*(11), 6205-6210. https://doi.org/10.1073/pnas.96.11.6205

Elserafy, M., Saric, M., Neuner, A., Lin, T. C., Zhang, W., Seybold, C., Sivashanmugam, L., & Schiebel, E. (2014, Jul 7). Molecular mechanisms that restrict yeast centrosome duplication to one event per cell cycle. *Curr Biol, 24*(13), 1456-1466. https://doi.org/10.1016/j.cub.2014.05.032

Eshel, D., Urrestarazu, L. A., Vissers, S., Jauniaux, J. C., van Vliet-Reedijk, J. C., Planta, R. J., & Gibbons, I. R. (1993, Dec 1). Cytoplasmic dynein is required for normal nuclear segregation in yeast. *Proc Natl Acad Sci U S A, 90*(23), 11172-11176. https://doi.org/10.1073/pnas.90.23.11172

Fitch, I., Dahmann, C., Surana, U., Amon, A., Nasmyth, K., Goetsch, L., Byers, B., & Futcher, B. (1992, Jul). Characterization of four B-type cyclin genes of the budding yeast Saccharomyces cerevisiae. *Mol Biol Cell, 3*(7), 805-818. https://doi.org/10.1091/mbc.3.7.805

Futcher, B. (1996, Dec). Cyclins and the wiring of the yeast cell cycle. *Yeast, 12*(16), 1635-1646. https://doi.org/10.1002/(SICI)1097-0061(199612)12:16%3C1635::AID-YEA83%3E3.0.CO;2-O

Gardner, J. M., & Jaspersen, S. L. (2014). Manipulating the yeast genome: deletion, mutation, and tagging by PCR. *Methods Mol Biol, 1205*, 45-78. https://doi.org/10.1007/978-1-4939-1363-3_5

Gauthier, N. P., Jensen, L. J., Wernersson, R., Brunak, S., & Jensen, T. S. (2010, Jan). Cyclebase.org: version 2.0, an updated comprehensive, multi-species repository of cell cycle experiments and derived analysis results. *Nucleic Acids Res, 38*(Database issue), D699-702. https://doi.org/10.1093/nar/gkp1044

Geissler, S., Pereira, G., Spang, A., Knop, M., Soues, S., Kilmartin, J., & Schiebel, E. (1996, Aug 1). The spindle pole body component Spc98p interacts with the gamma-tubulin-like Tub4p of Saccharomyces cerevisiae at the sites of microtubule attachment. *EMBO J, 15*(15), 3899-3911. https://www.ncbi.nlm.nih.gov/pubmed/8670895

Geymonat, M., Spanos, A., de Bettignies, G., & Sedgwick, S. G. (2009, Nov 16). Lte1 contributes to Bfa1 localization rather than stimulating nucleotide exchange by Tem1. *J Cell Biol, 187*(4), 497-511. https://doi.org/10.1083/jcb.200905114

Geymonat, M., Spanos, A., Smith, S. J., Wheatley, E., Rittinger, K., Johnston, L. H., & Sedgwick, S. G. (2002, Aug 9). Control of mitotic exit in budding yeast. In vitro

regulation of Tem1 GTPase by Bub2 and Bfa1. *J Biol Chem, 277*(32), 28439-28445. https://doi.org/10.1074/jbc.M202540200

Goffeau, A., Barrell, B. G., Bussey, H., Davis, R. W., Dujon, B., Feldmann, H., Galibert, F., Hoheisel, J. D., Jacq, C., Johnston, M., Louis, E. J., Mewes, H. W., Murakami, Y., Philippsen, P., Tettelin, H., & Oliver, S. G. (1996, Oct 25). Life with 6000 genes. *Science, 274*(5287), 546, 563-547. https://doi.org/10.1126/science.274.5287.546

Granovskaia, M. V., Jensen, L. J., Ritchie, M. E., Toedling, J., Ning, Y., Bork, P., Huber, W., & Steinmetz, L. M. (2010). High-resolution transcription atlas of the mitotic cell cycle in budding yeast. *Genome Biol, 11*(3), R24. https://doi.org/10.1186/gb-2010-11-3-r24

Gray, C. H., Good, V. M., Tonks, N. K., & Barford, D. (2003, Jul 15). The structure of the cell cycle protein Cdc14 reveals a proline-directed protein phosphatase. *EMBO J, 22*(14), 3524-3535. https://doi.org/10.1093/emboj/cdg348

Gruneberg, U., Campbell, K., Simpson, C., Grindlay, J., & Schiebel, E. (2000, Dec 1). Nud1p links astral microtubule organization and the control of exit from mitosis. *EMBO J, 19*(23), 6475-6488. https://doi.org/10.1093/emboj/19.23.6475

Guacci, V., Hogan, E., & Koshland, D. (1994, May). Chromosome condensation and sister chromatid pairing in budding yeast. *J Cell Biol, 125*(3), 517-530. https://doi.org/10.1083/jcb.125.3.517

Hanson, P. K. (2018). Saccharomyces cerevisiae: A Unicellular Model Genetic Organism of Enduring Importance. *Current Protocols Essential Laboratory Techniques, 16*(1), e21. https://doi.org/10.1002/cpet.21

Hartwell, L. H. (1967, May). Macromolecule synthesis in temperature-sensitive mutants of yeast. *J Bacteriol, 93*(5), 1662-1670. https://doi.org/10.1128/jb.93.5.1662-1670.1967

Hartwell, L. H. (1974, Jun). Saccharomyces cerevisiae cell cycle. *Bacteriol Rev, 38*(2), 164-198. https://doi.org/10.1128/br.38.2.164-198.1974

Hartwell, L. H., Culotti, J., Pringle, J. R., & Reid, B. J. (1974, Jan 11). Genetic control of the cell division cycle in yeast. *Science, 183*(4120), 46-51. https://doi.org/10.1126/science.183.4120.46

Hartwell, L. H., & Unger, M. W. (1977, Nov). Unequal division in Saccharomyces cerevisiae and its implications for the control of cell division. *J Cell Biol, 75*(2 Pt 1), 422-435. https://doi.org/10.1083/jcb.75.2.422

Hartwell, L. H., & Weinert, T. A. (1989, Nov 3). Checkpoints: controls that ensure the order of cell cycle events. *Science, 246*(4930), 629-634. https://doi.org/10.1126/science.2683079

Herskowitz, I. (1988, Dec). Life cycle of the budding yeast Saccharomyces cerevisiae. *Microbiol Rev, 52*(4), 536-553. https://doi.org/10.1128/mr.52.4.536-553.1988

Hofken, T., & Schiebel, E. (2004, Jan 19). Novel regulation of mitotic exit by the Cdc42 effectors Gic1 and Gic2. *J Cell Biol, 164*(2), 219-231. https://doi.org/10.1083/jcb.200309080

Holder, J., Poser, E., & Barr, F. A. (2019, Oct). Getting out of mitosis: spatial and temporal control of mitotic exit and cytokinesis by PP1 and PP2A. *FEBS Lett, 593*(20), 2908-2924. https://doi.org/10.1002/1873-3468.13595

Howell, R. S. M., Klemm, C., Thorpe, P. H., & Csikasz-Nagy, A. (2020, Nov). Unifying the mechanism of mitotic exit control in a spatiotemporal logical model. *PLoS Biol, 18*(11), e3000917. https://doi.org/10.1371/journal.pbio.3000917

Hu, F., Wang, Y., Liu, D., Li, Y., Qin, J., & Elledge, S. J. (2001, Nov 30). Regulation of the Bub2/Bfa1 GAP complex by Cdc5 and cell cycle checkpoints. *Cell, 107*(5), 655-665. https://doi.org/10.1016/s0092-8674(01)00580-3

Inoue, S. (1981, Dec). Cell division and the mitotic spindle. *J Cell Biol, 91*(3 Pt 2), 131s-147s. https://doi.org/10.1083/jcb.91.3.131s

Irniger, S., Piatti, S., Michaelis, C., & Nasmyth, K. (1995, Apr 21). Genes involved in sister chromatid separation are needed for B-type cyclin proteolysis in budding yeast. *Cell, 81*(2), 269-278. https://doi.org/10.1016/0092-8674(95)90337-2

Ito, K., Takahashi, A., Morita, M., Suzuki, T., & Yamamoto, T. (2011, Sep). The role of the CNOT1 subunit of the CCR4-NOT complex in mRNA deadenylation and cell viability. *Protein Cell, 2*(9), 755-763. https://doi.org/10.1007/s13238-011-1092-4

Iyer, V. R., Horak, C. E., Scafe, C. S., Botstein, D., Snyder, M., & Brown, P. O. (2001, Jan 25). Genomic binding sites of the yeast cell-cycle transcription factors SBF and MBF. *Nature, 409*(6819), 533-538. https://doi.org/10.1038/35054095

Jackson, L. P., Reed, S. I., & Haase, S. B. (2006, Mar). Distinct mechanisms control the stability of the related S-phase cyclins Clb5 and Clb6. *Mol Cell Biol, 26*(6), 2456-2466. https://doi.org/10.1128/MCB.26.6.2456-2466.2006

Jacobs, C. W., Adams, A. E., Szaniszlo, P. J., & Pringle, J. R. (1988, Oct). Functions of microtubules in the Saccharomyces cerevisiae cell cycle. *J Cell Biol, 107*(4), 1409-1426. https://doi.org/10.1083/jcb.107.4.1409

Jaspersen, S. L., Charles, J. F., & Morgan, D. O. (1999, Mar 11). Inhibitory phosphorylation of the APC regulator Hct1 is controlled by the kinase Cdc28 and the phosphatase Cdc14. *Curr Biol, 9*(5), 227-236. https://doi.org/10.1016/s0960-9822(99)80111-0

Jaspersen, S. L., Charles, J. F., Tinker-Kulberg, R. L., & Morgan, D. O. (1998, Oct). A late mitotic regulatory network controlling cyclin destruction in Saccharomyces cerevisiae. *Mol Biol Cell, 9*(10), 2803-2817. https://doi.org/10.1091/mbc.9.10.2803

Jaspersen, S. L., Giddings, T. H., Jr., & Winey, M. (2002, Dec 23). Mps3p is a novel component of the yeast spindle pole body that interacts with the yeast centrin homologue Cdc31p. *J Cell Biol, 159*(6), 945-956. https://doi.org/10.1083/jcb.200208169

Jaspersen, S. L., & Winey, M. (2004). The budding yeast spindle pole body: structure, duplication, and function. *Annu Rev Cell Dev Biol, 20*, 1-28. https://doi.org/10.1146/annurev.cellbio.20.022003.114106

Jativa, S., Calabria, I., Moyano-Rodriguez, Y., Garcia, P., & Queralt, E. (2019, Sep). Cdc14 activation requires coordinated Cdk1-dependent phosphorylation of Net1 and PP2A-Cdc55 at anaphase onset. *Cell Mol Life Sci, 76*(18), 3601-3620. https://doi.org/10.1007/s00018-019-03086-5

Jimenez, J., Bru, S., Ribeiro, M., & Clotet, J. (2015, Mar 2). Live fast, die soon: cell cycle progression and lifespan in yeast cells. *Microb Cell, 2*(3), 62-67. https://doi.org/10.15698/mic2015.03.191

Johnston, G. C., Ehrhardt, C. W., Lorincz, A., & Carter, B. L. (1979, Jan). Regulation of cell size in the yeast Saccharomyces cerevisiae. *J Bacteriol, 137*(1), 1-5. https://doi.org/10.1128/jb.137.1.1-5.1979

Johnston, G. C., Pringle, J. R., & Hartwell, L. H. (1977, Mar 1). Coordination of growth with cell division in the yeast Saccharomyces cerevisiae. *Exp Cell Res, 105*(1), 79-98. https://doi.org/10.1016/0014-4827(77)90154-9

Karess, R. (2005, Jul). Rod-Zw10-Zwilch: a key player in the spindle checkpoint. *Trends Cell Biol, 15*(7), 386-392. https://doi.org/10.1016/j.tcb.2005.05.003

Kellis, M., Birren, B. W., & Lander, E. S. (2004, Apr 8). Proof and evolutionary analysis of ancient genome duplication in the yeast Saccharomyces cerevisiae. *Nature, 428*(6983), 617-624. https://doi.org/10.1038/nature02424

Khmelinskii, A., Lawrence, C., Roostalu, J., & Schiebel, E. (2007, Jun 18). Cdc14-regulated midzone assembly controls anaphase B. *J Cell Biol, 177*(6), 981-993. https://doi.org/10.1083/jcb.200702145

Kilmartin, J. V. (2003, Sep 29). Sfi1p has conserved centrin-binding sites and an essential function in budding yeast spindle pole body duplication. *J Cell Biol, 162*(7), 1211-1221. https://doi.org/10.1083/jcb.200307064

Kilmartin, J. V. (2014, Sep 5). Lessons from yeast: the spindle pole body and the centrosome. *Philos Trans R Soc Lond B Biol Sci, 369*(1650). https://doi.org/10.1098/rstb.2013.0456

King, R. W., Deshaies, R. J., Peters, J. M., & Kirschner, M. W. (1996, Dec 6). How proteolysis drives the cell cycle. *Science, 274*(5293), 1652-1659. https://doi.org/10.1126/science.274.5293.1652

King, R. W., Peters, J. M., Tugendreich, S., Rolfe, M., Hieter, P., & Kirschner, M. W. (1995, Apr 21). A 20S complex containing CDC27 and CDC16 catalyzes the mitosis-

specific conjugation of ubiquitin to cyclin B. *Cell, 81*(2), 279-288. https://doi.org/10.1016/0092-8674(95)90338-0

Knaus, M., Cameroni, E., Pedruzzi, I., Tatchell, K., De Virgilio, C., & Peter, M. (2005, Sep 7). The Bud14p-Glc7p complex functions as a cortical regulator of dynein in budding yeast. *EMBO J, 24*(17), 3000-3011. https://doi.org/10.1038/sj.emboj.7600783

Knop, M., Pereira, G., & Schiebel, E. (1999, May-Jun). Microtubule organization by the budding yeast spindle pole body. *Biol Cell, 91*(4-5), 291-304. https://www.ncbi.nlm.nih.gov/pubmed/10518996

Knop, M., Siegers, K., Pereira, G., Zachariae, W., Winsor, B., Nasmyth, K., & Schiebel, E. (1999, Jul). Epitope tagging of yeast genes using a PCR-based strategy: more tags and improved practical routines. *Yeast, 15*(10B), 963-972. https://doi.org/10.1002/(SICI)1097-0061(199907)15:10B<963::AID-YEA399>3.0.CO;2-W

Kobayashi, H., Stewart, E., Poon, R., Adamczewski, J. P., Gannon, J., & Hunt, T. (1992, Nov). Identification of the domains in cyclin A required for binding to, and activation of, p34cdc2 and p32cdk2 protein kinase subunits. *Mol Biol Cell, 3*(11), 1279-1294. https://doi.org/10.1091/mbc.3.11.1279

Kocakaplan, D., Karaburk, H., Dilege, C., Kirdok, I., Bektas, S. N., & Caydasi, A. K. (2021, Oct 11). Protein phosphatase 1 in association with Bud14 inhibits mitotic exit in Saccharomyces cerevisiae. *Elife, 10*. https://doi.org/10.7554/eLife.72833

Koch, C., Moll, T., Neuberg, M., Ahorn, H., & Nasmyth, K. (1993, Sep 17). A role for the transcription factors Mbp1 and Swi4 in progression from G1 to S phase. *Science, 261*(5128), 1551-1557. https://doi.org/10.1126/science.8372350

Komarnitsky, S. I., Chiang, Y. C., Luca, F. C., Chen, J., Toyn, J. H., Winey, M., Johnston, L. H., & Denis, C. L. (1998, Apr). DBF2 protein kinase binds to and acts through the cell cycle-regulated MOB1 protein. *Mol Cell Biol, 18*(4), 2100-2107. https://doi.org/10.1128/MCB.18.4.2100

Kondo, A., Mostofa, M. G., Miyake, K., Terasawa, M., Nafisa, I., Yeasmin, A., Waliullah, T. M., Kanki, T., & Ushimaru, T. (2018, May 25). Cdc14 Phosphatase Promotes TORC1-Regulated Autophagy in Yeast. *J Mol Biol, 430*(11), 1671-1684. https://doi.org/10.1016/j.jmb.2018.04.007

Koranda, M., Schleiffer, A., Endler, L., & Ammerer, G. (2000, Jul 6). Forkhead-like transcription factors recruit Ndd1 to the chromatin of G2/M-specific promoters. *Nature, 406*(6791), 94-98. https://doi.org/10.1038/35017589

Koshland, D. E., Mitchison, T. J., & Kirschner, M. W. (1988, Feb 11). Polewards chromosome movement driven by microtubule depolymerization in vitro. *Nature, 331*(6156), 499-504. https://doi.org/10.1038/331499a0

Langan, T. A., Gautier, J., Lohka, M., Hollingsworth, R., Moreno, S., Nurse, P., Maller, J., & Sclafani, R. A. (1989, Sep). Mammalian growth-associated H1 histone kinase: a homolog of cdc2+/CDC28 protein kinases controlling mitotic entry in yeast and frog cells. *Mol Cell Biol, 9*(9), 3860-3868. https://doi.org/10.1128/mcb.9.9.3860-3868.1989

Latif, C., den Elzen, N. R., & O'Connell, M. J. (2004, Jul 15). DNA damage checkpoint maintenance through sustained Chk1 activity. *J Cell Sci, 117*(Pt 16), 3489-3498. https://doi.org/10.1242/jcs.01204

Lee, S. E., Frenz, L. M., Wells, N. J., Johnson, A. L., & Johnston, L. H. (2001, May 15). Order of function of the budding-yeast mitotic exit-network proteins Tem1, Cdc15,

Mob1, Dbf2, and Cdc5. *Curr Biol, 11*(10), 784-788. https://doi.org/10.1016/s0960-9822(01)00228-7

Lew, D. J., & Burke, D. J. (2003). The spindle assembly and spindle position checkpoints. *Annu Rev Genet, 37*, 251-282. https://doi.org/10.1146/annurev.genet.37.042203.120656

Lew, D. J., & Reed, S. I. (1995, Feb). Cell cycle control of morphogenesis in budding yeast. *Curr Opin Genet Dev, 5*(1), 17-23. https://doi.org/10.1016/s0959-437x(95)90048-9

Li, S., Sandercock, A. M., Conduit, P., Robinson, C. V., Williams, R. L., & Kilmartin, J. V. (2006, Jun 19). Structural role of Sfi1p-centrin filaments in budding yeast spindle pole body duplication. *J Cell Biol, 173*(6), 867-877. https://doi.org/10.1083/jcb.200603153

Li, Z., Vizeacoumar, F. J., Bahr, S., Li, J., Warringer, J., Vizeacoumar, F. S., Min, R., Vandersluis, B., Bellay, J., Devit, M., Fleming, J. A., Stephens, A., Haase, J., Lin, Z. Y., Baryshnikova, A., Lu, H., Yan, Z., Jin, K., Barker, S., Datti, A., Giaever, G., Nislow, C., Bulawa, C., Myers, C. L., Costanzo, M., Gingras, A. C., Zhang, Z., Blomberg, A., Bloom, K., Andrews, B., & Boone, C. (2011, Apr). Systematic exploration of essential yeast gene function with temperature-sensitive mutants. *Nat Biotechnol, 29*(4), 361-367. https://doi.org/10.1038/nbt.1832

Luo, X., Fang, G., Coldiron, M., Lin, Y., Yu, H., Kirschner, M. W., & Wagner, G. (2000, Mar). Structure of the Mad2 spindle assembly checkpoint protein and its interaction with Cdc20. *Nat Struct Biol, 7*(3), 224-229. https://doi.org/10.1038/73338

MacDougall, C. A., Byun, T. S., Van, C., Yee, M. C., & Cimprich, K. A. (2007, Apr 15). The structural determinants of checkpoint activation. *Genes Dev, 21*(8), 898-903. https://doi.org/10.1101/gad.1522607

Mah, A. S., Jang, J., & Deshaies, R. J. (2001, Jun 19). Protein kinase Cdc15 activates the Dbf2-Mob1 kinase complex. *Proc Natl Acad Sci U S A, 98*(13), 7325-7330. https://doi.org/10.1073/pnas.141098998

Maillet, L., Tu, C., Hong, Y. K., Shuster, E. O., & Collart, M. A. (2000, Oct 20). The essential function of Not1 lies within the Ccr4-Not complex. *J Mol Biol, 303*(2), 131-143. https://doi.org/10.1006/jmbi.2000.4131

Manzoni, R., Montani, F., Visintin, C., Caudron, F., Ciliberto, A., & Visintin, R. (2010, Jul 26). Oscillations in Cdc14 release and sequestration reveal a circuit underlying mitotic exit. *J Cell Biol, 190*(2), 209-222. https://doi.org/10.1083/jcb.201002026

Mapelli, M., Massimiliano, L., Santaguida, S., & Musacchio, A. (2007, Nov 16). The Mad2 conformational dimer: structure and implications for the spindle assembly checkpoint. *Cell, 131*(4), 730-743. https://doi.org/10.1016/j.cell.2007.08.049

Marschall, L. G., Jeng, R. L., Mulholland, J., & Stearns, T. (1996, Jul). Analysis of Tub4p, a yeast gamma-tubulin-like protein: implications for microtubule-organizing center function. *J Cell Biol, 134*(2), 443-454. https://doi.org/10.1083/jcb.134.2.443

Matellan, L., & Monje-Casas, F. (2020, Feb 12). Regulation of Mitotic Exit by Cell Cycle Checkpoints: Lessons From Saccharomyces cerevisiae. *Genes (Basel), 11*(2). https://doi.org/10.3390/genes11020195

McBride, H. J., Yu, Y., & Stillman, D. J. (1999, Jul 23). Distinct regions of the Swi5 and Ace2 transcription factors are required for specific gene activation. *J Biol Chem, 274*(30), 21029-21036. https://doi.org/10.1074/jbc.274.30.21029

McInerny, C. J., Partridge, J. F., Mikesell, G. E., Creemer, D. P., & Breeden, L. L. (1997, May 15). A novel Mcm1-dependent element in the SWI4, CLN3, CDC6, and CDC47 promoters activates M/G1-specific transcription. *Genes Dev, 11*(10), 1277-1288. https://doi.org/10.1101/gad.11.10.1277

Melo, J., & Toczyski, D. (2002, Apr). A unified view of the DNA-damage checkpoint. *Curr Opin Cell Biol, 14*(2), 237-245. https://doi.org/10.1016/s0955-0674(02)00312-5

Mendenhall, M. D. (1993, Jan 8). An inhibitor of p34CDC28 protein kinase activity from Saccharomyces cerevisiae. *Science, 259*(5092), 216-219. https://doi.org/10.1126/science.8421781

Mendenhall, M. D., & Hodge, A. E. (1998, Dec). Regulation of Cdc28 cyclin-dependent protein kinase activity during the cell cycle of the yeast Saccharomyces cerevisiae. *Microbiol Mol Biol Rev, 62*(4), 1191-1243. https://doi.org/10.1128/MMBR.62.4.1191-1243.1998

Michaelis, C., Ciosk, R., & Nasmyth, K. (1997, Oct 3). Cohesins: chromosomal proteins that prevent premature separation of sister chromatids. *Cell, 91*(1), 35-45. https://doi.org/10.1016/s0092-8674(01)80007-6

Miller, J. E., Zhang, L., Jiang, H., Li, Y., Pugh, B. F., & Reese, J. C. (2018, Jan 4). Genome-Wide Mapping of Decay Factor-mRNA Interactions in Yeast Identifies Nutrient-Responsive Transcripts as Targets of the Deadenylase Ccr4. *G3 (Bethesda), 8*(1), 315-330. https://doi.org/10.1534/g3.117.300415

Miller, M. E., & Cross, F. R. (2000, Jan). Distinct subcellular localization patterns contribute to functional specificity of the Cln2 and Cln3 cyclins of Saccharomyces cerevisiae. *Mol Cell Biol, 20*(2), 542-555. https://doi.org/10.1128/MCB.20.2.542-555.2000

Miller, R. K., & Rose, M. D. (1998, Jan 26). Kar9p is a novel cortical protein required for cytoplasmic microtubule orientation in yeast. *J Cell Biol, 140*(2), 377-390. https://doi.org/10.1083/jcb.140.2.377

Moens, P. B., & Rapport, E. (1971, Aug). Spindles, spindle plaques, and meiosis in the yeast Saccharomyces cerevisiae (Hansen). *J Cell Biol, 50*(2), 344-361. https://doi.org/10.1083/jcb.50.2.344

Mohl, D. A., Huddleston, M. J., Collingwood, T. S., Annan, R. S., & Deshaies, R. J. (2009, Feb 23). Dbf2-Mob1 drives relocalization of protein phosphatase Cdc14 to the cytoplasm during exit from mitosis. *J Cell Biol, 184*(4), 527-539. https://doi.org/10.1083/jcb.200812022

Morel, A. P., Sentis, S., Bianchin, C., Le Romancer, M., Jonard, L., Rostan, M. C., Rimokh, R., & Corbo, L. (2003, Jul 15). BTG2 antiproliferative protein interacts with the human CCR4 complex existing in vivo in three cell-cycle-regulated forms. *J Cell Sci, 116*(Pt 14), 2929-2936. https://doi.org/10.1242/jcs.00480

Morgan, D. O. (2007). *The cell cycle : principles of control*. Published by New Science Press in association with Oxford University Press ;
Distributed inside North America by Sinauer Associates, Publishers.

Mortimer, R. K., & Johnston, J. R. (1986, May). Genealogy of principal strains of the yeast genetic stock center. *Genetics, 113*(1), 35-43. https://doi.org/10.1093/genetics/113.1.35

Muhlrad, D., & Parker, R. (2005, Mar 9). The yeast EDC1 mRNA undergoes deadenylation-independent decapping stimulated by Not2p, Not4p, and Not5p. *EMBO J, 24*(5), 1033-1045. https://doi.org/10.1038/sj.emboj.7600560

Nasmyth, K. (1993, Apr). Control of the yeast cell cycle by the Cdc28 protein kinase. *Curr Opin Cell Biol, 5*(2), 166-179. https://doi.org/10.1016/0955-0674(93)90099-c

Newport, J. W., & Forbes, D. J. (1987). The nucleus: structure, function, and dynamics. *Annu Rev Biochem, 56*, 535-565. https://doi.org/10.1146/annurev.bi.56.070187.002535

Nguyen, T., Vinh, D. B., Crawford, D. K., & Davis, T. N. (1998, Aug). A genetic analysis of interactions with Spc110p reveals distinct functions of Spc97p and Spc98p, components of the yeast gamma-tubulin complex. *Mol Biol Cell, 9*(8), 2201-2216. https://doi.org/10.1091/mbc.9.8.2201

Nilsson, J., Yekezare, M., Minshull, J., & Pines, J. (2008, Dec). The APC/C maintains the spindle assembly checkpoint by targeting Cdc20 for destruction. *Nat Cell Biol, 10*(12), 1411-1420. https://doi.org/10.1038/ncb1799

Noguchi, E., Gadaleta, M. C., Springer Science+Business Media., & Springer Protocols. *Cell cycle control : mechanisms and protocols* (Second edition. ed.) [text] Click here for full text http://GW2JH3XR2C.search.serialssolutions.com/?sid=sersol&SS_jc=TC0001385580&title=Cell%20cycle%20control%20%3A%20mechanisms%20and%20protocols852

Nurse, P. (1975, Aug 14). Genetic control of cell size at cell division in yeast. *Nature, 256*(5518), 547-551. https://doi.org/10.1038/256547a0

O'Connell, M. J., & Cimprich, K. A. (2005, Jan 1). G2 damage checkpoints: what is the turn-on? *J Cell Sci, 118*(Pt 1), 1-6. https://doi.org/10.1242/jcs.01626

O'Connell, M. J., Walworth, N. C., & Carr, A. M. (2000, Jul). The G2-phase DNA-damage checkpoint. *Trends Cell Biol, 10*(7), 296-303. https://doi.org/10.1016/s0962-8924(00)01773-6

O'Toole, E. T., Winey, M., & McIntosh, J. R. (1999, Jun). High-voltage electron tomography of spindle pole bodies and early mitotic spindles in the yeast Saccharomyces cerevisiae. *Mol Biol Cell, 10*(6), 2017-2031. https://doi.org/10.1091/mbc.10.6.2017

Osborn, M. J., & Miller, J. R. (2007, Jun). Rescuing yeast mutants with human genes. *Brief Funct Genomic Proteomic, 6*(2), 104-111. https://doi.org/10.1093/bfgp/elm017

Oshidari, R., Strecker, J., Chung, D. K. C., Abraham, K. J., Chan, J. N. Y., Damaren, C. J., & Mekhail, K. (2018, Jul 2). Nuclear microtubule filaments mediate non-linear directional motion of chromatin and promote DNA repair. *Nat Commun, 9*(1), 2567. https://doi.org/10.1038/s41467-018-05009-7

Panasenko, O. O., & Collart, M. A. (2012, Feb). Presence of Not5 and ubiquitinated Rps7A in polysome fractions depends upon the Not4 E3 ligase. *Mol Microbiol, 83*(3), 640-653. https://doi.org/10.1111/j.1365-2958.2011.07957.x

Pardee, A. B. (1989, Nov 3). G1 events and regulation of cell proliferation. *Science, 246*(4930), 603-608. https://doi.org/10.1126/science.2683075

Pereira, G., Manson, C., Grindlay, J., & Schiebel, E. (2002, Apr 29). Regulation of the Bfa1p-Bub2p complex at spindle pole bodies by the cell cycle phosphatase Cdc14p. *J Cell Biol, 157*(3), 367-379. https://doi.org/10.1083/jcb.200112085

Pereira, G., & Schiebel, E. (2001, Dec). The role of the yeast spindle pole body and the mammalian centrosome in regulating late mitotic events. *Curr Opin Cell Biol, 13*(6), 762-769. https://doi.org/10.1016/s0955-0674(00)00281-7

Pereira, G., & Schiebel, E. (2003, Dec 19). Separase regulates INCENP-Aurora B anaphase spindle function through Cdc14. *Science, 302*(5653), 2120-2124. https://doi.org/10.1126/science.1091936

Pereira, G., & Schiebel, E. (2005, Jul 22). Kin4 kinase delays mitotic exit in response to spindle alignment defects. *Mol Cell, 19*(2), 209-221. https://doi.org/10.1016/j.molcel.2005.05.030

Pereira, G., Tanaka, T. U., Nasmyth, K., & Schiebel, E. (2001, Nov 15). Modes of spindle pole body inheritance and segregation of the Bfa1p-Bub2p checkpoint protein complex. *EMBO J, 20*(22), 6359-6370. https://doi.org/10.1093/emboj/20.22.6359

Peters, J. M. (2002, May). The anaphase-promoting complex: proteolysis in mitosis and beyond. *Mol Cell, 9*(5), 931-943. https://doi.org/10.1016/s1097-2765(02)00540-3

Planas-Silva, M. D., & Weinberg, R. A. (1997, Dec). The restriction point and control of cell proliferation. *Curr Opin Cell Biol, 9*(6), 768-772. https://doi.org/10.1016/s0955-0674(97)80076-2

Powers, B. L., & Hall, M. C. (2017, Aug 15). Re-examining the role of Cdc14 phosphatase in reversal of Cdk phosphorylation during mitotic exit. *J Cell Sci, 130*(16), 2673-2681. https://doi.org/10.1242/jcs.201012

Project, S. *SGD Project*. Retrieved 17.05.2022 from https://www.yeastgenome.org/search?category=locus&geneMode=wrap&page=0&q=mitotic%20cell%20cycle

Project, S. *SGD Project*. Retrieved 17.05.22 from https://www.yeastgenome.org/search?category=locus&feature_type=ORF&geneMode=wrap&page=0&page_size=100&q=hog%20pathway

Raleigh, J. M., & O'Connell, M. J. (2000, May). The G(2) DNA damage checkpoint targets both Wee1 and Cdc25. *J Cell Sci, 113 (Pt 10)*, 1727-1736. https://www.ncbi.nlm.nih.gov/pubmed/10769204

Reed, S. I. (1980, Jul). The selection of S. cerevisiae mutants defective in the start event of cell division. *Genetics, 95*(3), 561-577. https://doi.org/10.1093/genetics/95.3.561

Reid, B. J., & Hartwell, L. H. (1977, Nov). Regulation of mating in the cell cycle of Saccharomyces cerevisiae. *J Cell Biol, 75*(2 Pt 1), 355-365. https://doi.org/10.1083/jcb.75.2.355

Reiser, V., D'Aquino, K. E., Ee, L. S., & Amon, A. (2006, Jul). The stress-activated mitogen-activated protein kinase signaling cascade promotes exit from mitosis. *Mol Biol Cell, 17*(7), 3136-3146. https://doi.org/10.1091/mbc.e05-12-1102

Richardson, H. E., Wittenberg, C., Cross, F., & Reed, S. I. (1989, Dec 22). An essential G1 function for cyclin-like proteins in yeast. *Cell, 59*(6), 1127-1133. https://doi.org/10.1016/0092-8674(89)90768-x

Rock, J. M., & Amon, A. (2009, Dec 15). The FEAR network. *Curr Biol, 19*(23), R1063-1068. https://doi.org/10.1016/j.cub.2009.10.002

Rock, J. M., & Amon, A. (2011, Sep 15). Cdc15 integrates Tem1 GTPase-mediated spatial signals with Polo kinase-mediated temporal cues to activate mitotic exit. *Genes Dev, 25*(18), 1943-1954. https://doi.org/10.1101/gad.17257711

Romain Tavenard, J. F., Gilles Vandewiele, Felix Divo, Guillaume Androz, Chester Holtz, Marie Payne, Roman Yurchak, Marc Rußwurm, Kushal Kolar, Eli Woods. (2020). Tslearn, A Machine Learning Toolkit for Time Series Data. *Journal of Machine Learning Research, 21*(118), 1-6. http://jmlr.org/papers/v21/20-091.html

Rose, M. D., Biggins, S., & Satterwhite, L. L. (1993, Feb). Unravelling the tangled web at the microtubule-organizing center. *Curr Opin Cell Biol, 5*(1), 105-115. https://doi.org/10.1016/s0955-0674(05)80015-8

Ross, K. E., & Cohen-Fix, O. (2004, May). A role for the FEAR pathway in nuclear positioning during anaphase. *Dev Cell, 6*(5), 729-735. https://doi.org/10.1016/s1534-5807(04)00128-5

Rout, M. P., & Kilmartin, J. V. (1990, Nov). Components of the yeast spindle and spindle pole body. *J Cell Biol, 111*(5 Pt 1), 1913-1927. https://doi.org/10.1083/jcb.111.5.1913

Rowicka, M., Kudlicki, A., Tu, B. P., & Otwinowski, Z. (2007, Oct 23). High-resolution timing of cell cycle-regulated gene expression. *Proc Natl Acad Sci U S A, 104*(43), 16892-16897. https://doi.org/10.1073/pnas.0706022104

Rudner, A. D., & Murray, A. W. (2000, Jun 26). Phosphorylation by Cdc28 activates the Cdc20-dependent activity of the anaphase-promoting complex. *J Cell Biol, 149*(7), 1377-1390. https://doi.org/10.1083/jcb.149.7.1377

Ruthnick, D., Neuner, A., Dietrich, F., Kirrmaier, D., Engel, U., Knop, M., & Schiebel, E. (2017, Aug 7). Characterization of spindle pole body duplication reveals a regulatory role for nuclear pore complexes. *J Cell Biol, 216*(8), 2425-2442. https://doi.org/10.1083/jcb.201612129

Ruthnick, D., & Schiebel, E. (2016, May). Duplication of the Yeast Spindle Pole Body Once per Cell Cycle. *Mol Cell Biol, 36*(9), 1324-1331. https://doi.org/10.1128/MCB.00048-16

Ruthnick, D., Vitale, J., Neuner, A., & Schiebel, E. (2021, Mar 1). The N-terminus of Sfi1 and yeast centrin Cdc31 provide the assembly site for a new spindle pole body. *J Cell Biol, 220*(3). https://doi.org/10.1083/jcb.202004196

Sanchez, Y., Bachant, J., Wang, H., Hu, F., Liu, D., Tetzlaff, M., & Elledge, S. J. (1999, Nov 5). Control of the DNA damage checkpoint by chk1 and rad53 protein kinases through distinct mechanisms. *Science, 286*(5442), 1166-1171. https://doi.org/10.1126/science.286.5442.1166

Sarı, B. (2021). *A Novel Control Mechanism of Mitotic Exit in Saccharomyces cerevisiae* Koç University]. İstanbul.

Sbia, M., Parnell, E. J., Yu, Y., Olsen, A. E., Kretschmann, K. L., Voth, W. P., & Stillman, D. J. (2008, Apr 25). Regulation of the yeast Ace2 transcription factor during the cell cycle. *J Biol Chem, 283*(17), 11135-11145. https://doi.org/10.1074/jbc.M800196200

Schaerer, F., Morgan, G., Winey, M., & Philippsen, P. (2001, Aug). Cnm67p is a spacer protein of the Saccharomyces cerevisiae spindle pole body outer plaque. *Mol Biol Cell, 12*(8), 2519-2533. https://doi.org/10.1091/mbc.12.8.2519

Schiebel, E., & Bornens, M. (1995, May). In search of a function for centrins. *Trends Cell Biol, 5*(5), 197-201. https://doi.org/10.1016/s0962-8924(00)88999-0

Schneider, B. L., Zhang, J., Markwardt, J., Tokiwa, G., Volpe, T., Honey, S., & Futcher, B. (2004, Dec). Growth rate and cell size modulate the synthesis of, and requirement for,

G1-phase cyclins at start. *Mol Cell Biol, 24*(24), 10802-10813. https://doi.org/10.1128/MCB.24.24.10802-10813.2004

Schroeder, T. E. (1968, Oct). Cytokinesis: filaments in the cleavage furrow. *Exp Cell Res, 53*(1), 272-276. https://doi.org/10.1016/0014-4827(68)90373-x

Schwob, E., Bohm, T., Mendenhall, M. D., & Nasmyth, K. (1994, Oct 21). The B-type cyclin kinase inhibitor p40SIC1 controls the G1 to S transition in S. cerevisiae. *Cell, 79*(2), 233-244. https://doi.org/10.1016/0092-8674(94)90193-7

Seufert, W., Futcher, B., & Jentsch, S. (1995, Jan 5). Role of a ubiquitin-conjugating enzyme in degradation of S- and M-phase cyclins. *Nature, 373*(6509), 78-81. https://doi.org/10.1038/373078a0

Seybold, C., Elserafy, M., Ruthnick, D., Ozboyaci, M., Neuner, A., Flottmann, B., Heilemann, M., Wade, R. C., & Schiebel, E. (2015, Jun 22). Kar1 binding to Sfi1 C-terminal regions anchors the SPB bridge to the nuclear envelope. *J Cell Biol, 209*(6), 843-861. https://doi.org/10.1083/jcb.201412050

Seybold, C., & Schiebel, E. (2013, Oct 7). Spindle pole bodies. *Curr Biol, 23*(19), R858-860. https://doi.org/10.1016/j.cub.2013.07.024

Shaw, S. L., Yeh, E., Maddox, P., Salmon, E. D., & Bloom, K. (1997, Nov 17). Astral microtubule dynamics in yeast: a microtubule-based searching mechanism for spindle orientation and nuclear migration into the bud. *J Cell Biol, 139*(4), 985-994. https://doi.org/10.1083/jcb.139.4.985

Shirayama, M., Toth, A., Galova, M., & Nasmyth, K. (1999, Nov 11). APC(Cdc20) promotes exit from mitosis by destroying the anaphase inhibitor Pds1 and cyclin Clb5. *Nature, 402*(6758), 203-207. https://doi.org/10.1038/46080

Shou, W., Azzam, R., Chen, S. L., Huddleston, M. J., Baskerville, C., Charbonneau, H., Annan, R. S., Carr, S. A., & Deshaies, R. J. (2002, Apr 17). Cdc5 influences phosphorylation of Net1 and disassembly of the RENT complex. *BMC Mol Biol, 3*, 3. https://doi.org/10.1186/1471-2199-3-3

Shou, W., Seol, J. H., Shevchenko, A., Baskerville, C., Moazed, D., Chen, Z. W., Jang, J., Shevchenko, A., Charbonneau, H., & Deshaies, R. J. (1999, Apr 16). Exit from mitosis is triggered by Tem1-dependent release of the protein phosphatase Cdc14 from nucleolar RENT complex. *Cell, 97*(2), 233-244. https://doi.org/10.1016/s0092-8674(00)80733-3

Sikorski, R. S., & Hieter, P. (1989, May). A system of shuttle vectors and yeast host strains designed for efficient manipulation of DNA in Saccharomyces cerevisiae. *Genetics, 122*(1), 19-27. https://doi.org/10.1093/genetics/122.1.19

Snyder, M. (1994, Oct). The spindle pole body of yeast. *Chromosoma, 103*(6), 369-380. https://doi.org/10.1007/BF00362281

Spang, A., Courtney, I., Fackler, U., Matzner, M., & Schiebel, E. (1993, Oct). The calcium-binding protein cell division cycle 31 of Saccharomyces cerevisiae is a component of the half bridge of the spindle pole body. *J Cell Biol, 123*(2), 405-416. https://doi.org/10.1083/jcb.123.2.405

Spang, A., Courtney, I., Grein, K., Matzner, M., & Schiebel, E. (1995, Mar). The Cdc31p-binding protein Kar1p is a component of the half bridge of the yeast spindle pole body. *J Cell Biol, 128*(5), 863-877. https://doi.org/10.1083/jcb.128.5.863

Spang, A., Grein, K., & Schiebel, E. (1996, Sep). The spacer protein Spc110p targets calmodulin to the central plaque of the yeast spindle pole body. *J Cell Sci, 109 (Pt 9)*, 2229-2237. https://www.ncbi.nlm.nih.gov/pubmed/8886974

Spellman, P. T., Sherlock, G., Zhang, M. Q., Iyer, V. R., Anders, K., Eisen, M. B., Brown, P. O., Botstein, D., & Futcher, B. (1998, Dec). Comprehensive identification of cell cycle-regulated genes of the yeast Saccharomyces cerevisiae by microarray hybridization. *Mol Biol Cell, 9*(12), 3273-3297. https://doi.org/10.1091/mbc.9.12.3273

Stegmeier, F., & Amon, A. (2004). Closing mitosis: the functions of the Cdc14 phosphatase and its regulation. *Annu Rev Genet, 38*, 203-232. https://doi.org/10.1146/annurev.genet.38.072902.093051

Stegmeier, F., Huang, J., Rahal, R., Zmolik, J., Moazed, D., & Amon, A. (2004, Mar 23). The replication fork block protein Fob1 functions as a negative regulator of the FEAR network. *Curr Biol, 14*(6), 467-480. https://doi.org/10.1016/j.cub.2004.03.009

Stegmeier, F., Visintin, R., & Amon, A. (2002, Jan 25). Separase, polo kinase, the kinetochore protein Slk19, and Spo12 function in a network that controls Cdc14 localization during early anaphase. *Cell, 108*(2), 207-220. https://doi.org/10.1016/s0092-8674(02)00618-9

Stirling, D. A., Welch, K. A., & Stark, M. J. (1994, Sep 15). Interaction with calmodulin is required for the function of Spc110p, an essential component of the yeast spindle pole body. *EMBO J, 13*(18), 4329-4342. https://www.ncbi.nlm.nih.gov/pubmed/7925277

Sudakin, V., Chan, G. K., & Yen, T. J. (2001, Sep 3). Checkpoint inhibition of the APC/C in HeLa cells is mediated by a complex of BUBR1, BUB3, CDC20, and MAD2. *J Cell Biol, 154*(5), 925-936. https://doi.org/10.1083/jcb.200102093

Sullivan, M., Higuchi, T., Katis, V. L., & Uhlmann, F. (2004, May 14). Cdc14 phosphatase induces rDNA condensation and resolves cohesin-independent cohesion during budding yeast anaphase. *Cell, 117*(4), 471-482. https://doi.org/10.1016/s0092-8674(04)00415-5

Tanaka, K., & Russell, P. (2001, Nov). Mrc1 channels the DNA replication arrest signal to checkpoint kinase Cds1. *Nat Cell Biol, 3*(11), 966-972. https://doi.org/10.1038/ncb1101-966

Teixeira, D., & Parker, R. (2007, Jun). Analysis of P-body assembly in Saccharomyces cerevisiae. *Mol Biol Cell, 18*(6), 2274-2287. https://doi.org/10.1091/mbc.e07-03-0199

Temme, C., Zhang, L., Kremmer, E., Ihling, C., Chartier, A., Sinz, A., Simonelig, M., & Wahle, E. (2010, Jul). Subunits of the Drosophila CCR4-NOT complex and their roles in mRNA deadenylation. *RNA, 16*(7), 1356-1370. https://doi.org/10.1261/rna.2145110

Tomson, B. N., D'Amours, D., Adamson, B. S., Aragon, L., & Amon, A. (2006, Aug). Ribosomal DNA transcription-dependent processes interfere with chromosome segregation. *Mol Cell Biol, 26*(16), 6239-6247. https://doi.org/10.1128/MCB.00693-06

Traven, A., Hammet, A., Tenis, N., Denis, C. L., & Heierhorst, J. (2005, Jan). Ccr4-not complex mRNA deadenylase activity contributes to DNA damage responses in Saccharomyces cerevisiae. *Genetics, 169*(1), 65-75. https://doi.org/10.1534/genetics.104.030940

Udden, M. M., & Finkelstein, D. B. (1978, Mar). Reaction order of Saccharomyces cerevisiae alpha-factor-mediated cell cycle arrest and mating inhibition. *J Bacteriol, 133*(3), 1501-1507. https://doi.org/10.1128/jb.133.3.1501-1507.1978

Uhlmann, F., Wernic, D., Poupart, M. A., Koonin, E. V., & Nasmyth, K. (2000, Oct 27). Cleavage of cohesin by the CD clan protease separin triggers anaphase in yeast. *Cell, 103*(3), 375-386. https://doi.org/10.1016/s0092-8674(00)00130-6

Villoria, M. T., Ramos, F., Duenas, E., Faull, P., Cutillas, P. R., & Clemente-Blanco, A. (2017, Jan 4). Stabilization of the metaphase spindle by Cdc14 is required for recombinational DNA repair. *EMBO J, 36*(1), 79-101. https://doi.org/10.15252/embj.201593540

Visintin, R., Craig, K., Hwang, E. S., Prinz, S., Tyers, M., & Amon, A. (1998, Dec). The phosphatase Cdc14 triggers mitotic exit by reversal of Cdk-dependent phosphorylation. *Mol Cell, 2*(6), 709-718. https://doi.org/10.1016/s1097-2765(00)80286-5

Visintin, R., Hwang, E. S., & Amon, A. (1999, Apr 29). Cfi1 prevents premature exit from mitosis by anchoring Cdc14 phosphatase in the nucleolus. *Nature, 398*(6730), 818-823. https://doi.org/10.1038/19775

Visintin, R., Prinz, S., & Amon, A. (1997, Oct 17). CDC20 and CDH1: a family of substrate-specific activators of APC-dependent proteolysis. *Science, 278*(5337), 460-463. https://doi.org/10.1126/science.278.5337.460

Weinert, T. A., & Hartwell, L. H. (1988, Jul 15). The RAD9 gene controls the cell cycle response to DNA damage in Saccharomyces cerevisiae. *Science, 241*(4863), 317-322. https://doi.org/10.1126/science.3291120

Wittenberg, C., & Reed, S. I. (1988, Sep 23). Control of the yeast cell cycle is associated with assembly/disassembly of the Cdc28 protein kinase complex. *Cell, 54*(7), 1061-1072. https://doi.org/10.1016/0092-8674(88)90121-3

Wong, E. D., Karra, K., Hitz, B. C., Hong, E. L., & Cherry, J. M. (2013). The YeastGenome app: the Saccharomyces Genome Database at your fingertips. *Database (Oxford), 2013*, bat004. https://doi.org/10.1093/database/bat004

Yoder, T. J., Pearson, C. G., Bloom, K., & Davis, T. N. (2003, Aug). The Saccharomyces cerevisiae spindle pole body is a dynamic structure. *Mol Biol Cell, 14*(8), 3494-3505. https://doi.org/10.1091/mbc.e02-10-0655

Yoshida, S., Asakawa, K., & Toh-e, A. (2002, Jun 4). Mitotic exit network controls the localization of Cdc14 to the spindle pole body in Saccharomyces cerevisiae. *Curr Biol, 12*(11), 944-950. https://doi.org/10.1016/s0960-9822(02)00870-9

Yu, H. (2002, Dec). Regulation of APC-Cdc20 by the spindle checkpoint. *Curr Opin Cell Biol, 14*(6), 706-714. https://doi.org/10.1016/s0955-0674(02)00382-4

Zetterberg, A., Larsson, O., & Wiman, K. G. (1995, Dec). What is the restriction point? *Curr Opin Cell Biol, 7*(6), 835-842. https://doi.org/10.1016/0955-0674(95)80067-0

Zhou, H., Albuquerque, C. P., Liang, J., Suhandynata, R. T., & Weng, S. (2010, Sep 1). Quantitative phosphoproteomics: New technologies and applications in the DNA damage response. *Cell Cycle, 9*(17), 3479-3484. https://doi.org/10.4161/cc.9.17.13152

Zhu, G., Spellman, P. T., Volpe, T., Brown, P. O., Botstein, D., Davis, T. N., & Futcher, B. (2000, Jul 6). Two yeast forkhead genes regulate the cell cycle and pseudohyphal growth. *Nature, 406*(6791), 90-94. https://doi.org/10.1038/35017581

Chapter 7 : APPENDIX

7.1 Table of Strains

Table 7. 1: Table showing the strains used in this thesis.

Strain Name	Description	Reference
ESM356	*MATa ura3-52 leu2Δ1 his3Δ200 trp1Δ63.,*	*(Pereira & Schiebel, 2001)*
BY4741	*MATa; his3Δ1; leu2Δ0; met15Δ0; ura3Δ0.*	*(Li et al., 2011)*
SGY37-VIII,3	*MATa leu2 his3 trp1 ADE2 ura3-52::URA3-lexA-op-LacZ*	*(Geissler et al., 1996)*
IKY032	*ESM356 mCherry-Tub1 URA3 CDC14-GFP-KanMX6*	*This study*
IKY039	*ESM356 mCherry-Tub1 URA3 CDC14-GFP-KanMX6 bud14Δ::HIS3MX6*	*This study*
IKY233	*ESM356 mCherry-Tub1 URA3 CDC14-GFP-KanMX6 bfa1Δ::kITRP1*	*This study*
IKY234	*ESM356 mCherry-Tub1 URA3 CC14-GFP-KanMX6 bud14Δ::HIS3MX6 bfa1Δ::kITRP*	*This study*
IKY074	*YPH499 cdc15-1 mCherry-TUB1 LEU2 CDC14-GFP-KanMX6*	*This study*
IKY079	*YPH499 cdc15-1 mCherry-TUB1 LEU2 CDC14-GFP-KanMX6 bud14Δ::kITRP*	*This study*
IKY080	*YPH499 cdc15-1 mCherry-TUB1 LEU2 CDC14-GFP-KanMX6 spo12Δ::natNT2*	*This study*
DKY122	*SGY37-VIII,3 bfa1Δ::natNT2*	*This study*
IKY251	*SGY37-VIII,3 bud141Δ::kITRP*	*This study*
IKY299	*ESM356 mCherry-TUB1 URA3 CDC14-GFP-KanMX6 bud14Δ::HIS3MX6 BUD14-6HA LEU2 kITRP*	*This study*
IKY300	*ESM356 mCherry-TUB1 URA3 CDC14-GFP-KanMX6 bud14Δ::HIS3MX6 BUD14-F379A-6HA LEU2 kITRP*	*This study*
IKY301-1	*ESM356 mCherry-TUB1 URA3 CDC14-GFP-KanMX6 bud14Δ::HIS3MX6 LEU2*	*This study*
YPH499	*MATa ura3-52 lys2-801amber ade2-101ochre trp1Δ63 his3Δ200 leu2Δ1.*	*(Sikorski & Hieter, 1989)*
ESM1278	*YPH499 cdc15-1*	*(Sikorski & Hieter, 1989)*
Y08308	*cdc36-16 KanMX6*	*(Li et al., 2011)*

7.2 Table of Plasmids

Table 7. 2: Table showing the plasmids used in this thesis.

Plasmid Name	**Description**	**Reference**
pMM6	*p425-Gal1-Gal4-HA.*	(Geissler et al., 1996)
pMM5*	*p423-Gal1-lexA-Myc.*	(Geissler et al., 1996)
pHA69-1	*pMM5-BUD14*	Gift from G. Pereira
pHA70-1	*pMM6-BUD14*	Gift from G. Pereira
pCL4a-3	*pMM6-BFA1*	(Hofken & Schiebel, 2004)
pSM890a-1	*pMM6-CDC14*	
pSM993-1	*pMM5-CDC14*	
pCL3A-5	*pMM5-BFA1*	
pSP137-1	*pMM6-Cdc14-C283S*	
pSP132-1	*pMM5-Cdc14-C283S*	
IKY006	*pMM5-BUD14-5A*	(Kocakaplan et al., 2021)
IKY007	*pMM5-BUD14-F379A*	(Kocakaplan et al., 2021)
IKY008	*pMM5-BUD14-ΔSH3*	(Kocakaplan et al., 2021)
IKY010	*pMM6-BUD14-5A*	(Kocakaplan et al., 2021)
IKY011	*pMM6-BUD14-F379A*	(Kocakaplan et al., 2021)
IKY012	*pMM6-BUD14-ΔSH3*	(Kocakaplan et al., 2021)
pSMG02-1	*pRS405-BUD14*	This study
pSMG04-1	*pRS405-BUF14 F379A*	This study
pRS405	*LEU2-based integration vector*	
pAK011	*mCherry-TUB1-URA3-containing integration plasmid*	(Khmelinskii et al., 2007)
pBK067	*mCherry-TUB1-LEU2-containing integration plasmid*	(Caydasi et al., 2014)

7.3 Table of Primers

Table 7. 3: Table showing the plasmids used in this thesis.

Bud14-S1	GTGAAATACACGTAGTTTTTAGATAACATTCTCTGCTTGGTAAGAGAATGCGTACGCTGCAGGTCGAC
Bud14-S2	AAGTTCGTTGGATGAGAAAAAGACCAGGCTTTATTGTAAGGACAATATCAATCGATGAATTCGAGCTCG
Bud14-S3	TTGACAGAATGGATGTGTTGATGAAACAATTGGATGAAATTATTCGTAAACGTACGCTGCAGGTCGAC
Bfa1-S1	TGCGTACGCTGCAGGTCGACAGAAAAAAGTTCGAAAACTTTTGTAGCAGTTGAAAGTTTTGTATGCTA
Bfa1-S2	TGTACTCAAGATAACGGTAAAGAAACAGTTATAAGAAGGCTAAAGGGCTAATCGATGAATTCGAGCTCG
CDC14-S2	TAAGTTTTTTTATTATATGATATATATATATATAAAAATGAAATAAATTAATCGATGAATTCGAGCTCG
CDC14-S3	CTACAAGCGCCGCCGGTGGTATAAGAAAAATAAGTGGCTCCATCAAGAAACGTACGCTGCAGGTCGAC
S1-SPO12	AACAAAATAACATATACAGTAAGAACAATAGAAAACGTATTTATGCGTACGCTGCAGGTCGA
S2-SPO12	TAGTGTAGCATTTGGCTATTTTTGGATGACTAGAAAGGCAGATTTTTTTAATCGATGAATTCGAGCTCG

7.4 Table of Reagent, Buffer, and Chemicals

Table 7. 4: Table showing the reagents, buffers and chemicals used in this thesis.

Name	Description
TY agar with selective antibiotics (Ampicillin or Kanamycin)	5 g of NaCl (Merck, #106498), 5 g of Yeast Extract (Conda, #1702), 10 g of Tryptone (Biolife, #4122902), 20 g of Agar (Carl Roth, #5210.2), ddH2O up to 1000 mL. 100 µg/mL Ampicillin or 50 Kanamycin µg/mL
10X PCR Buffer	500mM Tris-HCl pH: 9.2 (Sigma, #T1503), 160mM (NH4)2SO4, 17.5mM MgCl2 (Fisher BioReagents, #BP214)
1X Blotting Buffer	25mM Tris, 190mM Glycine (AppliChem, #A1067), 0.025% SDS (Sigma, #75746), 20% methanol (Sigma, #32213)
1X Laemmli Running Buffer	25mM Tris, 192mM Glycine, 0.1% SDS, adjust pH to 8.3

1X PBS	137mM NaCl, 2.7mM KCl (Merck, #104936), 10mM Na2HPO4 (Merck, #106575), 1.76mM KH2PO4 (Fisher BioReagents, #BP362). Adjust pH to 7.2-7.4
1X PBS-T	137mM NaCl, 2.7mM KCl, 10mM Na2HPO4, 1.76mM KH2PO4. Adjust pH to 7.2-7.4 and add Tween-20 in final concentration of 0.02% (AppliChem, #A4974)
1X TAE Buffer	4.84 g of Tris, 1.14 mL of Glacial acetic acid (Isolab, #901016), 2 mL of 0.5M EDTA pH:8.0 (Sigma, #E5134), ddH2O up to 1000 mL.
2mM dNTPs mix	20 µL of dATP (100 mM), 20 µL dCTP (100 mM), 20 µL dTTP (100 mM) and 20 µL dGTP (100 mM), 920 µL ddH2O
Homemade ECL Solutions	Solution 1: 20 mL of 1M Tris-HCI pH: 8.5, 2 mL of 250mM Luminol (in DMSO, Sigma # A-8511), 889 µL of 90mM p-Coumaric acid (in DMSO, Sigma # C-9008), 178 mL of ddH2O Solution 2: 20 mL of 1M Tris-HCI pH: 8.5, 180 mL of ddH2O, 123 µL of 30% Hydrogen peroxide (H2O2, Sigma # H-1009)
HU-DTT	8M Urea (MP Biomedicals, #823048), 5% SDS, 200mM Tris-HCl pH: 6.8, 0.1mM EDTA, Bromophenol blue, 100mM 15 mg/mL DTT (Fisher BioReagnets, #BP172)
LiPEG	100mM LiOAc (Sigma, #L6883), 10mM Tris pH: 8.0, 1mM EDTA pH 8.0, 40% PEG3350 (Sigma, #P4338) ddH2O to complete the desired volume. Filter to sterilize.
LiSORB	100mM Lithium Acetate (LiOAc), 10mM Tris pH: 8.0, 1mM EDTA pH: 8.0, 1M Sorbitol (Merck, #107758), ddH2O to complete the desired volume. Filter to sterilize
P1 Buffer	50mM Tris-HCl pH:8.0, 10mM EDTA pH 8.0, 0.1 mg/mL RNase A
P2 Buffer	200mM NaOH, 1% SDS
P3 Buffer	3M KAc pH: 5.5
Ponceau S	0.2% (w/w) Ponceau S (Sigma #P3504) 3% (w/w) TCA in ddH2O

SC-X (X= URA, LEU, HIS or TRP)	3.4 g of Bacto Yeast Nitrogen Base (YNB) without amino acids with ammonium sulfate, 1 g of SC-X dropout amino acid mix, 10 g of D-(+)-Glucose, 0.05 g of Adenine hemisulfate salt (Sigma # A9126), ddH2O up to 500 mL
SC-X with selective antibiotics (Geneticin, Nourseothricin, or Hygromycin)	1.7 g of Yeast Nitrogen Base without amino acids without ammonium sulfate (Conda, #1553), 1 g of monosodium glutamic acid, 2 g of dropout amino acid mix, 20 g of D-(+)-Glucose, 20 g of Agar, ddH2O up to 500 mL were mixed and autoclaved, then mixed with 20 g of sterile agar in 500 mL ddH2O. 200 mg/L G418, 100 mg/L Nourseothricin or 300 mg/L Hygromycin into autoclaved agar
TY agar	5 g of NaCl, 5 g of Yeast Extract, 10 g of Tryptone, 20 g of Agar, ddH2O up to 1000 mL
TY medium	5 g of NaCl, 5 g of Yeast Extract, 10 g of Tryptone, ddH2O up to 1000 mL
TY medium with selective antibiotics (Ampicillin or Kanamycin)	5 g of NaCl, 5 g of Yeast Extract, 10 g of Tryptone, ddH2O up to 1000 mL. 100 μg/mL Ampicillin or 50 Kanamycin μg/mL
YPAD	5 g of Yeast Extract, 10 g of Peptone (Conda, #1616), 10 g of D-(+)-Glucose, 0.05 g of Adenine hemisulfate salt, ddH2O up to 500 mL
YPD with selective antibiotics (Geneticin, Nourseothricin, or Hygromycin)	10 g of Yeast Extract, 20 g of Peptone, 20 g of D-(+)-Glucose, 20 g of Agar, ddH2O up to 1000 mL. 200 mg/L G418, 100 mg/L Nourseothricin or 300 mg/L Hygromycin in autoclaved agar
YPAD for nocodazole arrest	5 g of Yeast Extract, 10 g of Peptone (Thermo, #211820), 10 g of D-(+)-Glucose, 0.05 g of Adenine hemisulfate salt, ddH2O up to 500 mL

7.5 WT Clustering Analysis

Table 7. 5: WT clustering analysis divided by the first time point value.

Gene	WT_30	WT_40	WT_50	WT_60	Cluster
YBR083W	1	1,151358	0,88884	0,764979	1
YOL069W	1	1,156266	0,969993	0,758443	1
YPL026C	1	1,136569	0,939153	0,747426	1
YEL075C	1	0,741969	0,593323	0,659899	2
YNL065W	1	0,804433	0,662546	0,694578	2
YOL123W	1	0,743052	0,585969	0,736812	2
YPL240C	1	0,713312	0,605817	0,791783	2
YAL055W	1	0,779729	0,774633	0,624971	2
YAL064C-A	1	0,815139	0,8115	0,616853	2
YAR066W	1	0,826615	0,75489	0,640634	2
YBL097W	1	0,847228	0,672483	0,63623	2
YBR298C	1	0,753113	0,713538	0,650225	2
YDR077W	1	1,002173	0,922154	0,653987	2
YDR156W	1	0,83226	0,677996	0,645067	2
YDR207C	1	0,806683	0,74893	0,609444	2
YDR403W	1	0,805546	0,774282	0,645054	2
YDR446W	1	0,89109	0,915319	0,592094	2
YEL037C	1	0,795455	0,804831	0,656198	2
YER072W	1	0,846898	0,784652	0,658099	2
YER103W	1	0,820176	0,738517	0,651036	2
YFL034C-B	1	1,000716	0,766926	0,638175	2
YFL037W	1	0,730323	0,707288	0,608095	2
YFL052W	1	0,908641	0,807082	0,576558	2
YGL162W	1	0,892855	0,709498	0,639329	2
YGL182C	1	1,007697	0,900027	0,597811	2
YGL201C	1	0,797744	0,77235	0,653935	2
YGR043C	1	0,752153	0,716048	0,577988	2
YGR143W	1	0,891445	0,780043	0,648315	2
YGR289C	1	0,799866	0,838201	0,620266	2
YHR116W	1	0,820918	0,746215	0,638886	2
YHR199C	1	0,78952	0,780919	0,656473	2
YIL053W	1	0,824984	0,780782	0,615776	2
YIL092W	1	0,953739	0,749783	0,635635	2
YIL093C	1	0,852976	0,827646	0,634852	2
YIR019C	1	0,863786	0,913196	0,556706	2
YJL012C	1	0,855564	0,772855	0,581639	2
YJL019W	1	0,885635	0,716185	0,645727	2

YJL083W	1	0,863889	0,848417	0,654108	2
YJL102W	1	0,864549	0,804672	0,577959	2
YJL159W	1	0,897536	0,907494	0,495631	2
YJL169W	1	0,756277	0,673705	0,647112	2
YJR129C	1	0,815505	0,752114	0,629139	2
YKL109W	1	1,031061	0,987242	0,641681	2
YKL129C	1	0,905795	0,879164	0,629575	2
YKR055W	1	0,963106	0,742388	0,6576	2
YKR098C	1	0,937563	0,754265	0,662595	2
YKR102W	1	0,776151	0,75171	0,626346	2
YLR045C	1	0,856147	0,739008	0,665694	2
YLR315W	1	0,977701	0,99129	0,6039	2
YLR373C	1	0,878451	0,712494	0,65558	2
YLR400W	1	0,789146	0,760659	0,625401	2
YML028W	1	0,803608	0,7385	0,621819	2
YML034W	1	0,941007	0,72521	0,635055	2
YML037C	1	0,889288	0,830804	0,643906	2
YML052W	1	0,761735	0,722047	0,55902	2
YMR016C	1	0,774889	0,727762	0,577289	2
YMR043W	1	0,81578	0,853891	0,622189	2
YMR068W	1	0,841078	0,769214	0,663753	2
YMR291W	1	0,852946	0,848614	0,558062	2
YNL112W	1	0,795697	0,766937	0,620023	2
YNL124W	1	0,763825	0,772158	0,651415	2
YNL172W	1	0,791071	0,684154	0,624478	2
YNL290W	1	0,771029	0,752014	0,615925	2
YOL151W	1	0,784091	0,673203	0,611085	2
YOR226C	1	0,795158	0,715063	0,589632	2
YOR301W	1	0,91388	0,943844	0,657083	2
YPL017C	1	0,733512	0,710592	0,59025	2
YPL058C	1	0,934917	0,753084	0,614375	2
YPR015C	1	0,790926	0,794679	0,647969	2
YPR032W	1	0,868827	0,742746	0,604481	2
YOL113W	1	1,032754	0,785871	0,670553	2
YGR074W	1	0,639425	1,217365	1,481013	3
YBR056W-A	1	1,920944	2,222404	2,423165	3
YHL041W	1	1,763905	1,694789	1,988559	3
YJL108C	1	1,512093	1,832358	1,790442	3
YKL001C	1	1,706063	1,941965	2,009223	3
YKL189W	1	1,518962	1,623145	1,784545	3
YLR366W	1	1,726732	1,98965	2,249616	3

YMR065W	1	1,546156	1,705889	2,010912	3
YOL159C	1	1,543476	1,67558	1,756497	3
YOR105W	1	1,632657	1,836797	2,169531	3
tT(AGU)H	1	0,896011	1,50663	1,417554	3
YBR076W	1	1,471654	1,587126	1,759479	3
YBR088C	1	1,102752	1,570955	1,868236	3
YBR144C	1	1,171679	1,500614	1,790136	3
YBR162C	1	1,106823	1,522475	1,690606	3
YBR208C	1	1,159033	1,628399	1,812098	3
YBR223C	1	1,40045	1,709084	1,97292	3
YCR009C	1	1,4136	1,59699	1,869531	3
YCR089W	1	1,395708	1,987555	1,961707	3
YDL196W	1	1,311577	1,528731	1,478723	3
YDL248W	1	1,290337	1,559893	1,629186	3
YER184C	1	1,220193	1,573095	1,660051	3
YFL031C-A	1	1,241633	1,563481	1,636532	3
YGR161C	1	1,307316	1,728729	1,565178	3
YHR007C	1	1,292612	1,686793	1,727467	3
YHR092C	1	0,985584	1,621954	1,558499	3
YHR209W	1	1,368372	1,618079	1,57563	3
YIL170W	1	1,099048	1,535229	1,511024	3
YIL171W	1	1,263842	1,731187	1,830209	3
YJL120W	1	1,352775	1,799789	1,733468	3
YJL218W	1	1,453238	1,70355	1,733714	3
YJR154W	1	1,106668	1,542785	1,465891	3
YKL102C	1	1,248499	1,606426	1,931438	3
YKL182W	1	1,103589	1,669226	1,648831	3
YLR080W	1	1,195759	1,590914	1,629387	3
YLR120C	1	1,131526	1,540043	1,814214	3
YLR121C	1	1,059361	1,691284	1,427815	3
YLR360W	1	1,351204	1,556697	1,611126	3
YML083C	1	1,095522	1,67988	1,812712	3
YMR020W	1	1,231088	1,601204	1,595633	3
YMR085W	1	0,949276	1,540928	1,560272	3
YMR195W	1	1,309911	1,581642	1,543076	3
YMR256C	1	1,378416	1,663757	1,701307	3
YNL104C	1	1,098412	1,504168	1,532372	3
YNL106C	1	1,232436	1,500235	1,7315	3
YNL217W	1	1,237159	1,799184	1,714311	3
YNR076W	1	1,292877	1,558171	1,604766	3
YOL162W	1	0,920808	1,537256	1,472987	3

YOR103C	1	1,405757	1,658546	1,768795	3
YOR134W	1	1,126077	1,509908	1,420755	3
YOR289W	1	1,200086	1,557227	1,708215	3
YOR316C	1	1,20006	1,651738	1,585447	3
YPR170C	1	1,243532	1,702287	1,570417	3
snR46	1	0,969705	1,233859	1,534821	3
YAL028W	1	1,228852	1,376524	1,508174	3
YBR056W	1	1,044113	1,363915	1,571612	3
YBR128C	1	1,139307	1,217534	1,588682	3
YBR157C	1	1,285744	1,406229	1,554622	3
YBR225W	1	1,315392	1,496462	1,646164	3
YBR287W	1	1,1836	1,425413	1,519055	3
YCL024W	1	1,278993	1,493549	1,605469	3
YCL054W-A	1	1,240418	1,377825	1,600955	3
YCL056C	1	1,315081	1,442592	1,827887	3
YCR005C	1	1,438284	1,4488	1,787264	3
YCR007C	1	1,156119	1,383712	1,584813	3
YDL069C	1	1,217498	1,45408	1,553245	3
YDL076C	1	1,182319	1,344953	1,628546	3
YDL206W	1	1,250794	1,332401	1,525504	3
YDR098C-B	1	1,11429	1,481127	1,759456	3
YDR248C	1	1,282643	1,409527	1,73224	3
YDR383C	1	1,280088	1,478154	1,642092	3
YDR433W	1	1,234385	1,486697	1,735026	3
YER133W-A	1	1,413241	1,494514	1,75364	3
YER187W	1	0,995378	1,3273	1,593494	3
YGL196W	1	1,132184	1,495247	1,587622	3
YGR001C	1	1,262718	1,35153	1,55444	3
YGR033C	1	1,281779	1,358139	1,617951	3
YGR060W	1	1,204011	1,390701	1,559955	3
YGR111W	1	1,129183	1,195517	1,551919	3
YGR131W	1	1,299184	1,434358	1,661541	3
YHL015W-A	1	1,262646	1,420776	1,814024	3
YHL016C	1	0,990247	1,459301	1,703584	3
YHR086W-A	1	1,064322	1,428513	1,525727	3
YIL002W-A	1	1,26087	1,328585	1,571652	3
YIL071C	1	1,303108	1,433995	1,518491	3
YIL079C	1	1,020923	1,171139	1,565743	3

YIL082W-A	1	1,190398	1,485329	1,563433	3
YIR001C	1	1,366376	1,423118	1,614656	3
YIR032C	1	0,839832	1,489215	1,640173	3
YIR039C	1	0,966892	1,367119	1,557343	3
YJL003W	1	1,281378	1,40301	1,604346	3
YJL147C	1	1,282031	1,456725	1,601201	3
YJL166W	1	1,333103	1,420644	1,639009	3
YJL187C	1	1,167047	1,352947	1,615673	3
YJR153W	1	1,24157	1,418928	1,547015	3
YJR161C	1	1,167148	1,386129	1,575917	3
YKL067W	1	1,103821	1,319334	1,605309	3
YKL101W	1	1,055089	1,244802	1,538182	3
YKL127W	1	1,069068	1,23175	1,513418	3
YKR039W	1	0,903642	1,318897	1,635607	3
YKR106W	1	1,199619	1,387932	1,530956	3
YLR128W	1	1,1186	1,471334	1,740574	3
YLR251W	1	1,209917	1,473448	1,50713	3
YLR395C	1	1,244417	1,412734	1,665543	3
YMR084W	1	0,99317	1,457091	1,546057	3
YMR175W-A	1	1,118263	1,331967	1,635204	3
YMR306W	1	1,1509	1,333111	1,594178	3
YMR319C	1	1,102453	1,462577	1,588334	3
YNL279W	1	1,18219	1,380197	1,552898	3
YNR059W	1	1,174961	1,248637	1,526662	3
YNR075W	1	1,151784	1,395434	1,592651	3
YOL058W	1	1,038132	1,184777	1,524715	3
YOL077W-A	1	1,166924	1,409136	1,666152	3
YOL156W	1	1,178253	1,492608	1,692852	3
YOL165C	1	1,053624	1,365769	1,545893	3
YOR220W	1	1,345507	1,496436	1,673048	3
YOR292C	1	1,087335	1,350889	1,597437	3
YOR390W	1	1,382896	1,434994	1,62919	3
YPL111W	1	0,849289	1,381525	1,694252	3
YPR035W	1	1,065388	1,413755	1,558303	3
YPR105C	1	1,216642	1,472923	1,695951	3
YBR169C	1	0,869949	1,308468	1,24196	3
YBR241C	1	0,760487	1,352506	1,367717	3
YBR302C	1	0,710259	1,1295	1,304086	3
YDL222C	1	0,741234	1,262995	1,235665	3
YIL032C	1	0,774294	1,298446	1,368947	3

YMR250W	1	0,857526	1,394906	1,450299	3
YNL142W	1	0,80476	1,24047	1,356442	3
YNL274C	1	0,968745	1,483456	1,472954	3
YPL278C	1	0,703589	1,266595	1,304717	3
ETS2-2	1	0,948204	1,108963	1,441358	3
Q0070	1	0,916322	1,361615	1,488973	3
snR85	1	0,923236	1,090516	1,434873	3
snR86	1	0,884812	1,227718	1,332439	3
YDR070C	1	0,943044	1,259901	1,432736	3
YDR173C	1	0,95184	1,172515	1,440847	3
YDR258C	1	0,877611	1,043921	1,340155	3
YGL052W	1	0,915805	1,35833	1,430064	3
YGR032W	1	0,896405	1,2062	1,411728	3
YIL123W	1	0,815954	1,148559	1,325973	3
YMR105C	1	0,793915	1,187841	1,271935	3
YMR251W-A	1	0,95596	1,24302	1,485029	3
YOL097W-A	1	0,924364	1,287712	1,474047	3
YOR139C	1	0,987673	1,182648	1,489095	3
YPL143W	1	0,816327	1,172236	1,296209	3
snR161	1	0,835537	0,614179	0,526496	4
tD(GUC)G1	1	0,881174	0,467476	0,569544	4
YBL046W	1	0,750913	0,663182	0,526387	4
YBR054W	1	0,822006	0,644846	0,425134	4
YBR105C	1	0,764568	0,610147	0,543213	4
YBR138C	1	0,893743	0,456067	0,41902	4
YBR296C-A	1	0,734106	0,513767	0,544826	4
YCL063W	1	0,798036	0,507697	0,423959	4
YCL064C	1	0,821252	0,57319	0,456155	4
YCR090C	1	0,952181	0,590367	0,385026	4
YDR281C	1	0,7469	0,522928	0,603624	4
YDR453C	1	0,701032	0,592988	0,468511	4
YDR502C	1	0,864594	0,651233	0,591275	4
YEL040W	1	0,7416	0,599424	0,538078	4
YEL069C	1	0,813607	0,663873	0,555608	4
YEL074W	1	1,023662	0,549722	0,458668	4
YEL076C	1	1,008393	0,588033	0,571624	4
YGL021W	1	0,7924	0,475971	0,44838	4
YGL116W	1	0,828053	0,576153	0,431632	4
YGL209W	1	0,829856	0,632644	0,459582	4
YGR035C	1	0,878061	0,499192	0,555122	4

YGR040W	1	1,02871	0,624846	0,466003	4
YGR108W	1	0,98165	0,639136	0,507883	4
YGR230W	1	0,940496	0,633595	0,617543	4
YHL034W-A	1	0,706564	0,468066	0,596558	4
YHR137W	1	0,806882	0,611848	0,580069	4
YHR140W	1	0,757945	0,571951	0,43469	4
YHR172W	1	0,830707	0,618328	0,539469	4
YIL024C	1	0,827895	0,632262	0,375432	4
YIL122W	1	0,818031	0,507414	0,42679	4
YIL134C-A	1	0,945769	0,412312	0,500935	4
YIL159W	1	0,787566	0,663859	0,603469	4
YJL051W	1	0,809844	0,51605	0,434682	4
YJL092W	1	0,810314	0,560302	0,448669	4
YJL153C	1	0,697276	0,473917	0,525609	4
YJR003C	1	1,066814	0,551602	0,382463	4
YJR048W	1	0,94747	0,57647	0,454179	4
YJR098C	1	0,933154	0,631832	0,437882	4
YKL029C	1	0,757076	0,602721	0,412573	4
YKL183W	1	0,706931	0,62202	0,390663	4
YKR012C	1	0,723261	0,648964	0,564105	4
YLL032C	1	0,993886	0,638432	0,610476	4
YLL067C	1	0,923584	0,534603	0,530323	4
YLR108C	1	0,899272	0,542957	0,543562	4
YLR109W	1	0,758617	0,628423	0,494914	4
YLR205C	1	0,777268	0,603953	0,548433	4
YLR214W	1	0,858381	0,636351	0,57637	4
YLR254C	1	0,811771	0,612573	0,591823	4
YLR297W	1	0,849125	0,517632	0,444985	4
YLR346C	1	0,7875	0,544753	0,408812	4
YLR353W	1	0,746587	0,512639	0,491396	4
YLR413W	1	0,781035	0,580858	0,548613	4
YLR415C	1	0,891248	0,460473	0,456522	4
YML131W	1	0,82504	0,631187	0,605977	4
YMR001C	1	0,828764	0,462077	0,390948	4
YMR132C	1	0,973535	0,571255	0,503057	4
YMR194C-B	1	0,714559	0,650818	0,462048	4
YNL058C	1	0,921457	0,586096	0,372647	4
YNL072W	1	0,702142	0,654487	0,494542	4
YNL298W	1	0,833051	0,644508	0,537628	4
YNR028W	1	0,849351	0,582545	0,566424	4

YOL136C	1	0,877872	0,614537	0,622958	4
YOL143C	1	0,878309	0,641139	0,549887	4
YOR058C	1	0,803254	0,565571	0,549227	4
YOR102W	1	0,786926	0,646377	0,609941	4
YOR153W	1	0,682874	0,595785	0,543731	4
YOR247W	1	0,930966	0,645233	0,532169	4
YOR315W	1	0,91082	0,609153	0,619153	4
YOR346W	1	0,897875	0,561428	0,484097	4
YOR372C	1	0,913142	0,63885	0,560731	4
YPL018W	1	0,731612	0,569459	0,524155	4
YPL019C	1	0,912149	0,660653	0,503884	4
YPL141C	1	0,89217	0,660788	0,567677	4
YPL189W	1	0,749311	0,611355	0,53657	4
YPL242C	1	0,913273	0,582009	0,526378	4
YPL280W	1	0,860545	0,634177	0,578506	4
YPR002W	1	0,95185	0,613807	0,437974	4
YPR124W	1	0,801564	0,611741	0,516821	4
tI(UAU)L	1	0,944087	0,679548	0,497226	4
tL(CAA)G2	1	0,835979	0,872532	0,326465	4
YAL064W-B	1	0,827345	0,708535	0,535228	4
YBR067C	1	0,933779	0,680717	0,43933	4
YBR123C	1	0,877602	0,668415	0,53297	4
YBR180W	1	0,865065	0,706444	0,45135	4
YBR202W	1	0,909467	0,713665	0,518928	4
YCL026C-A	1	0,773663	0,667268	0,524515	4
YCR063W	1	0,836057	0,73732	0,545952	4
YDL048C	1	0,843736	0,785164	0,398632	4
YDR191W	1	0,992107	0,746939	0,57376	4
YDR277C	1	0,829246	0,691191	0,460362	4
YDR523C	1	0,849218	0,673565	0,429035	4
YER034W	1	0,758103	0,707127	0,543997	4
YER188C-A	1	0,845981	0,84451	0,413224	4
YGL122C	1	0,809124	0,789155	0,48544	4
YHR126C	1	1,062156	0,813009	0,550637	4
YIL057C	1	0,951972	0,813544	0,490209	4
YIL106W	1	0,906549	0,694893	0,576115	4
YJL194W	1	1,319125	0,708149	0,40118	4
YLR120W-A	1	1,001715	0,833118	0,498079	4
YLR273C	1	1,17052	0,715516	0,528706	4
YLR274W	1	1,067308	0,765447	0,609804	4

YLR374C	1	0,922157	0,734403	0,388023	4
YOL114C	1	0,931774	0,771931	0,544224	4
YOR025W	1	0,92237	0,670612	0,602848	4
YOR066W	1	1,112768	0,825278	0,538791	4
YOR229W	1	0,755484	0,678395	0,560804	4
YPL061W	1	0,829928	0,688457	0,553446	4
YPL062W	1	0,94427	0,756018	0,59482	4
YPL187W	1	0,834476	0,777199	0,422928	4
YPR003C	1	1,008899	0,739822	0,631922	4
snR191	1	0,648755	0,749339	0,646199	5
snR82	1	0,655444	0,682794	0,754094	5
tD(GUC)N	1	0,665381	0,885366	0,752902	5
YAL039C	1	0,58377	0,88819	0,71409	5
YAL042W	1	0,643842	0,851468	0,652195	5
YAL061W	1	0,619373	0,870292	0,628327	5
YAL062W	1	0,657411	0,877565	0,694976	5
YAL063C-A	1	0,644343	0,824736	0,804676	5
YBL113C	1	0,66284	0,885035	0,627166	5
YCL033C	1	0,598914	0,912862	0,678305	5
YCR059C	1	0,631399	0,863511	0,639239	5
YDL016C	1	0,541278	0,840894	0,760858	5
YDL162C	1	0,648628	0,886986	0,799762	5
YDL221W	1	0,617003	0,734955	0,667158	5
YDR034C-A	1	0,656679	0,699128	0,751018	5
YDR188W	1	0,665786	0,836393	0,696583	5
YDR246W-A	1	0,54264	0,92375	0,682374	5
YDR412W	1	0,583397	0,769313	0,698379	5
YER018C	1	0,648737	0,862961	0,795553	5
YFR032C-A	1	0,624272	0,849184	0,716103	5
YFR034C	1	0,655945	0,830439	0,639632	5
YFR035C	1	0,609785	0,814152	0,679324	5
YGL198W	1	0,62833	0,907125	0,702913	5
YGR031W	1	0,666354	0,794734	0,631051	5
YHL006C	1	0,643128	0,824461	0,681725	5
YHR032W	1	0,652561	0,866793	0,70557	5
YIR036C	1	0,558698	0,9618	0,741427	5
YJL020C	1	0,649689	0,842949	0,689363	5
YJR019C	1	0,647392	0,922748	0,648	5
YLR255C	1	0,646502	0,610905	0,720641	5
YML122C	1	0,543387	0,752543	0,762267	5
YMR251W	1	0,666535	0,969328	0,777968	5

YNR073C	1	0,649805	0,854591	0,65886	5
YOL085C	1	0,586265	1,015807	0,666537	5
YOR050C	1	0,649542	0,718493	0,747983	5
YOR173W	1	0,661978	0,900068	0,721563	5
YOR181W	1	0,630303	0,822893	0,682871	5
YPL222W	1	0,648891	0,836822	0,742633	5
YPL252C	1	0,650138	0,852927	0,630363	5
YMR119W-A	1	0,684313	0,660068	0,676779	5
YAL038W	1	0,797274	0,845716	0,65048	5
YAR064W	1	0,764642	0,840117	0,661624	5
YBL013W	1	0,728939	0,738473	0,625699	5
YBR076C-A	1	0,753269	0,772216	0,640456	5
YBR108W	1	0,772122	0,807762	0,603469	5
YBR278W	1	0,681308	0,900242	0,625089	5
YCL034W	1	0,761261	0,869186	0,629266	5
YDL220C	1	0,747012	0,773103	0,589187	5
YDR024W	1	0,768576	0,986477	0,627977	5
YDR093W	1	0,698546	0,730617	0,64034	5
YDR171W	1	0,70863	1,000662	0,643507	5
YDR231C	1	0,731515	0,90907	0,654475	5
YDR343C	1	0,747792	1,004468	0,65081	5
YDR345C	1	0,818075	0,891543	0,633742	5
YEL032W	1	0,777856	0,816866	0,60361	5
YEL038W	1	0,700863	0,78181	0,644432	5
YFL016C	1	0,668673	0,747177	0,645853	5
YGL023C	1	0,694483	0,821675	0,665048	5
YGL025C	1	0,726155	0,760993	0,606444	5
YGL063W	1	0,668472	0,812273	0,646047	5
YGR013W	1	0,751306	0,763357	0,665291	5
YHL046C	1	0,808766	0,907503	0,552252	5
YHR057C	1	0,679856	0,797052	0,658767	5
YIL046W	1	0,694954	0,873796	0,65242	5
YIL153W	1	0,677555	0,921413	0,603356	5
YIR035C	1	0,712176	0,842839	0,653726	5
YJL130C	1	0,750871	0,762586	0,653583	5
YKL163W	1	0,946144	1,153657	0,609789	5
YLR035C-A	1	0,734659	0,859799	0,657287	5
YLR059C	1	0,743802	0,801108	0,632852	5
YLR141W	1	0,726322	0,743565	0,642764	5
YLR327C	1	0,70184	0,890231	0,647856	5
YLR348C	1	0,780925	0,924575	0,574214	5

YMR081C	1	0,786139	1,051948	0,542927	5
YMR105W-A	1	0,714577	0,737021	0,618409	5
YNL322C	1	0,6915	0,849369	0,650315	5
YNR041C	1	0,749292	0,976439	0,657285	5
YPR093C	1	0,690421	0,970557	0,625362	5
YER158C	1	0,891886	1,07919	0,673984	5
YHR189W	1	0,755616	1,078902	0,710236	5
snR24	1	1,743918	1,775576	2,664186	6
YCL075W	1	1,502214	1,958662	2,42327	6
YCL076W	1	1,553449	2,051489	2,530412	6
YDL003W	1	1,502469	1,771935	2,881081	6
YER135C	1	1,652391	1,41009	2,31394	6
YGL194C-A	1	1,502848	1,737629	2,435474	6
YGL258W-A	1	3,097357	2,791529	3,405688	6
YGR025W	1	3,598228	2,051284	4,219437	6
YIL071W-A	1	1,662578	1,300132	2,070437	6
YJL113W	1	1,544442	1,616073	2,415804	6
YJL114W	1	1,585472	1,354674	2,48945	6
YMR198W	1	1,582483	1,932209	2,580419	6
YMR232W	1	1,751113	1,955596	3,08725	6
YPR044C	1	1,606047	1,481957	2,079473	6
YCL074W	1	1,435461	1,791933	2,233369	6
YDR113C	1	1,268988	1,640402	2,026377	6
YDR480W	1	1,413477	1,584085	2,052965	6
YGL007C-A	1	1,373576	1,516659	2,085606	6
YGL053W	1	1,455012	1,920111	2,47661	6
YGL156W	1	0,95961	1,520666	2,002542	6
YGR122C-A	1	1,309043	1,753324	2,272245	6
YGR221C	1	1,36239	1,535103	2,093738	6
YHR054C	1	1,283859	1,656757	2,443269	6
YHR153C	1	1,448215	1,690263	2,454885	6
YIL083C	1	1,371402	1,531835	2,015133	6
YJR004C	1	1,361808	1,91475	2,307493	6
YKL128C	1	1,092355	1,584688	1,946665	6
YMR164C	1	1,141512	1,643091	2,087413	6
YMR180C	1	1,277575	1,683588	2,146686	6
YNL280C	1	1,134635	1,811539	2,397327	6
snR47	1	1,431189	1,291904	1,844793	6
snR59	1	1,144755	1,088539	1,907686	6
tE(UUC)C	1	1,202216	1,108588	1,685053	6

tE(UUC)K	1	1,062551	0,928956	1,63059	6
tK(UUU)O	1	1,041046	1,036703	1,951307	6
tP(AGG)C	1	1,394717	1,176738	2,051	6
tV(UAC)D	1	1,291736	0,683979	1,661215	6
YBL002W	1	1,38656	1,38462	2,675579	6
YBR009C	1	1,002021	1,057294	1,640762	6
YBR045C	1	1,082063	1,117493	1,718778	6
YBR085W	1	0,899246	1,285162	1,789035	6
YCR085W	1	0,891348	1,08946	1,72889	6
YDL214C	1	1,199066	1,199819	1,821324	6
YDL239C	1	1,211862	1,413488	1,881316	6
YDR085C	1	1,296259	1,491564	1,954587	6
YDR106W	1	0,973581	1,035558	1,799693	6
YDR154C	1	1,146961	1,117537	1,686789	6
YDR224C	1	1,156808	1,343374	1,838485	6
YDR249C	1	1,393283	1,408375	1,901896	6
YDR451C	1	1,095906	1,236182	2,311606	6
YER001W	1	1,181176	1,4518	2,714871	6
YER087C-A	1	0,938004	1,433982	2,089384	6
YER096W	1	0,90164	1,406424	2,037396	6
YFR057W	1	1,35111	1,215833	1,895707	6
YGL138C	1	1,246142	0,897003	2,204847	6
YGL184C	1	1,203686	1,477899	1,878432	6
YGL188C	1	0,973372	1,146173	1,79177	6
YGL217C	1	1,153061	1,125807	1,992782	6
YGR059W	1	0,876565	1,128309	1,628874	6
YGR222W	1	1,306667	1,369859	1,902638	6
YGR293C	1	0,969287	1,199087	1,94091	6
YHR071W	1	1,038639	1,078421	1,588194	6
YKL042W	1	1,382578	1,491145	2,085995	6
YKR034W	1	1,020457	0,923656	1,767735	6
YLR140W	1	1,055738	1,120081	1,737535	6
YLR452C	1	1,244247	1,439984	2,058815	6
YLR455W	1	1,065316	1,178382	1,64882	6
YML047C	1	1,46123	1,469894	2,274712	6
YMR182W-A	1	1,143454	1,335491	2,020869	6
YMR215W	1	1,040706	1,385753	1,833709	6
YNL028W	1	1,021226	1,296561	2,042445	6
YNL030W	1	1,004931	1,395771	2,131511	6
YNL031C	1	1,146147	1,403139	1,927752	6
YNL251C	1	1,064035	1,438592	1,922129	6

YNL269W	1	1,092553	1,172475	1,885649	6
YOL095C	1	1,237467	1,409138	1,973064	6
YOL155W-A	1	1,252405	1,070566	2,424867	6
YOL163W	1	0,977166	1,20116	1,637476	6
YOR130C	1	1,004942	1,383307	2,150331	6
YOR237W	1	1,031703	0,947083	1,684704	6
YOR238W	1	1,310129	1,399574	1,867381	6
YOR342C	1	1,215445	1,253703	1,718892	6
YOR365C	1	1,28055	1,119135	1,71736	6
YPL021W	1	0,70817	0,957653	1,81639	6
YPL201C	1	1,058383	0,995155	1,548676	6
YPL267W	1	1,224865	1,273695	2,150363	6
YPL279C	1	1,136509	1,238182	1,664936	6
YPR027C	1	1,233739	1,112973	1,750945	6
NME1	1	0,508019	0,511927	0,395739	7
RPR1	1	0,358016	0,509865	0,318953	7
snR17b	1	0,485942	0,402825	0,423361	7
snR190	1	0,351504	0,453976	0,33219	7
tL(UAA)J	1	0,481556	0,418414	0,300006	7
YAR071W	1	0,626508	0,368883	0,187321	7
YBR038W	1	0,601256	0,333362	0,178419	7
YBR093C	1	0,652984	0,463323	0,379112	7
YCL026C-B	1	0,584592	0,496497	0,339698	7
YDR397C	1	0,638265	0,560735	0,402586	7
YDR525W	1	0,47091	0,487175	0,410735	7
YDR534C	1	0,461401	0,492855	0,366261	7
YFL011W	1	0,542967	0,464546	0,349076	7
YGR228W	1	0,477785	0,542986	0,369966	7
YHR063W-A	1	0,501848	0,407795	0,184428	7
YHR136C	1	0,591441	0,377038	0,170496	7
YHR215W	1	0,620779	0,338018	0,148373	7
YIL158W	1	0,578464	0,321018	0,256829	7
YIL162W	1	0,552711	0,428231	0,326776	7
YJL079C	1	0,560786	0,521749	0,452839	7
YJL116C	1	0,608305	0,416102	0,392336	7
YJL118W	1	0,534251	0,511632	0,369321	7
YJR005C-A	1	0,363714	0,494283	0,296238	7
YJR092W	1	0,660078	0,369775	0,23004	7
YKL086W	1	0,522569	0,373435	0,239047	7
YKR075C	1	0,658574	0,502424	0,361057	7

YLR234W	1	0,607961	0,552316	0,379975	7
YLR307C-A	1	0,622868	0,49626	0,368792	7
YLR437C	1	0,543844	0,502891	0,324171	7
YML123C	1	0,62741	0,455455	0,282041	7
YMR032W	1	0,620038	0,309026	0,14814	7
YMR122C	1	0,649215	0,473469	0,402347	7
YNL043C	1	0,504936	0,423036	0,410972	7
YNL160W	1	0,565063	0,472016	0,341298	7
YOL050C	1	0,359619	0,636355	0,222193	7
YOR381W	1	0,574254	0,45259	0,396341	7
YOR382W	1	0,603258	0,460474	0,245492	7
YOR383C	1	0,499784	0,49088	0,316818	7
YPR156C	1	0,653685	0,523761	0,347239	7
YPR157W	1	0,633684	0,561606	0,377657	7
YAR018C	1	0,844074	0,44781	0,283939	7
YBR296C	1	0,761532	0,503526	0,28442	7
YDR033W	1	0,739428	0,420833	0,25759	7
YDR146C	1	0,73174	0,333449	0,202473	7
YLR131C	1	0,727885	0,450127	0,328773	7
YLR190W	1	0,699552	0,370748	0,280054	7
YML119W	1	0,77662	0,415966	0,323828	7
YMR001C-A	1	0,811877	0,226427	0,216765	7
YOR381W-A	1	0,676499	0,450624	0,461455	7
YPR149W	1	0,713769	0,466835	0,397041	7
tR(UCU)G1	1	0,492846	1,360363	0,94863	8
YDR136C	1	0,625621	1,300933	0,798794	8
YDR187C	1	0,49956	1,248389	0,719575	8
YEL049W	1	0,610633	1,091561	0,818706	8
YGL166W	1	0,664129	1,177138	0,716788	8
YGR176W	1	0,440691	1,180018	1,129271	8
YLL066C	1	0,617147	1,110037	0,905082	8
YMR304C-A	1	0,536211	1,074112	0,72973	8
YOL155C	1	0,596484	1,185683	1,017583	8
YOR053W	1	0,51613	1,153114	0,83498	8
YOR072W-A	1	0,485466	1,097099	0,830283	8
YOR183W	1	0,446531	1,167942	0,873526	8
YGR290W	1	0,83956	1,363692	0,658742	8
YJL052C-A	1	0,731873	1,126064	0,603893	8

YNR001W-A	1	0,682641	1,228219	0,620726	8
snR51	1	0,768194	1,534056	0,945533	8
YBR182C	1	1,017176	1,547956	1,069369	8
YCL001W-A	1	0,995594	1,688087	1,372945	8
YDL234C	1	1,031305	1,61571	1,259524	8
YFR015C	1	0,844769	1,576437	1,351764	8
YGL055W	1	0,988111	1,797302	1,347018	8
YGR008C	1	0,82668	1,636415	1,284668	8
YLL019C	1	1,068967	1,530921	1,194876	8
YML118W	1	1,074553	1,597111	1,263916	8
YML132W	1	1,053985	1,664514	1,328509	8
YOR032W-A	1	1,146715	1,817367	1,11971	8
YOR218C	1	0,887658	1,54123	0,987056	8
YPL275W	1	1,046396	1,543227	1,229647	8
YPR002C-A	1	1,005502	1,622597	1,283079	8
YBR005W	1	0,880679	1,412211	0,950993	8
YBR126C	1	0,753051	1,246991	1,07227	8
YDR516C	1	0,884093	1,458035	0,9755	8
YEL011W	1	0,787945	1,407758	1,000634	8
YEL060C	1	0,872436	1,4837	1,315433	8
YER020W	1	0,757815	1,230834	0,787066	8
YER152C	1	0,801776	1,482047	1,345381	8
YGR138C	1	0,780153	1,284891	0,746306	8
YGR203W	1	0,749567	1,178067	1,001359	8
YGR236C	1	0,72532	1,232859	0,919881	8
YGR248W	1	0,726977	1,188328	0,860442	8
YHR087W	1	0,742717	1,247206	1,013854	8
YHR145C	1	0,853482	1,486043	0,81894	8
YHR214C-E	1	0,764585	1,407567	0,980774	8
YIL101C	1	0,792832	1,347848	0,942569	8
YIL136W	1	0,755788	1,273842	0,914371	8
YIL169C	1	0,696275	1,317485	1,251931	8
YJL144W	1	0,821963	1,259908	1,064748	8
YJR120W	1	0,682628	1,109156	0,863204	8
YLR198C	1	0,691091	1,144006	0,741157	8
YML007C-A	1	0,75023	1,24831	1,094638	8
YML128C	1	0,845841	1,330353	1,194505	8
YMR056C	1	0,760298	1,29577	1,083888	8

YNL093W	1	0,736477	1,380367	1,083959	8
YOL014W	1	0,776044	1,399743	0,869334	8
YOR364W	1	0,670927	1,113629	0,887499	8
YPL231W	1	0,923764	1,413113	1,242751	8
YPR145C-A	1	0,883232	1,440777	0,9135	8
YDR247W	1	1,092973	1,376229	0,834812	8
YGR052W	1	1,032278	1,344187	0,748872	8
YLR358C	1	0,94796	1,320919	0,756852	8
YLR416C	1	0,957018	1,268001	0,815326	8
YLR466W	1	1,015076	1,407812	0,813883	8
YNR034W-A	1	0,93758	1,348264	0,787933	8
YOR268C	1	1,097813	1,432636	0,765247	8
YPL056C	1	0,932992	1,192858	0,765078	8
YMR242W-A	1	0,654696	2,005478	2,494575	9
tG(GCC)G1	1	1,934539	4,18001	5,14411	9
YBR040W	1	2,479405	4,093576	6,251651	9
YDL055C	1	1,759493	3,540192	4,698332	9
YDR124W	1	2,17134	3,084152	4,638515	9
YDR125C	1	1,919421	2,776254	3,984027	9
YDR340W	1	1,540604	3,224762	3,687038	9
YER070W	1	1,715049	3,391478	4,580618	9
YER124C	1	3,854136	9,379828	12,25153	9
YGL028C	1	2,510125	4,224349	4,648791	9
YGL089C	1	1,927924	4,335471	5,184665	9
YGR109W-B	1	1,521533	2,326761	2,844421	9
YHR143W	1	4,059095	14,33273	19,67882	9
YIL037C	1	2,18544	3,047278	4,22191	9
YIL140W	1	2,801475	5,615016	7,924442	9
YKL008C	1	1,625823	2,733554	3,327768	9
YKL221W	1	2,189523	2,914236	4,982472	9
YLR286C	1	3,056659	7,93782	9,716852	9
YNL015W	1	1,784694	3,124778	4,126296	9
YNL042W-B	1	1,721172	2,926237	4,685151	9
YOR316C-A	1	2,559171	6,912643	6,388597	9
YPL192C	1	2,27305	3,276851	4,872404	9
YPL256C	1	2,008982	2,928703	4,21676	9
YPR106W	1	2,584267	6,144079	6,128583	9
YPR141C	1	1,555278	2,299756	3,541613	9

tA(AGC)P	1	1,458891	2,141749	3,172718	9
tR(UCU)G3	1	1,315849	3,227293	5,107031	9
YBL003C	1	1,147853	1,661964	2,756535	9
YBR134W	1	1,115287	1,905965	2,661404	9
YDR107C	1	1,175409	1,957644	3,181602	9
YDR222W	1	1,112262	1,812798	3,134098	9
YDR225W	1	1,190681	2,126923	2,658607	9
YDR528W	1	1,444123	1,772783	3,290489	9
YGL230C	1	1,193338	2,306813	2,745497	9
YJL170C	1	1,45353	2,235813	2,970955	9
YKL096W-A	1	1,244558	2,521763	3,612721	9
YML027W	1	1,487448	2,058736	3,206838	9
YNL042W	1	1,191875	2,149805	2,801571	9
YNL277W-A	1	1,222303	2,749882	3,818579	9
YBR092C	1	0,670284	0,626115	0,79691	10
YOR298W	1	0,687451	0,599659	0,785478	10
YBR201C-A	1	1,530866	1,418967	1,370358	11
YEL008W	1	1,535013	1,163413	1,102474	11
YER138W-A	1	1,593518	1,267346	1,168165	11
YPL257W	1	1,512253	1,188121	1,322337	11
ICR1	1	1,248485	0,971801	0,587997	12
tL(CAA)N	1	1,451992	1,425189	0,588969	12
YDL246C	1	1,534771	1,228121	0,583836	12
YDR014W-A	1	1,316168	0,905342	0,487228	12
YEL050W-A	1	1,165757	1,367958	0,494097	12
YER189W	1	1,302656	1,101998	0,645612	12
YGR023W	1	1,053109	1,032838	0,612161	12
YJR038C	1	1,167264	1,035682	0,521754	12
YKL164C	1	1,48335	1,357716	0,594447	12
YKL185W	1	1,44837	1,244596	0,645457	12
YOL070C	1	1,096595	1,084091	0,65646	12
YOR391C	1	1,831503	0,815875	0,524261	12
YOR394C-A	1	1,334397	1,026401	0,652787	12
YPL130W	1	1,140111	1,224741	0,389074	12
YPL158C	1	1,642465	1,130937	0,60455	12
YPR092W	1	1,462442	0,765803	0,411006	12
tV(AAC)O	1	1,650295	1,208415	0,951106	12
YAL068C	1	1,69252	1,46624	0,774408	12

YCR010C	1	1,635418	1,278143	0,856273	12
YDL117W	1	1,673341	1,348386	0,817836	12
YDL179W	1	1,807172	1,281061	0,699666	12
YDR055W	1	1,725424	1,601798	0,760369	12
YFR052C-A	1	1,740735	1,450635	1,119797	12
YHL022C	1	1,769191	1,223742	0,708356	12
YIR040C	1	3,690951	2,798774	1,68458	12
YKL062W	1	1,512588	1,31637	1,086958	12
YKR091W	1	1,634477	1,397118	0,959342	12
YLR049C	1	2,010293	1,570936	1,061687	12
YNL130C-A	1	1,663366	1,475912	1,022248	12
YNL046W	1	1,414536	1,516761	0,828186	12
YIL141W	1	1,354554	0,875119	0,700564	12
YBR071W	1	1,427607	1,079534	0,740274	12
YDR250C	1	1,258888	1,043926	0,808855	12
YGL010W	1	1,291432	0,920007	0,806655	12
YGR190C	1	1,337951	1,022228	0,886412	12
YHR103W	1	1,351001	1,16859	0,772102	12
YKL116C	1	1,413947	1,090559	0,692682	12
YKL162C-A	1	1,452571	1,404091	0,793568	12
YKR053C	1	1,328329	1,089546	0,804195	12
YLR079W	1	1,400265	1,408377	0,91921	12
YML039W	1	1,298958	1,099602	0,822033	12
YMR323W	1	1,151238	1,07783	0,725729	12
YNL188W	1	1,353209	0,95756	0,870469	12
YNL211C	1	1,266386	0,90809	0,672281	12
YOL019W	1	1,422951	1,139511	0,914903	12
YOR177C	1	1,437847	1,316781	0,921502	12
YLR123C	1	1,131515	1,346569	0,7749	12
Q0045	1	0,545964	0,824104	1,114185	13
tG(GCC)D2	1	0,47371	0,841644	1,112338	13
tL(UAA)B1	1	0,655661	0,810369	0,991934	13
tV(AAC)K2	1	0,430161	1,001658	1,140386	13
YAL056C-A	1	0,636597	0,680316	0,96214	13
YBL073W	1	0,439333	0,674877	0,875062	13
YBR226C	1	0,455545	0,605944	1,465921	13
YCR050C	1	0,633392	0,807438	1,063546	13
YCR104W	1	0,617901	0,744145	1,152018	13
YDL009C	1	0,567335	0,899349	1,112047	13
YDL011C	1	0,530314	0,496651	1,133386	13
YDL094C	1	0,549768	1,013642	1,471505	13

YEL053W-A	1	0,521725	0,698244	1,367936	13
YFL058W	1	0,654868	0,898439	1,511964	13
YGL249W	1	0,60516	0,678398	1,040543	13
YGR011W	1	0,650842	0,585939	0,930447	13
YGR121W-A	1	0,447274	0,725744	0,920104	13
YHR021W-A	1	0,665686	1,017723	1,308619	13
YHR185C	1	0,611953	0,605415	0,868021	13
YLR281C	1	0,409987	0,364417	1,284011	13
YLR466C-B	1	0,536378	0,777363	1,171334	13
YML012C-A	1	0,536254	0,472931	1,001584	13
tF(GAA)D	1	0,800717	0,512355	1,086015	13
tS(UGA)E	1	0,985127	0,553001	1,216289	13
YDL158C	1	0,668405	0,592769	0,990199	13
YGR291C	1	0,819267	0,553105	1,065001	13
YOR029W	1	0,688865	0,550725	0,956238	13
YPL152W-A	1	0,919502	0,577282	1,063833	13
snR80	1	0,849245	0,845411	1,513275	13
tL(UAG)L1	1	0,676891	0,964372	1,599473	13
YBR047W	1	0,910237	0,987098	1,546365	13
YGL015C	1	0,878717	0,844919	1,592519	13
snR189	1	0,668876	0,807867	1,070874	13
tA(UGC)A	1	0,688986	0,809964	1,18583	13
tP(UGG)M	1	0,797819	0,858666	1,274921	13
YDR169C-A	1	0,769805	0,81959	1,204002	13
YDR273W	1	0,780015	1,028233	1,237862	13
YGR279C	1	0,699327	0,77258	1,109299	13
YIL160C	1	0,800993	0,968557	1,268586	13
YJL009W	1	0,91852	0,867208	1,445233	13
YML058W	1	0,784976	0,849212	1,197235	13
YMR133W	1	0,934044	1,025773	1,464209	13
YOL132W	1	0,719233	0,999489	1,194528	13
YOR242C	1	0,805355	0,798782	1,375626	13
YOR339C	1	0,920939	0,846588	1,443249	13
YPL025C	1	0,854473	0,909714	1,332155	13
YPL080C	1	0,770593	0,971513	1,228592	13
YPR151C	1	0,789314	0,780621	1,328415	13
Q0160	1	0,979448	0,795851	1,416262	13
snR71	1	0,934998	0,787978	1,265994	13

YGL149W	1	0,850046	0,794432	1,234134	13
YKR005C	1	0,912663	0,821279	1,279883	13
YML057C-A	1	0,974848	0,682779	1,244391	13
YNL289W	1	0,879456	0,675669	1,247406	13
snR30	1	0,462308	0,65523	0,587034	14
tL(CAA)L	1	0,531915	0,590969	0,554969	14
tQ(UUG)C	1	0,282594	0,72514	0,615232	14
YAL013W	1	0,63513	0,749777	0,53131	14
YAL020C	1	0,556124	0,795426	0,567478	14
YAL044C	1	0,610915	0,695574	0,579266	14
YAR053W	1	0,656519	0,603996	0,649964	14
YBL012C	1	0,511548	0,550477	0,441873	14
YBL095W	1	0,558801	0,721691	0,569074	14
YBL108W	1	0,4658	0,688065	0,261585	14
YBL109W	1	0,45369	0,84907	0,373369	14
YBR118W	1	0,548172	0,750922	0,557329	14
YBR213W	1	0,621963	0,771825	0,57487	14
YBR230W-A	1	0,498364	0,642033	0,480612	14
YBR231C	1	0,657599	0,682032	0,514735	14
YBR267W	1	0,549244	0,664496	0,57396	14
YCL040W	1	0,595207	0,883361	0,608978	14
YCR046C	1	0,54782	0,690176	0,487355	14
YCR047C	1	0,555216	0,860228	0,61809	14
YCR051W	1	0,542759	0,829953	0,577418	14
YCR073W-A	1	0,644636	0,84641	0,583086	14
YDL037C	1	0,663585	0,747352	0,522902	14
YDL039C	1	0,578302	0,714172	0,430421	14
YDR183C-A	1	0,533049	0,603401	0,40525	14
YDR327W	1	0,496439	0,891164	0,460058	14
YDR342C	1	0,60689	0,691722	0,596572	14
YDR413C	1	0,520523	0,623278	0,464153	14
YDR476C	1	0,57276	0,852254	0,552392	14
YDR482C	1	0,615952	0,923163	0,595494	14
YDR488C	1	0,577836	0,667105	0,504532	14
YDR510C-A	1	0,546778	0,55805	0,515009	14
YEL033W	1	0,639477	0,566849	0,625118	14
YEL066W	1	0,622328	0,700844	0,591384	14
YEL070W	1	0,618345	0,656999	0,470514	14
YER004W	1	0,663881	0,633933	0,420188	14

YER150W	1	0,609563	0,877901	0,407383	14
YFL014W	1	0,583414	0,539148	0,568951	14
YFL015C	1	0,481332	0,764992	0,576796	14
YFL021C-A	1	0,564039	0,780788	0,572812	14
YFL051C	1	0,596013	0,608397	0,563344	14
YFL065C	1	0,575663	0,715478	0,600292	14
YFL067W	1	0,561884	0,810871	0,475648	14
YFR017C	1	0,601033	0,726943	0,465118	14
YFR018C	1	0,562541	0,772626	0,628872	14
YGL236C	1	0,656573	0,718016	0,595313	14
YGR079W	1	0,647759	0,618494	0,647223	14
YGR087C	1	0,610877	0,595059	0,488254	14
YGR159C	1	0,606171	0,699606	0,605881	14
YGR192C	1	0,642856	0,837839	0,618348	14
YGR201C	1	0,638782	0,712142	0,604054	14
YGR249W	1	0,592021	1,076179	0,489301	14
YGR254W	1	0,598162	0,690693	0,441802	14
YHL020C	1	0,662629	0,834677	0,573966	14
YHL025W	1	0,620878	0,767098	0,525928	14
YHL040C	1	0,664162	0,692486	0,542869	14
YHL047C	1	0,644108	0,775776	0,633746	14
YHL048C-A	1	0,601438	0,975244	0,328736	14
YHL050C	1	0,629277	0,787146	0,607896	14
YHR032W-A	1	0,506131	0,881499	0,523373	14
YHR033W	1	0,546976	0,781371	0,5718	14
YHR041C	1	0,57287	0,803108	0,620141	14
YHR070W	1	0,59378	0,784867	0,625723	14
YHR173C	1	0,637099	0,662324	0,531637	14
YHR174W	1	0,642201	0,827991	0,604014	14
YIL102C	1	0,615189	0,612143	0,568209	14
YIR016W	1	0,639426	0,81315	0,604898	14
YJL007C	1	0,574202	0,645395	0,468871	14
YJL027C	1	0,21804	0,839303	0,428882	14
YJL052W	1	0,646961	0,827871	0,452569	14
YJL077W-B	1	0,601386	0,797263	0,517278	14
YJL213W	1	0,611298	0,607269	0,458284	14
YJR017C	1	0,565994	0,75779	0,544175	14
YJR073C	1	0,58362	0,665105	0,526613	14
YJR104C	1	0,555219	0,751619	0,548261	14
YJR115W	1	0,640512	0,677008	0,410842	14
YKL037W	1	0,628608	0,772961	0,623641	14

YKR048C	1	0,641179	0,786743	0,621983	14
YLR044C	1	0,577099	0,731277	0,513848	14
YLR099W-A	1	0,569622	0,793783	0,562048	14
YLR202C	1	0,463247	0,679378	0,605823	14
YLR222C-A	1	0,554763	0,981227	0,378924	14
YLR236C	1	0,537324	0,533274	0,471772	14
YLR316C	1	0,51955	0,675731	0,492901	14
YLR438C-A	1	0,609126	0,77612	0,65361	14
YLR438W	1	0,642909	0,692194	0,607373	14
YLR462W	1	0,502292	1,037104	0,546243	14
YML009C-A	1	0,520689	0,625635	0,345268	14
YML101C	1	0,660141	0,745659	0,487761	14
YML102W	1	0,653276	0,692523	0,53526	14
YML113W	1	0,61682	0,730903	0,582778	14
YMR042W	1	0,590477	0,775689	0,619216	14
YMR046W-A	1	0,373634	0,709558	0,647291	14
YMR116C	1	0,627048	0,675245	0,567523	14
YMR173W-A	1	0,421822	0,812271	0,449176	14
YMR244C-A	1	0,281551	0,728174	0,442675	14
YMR244W	1	0,593313	0,710597	0,371849	14
YMR303C	1	0,563272	0,835353	0,607515	14
YNL240C	1	0,575233	0,762942	0,564496	14
YNL285W	1	0,584435	0,585393	0,635942	14
YNR014W	1	0,587729	0,741767	0,465585	14
YOL067C	1	0,647207	0,774662	0,598946	14
YOL086C	1	0,528896	0,751106	0,495371	14
YOR083W	1	0,51518	0,565657	0,456997	14
YOR161C-C	1	0,590364	0,617781	0,554898	14
YOR314W	1	0,39981	0,604223	0,483727	14
YPR080W	1	0,578217	0,762347	0,596122	14
YPR087W	1	0,370116	0,818392	0,629733	14
YPR170W-B	1	0,591703	0,741329	0,654497	14
YPR182W	1	0,597216	0,848845	0,622744	14
YPR204W	1	0,614573	0,853707	0,59883	14
YAL005C	1	0,70689	0,646686	0,568875	14
YEL065W	1	0,673642	0,641032	0,613654	14
YNL304W	1	0,69085	0,608552	0,580993	14

YOR084W	1	0,715094	0,6636	0,552444	14
YPL155C	1	0,675508	0,632118	0,492697	14
tN(GUU)K	1	0,67681	0,958294	0,530935	14
YAL022C	1	0,707938	0,78804	0,554089	14
YAL060W	1	0,687163	0,705738	0,540525	14
YAL065C	1	0,678176	0,824479	0,597516	14
YAR068W	1	0,709813	0,787598	0,493019	14
YBL082C	1	0,696887	0,712429	0,607457	14
YBR240C	1	0,687147	0,734386	0,520207	14
YEL010W	1	0,741716	0,797527	0,502322	14
YEL077C	1	0,714792	0,79763	0,542437	14
YER147C	1	0,69601	0,759474	0,609678	14
YHR040W	1	0,668991	0,783596	0,586228	14
YHR219W	1	0,690641	0,779066	0,595292	14
YIL177C	1	0,704307	0,707844	0,396495	14
YJL063C	1	0,671228	0,766053	0,542345	14
YJL077C	1	0,710052	0,704463	0,474585	14
YJR113C	1	0,679964	0,782517	0,547827	14
YJR116W	1	0,695212	0,701021	0,61916	14
YLR013W	1	0,682537	0,916057	0,577632	14
YLR308W	1	0,678521	0,849188	0,493847	14
YMR276W	1	0,679742	0,798597	0,58068	14
YNL034W	1	0,707316	0,992194	0,492088	14
YNL144C	1	0,707654	0,7105	0,458052	14
YOL059W	1	0,709695	0,718547	0,482545	14
YPL055C	1	0,696247	0,740743	0,562124	14
YPR152C	1	0,680584	0,778349	0,59148	14
YBR090C	1	0,569561	1,412374	0,797122	15
YDR366C	1	0,500259	1,286381	0,649316	15
YHR218W	1	0,561951	1,302128	0,609646	15
YLR349W	1	0,609074	1,291231	0,497332	15
YML100W-A	1	0,623376	2,340677	1,211984	15
YMR316C-A	1	0,278711	1,17144	0,506419	15
YOL052C-A	1	0,610646	1,250708	0,606639	15
YOL085W-A	1	0,645007	1,637308	0,675474	15
YIR041W	1	1,388635	1,870184	0,364239	15
YLR041W	1	1,439396	2,107392	0,49962	15
YGL261C	1	1,55194	3,187662	1,558152	15
tN(GUU)G	1	0,899245	1,825496	0,818222	15

tP(UGG)O3	1	0,802376	1,733496	0,824991	15
YAR075W	1	1,338624	3,549123	1,361402	15
YBR219C	1	1,419353	2,301349	0,751994	15
YDL240C-A	1	0,714128	2,437344	1,240532	15
YEL045C	1	0,778226	1,902311	1,085595	15
YER158W-A	1	0,767774	3,481779	1,563031	15
YGL118C	1	1,11018	2,655862	1,057864	15
YKL202W	1	1,133014	1,684646	0,768578	15
YLR232W	1	1,24707	1,828494	0,930028	15
YML034C-A	1	0,790145	1,849937	0,924164	15
YMR107W	1	0,765791	2,449555	1,100949	15
YOL131W	1	1,042406	0,721788	1,082751	16
Q0075	1	0,577831	0,365227	0,932834	17
Q0158	1	0,358778	0,365632	0,462539	17
snR19	1	0,409232	0,510495	0,557128	17
snR52	1	0,60142	0,459501	0,580704	17
snR74	1	0,38512	0,404994	0,649994	17
tG(CCC)O	1	0,520917	0,602895	0,748601	17
YAL018C	1	0,46624	0,351485	0,597135	17
YBL044W	1	0,290878	0,130709	0,691648	17
YBR301W	1	0,217023	0,462209	0,672249	17
YJR079W	1	0,409596	0,188144	0,45767	17
YKL131W	1	0,401638	0,528998	0,676795	17
YMR294W-A	1	0,21632	0,444599	0,562513	17
YNL303W	1	0,48623	0,529833	0,62477	17
YOR135C	1	0,462237	0,401537	0,65014	17
YOR388C	1	0,646632	0,52777	0,628141	17
YOR396W	1	0,372153	0,386438	0,600923	17
YPR126C	1	0,62103	0,235463	0,683925	17
YNL149C	1	0,701944	0,4556	0,741097	17
tG(GCC)P1	1	0,646973	0,737087	0,844883	18
YCL036W	1	0,635171	1,001622	0,990249	18
YDR215C	1	0,533305	0,827978	0,837087	18
YGL126W	1	0,654799	0,88517	0,853137	18
YGR063C	1	0,655895	0,878589	0,944314	18
YGR294W	1	0,622883	0,979653	1,010079	18
YHR079C-A	1	0,560947	1,071351	1,098024	18
YKL031W	1	0,63939	0,970618	0,847341	18
YKL097C	1	0,55044	0,97768	1,079483	18

YKL183C-A	1	0,568106	0,876044	0,925525	18
YMR069W	1	0,52822	0,819953	0,832755	18
YNL208W	1	0,620402	1,032556	0,895959	18
YPL121C	1	0,639135	1,089359	1,181065	18
YPL277C	1	0,63512	1,01791	1,019114	18
YAR073W	1	0,703258	1,137367	1,172168	18
YHR095W	1	0,67177	1,019709	0,981534	18
YIL066C	1	0,666672	1,089921	1,028594	18
YKL096C-B	1	0,701457	1,055099	0,9927	18
YMR007W	1	0,714005	1,051654	1,193095	18
YOR387C	1	0,757787	1,055815	1,176162	18
snR72	1	1,162837	0,651678	1,255944	19
YBL100C	1	1,511223	1,282673	1,647118	19
YDR043C	1	1,7164	1,581131	1,928126	19
YDR379C-A	1	1,646785	1,521786	1,948712	19
YDR467C	1	1,695029	1,641878	1,795052	19
YFR012W-A	1	1,78291	1,430693	2,009071	19
YGL074C	1	1,561044	1,433952	1,881859	19
YHR014W	1	1,511987	1,508995	1,647978	19
YKL061W	1	1,53721	1,452941	1,598299	19
YPR078C	1	1,573961	1,497951	1,897995	19
snR61	1	1,075651	0,993891	1,520423	19
snR68	1	1,026389	1,0021	1,507804	19
YBR156C	1	1,40303	1,272429	1,609442	19
YBR188C	1	1,292962	1,29844	1,514846	19
YBR194W	1	1,451312	1,353426	1,562214	19
YCL012C	1	1,278514	1,263576	1,600883	19
YDL135C	1	1,265534	1,298038	1,571007	19
YDR538W	1	1,446454	1,376813	1,515042	19
YER044C	1	1,200281	1,17758	1,505829	19
YER048W-A	1	1,320334	1,300227	1,640632	19
YFL012W	1	1,300011	1,121536	1,53939	19
YGL038C	1	1,478001	1,322525	1,518033	19
YGL194C	1	1,300821	1,240195	1,517264	19
YGL223C	1	1,407536	1,369411	1,525985	19
YGR242W	1	1,148701	1,131442	1,510791	19
YHR001W-A	1	1,409856	1,422652	1,682136	19
YHR101C	1	1,212508	1,252084	1,549131	19
YJL089W	1	1,117068	1,105519	1,5694	19

YKL068W-A	1	1,392346	1,211367	1,703829	19
YLR053C	1	1,486737	1,229191	1,75149	19
YLR341W	1	1,407835	1,035822	1,567791	19
YLR453C	1	1,452578	1,397485	1,551112	19
YML046W	1	1,487486	1,397415	1,711199	19
YMR316C-B	1	1,159837	1,162597	1,56786	19
YMR320W	1	1,398175	1,232443	1,602947	19
YNL070W	1	1,467919	1,239347	1,624813	19
YOL157C	1	1,320877	1,287528	1,682994	19
YOR302W	1	1,494694	1,105499	1,556379	19
YPL156C	1	1,463204	1,347461	1,835976	19
YPL191C	1	1,469269	1,460006	1,627126	19
YPL225W	1	1,292526	1,213336	1,51016	19
YPR010C-A	1	1,419534	1,400055	1,596748	19
snR36	1	1,128388	0,927209	1,439521	19
YAR047C	1	1,133509	0,880607	1,425831	19
YLR445W	1	1,106368	0,934846	1,4833	19
YPL249C-A	1	1,14005	0,960545	1,457059	19
snR48	1	1,941979	1,796054	1,94217	20
snR67	1	1,616469	1,702099	1,382382	20
tD(GUC)O	1	1,547305	1,779172	1,604403	20
tK(UUU)L	1	2,096258	2,444522	1,12744	20
tV(AAC)M2	1	2,806762	3,068307	1,94087	20
YDL034W	1	1,528719	1,720177	1,612757	20
YDL119C	1	2,120649	2,387822	1,892862	20
YDR102C	1	1,70909	1,73709	1,703342	20
YDR119W-A	1	2,006487	2,648859	1,268037	20
YER121W	1	1,589191	1,945398	1,775293	20
YGL259W	1	1,755844	1,834258	1,899356	20
YGR015C	1	1,557918	1,530397	1,397367	20
YGR044C	1	1,965922	2,433357	1,674556	20
YGR149W	1	1,989889	2,065034	1,8181	20
YHL037C	1	2,164772	2,472392	2,276119	20
YJL106W	1	1,714244	1,646344	1,3242	20
YJL107C	1	1,788665	2,054705	2,056781	20
YJL119C	1	1,80475	2,873428	1,782393	20
YJL189W	1	1,556158	1,595975	1,484554	20
YKL161C	1	2,43282	2,726669	2,365195	20
YLR012C	1	1,753538	1,592251	1,607189	20

YLR461W	1	1,915935	1,814548	1,456637	20
YMR315W-A	1	1,678526	1,859863	1,36177	20
YNL078W	1	1,691691	1,933391	1,412698	20
YNL318C	1	2,19843	2,66827	2,211623	20
YNL327W	1	1,839616	2,434363	1,525742	20
YOR024W	1	1,838552	1,638589	1,352502	20
YOR264W	1	1,977519	2,436552	1,794669	20
YPL066W	1	1,697887	1,689245	1,389258	20
YPR005C	1	2,358971	1,994271	1,646079	20
YBR182C-A	1	1,479734	1,831784	1,322561	20
YCR099C	1	1,422859	1,542452	1,251011	20
YDR481C	1	1,198971	1,589901	1,09047	20
YDR540C	1	1,367312	1,83596	1,627	20
YEL059W	1	1,345003	1,630952	1,38282	20
YER078W-A	1	1,395159	1,631206	0,925275	20
YGL007W	1	1,317346	1,729786	1,328255	20
YGR086C	1	1,315322	1,594176	1,217826	20
YGR107W	1	1,432752	1,695792	1,186492	20
YGR234W	1	1,299239	1,76288	1,535888	20
YHR030C	1	1,456733	1,519417	1,364559	20
YIL055C	1	1,2707	1,761996	1,398208	20
YJL043W	1	1,213228	1,574965	1,340641	20
YLR194C	1	1,36576	1,696985	0,867417	20
YLR252W	1	1,205935	1,587043	1,342516	20
YLR257W	1	1,410256	1,716091	1,630185	20
YLR300W	1	1,484329	1,838868	1,497629	20
YLR406C-A	1	1,212331	1,586656	1,123901	20
YMR175W	1	1,240772	1,673585	0,996943	20
YMR306C-A	1	1,439928	1,791691	1,258041	20
YNL009W	1	1,36684	1,54166	1,430646	20
YNL173C	1	1,210872	1,552818	1,331405	20
YNL192W	1	1,418085	1,523364	1,339603	20
YNL328C	1	1,474227	1,625988	1,36382	20
YNR065C	1	1,264178	1,512149	1,309161	20
YOL047C	1	1,200791	2,026475	1,302363	20
YOL122C	1	1,355822	1,526637	1,317346	20
YOR032C	1	1,282577	1,666786	1,06263	20
YPL088W	1	1,430146	1,822196	1,409756	20
YPL163C	1	1,483478	1,507561	1,423149	20

YPR064W	1	1,254033	1,590665	1,428889	20
LSR1	1	0,309732	0,330162	0,271643	21
Q0020	1	0,107735	0,124556	0,155995	21
Q0050	1	0,306414	0,131822	0,284153	21
Q0055	1	0,244133	0,172626	0,312041	21
SCR1	1	0,119033	0,183236	0,121556	21
snR17a	1	0,310186	0,247524	0,225905	21
YLL066W-B	1	0,331549	0,235987	0,199002	21
YBR285W	1	1,047497	1,180337	0,746981	22
YIL054W	1	1,041305	1,252269	0,784251	22
YPL014W	1	0,999613	1,115064	0,703065	22
tR(ACG)E	1	2,431434	1,835559	6,092701	23
YDL227C	1	1,873372	4,026924	8,835852	23
YGR109C	1	4,461076	9,239464	25,85479	23
YJL152W	1	1,652685	1,467921	3,817984	23
YOL007C	1	1,521077	2,121719	4,466346	23
tA(AGC)H	1	1,292913	2,843487	5,924502	23
tD(GUC)L2	1	0,923019	2,013805	4,709967	23
tH(GUG)E2	1	1,18278	4,101554	9,458606	23
tI(AAU)I2	1	1,143554	1,927998	3,619325	23
tR(ACG)L	1	1,407286	3,416833	6,380187	23
YNL300W	1	0,901063	1,379841	5,048317	23
YNL332W	1	0,879417	1,319586	2,887538	23
YDR218C	1	1,470195	0,589573	1,070753	24
RNA170	1	1,925647	1,266806	1,465569	24
snR79	1	1,754594	1,307076	1,688384	24
tG(GCC)M	1	2,04356	1,187647	1,851581	24
YAL044W-A	1	1,967987	1,055271	1,602143	24
YBL108C-A	1	1,563788	1,146013	1,092304	24
YBR200W-A	1	2,108378	1,106211	1,623397	24
YCR102W-A	1	1,966603	1,541022	1,490398	24
YDR182W-A	1	1,556689	0,863577	1,123603	24
YDR455C	1	1,659094	1,059538	1,297726	24
YDR542W	1	1,799159	1,159023	1,405928	24
YER053C-A	1	1,723697	1,134057	1,138422	24
YER106W	1	1,593966	0,770372	0,894957	24
YGR016W	1	1,786624	1,442969	1,395417	24
YGR273C	1	2,172104	0,683152	0,887837	24

YHL045W	1	1,99756	1,359802	1,477004	24
YJL127W-A	1	1,593866	1,043169	1,406533	24
YJL202C	1	2,860195	1,92496	2,514597	24
YJL220W	1	2,595382	1,250857	3,047524	24
YJR157W	1	2,817769	1,567991	1,870442	24
YJR159W	1	1,840695	1,479368	1,381444	24
YLR269C	1	2,427198	1,221829	1,686297	24
YLR296W	1	1,973857	0,768914	1,053662	24
YLR365W	1	2,770562	1,98004	1,909287	24
YMR151W	1	1,806156	1,165535	1,372838	24
YOL037C	1	3,124705	1,943534	3,294304	24
YOR255W	1	1,816168	1,167136	1,380349	24
YPL060C-A	1	1,537369	0,822052	0,986605	24
YPR150W	1	2,965268	0,766871	2,122896	24
tK(UUU)P	1	1,385784	0,829403	1,038863	24
YNL179C	1	1,462059	0,974701	1,315308	24
YOL024W	1	1,421407	0,935944	1,036465	24
YOR248W	1	1,397521	0,821738	1,245082	24
tH(GUG)M	1	0,442918	1,657301	1,227551	25
tV(AAC)G2	1	0,646499	2,472099	1,975527	25
YLR434C	1	0,587117	1,845748	1,309034	25
snR58	1	1,569825	2,294802	2,679626	25
YBR158W	1	2,134448	2,774696	3,045496	25
YDR133C	1	1,83505	2,64981	2,756991	25
YER185W	1	1,641831	2,381336	2,399143	25
YFL021W	1	1,651923	2,954178	2,157677	25
YGR041W	1	1,825793	3,218375	2,843647	25
YKL096W	1	1,843667	3,004902	2,86655	25
YLR258W	1	1,753558	3,525965	2,874188	25
YNL066W	1	1,633456	3,150514	2,947225	25
YNL103W-A	1	1,573172	3,755805	3,641731	25
YNR067C	1	2,122032	3,408353	2,542195	25
YOR263C	1	1,761155	4,492986	3,140195	25
IRT1	1	1,237819	2,204606	2,49984	25
RUF23	1	1,133106	2,626957	1,795614	25
snR39B	1	1,308071	2,012486	2,165248	25
tA(UGC)O	1	0,836446	1,687859	1,454646	25
tY(GUA)D	1	0,72148	1,7341	1,522442	25
YBR072C-A	1	1,364156	2,61819	2,68788	25
YCL073C	1	1,326723	3,328881	3,186152	25
YDL050C	1	1,097499	2,003325	1,933864	25

YDL118W	1	1,240236	2,356121	1,789293	25
YDR095C	1	1,395159	2,623768	2,157275	25
YDR157W	1	1,441139	2,89829	2,303953	25
YER019W	1	0,919484	2,063592	1,854943	25
YFR032C	1	0,99899	2,03648	2,15605	25
YGL229C	1	1,492771	2,406506	2,662228	25
YHR094C	1	1,177268	2,169566	1,679015	25
YJL028W	1	1,414224	2,461822	2,054883	25
YJL078C	1	0,79608	1,679339	1,415574	25
YJL150W	1	0,742719	2,273502	2,103813	25
YLR285C-A	1	0,907318	3,479181	2,89618	25
YML100W	1	1,03742	2,754176	2,686391	25
YMR230W-A	1	1,146186	2,426507	1,565368	25
YMR247W-A	1	1,427362	2,643069	2,295262	25
YMR316W	1	1,222245	1,90243	1,76038	25
YOL016C	1	0,957674	1,80108	1,389722	25
YOR230W	1	1,189204	1,898795	2,141322	25
YOR374W	1	1,032424	2,423852	2,418319	25
YOR385W	1	1,205683	1,91309	1,676396	25
YPR160W	1	1,32603	2,826457	2,784567	25
Q0065	1	1,418246	0,553942	0,706408	26
RDN5-1	1	0,956091	0,614816	0,685491	26
snR65	1	0,804574	0,598591	0,670382	26
snR66	1	0,890726	0,640415	0,90709	26
YAL024C	1	0,939726	0,624816	0,64416	26
YBR098W	1	0,887257	0,611173	0,669671	26
YDR360W	1	0,831274	0,631495	0,70818	26
YDR380W	1	0,938347	0,663164	0,714069	26
YEL009C-A	1	1,084061	0,543299	1,085641	26
YEL030C-A	1	0,995768	0,474463	0,623246	26
YER181C	1	0,931908	0,386141	0,954741	26
YGL183C	1	1,005764	0,65059	1,02171	26
YHR049C-A	1	1,31597	0,640211	0,592004	26
YIL119C	1	1,134145	0,64614	0,628585	26
YJL075C	1	1,103323	0,624776	0,857747	26
YKL108W	1	0,921264	0,665218	0,646418	26
YKR073C	1	1,134081	0,511885	0,997127	26
YLL042C	1	0,978167	0,545877	0,761217	26
YLR084C	1	0,915445	0,629153	0,669879	26
YLR412C-A	1	0,988461	0,495187	0,976114	26

YML099W-A	1	0,972213	0,586922	0,706605	26
YMR144W	1	0,964155	0,645478	0,70102	26
YNL150W	1	0,944599	0,313083	0,598646	26
YNL319W	1	1,006569	0,395182	0,857868	26
YNR009W	1	0,73257	0,550917	0,713848	26
YOL046C	1	0,957345	0,436581	1,027193	26
YOR214C	1	0,98298	0,474699	0,891759	26
YOR293C-A	1	0,778228	0,347663	0,783201	26
YPL124W	1	0,978612	0,666199	0,724	26
YPL255W	1	0,947407	0,610348	0,735134	26
YPR119W	1	0,892514	0,600804	0,651539	26
YPR203W	1	1,052868	0,599238	0,677263	26
YBR085C-A	1	1,044304	0,773479	0,657095	26
YHR127W	1	0,937354	0,66872	0,660411	26
YMR101C	1	1,108314	0,693945	0,650355	26
YMR211W	1	0,994976	0,735812	0,655579	26
YPR016W-A	1	1,001228	0,710458	0,632346	26
YAL037C-A	1	1,087918	0,700604	0,802569	26
YBR018C	1	1,099795	0,711778	0,754051	26
YDL211C	1	1,323794	0,819855	1,055658	26
YGR146C	1	1,183086	0,714655	0,770064	26
YGR225W	1	1,283412	0,789259	0,721502	26
YJL038C	1	1,280096	0,817686	0,831598	26
YML090W	1	1,320057	0,854768	0,821555	26
YMR321C	1	1,216418	0,809052	0,797314	26
YOR114W	1	1,223797	0,689043	0,81925	26
YOR313C	1	1,206346	0,793713	0,973246	26
YPR096C	1	1,255079	0,797531	1,046696	26
YPR123C	1	1,266552	0,808755	0,704637	26
YPR130C	1	1,035369	0,682982	0,864877	26
YBL111C	1	1,13161	0,781822	0,677474	26
YOR199W	1	1,181812	0,7954	0,7818	26

7.6 *cdc36-16* Clustering Analysis

Table 7. 6: *cdc36-16* clustering analysis divided by the first timepoint value

Gene	*cdc36-16*_40	*cdc36-16*_50	*cdc36-16*_60	*cdc36-16*_70	Cluster
YBR098W	1	0,940444989	0,657035915	0,677945508	1
YIL057C	1	0,909981453	0,614153158	0,716657177	1

YLR460C	1	1,081762281	0,64565207	0,764991495	1
YPR135W	1	0,948081152	0,654149348	0,667491402	1
snR40	1	1,113591906	1,100050596	0,631433657	1
YAL007C	1	0,934372227	0,783043167	0,590679484	1
YAL018C	1	0,90402721	0,745579931	0,582880334	1
YAL019W	1	0,839335614	0,699225697	0,661858068	1
YAL023C	1	0,79406846	0,704058117	0,616963292	1
YAR007C	1	1,001017965	0,848894831	0,656733644	1
YAR066W	1	0,934905325	0,911406754	0,545358443	1
YBL002W	1	0,977357092	0,812475106	0,655346981	1
YBL010C	1	0,961451377	0,803022248	0,635118417	1
YBL031W	1	0,937131576	0,830814214	0,625426899	1
YBL046W	1	0,825217629	0,758546523	0,565702054	1
YBL061C	1	0,898072124	0,738214836	0,643817721	1
YBR007C	1	1,034840885	0,819928951	0,651099874	1
YBR018C	1	0,909190583	0,667072579	0,648219292	1
YBR025C	1	0,840181397	0,753042744	0,656524261	1
YBR067C	1	0,862176546	0,69999444	0,599648005	1
YBR087W	1	0,955372144	0,802053142	0,603136174	1
YBR123C	1	0,983295162	0,743224704	0,642226323	1
YBR160W	1	0,925975189	0,836268937	0,637036895	1
YBR180W	1	0,926981605	0,790454898	0,662695471	1
YBR243C	1	0,940829858	0,807625336	0,637752437	1
YBR249C	1	0,794512314	0,73639152	0,649955249	1
YCL019W	1	0,962587455	0,915737501	0,611944212	1
YCL064C	1	0,848616471	0,701495428	0,622474131	1
YCR090C	1	0,891160456	0,818029394	0,565685095	1
YDL090C	1	0,979166475	0,898229739	0,644696652	1
YDL093W	1	0,850148767	0,683583298	0,604291095	1
YDL095W	1	0,858004226	0,695412426	0,658160185	1
YDL102W	1	0,914876331	0,725304586	0,58103171	1
YDL164C	1	0,930928682	0,708455583	0,625143831	1
YDR112W	1	0,786033347	0,754681985	0,588375945	1
YDR279W	1	0,95628515	0,838587717	0,646803104	1
YDR297W	1	0,824092268	0,749763993	0,597314534	1
YDR348C	1	0,893220585	0,785342072	0,645256807	1
YEL032W	1	0,774638962	0,683452476	0,610814865	1
YEL055C	1	0,932287941	0,719258727	0,63484699	1
YER028C	1	0,760257565	0,696345151	0,617072547	1
YER087C-B	1	0,964059182	0,817327801	0,666456732	1
YER131W	1	0,810593478	0,750241156	0,616511007	1

YER138W-A	1	0,995909382	0,696557634	0,601800017	1
YER148W-A	1	1,210914877	1,105885991	0,638333719	1
YER156C	1	0,884498328	0,811227014	0,595276403	1
YER170W	1	0,85503582	0,811780005	0,563073244	1
YFL034C-B	1	0,968310248	0,784747271	0,618719791	1
YFL045C	1	0,923807692	0,824878344	0,657033333	1
YFR027W	1	0,946734096	0,805978902	0,612965591	1
YFR041C	1	1,007713683	0,861392667	0,662053347	1
YGL012W	1	0,823825405	0,712323437	0,600800379	1
YGL061C	1	1,035244733	0,863763996	0,652666587	1
YGL102C	1	0,855256917	0,823308661	0,545810842	1
YGL109W	1	0,821008054	0,781978547	0,586490759	1
YGL201C	1	0,803389727	0,68054678	0,637205788	1
YGL225W	1	0,854493765	0,734859552	0,639235855	1
YGL253W	1	0,830618716	0,749232759	0,663688963	1
YGR035C	1	0,87688259	0,766253715	0,651996495	1
YGR189C	1	0,85015572	0,801531634	0,663337098	1
YGR229C	1	0,889614941	0,750410297	0,5810336	1
YGR230W	1	1,066086086	0,836996671	0,665225196	1
YHL015W	1	0,863767495	0,808581543	0,645130804	1
YHR050W	1	0,853734656	0,752164034	0,569490796	1
YHR142W	1	0,881522852	0,749718692	0,636100221	1
YHR214W-A	1	0,874209129	0,727723215	0,659162841	1
YIL069C	1	0,851846843	0,804312699	0,660680701	1
YIL096C	1	0,787813855	0,691998157	0,664188569	1
YIL106W	1	0,901654706	0,757908567	0,627273186	1
YJL012C	1	0,908457321	0,765668326	0,666211675	1
YJL095W	1	0,925371959	0,751415331	0,612952557	1
YJL115W	1	0,840898097	0,751057717	0,647113048	1
YJL173C	1	0,917753743	0,842839028	0,631277063	1
YJL196C	1	0,889117014	0,857549391	0,617432215	1
YJL208C	1	0,817743029	0,739627765	0,637674993	1
YJR071W	1	1,086397069	0,881827092	0,595224915	1
YJR118C	1	0,866159332	0,758420074	0,60417833	1
YKL042W	1	1,018910542	0,891966583	0,662904807	1
YKL045W	1	1,001102931	0,83497833	0,557598176	1
YKL089W	1	0,90277725	0,839217774	0,627843999	1
YKR080W	1	0,810718827	0,680304176	0,623918956	1
YLL021W	1	0,852022069	0,689497183	0,617095248	1

YLL032C	1	0,977312673	0,7243584	0,603112748	1
YLR042C	1	0,881558003	0,774890677	0,579504644	1
YLR108C	1	1,004593	0,680821596	0,613152866	1
YLR233C	1	1,039244714	0,832682053	0,623321364	1
YLR273C	1	1,11980696	0,878103869	0,656156602	1
YLR274W	1	0,968458282	0,778345908	0,592153996	1
YLR313C	1	0,925515107	0,713955143	0,596727161	1
YLR341W	1	0,885070656	0,736142818	0,652051629	1
YLR342W-A	1	0,834759897	0,688982705	0,6496936	1
YLR373C	1	0,910525328	0,772898412	0,60440719	1
YLR376C	1	1,000085924	0,721820706	0,654980247	1
YLR381W	1	1,051114502	0,739361296	0,609330965	1
YLR386W	1	0,963989829	0,764737349	0,64005463	1
YLR388W	1	0,884738407	0,790914879	0,638266348	1
YLR457C	1	0,969235015	0,791700786	0,665802081	1
YML037C	1	0,852015592	0,7331566	0,655126062	1
YML061C	1	0,929743381	0,743002222	0,569440794	1
YML085C	1	0,830985622	0,746953722	0,66313979	1
YML097C	1	0,970412658	0,766152157	0,660905757	1
YMR010W	1	1,03883859	0,780148888	0,621190458	1
YMR101C	1	0,865660397	0,798172708	0,650012101	1
YMR211W	1	0,903789705	0,773739065	0,659661868	1
YMR321C	1	0,895857943	0,799495328	0,588725102	1
YNL088W	1	0,99533835	0,768155684	0,665101491	1
YNL182C	1	0,821965913	0,700760769	0,657624813	1
YNL188W	1	1,050412582	0,904355423	0,569865864	1
YNL220W	1	0,853954311	0,787628434	0,65501417	1
YNL225C	1	1,040669834	0,820390641	0,608582279	1
YNL312W	1	0,918866186	0,853075062	0,632541685	1
YNL313C	1	0,844406934	0,67164494	0,649215586	1
YNR028W	1	0,909675608	0,792216275	0,596925981	1
YOL034W	1	0,893869899	0,723381996	0,634453867	1
YOR025W	1	0,92911682	0,782560111	0,563777726	1
YOR026W	1	0,9022374	0,794428617	0,656247588	1
YOR058C	1	0,966601929	0,724143046	0,59483757	1
YOR101W	1	0,81562823	0,761411246	0,646174314	1
YOR114W	1	1,043046159	0,826570616	0,540896389	1
YOR127W	1	0,991499204	0,804454111	0,665634895	1
YOR184W	1	0,821130664	0,741993958	0,665291028	1
YOR279C	1	1,000049202	0,835631741	0,62584235	1
YOR344C	1	0,921790413	0,776314966	0,66402169	1

YPL141C	1	0,895922001	0,697801859	0,628901757	1
YPL153C	1	0,98931172	0,740638697	0,640091357	1
YPL163C	1	0,916690719	0,855892973	0,575390616	1
YPL209C	1	1,057979621	0,806763221	0,62852479	1
YPL227C	1	0,971744922	0,807308819	0,578349971	1
YPR012W	1	0,868675574	0,908998872	0,520728935	1
YPR018W	1	0,980263163	0,764441432	0,56775835	1
YPR125W	1	0,8990754	0,803196108	0,649485724	1
YER106W	1	1,224076445	0,977731845	0,736406234	1
YER111C	1	1,223185428	0,890323111	0,667112026	1
YFR042W	1	1,060124165	0,880808365	0,671863866	1
YGR168C	1	1,087966774	0,896067161	0,724792102	1
YHL022C	1	1,117908128	0,793304128	0,710605787	1
YKL092C	1	1,081860428	0,724534475	0,677779496	1
YKL116C	1	1,10970686	1,025197894	0,69688238	1
YKR083C	1	1,111499548	0,953556969	0,714254611	1
YML091C	1	1,185080332	0,887288495	0,779977919	1
YMR117C	1	1,148202408	0,944069233	0,68569201	1
YOL113W	1	1,07699459	0,843375095	0,703569716	1
YPL158C	1	1,214206425	1,0831648	0,701621231	1
Q0092	1	2,777190607	2,312544	2,905004157	2
tE(UUC)G1	1	1,748774119	1,542777477	2,344334107	2
tP(UGG)N2	1	1,665035604	1,31046595	1,643197988	2
tV(UAC)D	1	1,905614622	1,808013195	2,142413648	2
YCL073C	1	2,821978836	2,035471319	3,327225311	2
YDR446W	1	1,898131638	1,23288807	2,037163149	2
YER135C	1	1,579838761	1,280761271	1,669676078	2
YGL168W	1	2,490115021	1,737164689	2,848596664	2
YGR174W-A	1	1,525251735	1,300952965	2,084402494	2
YGR228W	1	2,012899124	1,733447278	2,65069474	2
YJL164C	1	1,67370062	1,670938	2,055396465	2
YJR150C	1	1,600715786	1,154213037	1,961973388	2
YLR111W	1	1,704674251	1,364309709	1,770185612	2
YOL037C	1	1,511660948	1,290092265	1,655138898	2
YOL084W	1	1,522609758	1,247850789	1,981154979	2
YOL163W	1	1,671314519	1,545304162	2,004385218	2
YOR102W	1	2,052813438	1,616707022	2,229486255	2
YPL033C	1	1,598425119	1,249834823	1,77947125	2
RNA170	1	1,299999858	1,315662352	1,740225196	2
tL(UAG)L1	1	0,97104974	1,008310619	1,511501708	2
tV(AAC)G2	1	1,095062203	1,020164968	1,612979137	2

YBR128C	1	1,245104	1,18821865	1,539930901	2
YBR132C	1	1,207242298	1,195738723	1,611293427	2
YBR144C	1	1,459435742	1,358544824	2,233557564	2
YDL021W	1	1,278643095	1,305813266	1,633314756	2
YDL159W-A	1	1,137553644	1,016896721	1,535517391	2
YDL239C	1	1,405377009	1,353496815	1,989643484	2
YFL019C	1	0,920132488	0,918673043	1,541596135	2
YGR122C-A	1	1,345269995	1,303568858	1,9541389	2
YGR236C	1	1,223969637	0,939433193	1,611979527	2
YHR022C-A	1	1,390039152	0,760449584	1,649624464	2
YHR096C	1	1,276050617	1,289381073	1,671713518	2
YHR157W	1	0,988518114	1,05885236	1,684180137	2
YIL045W	1	1,375344006	1,399464156	1,743405305	2
YIL071W-A	1	1,481059882	0,998305144	1,901211693	2
YIL082W-A	1	1,022500488	1,077763802	1,712549362	2
YIL111W	1	1,111186954	1,168496421	1,529942669	2
YJL016W	1	1,186522841	1,133018555	1,588470304	2
YJL089W	1	1,315881541	1,135176092	1,993573278	2
YJR004C	1	1,021413766	1,048481754	1,615169652	2
YJR005C-A	1	1,157958352	1,065731797	1,585695259	2
YJR120W	1	1,138531101	1,000764009	1,553020839	2
YKL076C	1	1,086001412	0,988809623	1,588222376	2
YKR005C	1	1,141536662	1,161561492	1,767263083	2
YLR311C	1	1,264615309	0,877296251	1,5354361	2
YML057C-A	1	1,243578183	1,082426065	1,629844937	2
YMR169C	1	1,261769513	1,200020764	1,902302649	2
YMR194C-A	1	1,25126272	1,125569737	1,705453107	2
YNL009W	1	1,251908328	1,271718475	1,603865854	2
YOL085W-A	1	1,437493305	1,344485747	1,909693057	2
YOL132W	1	1,189852118	0,976773059	1,513799318	2
YOL155W-A	1	1,421555222	1,411267218	2,04897068	2
YOL159C-A	1	1,408605515	1,323381843	1,751940725	2
YPL027W	1	1,147391308	1,184051526	1,706383641	2
YPL276W	1	1,239436261	1,161661715	1,505892355	2
YPR126C	1	1,29045852	0,982791123	1,599672257	2
YDL050C	1	1,328401	0,690344277	1,462295417	2
YER188C-A	1	1,259759136	0,781040491	1,486159746	2
YOR034C-A	1	1,167605056	0,726260825	1,426511669	2

snR11	1	0,943407874	0,880053741	1,366755845	2
YBR250W	1	1,099698018	0,904538738	1,403102499	2
YLL013C	1	1,007799233	0,894494279	1,364564705	2
YLR187W	1	0,998350594	0,922753901	1,393376734	2
YOR388C	1	0,981291386	0,924245012	1,459908713	2
YHR044C	1	0,621162273	0,590442329	0,56588533	3
YJL118W	1	0,63717227	0,563588554	0,516138187	3
YOR382W	1	0,663916342	0,557131676	0,431155519	3
snR13	1	0,698836346	0,550759376	0,571285223	3
snR32	1	0,812320463	0,463953153	0,494519722	3
snR49	1	0,813389666	0,648189973	0,596401541	3
YAR008W	1	0,806141064	0,631117304	0,477210627	3
YAR018C	1	0,847589451	0,602343656	0,403599692	3
YAR064W	1	0,721906602	0,652606016	0,523274964	3
YBL009W	1	0,741817117	0,489114493	0,367001391	3
YBL035C	1	0,806275946	0,663529009	0,553091234	3
YBR202W	1	0,811258239	0,630124598	0,432630901	3
YBR275C	1	0,889947417	0,651957553	0,563086856	3
YCL063W	1	0,781817671	0,505996432	0,33656187	3
YDL211C	1	0,891391823	0,663138776	0,554901395	3
YDR097C	1	0,81431368	0,54377108	0,507131809	3
YDR146C	1	0,856417109	0,526481556	0,326716054	3
YDR281C	1	0,814238391	0,644344974	0,500205348	3
YDR451C	1	0,731917297	0,483549275	0,412569955	3
YDR507C	1	0,789318138	0,535108977	0,327233764	3
YDR523C	1	0,842993799	0,607100237	0,543022352	3
YEL040W	1	0,684729857	0,592794234	0,475525949	3
YER070W	1	0,807880809	0,547537028	0,463061863	3
YFL064C	1	0,673720413	0,643675039	0,522776814	3
YGL021W	1	0,886548591	0,572247948	0,427103164	3
YGL116W	1	0,814596981	0,575899538	0,416579498	3
YGL162W	1	0,757935107	0,648328594	0,569415587	3
YGR014W	1	0,814526813	0,587384303	0,646403933	3
YGR040W	1	0,815118259	0,602799531	0,443118235	3
YGR140W	1	0,838132733	0,664175239	0,556296367	3
YHR049C-A	1	1,045465656	0,598240172	0,640829659	3
YHR140W	1	0,865130649	0,615524055	0,574512601	3
YHR149C	1	0,722381199	0,540396122	0,388258943	3
YHR154W	1	0,945673586	0,601235999	0,401510522	3
YHR172W	1	0,927119652	0,555228078	0,433584818	3
YIL026C	1	0,951084568	0,642273859	0,433127986	3

YIL053W	1	0,749471432	0,662253597	0,438193481	3
YIL158W	1	0,791941	0,565731484	0,422609878	3
YIL159W	1	0,84173412	0,628868218	0,573629312	3
YIL162W	1	0,850984426	0,611902006	0,457611876	3
YJL009W	1	1,085325177	0,570499119	0,617199411	3
YJL051W	1	0,84536369	0,609097032	0,501884688	3
YJL074C	1	0,8729629	0,541780138	0,349713297	3
YJL080C	1	0,858990964	0,614418919	0,59361073	3
YJL158C	1	0,757448698	0,610846502	0,595499305	3
YJL194W	1	0,998691213	0,635409699	0,417882607	3
YJR003C	1	0,920704022	0,633879049	0,410703723	3
YJR048W	1	0,826980195	0,636993199	0,440380316	3
YJR092W	1	0,83943385	0,514221047	0,356239956	3
YJR143C	1	0,861086098	0,624222639	0,618933658	3
YKL108W	1	0,866399831	0,601958535	0,404204576	3
YKL165C	1	0,880006222	0,644361528	0,591866266	3
YKR012C	1	0,910488544	0,50994954	0,445832904	3
YKR013W	1	0,668312182	0,628847447	0,490196511	3
YKR075C	1	0,712613769	0,641319702	0,529739173	3
YLL002W	1	0,927390552	0,643595285	0,54848985	3
YLL012W	1	0,778156621	0,614575998	0,5442522	3
YLR084C	1	0,791965356	0,533893672	0,404685844	3
YLR103C	1	0,851638362	0,652491018	0,550450581	3
YLR131C	1	0,935572681	0,591515869	0,508547856	3
YLR183C	1	0,863190408	0,605106603	0,400876721	3
YLR190W	1	0,834240722	0,663141947	0,501532102	3
YLR212C	1	0,778040147	0,653441579	0,441114517	3
YLR278C	1	0,834265398	0,610087758	0,52786967	3
YLR297W	1	0,936926475	0,625975862	0,586979098	3
YLR342W	1	0,817760182	0,587564055	0,493913843	3
YLR385C	1	0,684915797	0,554922274	0,467460305	3
YLR413W	1	0,714500478	0,486501001	0,479185852	3
YLR462W	1	0,767316996	0,653513033	0,479997554	3
YML060W	1	0,777615819	0,619991209	0,503424148	3
YML090W	1	1,018009488	0,636073271	0,570352808	3
YML109W	1	0,855510683	0,61381412	0,47578473	3
YML119W	1	0,88215347	0,602987809	0,396407704	3
YML123C	1	0,780874775	0,631261979	0,494201966	3
YML133C	1	0,823623353	0,582770381	0,630774109	3
YMR001C	1	0,839861584	0,563362976	0,433587044	3
YMR001C-A	1	0,757564733	0,501083259	0,320245251	3

YMR032W	1	0,786789213	0,465044041	0,279819911	3
YMR119W-A	1	0,808082418	0,456668078	0,538070949	3
YMR132C	1	0,873312268	0,628779778	0,507910684	3
YMR144W	1	0,893916629	0,649321428	0,358883135	3
YMR179W	1	0,911533795	0,620628514	0,475860082	3
YNL043C	1	0,882994604	0,604097528	0,550804472	3
YNL072W	1	0,73472605	0,646530478	0,431017684	3
YNL102W	1	0,862184895	0,572956633	0,434968449	3
YNL231C	1	0,861045861	0,631293971	0,455271296	3
YNL273W	1	0,932145977	0,641307621	0,506153331	3
YNL298W	1	0,797230967	0,509455976	0,424028376	3
YOL017W	1	0,960991725	0,664144546	0,412966617	3
YOL059W	1	0,696702353	0,621208951	0,571259228	3
YOL136C	1	0,865438556	0,61978165	0,5332274	3
YOR225W	1	0,759771693	0,362728229	0,57299629	3
YOR247W	1	0,825853937	0,561361132	0,377603268	3
YOR372C	1	0,901804327	0,639312475	0,533824079	3
YPL058C	1	0,693759694	0,432075139	0,532408664	3
YPL081W	1	0,67578283	0,562004882	0,554852361	3
YPL124W	1	0,963332108	0,639944824	0,421281487	3
YPL155C	1	0,765871425	0,663913152	0,598801637	3
YPL189W	1	0,828292264	0,54623263	0,609073493	3
YPL255W	1	0,8143278	0,553501019	0,453535053	3
YPL267W	1	0,874920358	0,604062093	0,502860649	3
YPR002W	1	0,790138527	0,522346452	0,531880529	3
YPR119W	1	0,794466657	0,569123154	0,444999089	3
YPR156C	1	0,791611932	0,603986092	0,58373617	3
YPR157W	1	0,730779344	0,495740905	0,61807341	3
YPR175W	1	0,788716192	0,524394043	0,44504584	3
ICR1	1	0,968512729	0,66795345	0,519877266	3
YAL024C	1	0,950242302	0,685549352	0,531014777	3
YAR068W	1	0,712756805	0,67683145	0,532340164	3
YBL023C	1	0,85642932	0,668287297	0,556959349	3
YBL111C	1	0,917714262	0,739954512	0,505370023	3
YBR064W	1	0,688385147	0,672883722	0,445879714	3
YBR070C	1	0,966986738	0,709101558	0,488176325	3
YBR073W	1	0,942276346	0,727016292	0,567329375	3
YBR138C	1	0,989480245	0,714028429	0,508885787	3
YBR233W	1	0,886976401	0,707603436	0,50597435	3
YBR296C-A	1	0,871663128	0,7834659	0,498969275	3

YCL054W-A	1	1,016903213	0,693137648	0,381400573	3
YCL061C	1	0,972925988	0,738441544	0,560696739	3
YCR034W	1	0,856599672	0,707728367	0,572701101	3
YDL003W	1	1,024676685	0,733576989	0,515953351	3
YDL105W	1	1,01300521	0,687818853	0,530944772	3
YDR309C	1	0,875368998	0,669852464	0,500639484	3
YDR399W	1	0,784389682	0,706837183	0,477513486	3
YER118C	1	0,877406131	0,687692617	0,453229528	3
YER149C	1	0,747257125	0,725881375	0,53859294	3
YER181C	1	0,780733288	0,968617945	0,310256261	3
YER190W	1	0,897250708	0,713986082	0,26621129	3
YFL008W	1	0,961182901	0,733239422	0,551471964	3
YFL037W	1	0,753635337	0,684427559	0,514158385	3
YGR108W	1	1,064419421	0,761000936	0,445322454	3
YGR146C	1	0,876256911	0,672601218	0,545494827	3
YGR152C	1	0,876992201	0,676819648	0,483706643	3
YHR061C	1	0,829753722	0,715256406	0,529843794	3
YHR127W	1	0,87459475	0,702681517	0,462468556	3
YHR136C	1	0,845433653	0,697633568	0,414259147	3
YIL122W	1	0,831244083	0,669023797	0,513228657	3
YJL019W	1	0,872597187	0,707017199	0,528931053	3
YJL092W	1	0,984725596	0,685998788	0,587310981	3
YJR043C	1	0,875883473	0,676182457	0,461767886	3
YJR098C	1	0,835407055	0,71102677	0,530954814	3
YKL113C	1	0,924154633	0,691727804	0,497002429	3
YKR073C	1	0,829020538	0,938690274	0,350310217	3
YLR045C	1	0,899094968	0,678675987	0,565536106	3
YLR214W	1	0,822128164	0,689247292	0,565043521	3
YLR234W	1	0,73878852	0,687715331	0,503744256	3
YLR272C	1	0,935549937	0,687322693	0,555205457	3
YLR296W	1	0,740429386	0,89330024	0,362531417	3
YLR383W	1	0,8831604	0,67677368	0,560691223	3
YMR076C	1	0,964193854	0,69916082	0,558366151	3
YMR078C	1	0,945499609	0,688469869	0,526340547	3
YMR199W	1	0,876829567	0,702765697	0,417241022	3
YMR307W	1	0,806901415	0,670808858	0,459987208	3
YNL058C	1	0,941143377	0,706675467	0,517382999	3
YNL082W	1	0,999221069	0,678760496	0,490912317	3
YNL233W	1	0,966671198	0,716929327	0,573842942	3
YNL290W	1	0,78716863	0,767721129	0,523275832	3
YNL291C	1	0,910664007	0,697249373	0,526662068	3

YNL304W	1	0,876246638	0,776294323	0,527457341	3
YNL309W	1	0,834555543	0,70263275	0,529434813	3
YNR009W	1	0,821208609	0,678516459	0,528855459	3
YOR144C	1	0,951582753	0,727858338	0,478185878	3
YOR218C	1	1,044801603	0,688693087	0,305272606	3
YOR226C	1	0,798702783	0,743901295	0,495722688	3
YOR315W	1	0,832231379	0,697512808	0,512086231	3
YPL014W	1	0,964246268	0,713388673	0,522775201	3
YPL019C	1	0,938010624	0,680851743	0,512601505	3
YPL242C	1	0,957965958	0,707575295	0,537219407	3
YPR120C	1	0,897680595	0,722396512	0,483757213	3
YHR079C-A	1	0,636672256	2,171394491	1,519685934	4
tH(GUG)M	1	1,558751774	2,27529733	2,188474031	4
tL(CAA)G2	1	2,237592845	2,479438008	2,550815499	4
YBR158W	1	1,50996142	2,061401142	2,149837203	4
YBR184W	1	1,53373838	2,105703199	1,620701911	4
YDL119C	1	1,5646873	1,99961661	1,899335548	4
YDR119W-A	1	1,752489653	2,624118339	2,813259029	4
YDR157W	1	2,86324528	4,899151889	4,458068505	4
YGL096W	1	1,553858941	1,875711091	1,63880341	4
YGL229C	1	1,923956986	2,462465207	2,789509264	4
YGR044C	1	1,650559034	2,432298601	2,357775212	4
YGR052W	1	2,398010391	2,648473986	2,904134402	4
YHR131W-A	1	2,301443279	2,45851988	2,725522165	4
YHR213W	1	1,699148776	2,324692913	2,003870824	4
YMR195W	1	1,704866526	2,382416084	2,458135728	4
YMR322C	1	2,579544478	2,452732922	2,729739321	4
YNL067W-A	1	1,584673332	2,265011834	1,658882303	4
YOR264W	1	1,701328993	2,374145494	2,187774946	4
YPR043W	1	1,895091079	3,162432067	2,757226857	4
YPR100W	1	1,543222999	2,153070155	1,709194775	4
YPR170C	1	2,130676807	2,707751878	2,752249517	4
tE(UUC)K	1	1,152677387	2,291010226	1,803997667	4
tS(AGA)D2	1	1,197796943	1,688787596	1,642434854	4
YBL071C-B	1	1,464570353	2,900793076	2,244004962	4
YBL091C-A	1	1,093100336	1,671534173	1,681123861	4
YBR302C	1	1,128922745	1,769842983	1,645524392	4
YCL001W-A	1	1,174072389	1,80691264	1,880240042	4

YCR007C	1	1,224664617	1,617971935	1,56398434	4
YDL110C	1	1,146953105	1,933483199	1,982372587	4
YDL169C	1	1,275428561	1,64820018	1,61138685	4
YDL181W	1	1,435790948	2,096547907	2,156810935	4
YDR089W	1	1,49272392	1,862480508	1,887364001	4
YDR225W	1	1,255619392	1,82704824	1,931601412	4
YDR417C	1	0,95364403	1,915064838	1,353544306	4
YDR516C	1	1,163472359	1,773225271	1,945696515	4
YEL035C	1	1,376314387	2,119884871	2,189842522	4
YEL045C	1	1,055388748	1,829358683	1,473880316	4
YEL076C	1	1,366209898	2,227859274	1,647470131	4
YER121W	1	1,252037714	1,695842857	1,693949076	4
YER152C	1	0,885141256	1,589446236	1,539937773	4
YER153C	1	1,038119653	1,676939494	1,450631402	4
YFL012W	1	1,408514807	1,857900957	1,611858387	4
YFL020C	1	0,781347371	1,546015056	1,614539222	4
YFR003C	1	1,234320049	1,628547599	1,596589318	4
YFR017C	1	0,977089394	1,594861253	1,556523993	4
YFR053C	1	1,400426236	1,813580048	1,742166969	4
YGR021W	1	1,116702715	1,56293693	1,519588868	4
YGR041W	1	1,412832107	1,956484679	2,114952337	4
YGR121W-A	1	0,978352264	1,735236608	1,454535101	4
YGR203W	1	0,801369982	1,637491591	1,47668225	4
YHR032W-A	1	0,966792146	2,018826682	1,340074236	4
YHR214C-E	1	1,030493682	3,035818043	1,85486116	4
YIL054W	1	1,083006179	1,860635031	1,716064235	4
YIR032C	1	0,751175487	1,574772239	1,516582841	4
YJL043W	1	0,969201165	3,753235416	2,900945887	4
YLL041C	1	1,412359326	1,905326207	1,956449156	4
YLL052C	1	1,124509694	1,592497568	1,618362814	4
YLL053C	1	1,086604749	1,921840449	1,931613161	4
YLR194C	1	1,093566545	1,871585186	1,640967211	4
YLR395C	1	1,271317742	1,750197222	1,761324758	4
YLR434C	1	1,439938426	2,408069056	2,250265377	4
YML100W-A	1	0,709716752	1,603600132	1,395587145	4
YMR180C	1	1,316886929	1,723925252	1,689815425	4
YMR262W	1	1,176122296	1,649746648	1,651029024	4
YNL098C	1	1,103941854	1,597295503	1,631748038	4
YNL173C	1	1,41847485	2,100215719	2,214114941	4

YNL217W	1	1,256499174	1,85417604	2,022419909	4
YNL266W	1	1,279195181	2,071425319	2,071132563	4
YNL327W	1	1,355413933	1,70187065	1,650906568	4
YOL082W	1	1,36216987	1,756055951	1,750320273	4
YOL110W	1	0,888811305	1,734634558	1,410548939	4
YOR134W	1	1,252379273	1,644718679	1,703318896	4
YPL021W	1	1,016641598	1,555779993	1,580108498	4
YPL025C	1	1,410006586	2,363720565	1,814143987	4
YPR130C	1	1,132367507	1,798287604	1,577039941	4
Q0130	1	1,519006687	1,390557007	1,110540217	5
Q0075	1	1,290345589	1,196201846	0,757646555	5
YDL117W	1	1,235451284	1,142864859	0,818691461	5
YKL164C	1	1,228044838	1,202297659	0,799406619	5
YHL006W-A	1	0,963522175	1,163146572	0,76655747	5
tD(GUC)G1	1	0,653876452	1,012333009	0,895697137	6
YBL071W-A	1	0,656234248	0,938596655	1,000788471	6
YCR047C	1	0,647580237	0,963804718	0,97281467	6
YHL048C-A	1	0,558137057	1,220908294	1,04965355	6
YOL014W	1	0,650125918	0,996609979	0,946327228	6
YOL085C	1	0,658719281	1,546604726	1,246897832	6
Q0120	1	0,903837115	1,574704023	1,131786495	6
YJL220W	1	0,961172797	1,630025225	1,177602358	6
YMR135W-A	1	1,135854129	1,541646539	1,324831744	6
YPR123C	1	1,091116521	1,614236185	1,158266272	6
RPR1	1	0,713169046	1,2450461	1,175413358	6
snR43	1	0,719698176	1,479739307	1,327301923	6
YAL039C	1	0,75664429	1,1614809	1,035980659	6
YAR035W	1	0,826967853	1,442476326	1,166983337	6
YBL033C	1	0,839262801	1,300510961	1,263339192	6
YCL033C	1	0,684414486	1,20666658	1,053904112	6
YCL036W	1	0,731033868	1,252993203	1,268546176	6
YCL057C-A	1	0,81251659	1,290467938	1,233916946	6
YCR046C	1	0,730827726	1,203100662	0,940664991	6
YCR051W	1	0,695862436	1,121914079	0,948718731	6
YDR039C	1	0,924879401	1,460807423	1,413175362	6
YDR215C	1	0,718107268	1,241783444	1,240786908	6
YDR476C	1	0,743923021	1,179140716	1,165728096	6
YDR482C	1	0,704122522	1,09990051	0,918980639	6
YEL059C-A	1	0,840366558	1,332562491	1,354056623	6

YFL031W	1	0,858512367	1,298179117	1,329207134	6
YFR018C	1	0,863213976	1,389961645	1,194717785	6
YGR294W	1	0,739837944	1,379688003	1,164750126	6
YHR014W	1	0,860687439	1,417509697	1,191791974	6
YHR070W	1	0,674381928	1,023692822	1,00597059	6
YIL154C	1	0,739531489	1,386836397	1,075676349	6
YIR036C	1	0,685516143	1,303821579	1,281598286	6
YJL062W-A	1	0,872014854	1,319304347	1,027711092	6
YJR019C	1	0,79821248	1,395517191	1,269820878	6
YJR074W	1	0,838593841	1,400950491	1,387197506	6
YJR104C	1	0,724162629	1,112730812	0,95214504	6
YKL018C-A	1	0,80806539	1,248513936	1,063023557	6
YLL067C	1	0,7332642	1,126422424	1,091522487	6
YLR141W	1	0,801009833	1,230766988	0,973546067	6
YLR445W	1	0,690709866	1,16879947	1,050165481	6
YMR069W	1	0,753966238	1,134891708	1,176326792	6
YMR173W-A	1	0,847619206	1,308847739	1,208825699	6
YMR295C	1	0,858368055	1,407348794	1,333138645	6
YMR303C	1	0,922032165	1,389188391	1,402207726	6
YNL208W	1	0,707520714	1,256462745	1,143957359	6
YNL269W	1	0,802436852	1,220246804	1,090351088	6
YOR255W	1	0,708087167	1,352886018	1,317209451	6
YPR002C-A	1	0,758407529	1,248880786	1,112936966	6
YPR182W	1	0,678621777	1,200548457	0,975110076	6
YHR032W	1	0,759818963	1,07028176	1,145119421	6
snR30	1	0,657206443	0,950897953	1,576336061	7
YAR075W	1	0,534311542	1,257479769	1,302800079	7
YBR267W	1	0,6062054	0,8840651	0,98306268	7
YDL162C	1	0,470094269	0,801574087	1,140759124	7
YDL240C-A	1	0,473965653	1,219950793	1,394885051	7
YDL246C	1	0,635340841	1,260165478	1,489502555	7
YGL149W	1	0,420831869	0,825309781	1,221844732	7
YJL052C-A	1	0,449167317	0,860377179	1,221740009	7
YJL119C	1	0,661798975	0,816173194	1,219527948	7
YKL031W	1	0,514792155	1,11873169	1,201654345	7
YLR261C	1	0,665229788	1,40487384	1,578632834	7
YLR331C	1	0,357332227	1,00619821	1,243845776	7
YLR349W	1	0,483292792	0,751500768	1,157660601	7
YMR254C	1	0,540839477	0,827980208	1,025299733	7
YMR294W-A	1	0,603773038	1,034014399	1,296691153	7

YNL319W	1	0,492585291	1,03090244	1,203843925	7
YNL337W	1	0,453277066	1,038242778	1,358749595	7
YOR139C	1	0,545512736	0,701415258	1,084171315	7
YPL238C	1	0,290250736	0,978716918	1,092109212	7
snR58	1	0,759006375	1,04843267	1,652707705	7
YCL037C	1	0,937617498	0,993179391	1,527139969	7
YCR089W	1	0,878658827	0,96259288	1,513686241	7
YDL218W	1	0,831562876	1,04710973	1,561994518	7
YGR279C	1	0,858588194	1,183401927	1,816438881	7
YJL152W	1	0,836845916	1,000493196	1,529520644	7
YJR047C	1	0,707233101	1,041720905	1,546200978	7
YKL066W	1	0,822001569	1,297433946	1,542145648	7
YNL285W	1	0,780860342	1,097294654	1,503065253	7
tG(GCC)D2	1	0,717668735	1,120270362	1,321330025	7
YER088C-A	1	0,780132844	1,186574335	1,354213268	7
YJR073C	1	0,744278034	1,207311806	1,353505532	7
YOL155C	1	0,783929572	1,215599607	1,499629518	7
YOR181W	1	0,770800728	1,291497748	1,471097609	7
snR31	1	0,727624886	0,958320679	1,210251464	7
tK(UUU)L	1	0,673394806	0,94945488	1,272066591	7
tL(UAA)J	1	0,87253007	1,18788413	1,389212228	7
YAL008W	1	0,844543065	0,987022872	1,330593188	7
YBR085W	1	0,78489486	1,168714822	1,339938179	7
YBR092C	1	0,784637136	1,043663672	1,188381991	7
YCL009C	1	0,710407074	1,011974369	1,225108376	7
YCL075W	1	0,763163584	1,00404863	1,15066342	7
YCR021C	1	0,708247043	0,862391181	1,116625815	7
YDL016C	1	0,797467751	1,02181764	1,319852015	7
YDL171C	1	0,896769788	1,058557966	1,388453541	7
YEL033W	1	0,816787415	1,020910122	1,252261252	7
YEL049W	1	0,776297866	0,791722396	1,275198656	7
YER096W	1	0,890591937	1,166984168	1,491429754	7
YER137C	1	0,799427296	0,90024289	1,34943835	7
YER150W	1	0,856016525	1,05590428	1,318773418	7
YFR032C	1	0,816936347	1,198427421	1,382544547	7
YGL074C	1	0,81562997	0,994634783	1,384117417	7
YGR068C	1	0,816926075	1,158936109	1,357553578	7
YIL169C	1	0,783151196	1,170959303	1,466785584	7
YJL088W	1	0,840152186	0,858529159	1,325411826	7
YJL144W	1	0,882860976	1,159803068	1,407920036	7
YKL032C	1	0,864330988	1,091578318	1,420928917	7

YKL125W	1	0,872762027	1,00670951	1,362165609	7
YKR042W	1	0,747453391	0,911016825	1,455788697	7
YLR466W	1	0,752377755	0,837590543	1,181930424	7
YMR304C-A	1	0,771480814	0,791055869	1,272605002	7
YOL058W	1	0,828738961	1,10281187	1,477086104	7
YOR008W-B	1	0,896277435	1,046766826	1,434566907	7
YOR263C	1	0,751763212	0,823317878	1,276401116	7
YPR064W	1	0,732624887	0,88859094	1,128516298	7
tI(AAU)I2	1	1,626854535	1,72308326	2,771626533	8
tX(XXX)L	1	2,083723944	1,860534778	3,111177354	8
YAL064W	1	3,931580906	4,474680698	5,180653968	8
YBR226C	1	1,790436801	2,089705235	2,577933385	8
YEL039C	1	1,688224186	2,227600953	2,928558544	8
YER054C	1	2,016034171	2,723438974	3,486099176	8
YGL028C	1	1,669503857	2,780753848	3,215263611	8
YHL021C	1	1,501816936	2,041468049	2,554083316	8
YLR258W	1	1,886673232	2,755811586	3,100450657	8
YML100W	1	2,270748162	3,400287851	4,228162857	8
YMR105C	1	1,535195592	2,52659441	3,388703893	8
YMR242W-A	1	3,183269547	4,752993383	5,42494679	8
YNL015W	1	1,786982815	2,750441376	3,323688093	8
YNL036W	1	1,718166467	2,433922256	2,918880208	8
YNR067C	1	1,71732316	2,592372793	2,835141383	8
YOR316C-A	1	1,620419967	3,193056519	3,463026784	8
YPL230W	1	1,774029644	2,467461248	2,777933448	8
YPR106W	1	1,910497288	3,616554279	4,616432124	8
YPR160W	1	2,17541721	3,291484969	4,471369204	8
YPR184W	1	1,702942187	2,09631163	2,832640594	8
YAL061W	1	1,149304643	1,957246065	2,539370769	8
YBR126C	1	1,106940288	1,799031301	2,195446265	8
YBR169C	1	1,450476884	1,95839253	2,751974072	8
YBR208C	1	1,318978889	1,766474907	2,679766882	8
YBR241C	1	1,107984053	2,40367565	3,21387813	8
YCL025C	1	1,204569313	1,548564334	2,24890738	8
YCL048W-A	1	1,199334923	2,064452969	2,610086883	8
YDL055C	1	1,398220839	2,441948951	2,811888461	8
YDR107C	1	1,235558614	1,750565841	2,575314076	8
YDR124W	1	1,210755136	1,739061058	2,308774423	8

YDR125C	1	1,043191535	1,530633808	2,123897269	8
YDR258C	1	1,453442444	2,098080014	3,017814793	8
YEL011W	1	1,42981359	2,020015979	2,962037715	8
YEL060C	1	1,034437517	1,520302202	2,257195138	8
YER019W	1	0,929836923	1,948140942	2,112695574	8
YER185W	1	1,30332115	1,953717311	2,743377399	8
YFL021W	1	1,447576856	2,367485273	3,226846354	8
YFR015C	1	1,376204309	2,002350736	2,579447742	8
YGR008C	1	1,447485918	2,528515271	3,383262507	8
YGR248W	1	1,303671377	2,507286636	3,439673522	8
YHL045W	1	1,130241864	1,747937889	2,66678572	8
YHR087W	1	1,40600178	2,310179944	3,204776624	8
YHR094C	1	1,35984578	2,221361113	2,55953707	8
YIL086C	1	0,906496623	1,556248973	2,093723829	8
YIL113W	1	1,43455573	2,244682239	2,784518001	8
YIL136W	1	1,135646022	1,975687062	2,862916747	8
YIL140W	1	1,458934268	2,347508449	3,446736304	8
YJL150W	1	1,074937541	1,977778822	2,639817659	8
YJL170C	1	1,1023279	1,880936504	2,995379282	8
YLL023C	1	1,128110289	1,628427234	2,138627462	8
YLL026W	1	1,266241872	1,696881874	2,236058589	8
YLR128W	1	1,324990345	1,93017845	2,561315781	8
YLR184W	1	0,870028697	1,857075588	2,218524006	8
YLR452C	1	1,217407928	1,782581959	2,491289702	8
YML128C	1	1,351990433	1,963495942	3,023722032	8
YMR250W	1	1,375981793	2,044085784	3,288892824	8
YMR251W-A	1	1,157174962	1,918163104	2,262596205	8
YNL042W-B	1	1,284884837	1,65520341	2,532777061	8
YNL066W	1	1,357941781	2,303147073	2,596789696	8
YNL195C	1	1,07400305	1,921219834	2,590571772	8
YNL251C	1	1,160353695	1,744792635	2,854403703	8
YNL274C	1	1,276352863	1,905716729	2,519666116	8
YNL332W	1	1,004082436	2,0811186	2,647910008	8
YNR001W-A	1	1,254999879	3,086007982	3,389636953	8
YOR230W	1	1,196034766	2,007334161	2,652742269	8
YOR348C	1	1,028427063	1,790998594	2,500885605	8
YPL062W	1	1,200857812	1,671157353	2,325905862	8
YPL192C	1	1,303945034	1,815727935	2,789126734	8
YPR026W	1	1,367062934	1,738480994	2,490459585	8

RUF23	1	0,89151165	1,355938471	1,949459267	8
tR(ACG)L	1	1,225216708	1,459842295	2,276123672	8
YCR005C	1	1,018676221	1,399701654	2,057430727	8
YJR095W	1	1,203528942	1,480845395	2,388806505	8
YML058W	1	0,938210553	1,468219035	2,143213029	8
YNL202W	1	1,125591356	1,395257488	2,146110345	8
YLR162W-A	1	110,0741137	0,826229067	1,4460606	9
YAL064W-B	1	0,596956566	0,78663374	0,832253173	10
YCR102C	1	0,654993157	0,772991481	0,7804633	10
YHL049C	1	0,589874836	0,688740375	0,825347996	10
YKL078W	1	0,590907622	0,633058675	0,748880487	10
YMR158W-B	1	0,654507226	0,654037745	0,796617803	10
tL(CAA)L	1	0,679107085	0,625791211	0,80067343	10
YBR113W	1	0,734350126	0,635961952	0,845740828	10
YBR238C	1	0,772493359	0,662527864	0,72146258	10
YDL049C	1	0,691483059	0,64290736	0,737425201	10
YDR360W	1	0,708688369	0,605542426	0,787573525	10
YEL065W	1	0,782768376	0,572458112	0,659116075	10
YGL170C	1	0,797972494	0,575060336	0,767435954	10
YJL075C	1	0,745534896	0,655257584	0,718969711	10
YML045W	1	0,678348338	0,662587766	0,853992146	10
YMR058W	1	0,767315744	0,608575845	0,710425209	10
YNL077W	1	0,758875479	0,643977967	0,644299085	10
YNL112W	1	0,673032914	0,631307829	0,64360129	10
YNL203C	1	0,74034855	0,637915377	0,833899502	10
YPL080C	1	0,673386934	0,623030404	0,778838827	10
YPL265W	1	0,842172099	0,664992447	0,843813682	10
YLR279W	1	1,410538272	1,534147139	1,239645643	11
snR10	1	0,328896649	0,722294639	0,353248337	12
snR128	1	0,449025244	0,604747348	0,554344169	12
snR52	1	0,379708115	0,281779679	0,469480446	12
snR64	1	0,515569569	0,385019875	0,578005164	12
snR65	1	0,444052737	0,506660194	0,52001683	12
YBR093C	1	0,624763771	0,418366636	0,272542369	12
YBR126W-A	1	0,28099683	0,466159643	0,440807965	12
YCL026C-A	1	0,570086131	0,595536081	0,440803422	12
YCR064C	1	0,333993294	0,600285707	0,503481969	12
YDR014W-A	1	0,421278771	0,48123816	0,288369367	12

YDR095C	1	0,353202138	0,284374324	0,320511187	12
YDR345C	1	0,579270626	0,510614781	0,482119458	12
YDR397C	1	0,458265565	0,699056968	0,372188165	12
YER189W	1	0,572647237	0,593399052	0,357645803	12
YHR063W-A	1	0,59729928	0,197042379	0,269064075	12
YKL029C	1	0,56139447	0,360956854	0,260264014	12
YLR400W	1	0,576171982	0,530729526	0,58845089	12
YMR120C	1	0,614805989	0,45914709	0,342367309	12
YMR244C-A	1	0,544511322	0,655367882	0,271949632	12
YNL289W	1	0,460149974	0,247921436	0,136075614	12
YAR071W	1	0,667099102	0,351070144	0,188129307	12
YBR038W	1	0,689464237	0,396248119	0,331579412	12
YHR173C	1	0,679370042	0,527517738	0,29549295	12
YHR215W	1	0,736517038	0,39420435	0,21512417	12
tS(UGA)E	1	0,60382474	0,511345997	1,412035092	13
YBR300C	1	0,605092926	0,513230302	1,805683028	13
YHL034W-A	1	0,450536544	0,753472291	1,635885013	13
snR17a	1	0,9926583	0,660037617	2,837511269	13
YOL166C	1	0,774709851	0,57232823	1,643792214	13
YDR396W	1	1,860228591	0,784692897	2,393035103	13
YIL032C	1	1,598464887	1,042887439	2,451282243	13
LSR1	1	1,111377352	1,017444997	2,877859339	13
NME1	1	1,077717857	1,102728789	2,221302625	13
Q0050	1	1,497441398	1,432830778	3,128647969	13
Q0085	1	0,889351308	0,896479932	1,897116414	13
RDN5-1	1	0,946193805	0,718144058	1,586430573	13
snR17b	1	0,923490237	0,930777072	2,390745334	13
snR19	1	1,366958627	1,354819953	2,611571221	13
snR190	1	1,024877286	0,960293424	2,088467783	13
tA(UGC)A	1	1,042355452	0,903601966	1,718284688	13
tM(CAU)O2	1	0,892074287	0,829378278	1,588638543	13
tR(ACG)K	1	1,130697514	1,269077211	2,574184304	13
YBL073W	1	1,214586001	0,790311303	1,990005346	13
YBR045C	1	1,105176328	1,28269357	2,131136577	13
YBR072W	1	0,958186998	1,349278158	2,566025671	13
YBR117C	1	1,005886524	1,140578321	1,886643604	13
YER053C-A	1	1,001037769	1,190017374	1,892784865	13
YER125W	1	1,101774414	1,055870069	1,88730126	13
YGL062W	1	1,168976956	1,250758818	2,107767957	13

YGR088W	1	1,160054991	1,302507086	2,228411945	13
YGR109W-B	1	1,072633889	1,132843453	1,881553096	13
YKL065W-A	1	1,246764291	0,785031559	1,901684142	13
YKR039W	1	1,007563174	1,193073176	1,993597127	13
YLR416C	1	0,907701362	0,7537818	1,500557195	13
YLR461W	1	0,784813619	0,774527411	1,63896535	13
YMR175W	1	1,442932525	1,052083024	2,358624539	13
YMR306C-A	1	1,306085983	1,093074298	2,60829168	13
YMR316C-A	1	1,120938694	0,788138677	1,868506586	13
YOR024W	1	0,740591269	0,732251675	2,225120082	13
YOR186W	1	0,8175917	1,045130919	1,771142035	13
YOR214C	1	1,060254376	0,750657377	2,047284066	13
YOR376W	1	0,928685537	1,238456709	2,153905392	13
YOR389W	1	1,227486838	1,295218626	2,200084372	13
YKL153W	1	0,828612611	0,772800175	1,431472201	13
YNL190W	1	0,981592161	0,80498203	1,26988513	14
YOR298W	1	1,033953784	0,816832097	1,268240807	14
tI(UAU)D	1	0,576582217	0,8908201	0,841230116	15
YAL059W	1	0,655166066	0,856724301	0,911209665	15
YGR079W	1	0,590496151	0,88274174	0,871947037	15
YDR074W	1	1,589105619	1,803654784	2,09343312	16
YGL262W	1	1,535800282	1,634289724	2,164989492	16
YJL106W	1	1,622009202	1,843778023	2,024662377	16
YLR149C	1	1,561840807	1,68236222	1,937809757	16
YOR387C	1	1,515341555	1,698028821	1,893950901	16
YPR149W	1	1,504563105	1,746639785	2,208860682	16
tD(GUC)L2	1	1,492410078	1,873356525	2,184388429	16
tK(UUU)D	1	1,331633922	1,583247868	1,8195193	16
tW(CCA)M	1	1,243819449	1,523155462	1,859026903	16
tY(GUA)M1	1	1,049235772	1,535021509	1,811198841	16
YBR046C	1	1,277897966	1,602039202	2,126344424	16
YBR047W	1	1,298987569	1,539707331	1,881035101	16
YBR056W-A	1	1,281628861	1,581162435	1,791178461	16
YBR157C	1	1,352133995	1,504550133	1,874690134	16
YBR230C	1	1,107138916	1,582813442	1,785945543	16
YCL012C	1	1,27274575	1,549754524	1,806136087	16
YCR083W	1	1,118700941	1,616217867	1,844655685	16
YDL085W	1	1,121857506	1,513384447	1,896935053	16

YDL149W	1	1,27542681	1,564039069	1,806763037	16
YDL238C	1	1,190924942	1,549798001	1,744818657	16
YDR031W	1	1,340936158	1,817949805	2,098539358	16
YDR248C	1	1,205181537	1,591267402	1,891677656	16
YDR379C-A	1	1,229622127	1,536050261	1,709632603	16
YDR391C	1	1,152959488	1,631630808	1,957143055	16
YER053C	1	1,165561459	1,577931444	1,946831407	16
YER079W	1	1,43776863	1,752434332	2,288040271	16
YFL011W	1	1,49306982	1,805697308	2,066323196	16
YGL156W	1	1,340591933	1,610413974	2,030596204	16
YGL184C	1	1,012293482	1,62924666	1,970539806	16
YGL194C-A	1	1,28434855	1,539726583	1,718635564	16
YGL196W	1	1,301726588	1,509323749	1,844084083	16
YGL230C	1	1,487791447	1,748148622	2,069393648	16
YGR019W	1	1,104054914	1,519258995	1,992576708	16
YGR131W	1	1,451287333	1,712983929	2,067817012	16
YHR001W-A	1	1,488049238	1,866046781	2,261346935	16
YHR092C	1	1,252838018	1,509105334	1,65256699	16
YHR104W	1	1,12703441	1,523357467	1,79120915	16
YIL055C	1	1,267048118	1,55816069	2,187050917	16
YIL160C	1	1,171066965	1,59396537	2,098226991	16
YIR039C	1	1,485981456	1,776497351	2,104024112	16
YJL003W	1	1,253748678	1,636236803	1,86620308	16
YJL153C	1	1,040305084	1,546008712	1,702364766	16
YJL161W	1	1,323763495	1,601817609	1,932478166	16
YJL166W	1	1,228868474	1,500578904	1,754841968	16
YJR008W	1	1,275306325	1,573165916	1,925128004	16
YKL001C	1	1,117653002	1,530205288	1,813741681	16
YKL008C	1	1,237237647	1,598913152	1,734300168	16
YKL124W	1	1,286674192	1,515009562	1,76966818	16
YKL148C	1	1,243288499	1,740465208	2,131240211	16
YKL150W	1	1,226472388	1,556863247	1,710930951	16
YKL182W	1	1,268656387	1,574945391	1,807651515	16
YLL039C	1	1,132885326	1,50591033	1,671373456	16
YLR012C	1	1,229399985	1,529620008	1,729313953	16
YLR080W	1	1,08505555	1,572815791	1,944276951	16
YLR178C	1	0,975777256	1,56093357	1,947939361	16
YLR257W	1	1,351542841	1,689261304	1,814064982	16
YLR270W	1	1,340552209	1,675774059	2,102727904	16
YLR289W	1	1,326165873	1,501500764	1,844890024	16
YML132W	1	1,058935903	1,622672812	1,757510984	16

YMR110C	1	1,240668479	1,529804492	1,94803985	16
YMR181C	1	1,434734644	1,728372196	1,97987346	16
YMR182C	1	1,058933157	1,556673846	1,750723636	16
YMR182W-A	1	0,90546486	1,526996791	1,851598964	16
YMR256C	1	1,316134609	1,534931085	1,831169296	16
YMR261C	1	1,323166546	1,619003599	1,84688368	16
YMR278W	1	1,26830233	1,5024489	1,664597813	16
YNL078W	1	1,292020851	1,596536395	1,985479745	16
YNL200C	1	1,079130689	1,525314012	1,802582871	16
YNL270C	1	1,227919401	1,504244797	1,812450384	16
YOL077W-A	1	1,212493665	1,593361174	1,707919235	16
YOR065W	1	1,282162629	1,616116271	1,744338056	16
YOR185C	1	1,328777535	1,746087155	2,073019247	16
YOR289W	1	1,416307633	1,823020858	2,257783141	16
YOR292C	1	1,40511525	1,593384632	1,812126807	16
YOR316C	1	1,246127504	1,63909331	1,727993777	16
YPL003W	1	1,25196079	1,520654973	1,781447245	16
YPL004C	1	1,393082475	1,631037429	2,061140622	16
YPL123C	1	1,360634918	1,649500922	1,854345762	16
YPL186C	1	1,241150236	1,654575334	2,144224016	16
YPL247C	1	1,358677855	1,643215131	1,844264865	16
YPL264C	1	1,359277433	1,582283016	2,18155621	16
YPL278C	1	1,303006607	1,53310569	2,212635502	16
YPR141C	1	1,131869754	1,502918311	1,930013119	16
YAL054C	1	1,086815864	1,354370541	1,755597722	16
YAR073W	1	1,211571452	1,354921133	1,626817804	16
YBL042C	1	0,99380213	1,467709051	1,650415368	16
YBL043W	1	0,995280128	1,363724925	1,956248095	16
YBL049W	1	1,143354476	1,453116433	1,652370197	16
YBR006W	1	1,192678047	1,49327015	1,850915948	16
YBR026C	1	1,084592692	1,194067105	1,554471555	16
YBR052C	1	1,046530827	1,376010545	1,523639706	16
YBR056W	1	1,130992955	1,42599397	1,835946088	16
YBR086C	1	1,076343911	1,266023721	1,525554806	16
YBR177C	1	1,252454997	1,378542177	1,659561643	16
YBR214W	1	1,162888226	1,416340319	2,113625612	16
YBR222C	1	1,084666478	1,343551043	1,506578046	16
YBR280C	1	1,283600445	1,373823933	1,944063256	16
YBR284W	1	1,182229981	1,272736506	1,615904044	16
YCL008C	1	0,902008273	1,225260981	1,586710998	16

YCR009C	1	1,190172475	1,445790539	1,66511939	16
YCR061W	1	1,155390636	1,412046284	2,075614414	16
YDL025C	1	1,202661654	1,2939195	1,602915087	16
YDL215C	1	1,278811392	1,363300623	1,732710067	16
YDL227C	1	1,151288975	1,245776039	1,992488109	16
YDL234C	1	1,099619215	1,22910251	1,534022914	16
YDR001C	1	1,221832658	1,47011012	1,850323133	16
YDR030C	1	1,056214902	1,41405766	1,588058645	16
YDR034W-B	1	1,237115286	1,432624321	1,727916478	16
YDR106W	1	1,168331499	1,372290027	1,655523332	16
YDR129C	1	1,02620834	1,294308536	1,535013115	16
YDR195W	1	1,109550617	1,298015214	1,555257723	16
YDR204W	1	1,00767012	1,319218688	1,576966034	16
YDR273W	1	1,110784328	1,199524147	1,557492733	16
YDR405W	1	0,929314834	1,324380776	1,517817614	16
YDR461W	1	0,965042282	1,352346598	1,806372103	16
YDR467C	1	1,111227892	1,215225248	1,823612443	16
YDR528W	1	1,089169092	1,342034491	1,631614505	16
YEL020C	1	1,074969522	1,357848641	1,645513303	16
YER039C	1	1,085194041	1,41791613	1,506586882	16
YER044C	1	1,133939474	1,214354985	1,540596783	16
YER084W	1	1,000771818	1,113891941	1,552234788	16
YER119C	1	0,913809452	1,245928035	1,502907852	16
YER128W	1	1,077691429	1,199126813	1,577661647	16
YER169W	1	1,07517575	1,293504393	1,584424392	16
YER187W	1	0,84752186	1,378207537	1,732958087	16
YFL030W	1	0,926572893	1,268515705	1,558034808	16
YFR011C	1	1,040337305	1,469275637	1,546126966	16
YGL006W	1	1,236227807	1,403232483	1,755875632	16
YGL007W	1	1,062003823	1,181929847	1,662635146	16
YGL055W	1	0,981319059	1,291078981	1,695206156	16
YGL104C	1	0,973640006	1,220950472	1,565019672	16
YGL121C	1	1,023157817	1,283008492	1,650554619	16
YGL197W	1	1,167122112	1,266634145	1,609209755	16
YGL217C	1	1,283893147	1,446911034	2,069320902	16
YGL258W-A	1	1,133663713	1,441695942	1,761470825	16
YGR111W	1	1,152898045	1,326130846	1,601990536	16
YGR161C	1	1,157350227	1,426068997	1,857607555	16
YGR194C	1	1,315214368	1,476074729	1,797302594	16
YGR243W	1	1,211486974	1,404443056	1,712610092	16

YHL002W	1	1,088909824	1,277847127	1,558538604	16
YHL016C	1	1,136731791	1,275058115	1,638123886	16
YHL028W	1	0,946713907	1,428417536	1,912057712	16
YHR016C	1	1,092958336	1,458199652	1,780239342	16
YHR037W	1	1,182647593	1,441362448	1,78779801	16
YHR050W-A	1	0,910374482	1,417493611	1,828268702	16
YHR097C	1	1,166947385	1,40153568	1,581443132	16
YHR101C	1	1,179751177	1,436227179	1,598813647	16
YHR138C	1	1,202599197	1,448494232	1,787357112	16
YHR209W	1	1,261047447	1,464383251	1,713051489	16
YIL037C	1	1,17865608	1,400291207	1,910488848	16
YIL066C	1	1,051566676	1,202049023	1,769362297	16
YIL087C	1	1,031887412	1,349015162	1,636548436	16
YIL101C	1	1,302491701	1,430884371	2,144230564	16
YIL155C	1	1,106003724	1,377864564	1,777174903	16
YIR007W	1	1,198089953	1,283122413	1,786620009	16
YJL066C	1	1,027628975	1,479347905	1,527390951	16
YJL078C	1	0,930676524	1,346908386	1,569584202	16
YJL185C	1	1,179397735	1,298275042	1,805382512	16
YJR059W	1	1,264385667	1,482791094	1,81573212	16
YJR096W	1	1,067231134	1,344026693	1,681802349	16
YJR114W	1	0,904042974	1,404456517	1,729109484	16
YJR147W	1	0,954186302	1,401006424	1,816933345	16
YKL026C	1	1,154562749	1,255870278	1,543834996	16
YKL035W	1	1,114719919	1,388337015	1,566252207	16
YKL067W	1	1,196293927	1,455669695	1,743036352	16
YKL085W	1	1,029766496	1,491393364	1,616967791	16
YKL091C	1	1,1073646	1,331798062	1,591188709	16
YKL103C	1	1,102252599	1,356910759	1,576677886	16
YKL141W	1	1,103369796	1,429828118	1,556223258	16
YKL151C	1	0,914478231	1,261964368	1,597567631	16
YKL219W	1	1,073742314	1,306339159	1,580865539	16
YKR076W	1	1,047026601	1,201982592	1,649815634	16
YLL019C	1	1,335390269	1,421336884	1,844805036	16
YLL058W	1	0,981083741	1,280437214	1,509021992	16
YLR123C	1	1,09421728	1,235654396	1,526947291	16
YLR152C	1	1,257249128	1,352526817	1,80078623	16
YLR251W	1	1,239697551	1,383153797	1,640921932	16
YLR337C	1	0,959763815	1,404909169	1,650549836	16
YLR438W	1	1,025298048	1,296314617	1,583940538	16
YML042W	1	1,205115997	1,418542031	1,691181279	16

YML068W	1	1,144263639	1,416348535	1,631335569	16
YMR007W	1	1,17360068	1,360378752	2,06414914	16
YMR008C	1	1,021500144	1,320576471	1,634452453	16
YMR020W	1	1,070966688	1,365047818	1,59408044	16
YMR035W	1	1,095742451	1,322139777	1,596196146	16
YMR040W	1	1,114226964	1,405938337	1,714603595	16
YMR084W	1	1,144322874	1,468712148	1,992564636	16
YMR085W	1	0,999406298	1,129659204	1,521321651	16
YMR133W	1	1,065527953	1,346364772	1,772799647	16
YMR164C	1	1,09762693	1,28627888	1,734295055	16
YMR174C	1	1,134281373	1,496806324	2,095992836	16
YMR183C	1	1,092808517	1,419161743	1,679828199	16
YMR198W	1	0,929752692	1,277800493	1,581295363	16
YMR215W	1	1,060533754	1,423527386	1,665691472	16
YMR232W	1	1,014781403	1,222448183	1,74351225	16
YMR315W	1	1,089019203	1,348210899	1,530090853	16
YNL042W	1	1,096251435	1,471939839	2,007000836	16
YNL093W	1	1,201381538	1,360014704	1,799538067	16
YNL099C	1	1,020444904	1,313142186	1,539092752	16
YNL115C	1	1,16828667	1,445115965	1,934670057	16
YNL142W	1	0,899964928	1,190815287	1,790774543	16
YNL194C	1	1,297911636	1,371459268	1,946047576	16
YNL253W	1	1,062892445	1,321246396	1,616690468	16
YNR001C	1	1,250361986	1,404336019	1,796970275	16
YNR014W	1	0,966048194	1,494900532	1,560491384	16
YNR064C	1	0,991874158	1,293679275	1,806662544	16
YNR065C	1	1,204940237	1,321540647	1,59978223	16
YNR076W	1	1,176603688	1,298809349	1,637651112	16
YOL045W	1	1,17818618	1,333660456	1,592219507	16
YOL071W	1	1,277019766	1,478747893	1,688561773	16
YOL106W	1	0,970982841	1,193931511	1,526998394	16
YOR001W	1	1,069705162	1,233331433	1,558159835	16
YOR111W	1	1,057107986	1,190596877	1,550611904	16
YOR130C	1	1,017343114	1,169754308	1,510630897	16
YOR137C	1	1,235175563	1,300904701	1,678031263	16
YOR142W	1	1,129153092	1,407079603	1,546144953	16
YOR161C	1	1,226910222	1,432373556	1,782773147	16
YOR215C	1	1,201659773	1,493382872	1,612660383	16
YOR302W	1	1,104393865	1,259607854	1,570272569	16
YOR303W	1	1,0011162	1,182412137	1,548179672	16
YOR317W	1	1,190774065	1,468826037	1,73682981	16

YOR347C	1	1,225905577	1,494698168	1,669585658	16
YPL006W	1	1,21792551	1,363456109	1,963754507	16
YPL087W	1	1,15481601	1,389053142	1,651444441	16
YPL111W	1	1,020651022	1,426527558	1,931411991	16
YPL121C	1	1,168163677	1,243532646	1,846058914	16
YPL154C	1	0,994592251	1,289220711	1,578186133	16
YPL171C	1	0,968215569	1,425874725	1,701201136	16
YPL277C	1	1,13525213	1,390405532	1,96644502	16
YPR010C-A	1	1,225826051	1,477643682	1,92665383	16
YPR145C-A	1	1,122757749	1,398587757	1,775999315	16
YPR172W	1	1,170692811	1,378852226	1,647560592	16
YFL062W	1	0,914136111	1,428086463	1,459755769	16
YKR049C	1	0,875627767	1,318964434	1,47375365	16
YBR089C-A	1	0,92077955	1,301446842	1,42465921	16
YCL039W	1	0,922637329	1,209621497	1,465105574	16
YCR068W	1	0,960377731	1,32053716	1,461096568	16
YDR032C	1	0,903262387	1,26582966	1,440048104	16
YGR051C	1	0,900086052	1,206096569	1,378781612	16
YIR034C	1	0,98923737	1,13897724	1,486526387	16
YKR046C	1	0,884899305	1,263830406	1,496210702	16
YMR297W	1	0,924015818	1,311096937	1,411723336	16
YNR063W	1	0,990655184	1,18151308	1,488954545	16
YOL016C	1	0,936269804	1,334330037	1,499097519	16
YOL086W-A	1	0,937592703	1,352933154	1,460694948	16
YOL156W	1	0,891538959	1,225863106	1,37488982	16
snR81	1	0,476199111	0,953658659	0,608957635	17
snR85	1	0,59929689	0,958852628	0,524878723	17
YAR019W-A	1	0,505280626	1,010342467	0,754764937	17
YBL109W	1	0,617618963	1,09720123	0,601370741	17
YBR230W-A	1	0,617959372	1,151879408	0,871319858	17
YDL186W	1	0,624970485	1,149793575	0,851624691	17
YDR008C	1	0,497690449	1,361834612	0,797373069	17
YDR024W	1	0,400656354	0,892794042	0,680542615	17
YDR320W-B	1	0,519475058	1,35438814	0,729165768	17
YGL166W	1	0,642443351	1,193789324	0,945771105	17
YGL261C	1	0,649502368	1,417746781	0,726041206	17
YHR021W-A	1	0,567373363	1,044349059	0,493123115	17
YHR125W	1	0,447264331	1,221566014	0,731404478	17

YJL027C	1	0,278875862	0,873826538	0,399682815	17
YLR099W-A	1	0,639882539	1,118903191	0,844783536	17
YLR358C	1	0,382008672	1,634236066	0,663009531	17
YML009C-A	1	0,615085033	1,067999467	0,733289464	17
YML047W-A	1	0,350096015	1,071159676	0,811218787	17
YML122C	1	0,534524385	1,177495682	0,855662104	17
YMR230W-A	1	0,398904397	0,825749189	0,755513852	17
YOR072W-A	1	0,615440964	1,182905716	0,924829243	17
YOR083W	1	0,426915716	0,80437854	0,576698055	17
YOR300W	1	0,226638533	1,310066482	0,852759352	17
YPL252C	1	0,653462525	1,05918459	0,80892065	17
tK(UUU)K	1	0,827507566	1,425898015	0,64845178	17
YAL031W-A	1	0,816593099	1,345223369	0,417069478	17
YBL044W	1	0,716688916	2,115399585	1,174239431	17
snR62	1	0,6696532	1,308188667	0,983306383	17
snR8	1	0,808637537	1,28550405	0,868989572	17
YBR109W-A	1	0,848448623	1,426236566	0,763262808	17
YER018C	1	0,829825832	1,253155312	0,755824064	17
YER107W-A	1	0,88255023	1,38358119	0,885118649	17
YFR034C	1	0,760750516	1,423021472	0,890054776	17
YGL126W	1	0,804268124	1,416942399	0,984555669	17
YIL102C	1	0,680476317	1,305049358	0,776651006	17
YCR102W-A	1	0,896397078	1,320640255	0,773932864	17
YDR442W	1	0,894419215	1,231960811	0,735897631	17
YEL074W	1	0,927980051	1,341797079	0,833391131	17
YKL097C	1	0,901846591	1,268122836	0,743160382	17
YKL165C-A	1	0,977205793	1,392254427	0,826608092	17
YIR013C	1	1,302969897	0,549169713	0,453396845	18
YOR248W	1	1,541409637	0,639292893	0,462752522	18
snR6	1	1,559138757	0,787352012	0,491512013	18
tY(GUA)J1	1	1,275783647	0,915263055	0,58152657	18
YCL042W	1	1,492146114	0,951109134	0,452206633	18
YLR236C	1	1,354609472	0,912058637	0,574182453	18
YMR290W-A	1	1,410724295	1,072870963	0,648532123	18
YPL152W-A	1	2,012609237	0,784093527	0,496312812	18

YGR290W	1	1,997125625	0,846941834	0,980678091	18
YLR140W	1	2,551300196	0,678572288	1,006385533	18
YML089C	1	2,984860639	1,741568389	0,783315499	18
RUF21	1	1,489922783	0,822279433	0,695002745	18
YOR105W	1	1,347977035	0,883997696	0,673747824	18
tG(GCC)G1	1	0,566271833	0,821301547	0,838772037	19
YAL044C	1	0,634866236	0,714377849	0,593343628	19
YCL026C-B	1	0,619611845	0,713033714	0,579075064	19
YCR013C	1	0,638290174	0,690286006	0,614485769	19
YDR118W-A	1	0,483526834	0,671720902	0,56066822	19
YDR366C	1	0,579390038	0,789149798	0,779389098	19
YFL067W	1	0,634281588	0,784989643	0,569345829	19
YGR159C	1	0,630116346	0,852489309	0,751288574	19
YLR198C	1	0,573573416	0,769386179	0,572827897	19
YLR316C	1	0,621500833	0,833326261	0,775157714	19
YML113W	1	0,663982736	0,873807611	0,797702547	19
YNL103W-A	1	0,550951356	0,777205715	0,776100589	19
YPR150W	1	0,507152639	0,785551908	0,674216251	19
YOR294W	1	0,697378638	0,645931304	0,618142716	19
snR47	1	0,778198111	0,910016101	0,651077429	19
YAL022C	1	0,786151417	0,830170884	0,655261609	19
YAR015W	1	0,743404903	0,727739298	0,6271514	19
YBL012C	1	0,832455419	1,063773477	0,560198993	19
YBL113C	1	0,723796766	0,771189299	0,599408042	19
YBR054W	1	0,682735578	0,680598475	0,628022734	19
YBR088C	1	0,843240796	0,850240554	0,650801148	19
YBR231C	1	0,771352342	0,770814856	0,613243815	19
YDL009C	1	0,795544333	0,810865303	0,639381098	19
YDR316W-B	1	0,850992908	0,908222328	0,570087736	19
YDR524C-B	1	0,730446057	0,871495991	0,639703146	19
YEL008W	1	0,79538508	1,090201842	0,663316736	19
YER004W	1	0,817471453	0,812696102	0,662455538	19
YFL065C	1	0,762151607	0,914215585	0,475419878	19
YFR032C-B	1	0,832472278	1,02854673	0,615934971	19
YGL034C	1	0,735412755	0,82344575	0,639608425	19
YGL147C	1	0,763526887	0,790188679	0,638995005	19
YGL209W	1	0,747029039	0,737871427	0,613504036	19
YHR219W	1	0,74001895	0,895531419	0,610961762	19
YJL122W	1	0,738496909	0,69787072	0,622187514	19

YJR020W	1	0,683729974	0,960664745	0,509534847	19
YKL037W	1	0,667947851	0,923978273	0,570294752	19
YKL086W	1	0,869136643	1,030390273	0,658327396	19
YKL183W	1	0,768622615	0,775937017	0,594524614	19
YLL022C	1	0,750682931	0,787402875	0,639652551	19
YLR109W	1	0,825140267	0,826425156	0,621179999	19
YLR122C	1	0,78132003	0,969352293	0,469522175	19
YLR315W	1	0,76614797	0,818728296	0,663674313	19
YLR340W	1	0,744948722	0,720938782	0,642881198	19
YLR348C	1	0,728338863	0,796979439	0,518437544	19
YLR437C	1	0,738059253	0,869992226	0,591193532	19
YML028W	1	0,762391106	0,783048513	0,597137372	19
YML058W-A	1	0,850202973	0,947183817	0,663448791	19
YML101C	1	0,795523172	1,045315003	0,64979652	19
YML102W	1	0,747625402	0,787949523	0,578811531	19
YMR116C	1	0,732056961	0,736119032	0,570342905	19
YMR244W	1	0,741928455	0,987669296	0,653116831	19
YNL301C	1	0,69288946	0,677155676	0,65356099	19
YOL143C	1	0,741570935	0,781188579	0,643838306	19
YOR183W	1	0,913763106	1,099151561	0,620040522	19
YPL187W	1	0,742025164	0,887678643	0,665126827	19
tA(AGC)H	1	0,437217824	1,262393327	2,514159018	20
YDL204W	1	1,603242424	2,85856787	4,697747609	20
YDL222C	1	1,658459324	2,63086916	5,134795845	20
YER124C	1	2,565173268	5,219325379	7,132523473	20
YHR054C	1	2,480981758	5,180715642	10,22718666	20
YHR143W	1	2,56112519	5,905219412	10,05863712	20
YLR286C	1	1,892347352	3,858940982	5,483858861	20
YNL277W-A	1	2,082444884	6,617866572	8,283379895	20
YOL052C-A	1	2,076446607	3,456424224	5,345687908	20
YOR374W	1	1,784235851	3,151690187	4,639953247	20
IRT1	1	0,813184752	2,066874525	3,394458761	20
tH(GUG)E2	1	0,978551358	2,167072249	3,483728515	20
tR(UCU)G3	1	1,398686416	2,899727972	4,715523523	20
YBR040W	1	1,439582537	1,942169278	3,588336209	20
YDR070C	1	1,479849435	2,039722928	3,54773759	20
YFL014W	1	1,14735971	2,065855861	3,307287721	20
YFL058W	1	1,100221304	2,238128618	3,584856073	20
YLR285C-A	1	1,16377635	3,363063432	5,903150279	20
YMR107W	1	1,443023912	1,926862991	3,624108384	20

YNR034W-A	1	1,470532502	2,572309879	4,263408596	20
YOR173W	1	1,265849958	2,231325883	4,473220932	20
YPR092W	1	1,150101501	2,846195759	6,583605721	20
Q0020	1	1,425532808	1,434524645	3,825316902	20
Q0055	1	1,123223129	1,324231419	3,217140425	20
SCR1	1	0,908433785	1,209075338	3,828301996	20
tE(UUC)C	1	0,709631864	0,889562584	3,172818402	20
YDL223C	1	1,118094804	1,418512876	2,947481874	20
Q0158	1	1,575459807	1,475444748	1,750960395	21
YEL020W-A	1	1,680910614	1,670863947	1,495414925	21
YGR149W	1	1,612842392	1,848592251	1,771417525	21
YIL046W-A	1	1,709520947	1,522743461	1,623714928	21
YML012C-A	1	1,555231114	1,348144689	1,487335333	21
YOR028C	1	1,780655402	1,73822486	1,948369492	21
YOR177C	1	1,590763702	1,737143443	1,800206424	21
YPL201C	1	1,555831644	1,327823635	1,450517507	21
YPR005C	1	1,545216377	1,662078719	1,411029273	21
tD(GUC)G2	1	1,468176155	1,700166419	1,750810335	21
YBR183W	1	1,498703803	1,564451932	1,662023006	21
YDR055W	1	1,436784585	1,667785357	1,350507147	21
YDR171W	1	1,312361866	1,647376551	1,665153028	21
YDR202C	1	1,362845776	1,598013605	1,683489922	21
YDR358W	1	1,331073372	1,601246315	1,652470124	21
YDR529C	1	1,234694492	1,502410831	1,512855467	21
YEL024W	1	1,224235636	1,532453982	1,495363944	21
YER045C	1	1,214229914	1,571975363	1,58956501	21
YGR112W	1	1,240290925	1,520737154	1,566561294	21
YGR183C	1	1,228840663	1,510033346	1,419561634	21
YHL037C	1	1,414037657	1,508775549	1,63797699	21
YJL047C-A	1	1,241693306	1,531644945	1,445787251	21
YJL057C	1	1,366626408	1,519893981	1,706707645	21
YJL067W	1	1,448022742	1,701794333	1,602542005	21
YJL218W	1	1,348261415	1,611208102	1,51645531	21
YJR108W	1	1,322499294	1,598120271	1,478136373	21
YKL061W	1	1,252538198	1,525664277	1,589527636	21
YKR058W	1	1,416404829	1,574444879	1,581480411	21
YLR345W	1	1,410119642	1,532237521	1,576581982	21
YMR057C	1	1,181823041	1,535296602	1,549607152	21
YNL046W	1	1,237298233	1,644982874	1,328816485	21
YNL328C	1	1,371647212	1,59161855	1,437246124	21
YOL048C	1	1,364201293	1,516651563	1,672857915	21

YPL203W	1	1,352751734	1,576535459	1,561101677	21
YBL029C-A	1	1,284389202	1,499094724	1,555227874	21
YBL039W-B	1	1,275503991	1,283510088	1,517505164	21
YBL045C	1	1,195142143	1,39567673	1,555898834	21
YBR003W	1	1,223094278	1,476088131	1,513242982	21
YBR090C	1	1,497425648	1,390496188	1,520095912	21
YBR147W	1	1,368536554	1,287480927	1,524176493	21
YCL047C	1	1,220341367	1,372355685	1,542521407	21
YDL214C	1	1,189180233	1,291094144	1,512214293	21
YDR178W	1	1,232393801	1,47293384	1,538840701	21
YDR218C	1	1,413424024	1,487715505	1,665183549	21
YDR253C	1	1,245906333	1,242708081	1,522398453	21
YEL005C	1	1,305377312	1,4801345	1,624899546	21
YEL012W	1	1,226881902	1,409142607	1,577861628	21
YEL014C	1	1,38286869	1,372779214	1,594296144	21
YER182W	1	1,250678972	1,410022021	1,616617055	21
YFR008W	1	1,31686451	1,451227889	1,590387892	21
YFR014C	1	1,215478324	1,376090974	1,536510644	21
YGL250W	1	1,211688784	1,435877549	1,526853058	21
YGR053C	1	1,220562103	1,379757614	1,578375726	21
YGR059W	1	1,36359293	1,438612895	1,623471395	21
YGR110W	1	1,159013121	1,347732957	1,503981574	21
YGR127W	1	1,388844009	1,486757047	1,606971636	21
YHL044W	1	1,371549135	1,455442604	1,716442711	21
YHL048W	1	1,204284338	1,417944027	1,519868538	21
YHR160C	1	1,360465711	1,338305392	1,604490117	21
YHR171W	1	1,314645811	1,443390205	1,559956624	21
YIR001C	1	1,233706327	1,434004491	1,606974419	21
YJL005W	1	1,239668379	1,377039614	1,510942096	21
YJL042W	1	1,18787196	1,455289914	1,55166954	21
YJL070C	1	1,31531553	1,34003511	1,637904159	21
YJL141C	1	1,316045145	1,428394903	1,569623629	21
YJL163C	1	1,265539429	1,481285234	1,510434512	21
YJR102C	1	1,161475897	1,377143021	1,54252714	21
YJR121W	1	1,157064818	1,314894636	1,53121039	21
YKR003W	1	1,249127202	1,357390677	1,578830247	21
YLR294C	1	1,243513285	1,243895043	1,516779883	21
YLR356W	1	1,165114216	1,44125968	1,526254341	21
YML120C	1	1,345518427	1,484313362	1,513498121	21
YMR031C	1	1,25968927	1,291373224	1,562614458	21
YNL336W	1	1,271231352	1,363623424	1,54515242	21

YNR007C	1	1,269625126	1,479386263	1,618126617	21
YNR034W	1	1,213808537	1,426788477	1,583129942	21
YNR066C	1	1,36940376	1,408839735	1,538346439	21
YNR075W	1	1,229897947	1,443703092	1,500160231	21
YOL046C	1	1,496969786	1,386455942	1,500017658	21
YOL083W	1	1,313630148	1,31297672	1,54682799	21
YOL097W-A	1	1,390107931	1,334394249	1,535184904	21
YOR005C	1	1,2633859	1,288897809	1,532470773	21
YOR020W-A	1	1,143399175	1,363844998	1,512359974	21
YOR036W	1	1,146219264	1,442990837	1,534144372	21
YOR219C	1	1,151326931	1,251029624	1,516162012	21
YOR386W	1	1,375269706	1,3841387	1,564780604	21
YPL024W	1	1,22060145	1,492242215	1,516441374	21
YPL147W	1	1,336745113	1,313241391	1,530525622	21
YPL191C	1	1,343781902	1,442193365	1,508448457	21
YPR020W	1	1,24405557	1,414389931	1,554030246	21
YPR191W	1	1,219514878	1,44905432	1,538269038	21
tG(CCC)O	1	0,340141963	0,558175918	0,649779767	22
tK(UUU)P	1	0,46970224	0,546040471	0,713021161	22
tP(AGG)N	1	0,318352215	0,516137927	0,93330474	22
tR(ACG)E	1	0,311669698	0,454055427	0,873263144	22
YAR070C	1	0,343290878	0,52542561	0,977080206	22
YBR103C-A	1	0,377560055	0,373722995	0,643333743	22
YDR340W	1	0,424139285	0,599492107	1,249389246	22
YFR012W-A	1	0,566216141	0,472390986	0,913298601	22
YHR218W	1	0,535398501	0,495374532	0,919300405	22
YIL100W	1	0,194507402	0,307695434	0,73185785	22
YJR037W	1	0,430196812	0,425667908	1,155862126	22
YLR374C	1	0,328889537	0,379554288	0,867563265	22
YNL198C	1	0,257954448	0,29821714	0,630445421	22
YOL050C	1	0,432193683	0,343705927	0,570692691	22
YOR314W	1	0,332779358	0,428819247	0,66467826	22
YOR391C	1	0,377489515	0,613810805	0,801283081	22
YFL002W-A	1	1,12256092	0,534749458	0,776030364	23
YFR023W	1	1,212832359	0,60167339	0,798501598	23
YHR185C	1	1,50331807	0,598524978	1,032232222	23
YPR076W	1	1,905512854	0,539675673	1,192384036	23
snR39B	1	1,588951156	1,033071629	1,199443771	23
tL(UAA)B1	1	2,507973474	1,340102953	1,38018938	23

YAR035C-A	1	1,666384329	0,717018707	1,120567171	23
YBR126W-B	1	2,263205881	1,131994421	1,784621424	23
YCR095W-A	1	1,500065716	1,236046	1,361618803	23
YDR182W-A	1	2,149612996	0,873082415	1,331275681	23
YDR433W	1	1,893818953	1,158633656	1,202543092	23
YEL075C	1	2,229407798	1,454865026	1,51856583	23
YER078W-A	1	1,778710995	1,353491002	1,33468847	23
YER087C-A	1	1,936769585	1,444843893	1,374982289	23
YGL006W-A	1	1,51556333	1,025737617	1,142530807	23
YGR109C	1	1,641041692	1,278774058	1,234053159	23
YHL046C	1	1,701722952	1,312651591	1,509283195	23
YLR013W	1	1,547726687	0,751125834	1,301342027	23
YLR222C-A	1	1,512671763	0,73075618	1,395937143	23
YLR415C	1	2,276506012	1,39560851	1,760759783	23
YMR247W-A	1	2,390080826	1,419862752	2,045609726	23
YOL131W	1	1,565831649	1,321593702	1,164179376	23
YOL160W	1	2,18391917	1,676163367	1,758000584	23
ETS2-2	1	1,259704077	0,755335138	0,93727857	23
tN(GUU)P	1	1,212629245	0,792887181	0,963639047	23
tV(AAC)M2	1	1,373613933	0,694988925	0,866065674	23
YDR102C	1	1,166798161	0,732907141	0,978062103	23
YFL010W-A	1	1,298638978	0,727391483	1,158001567	23
YFR054C	1	1,43132043	0,943058492	1,148774253	23
YJR079W	1	1,168089003	0,742303274	0,996962106	23
YOR178C	1	1,161911629	0,728773359	0,853689477	23
YLR202C	1	1,348557885	0,965516493	0,861298879	23
YLR307C-A	1	1,309943087	0,888116708	0,819659464	23
YGL258W	1	1,300899833	0,87074548	1,31964935	23
YNL130C-A	1	0,647029789	0,29821714	0,937360879	24
YOR394C-A	1	0,623574211	0,453335696	1,039804666	24
YPL200W	1	0,649496933	0,370809553	1,180823311	24
snR191	1	0,913458669	0,614563677	1,305960242	24
snR36	1	0,830301135	0,567266463	0,934142452	24
snR48	1	0,770723351	0,649597242	0,929195007	24
tP(UGG)O3	1	0,731785827	0,467868956	1,003768963	24
YAL037C-A	1	0,997932502	0,606449491	0,997346497	24
YAL063C-A	1	0,897701783	0,514492655	0,860183656	24

YBL100W-C	1	0,907354701	0,598448113	0,987783288	24
YBR196C-A	1	0,797418013	0,623555891	1,248108157	24
YDL221W	1	0,803531437	0,647473523	1,165730746	24
YGL015C	1	0,884771458	0,596477208	0,952556688	24
YGR025W	1	0,957669347	0,571055336	0,899991181	24
YGR045C	1	0,8752129	0,426592584	0,93239805	24
YGR249W	1	0,903382857	0,537857132	0,802497803	24
YIL134C-A	1	0,694812192	0,483254195	0,989767731	24
YIR040C	1	1,156271483	0,390542575	0,986827313	24
YJL142C	1	0,915532565	0,453409281	0,849695808	24
YJL202C	1	0,880763512	0,656846169	0,954317955	24
YJR128W	1	0,687545701	0,505797962	0,757096157	24
YKL044W	1	1,038017366	0,647160273	1,263466433	24
YKL115C	1	0,886609931	0,583145589	0,861232456	24
YKL183C-A	1	0,871988006	0,569969206	0,890350245	24
YLR412C-A	1	0,983564136	0,51492776	1,414803431	24
YML034C-A	1	0,800755901	0,496728293	0,695445128	24
YML099W-A	1	0,822905259	0,580211945	0,915836044	24
YOR313C	1	0,796788716	0,544064008	0,831252439	24
YPL119C-A	1	1,022956851	0,638645673	1,030037478	24
YPL143W	1	0,696824902	0,424642699	0,811967186	24
YPL275W	1	0,848259414	0,631566714	0,945158222	24
YOL013W-B	1	1,107641483	0,681202983	1,19017149	24
YMR323W	1	0,892505786	0,669906413	1,150596833	24
YOR339C	1	0,971649703	0,766995196	1,222548525	24
YGL182C	1	1,14200891	1,660303131	0,66544349	25
YIL177C	1	1,035073133	1,529282152	0,485309858	25
YOR381W-A	1	1,535934179	1,381982255	0,586272827	25
snR74	1	1,68177891	2,030071722	1,584388231	25
tV(AAC)O	1	1,579467309	2,412956835	1,188070254	25
YBR051W	1	2,771438945	3,400332838	2,174717112	25
YBR219C	1	1,792001885	2,913961503	1,341916193	25
YCR085W	1	2,501366189	3,235013309	1,046809071	25
YDR455C	1	3,033704955	4,406647775	1,589055464	25
YER097W	1	2,533814106	2,708892226	2,221217076	25
YJL007C	1	2,250823488	1,824935297	1,330886981	25
YJR159W	1	1,893873044	1,99305372	1,295862854	25
YLL066W-B	1	1,793930191	1,809059676	1,100161142	25

YLR120W-A	1	1,70073887	2,047795567	1,44614239	25
YLR366W	1	1,588200488	1,548536055	0,719710631	25
YOR135C	1	2,164742325	2,139361224	1,345054179	25
YPL280W	1	2,39258048	3,173999365	1,813346319	25
snR77	1	1,136613802	1,710954116	1,011108408	25
tP(AGG)C	1	1,312504092	1,543452412	1,087964299	25
tR(UCU)G1	1	1,043230217	2,07043041	0,79083929	25
tW(CCA)P	1	1,204726513	1,611170403	1,056709494	25
YBR298C-A	1	1,197217696	1,565123555	1,02551815	25
YCL041C	1	1,477427026	1,509796484	0,84530834	25
YDL011C	1	1,486970444	2,390864885	0,827110165	25
YDR542W	1	1,334585073	1,756078948	0,901426942	25
YEL053W-A	1	1,312392348	1,963675535	0,944674378	25
YHR086W-A	1	1,475661188	1,556826736	0,947524232	25
YMR175W-A	1	1,464828296	1,924884945	1,419876413	25
Q0070	1	1,234048802	1,451308866	0,754742972	25
snR38	1	1,314015807	1,305039857	0,816763726	25
Q0045	1	1,29958483	1,361761373	0,895044752	25
YDR187C	1	1,173992504	1,452077037	0,836440242	25